Sensing and Signalling Intercalary Growth in *Epichloë festucae*

A thesis presented in the partial fulfilment of the requirements for the degree of

Doctor of Philosophy (PhD)

in

Genetics

at Massey University, Manawatu, New Zealand

Aslinur Ozturk

2019

ABSTRACT

Epichloë festucae is a seed-transmitted symbiont that colonises the aerial parts of grasses and provides protection from biotic and abiotic stress. Although fungal hyphae normally extend at apical tips, exceptions to polar growth characterise the ecology of many important species. Recently, *E. festucae* has been shown to undergo intercalary growth during host colonization, where hyphae elongate and new compartments are created between existing compartments. Intercalary growth enables the synchronized growth of *E. festucae* hyphae and plant cells, and rapid hyphal elongation in plant intercellular tissue. Intercalary growth in *E. festucae in vitro* has been shown to be stimulated by mechanical stretch, mimicking the forces thought to be imposed on hyphae in plants due to their attachment to growing host cells. This research also showed that the High Affinity Calcium Uptake (HAC) and Cell Wall Integrity (CWI) systems influence intercalary growth, however, the mechanisms that regulate cell wall plasticity and compartmentalization are still largely unknown. **The aim of this study was to identify the global gene responses to mechanical stress in *E. festucae* and to further investigate the roles of HACS and CWI in cell wall plasticity and intercalary growth.**

First, the role of *E. festucae* MidA, a homolog of the *S. cerevisiae* Mid1 stress-activated calcium influx channel complex, was addressed to better understand its involvement in intercalary growth and host colonisation. *E. festucae* MidA had been partly characterized previously and found to regulate vegetative growth, cell wall morphology, calcium influx and colonisation of the intercalary growth zone of ryegrass leaves. In this study, *L. perenne* seedlings were inoculated with *E. festucae* wild type, Δ*midA*, and *midA* complementation strains. The effects of *midA* deletion on rates of plant colonisation, and the phenotype of infected plants was determined, and found to be the same as the wild type, although hyphae were more difficult to detect. The biomass of the different strains in host tissues, enriched either for the shoot apex (including the meristem) or surrounding leaf tissues, was quantified. The results revealed that *E. festucae* Δ*midA* colonization in both tissue types was reduced compared to wild type (WT), but the effect was most convincing during growth in leaf tissues. These findings

suggests that MidA function is required for host colonization, particularly in the leaf expansion zone where intercalary growth occurs.

The role of MidA in cell wall plasticity and hyphal growth responses to mechanical stretch was next addressed. *E. festucae* WT and Δ*midA* strains were grown on Potato Dextrose Agar (PDA), with or without 50 mM $CaCl_2$ supplementation in a custom stretching device. When grown on PDA without calcium supplementation, the cell walls of WT and *midA*-complemented deletion strains were able to withstand mechanical stretching equivalent to 6.5% of their hyphal length (applied over approximately 15 min). However, when grown in the presence of 50 mM $CaCl_2$, wild type hyphae and *midA*-complemented deletion strains were able to withstand 26% of mechanical stretch without visible evidence of cell wall fracture. In contract, Δ*midA* strains grown on PDA alone were damaged after 2% of mechanical stress. Supplemental calcium was able to partly rescue this defect, and the Δ*midA* strains were able to undergo 8.9% of stretch in PDA plus 50 mM $CaCl_2$. These findings showed that supplemental calcium increases the resilience of *E. festucae* cell walls to mechanical stretch, and that *midA* is required for this, presumably by facilitating calcium influx and cell wall plasticity.

Next, a transcriptomics study was conducted on *E. festucae* cultures undergoing various degrees of stretch. Hyphae were grown *in vitro* on silicon membranes and stretching forces applied to induce intercalary compartment extension and division, as observed in developing leaves. In cultures harvested 5 min after stretch, 105 genes were differentially expressed, whereas after 3 h, that number increased to 403. Analysis of these genes suggested that reprogramming of primary metabolism and plasma membrane organisation occurs almost immediately in response to mechanical stress, and mobilisation of cell wall enzymes and hyphal growth occurs over a longer time period.

Finally, previous research as shown that deletion of *E. festucae* WscA, a homologue of the *S. cerevisiae* mechano-sensor Wsc1, induced cell wall and hyphal growth defects during growth in culture, however deletion strains were able to colonise ryegrass plants similarly to the wild type. To further elucidate the role of the CWI pathway in intercalary growth, a comprehensive bioinformatics study was conducted to identify additional *E. festucae* Wsc proteins which may function upstream of the CWI pathway. A putative *E. festucae* WscB homolog was identified, plus a new putative cell wall protein with a unique domain. Phylogenetic analysis showed similar proteins in 17 other

Epichloë species and entomopathogenic fungi, suggesting the presence of an *E. festucae* sensor protein that has been evolutionarily conserved. Vectors to delete these genes were constructed and *E. festucae* antibiotic-resistant colonies recovered. The putative deletion mutants of both strains were very small and compact compared to wild type growth in culture. Efforts to confirm the deletion loci and functionally characterise the mutants will be part of future research.

In conclusion, a transcriptomics study has revealed that mechanical stretching induces metabolic changes during early and late responses in *E. festucae*, promoting early induction of primary metabolism and later changes associated with hyphal growth and cell wall remodelling. Moreover, further investigation of MidA revealed its importance for cell wall plasticity during intercalary expansion, and indicated that calcium is an essential requirement for hyphal resilience to mechanical stretch. Finally a new protein was discovered that responded to mechanical stress and could be a potential mechanosensor protein. This PhD project attempted to broaden our understanding of intercalary growth in *E. festucae* and pave the way for future studies on mechanical stress response in fungi.

Acknowledgements

I'd like to start by thanking my main supervisor Dr Christine Voisey for her endless support and encouragement throughout my PhD. She has been an immense source of inspiration. She always believed in me and pushed me in the right direction, watching me take baby steps with patience. She always put me first and gave me her hundred percent. I truly feel fortunate to have been her student. From the bottom of my heart, thank you.

I also would like to thank Prof Rosie Bradshaw for her gentle guidance and immense support throughout my PhD. Her expertise shaped this project tremendously. She always prioritized me and came all the way from Massey campus to AgResearch even in her busiest times. I will forever be grateful for her kindness and generosity. Thank you for everything.

I would like to acknowledge Dr Pierre-Yves Dupont and Dr. Carla Eaton for their contributions. Special thanks to Dr Dupont for his help in phylogenetic analyses and bioinformatics suggestions.

I would like to acknowledge Dr John Koolaard for his statistical assistance in my mechanical stretching set up and incredibly smart suggestions to make life easier in the lab. May he rest in peace. I would also like to thank Paul Mclean for his tremendous contribution to transcriptomics analyses. Without his help I wouldn't be able to finish the analysis.

I also want to thank all Plant Microbe Interactions team for all their help, big and small. Thank you Dr Natasha Forester for giving me all your wet lab tips and sharing your experience on all things *Epichloë*. Thank you Dr Pranav Chettri for helping me with my transormations, biomass analyses and answering any questions I have. Thank you Jaspreet, Debbie, Thomas, Anouck, Wade, Editha, Marissa, Wei and everyone in our team. It has been wonderful to work with you and learn so much from you.

A big thank you to Dr Sameera Ariyawansa for initiating this project and being very supportive throughout my studies. I am thankful that you returned from Sri Lanka and showed me the proper way to set up the mechanical stretching experiment in your busiest time, and thank you for providing *E. festucae* Δ*midA*, complement and pYH2a strains.

My wonderful family deserves a big thank you for being patient with me and always supporting me. My loving father Mustafa, my beautiful mother Sema and my dearest brother Halil were always there for me, one call away. They are the best family anyone can have in this life. Let me also thank my adorable goofy dog Tarcin, who cheered me on from afar. I would also like to thank my beloved in laws Galip, Nimet, Buket and Elifnur for supporting me, checking on me and always keeping me in their thoughts.

My dearest friends Grace and Rachel. Thank you for the laughter, fun times, hugs, talks and everything else. You two have become my sisters.

My loving husband deserves the biggest thanks for always being there, making me smile, taking me on adventures and being a wonderful and understanding partner in every way. Thank you for always listening. Thank you for believing in me. Thank you for making me feel like the most special person in the world. Thank you for being my biggest supporter. Together we are invincible.

I would like to acknowledge AgResearch Ltd for funding me throughout my PhD project.

Finally, I would like to thank the kind people of New Zealand. You welcomed me and made me feel at home, it has been a priviledge to study in this beautiful country. Oh, and a big thank you to the biggest fluffball Murphy boy, the best neighbour in the world. I will miss you heaps.

Table of Contents

List of Tables

List of Figures

List of Abbreviations

aa	Amino acid
ATP	Adenosine triphosphate
BAPTA	1, 2-bis(o-aminophenoxy)ethane-N,N,N',N'-tetraacetic acid
BLAST	Basic Local Alignment Search Tool
bp	Base pair(s)
BS	Blocking solution
bZIP	basic leucine zipper
CaM	Calmodulin
cAMP	adenosine 3, 5-cyclic monophosphate
CDPK	Ca^{2+} dependent protein kinases
cm	Centimetre
CR	Congo Red
CT	Cytoplasmic tail
CTF	CCAAT box-binding domain
CW	Calcofluor White
CWI	Cell wall integrity

DIC	Differential interference contrast
DNA	Deoxyribonucleic acid
dNTP	Deoxynucleotide triphosphates
E value	Expect value
EF	Elongation factor
EGFP	Enhanced Green Fluorescent Protein
ER	Early Response
FHA	Forkhead associated domain
FTFD	Fungal Transcription Factor Database
g	Gram
GH	Glycoside hydrolase
GO	Gene Ontology
h	Hour(s)
HACS	High affinity calcium system
HLH	Helix loop helix
HsbA	Hydrophobic surface binding protein A

HSP	Heat shock protein
HygR	Hygromycin resistant
IAP	Inhibitor of apoptosis protein
JGI	Joint Genome Institute
Kb	Kilobase(s)
LACS	Low-affinity calcium system
LR	Late Response
M	Molar
MAPK	Mitogen-activated protein kinases
MAPKK	Mitogen-activated protein kinase kinase
MAPKKK	Mitogen-activated protein kinase kinase kinase
EGTA	Ethylene glycol-bis (2-aminoethylether)-N,N,N,N-tetraacetic acid
ER	Endoplasmic reticulum
mg	Milligrams
min	Min
mm	Millimeter
mM	Millimole

NADPH	Nicotinamide adenine dinucleotide phosphate
NCBI	National Center for Biotechnology Information
ng	Nanogram(s)
nM	Nanomole
nm	Nanometer(s)
Nox	Nicotinamide adenine dinucleotide phosphate complex
NRPS	Non ribosomal peptide synthetase
PBSA	Polybutylene succinate-co-adipate
PCR	Polymerase chain reaction
PDA	Potato dextrose agar
PDB	Potato dextrose broth
PEG	Polyethylene glycol
PKC	Protein kinase C
rcf	Relative centrifugal force
RE	Restriction enzyme
ROS	Reactive oxygen species

qPCR	Quantitative Polymerase Chain Reaction
rpm	Revolutions per minute
RT	Room temperature
s	Second(s)
SAM	Shoot apical meristem
SD	Standard deviation
SDS	Sodium dodecyl sulphate
SP	Signal peptide
STR	Serine threonine rich region
TAE	Tris-acetate-EDTA
tBLASTn	Translated nucleotide database search using a protein query
TEM	Transmission Electron Microscopy
TF	Transcription factor
TMH	Transmembrane Domain
TOR	Target of rapamycin
USA	United States of America
wk	Week(s)

v/v	Volume/volume ratio
w/v	Weight/volume ratio
WT	Wild type
WSC	Wall stressor component
YFP	Yellow fluorescent Protein
YH2A	Histone protein HH2A fused to yellow fluorescent protein
µg	Micrograms
µL	Microliters
µm	Micrometers
µM	Micromolar
^{o}C	Degrees Celsius

1. Introduction

1.1. *Epichloë festucae*: a Symbiotic Endophyte of Temperate Grasses

Epichloë festucae is a fungus of the Clavicipitaceae family in the Sordariomycetes subclass within the Ascomycota division (Figure 1.1). This endophytic fungus is known to have long term symbiotic interactions with cool season grasses of the Poaceae family and provide them with protection against herbivory, abiotic stresses and insects (Schardl, 1996; Schardl, 2002; Scott, 2001; Tadych et al., 2012). Exclusive associations have been defined between individual *Epichloë* species and their specific species of hosts (Leuchtmann et al., 2014). *E. festucae* var. *lolii* colonises *Lolium perenne*, however other strains of *E. festucae* are known to be able to infect different hosts such as *Festuca rubra*, *Koeleria pyramidata* and *Schedonorus giganteus* (Leuchtmann et al., 2014, Hill et al., 2013; Li et al., 2015; Schardl, 1996).

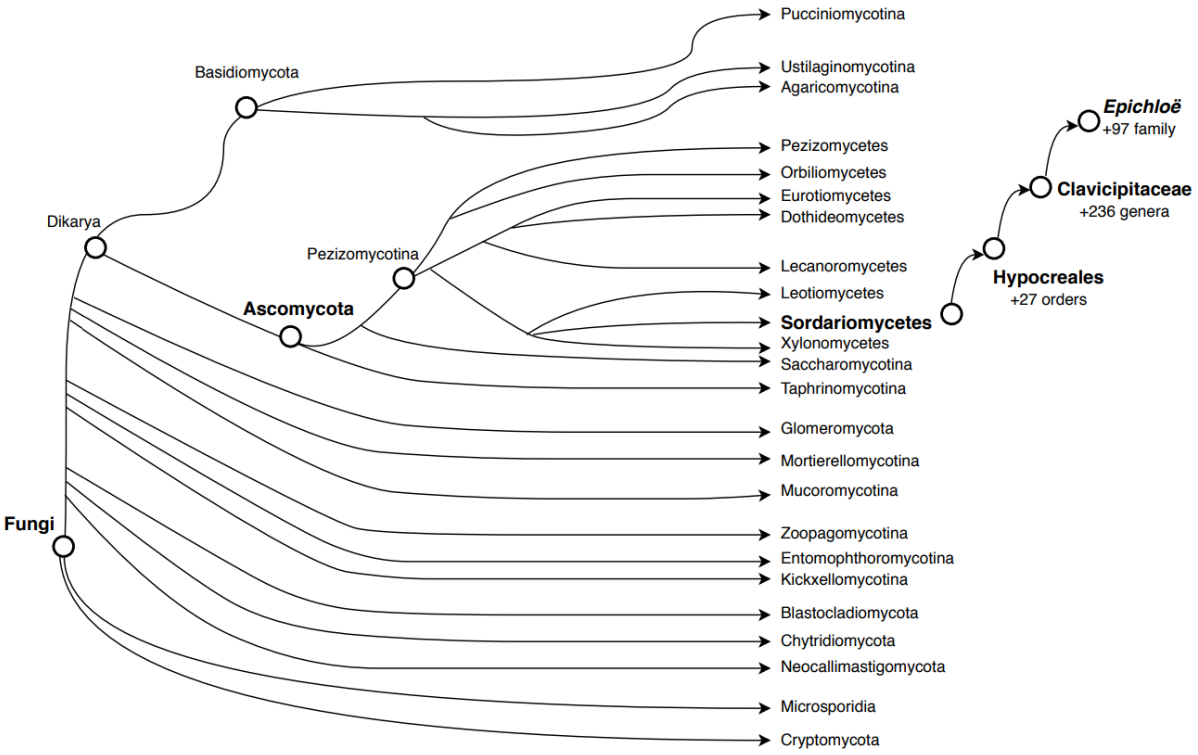

Figure 1.1 Taxonomic classification of *Epichloë* endophytes within the fungi kingdom. Adapted from MycoCosm portal: gearing up for 1000 fungal genomes (Grigoriev et al, 2014).

L. perenne is an economically important forage plant widely distributed around the world (Hill et al, 2013; Schardl, 1996; Scott, 2001). While *E. festucae* takes advantage of the nutrition, environmental protection and reproduction privileges that its host provides, the

plant may gain protection from biotic and abiotic stresses through the production of fungal alkaloids that are insecticidal, or deter certain vertebrates and insects (Schardl, 2002; Guerre et al., 2014), or improve host resilience to drought (Schardl, 1996; Scott, 2001). Ergot alkaloids, lolines, peramines and indole diterpenes are the best known classes of secondary metabolites produced by *Epichloë* (Scott, 2001; Schardl, 2013). Among them, peramine and lolines have insect deterrent properties that are advantageous in agriculture, especially for protection of grasses against Argentine stem weevil and other insects (Schardl, 2001; Scott, 2001). Ergot alkaloids (ergovalines) and indole diterpenes also show insect deterrent properties, but they are mostly notorious for causing circulatory or neurotoxic disturbances in herbivores which are manifested as ergotism and ryegrass staggers respectively (Guerre et al., 2015; Scott, 2001).

1.2. Ryegrass Growth

L. perenne, also known as perennial ryegrass, belongs to the Pooideae subfamily within Poaceae family (Freeman, 1904; Schardl, 2004). Growth of grasses in the Pooideae subfamily was initially studied on *L. temulentum*, which is known as darnel or poison ryegrass due to its nauseating effects when consumed (Freeman, 1904). Grasses of *Lolium spp*. are widely utilized in grazing due to their ability to vegetatively grow from their basal meristem and produce tillers (Jewiss, 1972). The gross anatomy of ryegrass consists of roots, crown, leaf sheath, tillers and leaves (Figure 1.2).

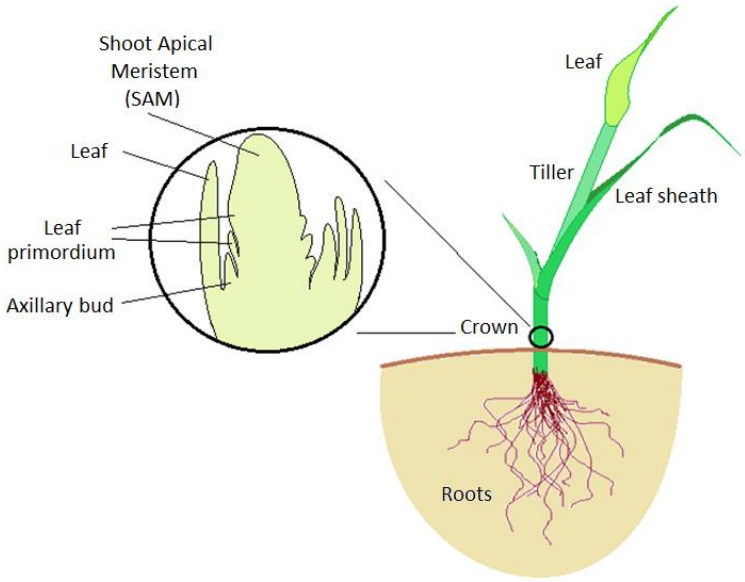

Figure 1.2 Anatomy of *L. perenne* and the longitudinal section of shoot apex reproduced from Sharman, 1945.

Their ability to grow after grazing originates from the structure of shoot apex, also known as growing point, and its close location to the soil that protects it from damage (Langer, 1972). The shoot apex contains a meristematic region and leaf primordia, which eventually develop into new leaves (Langer, 1972). During growth, cells rapidly divide in the outer layer of the SAM, giving rise to a new leaf primordium that encircles the Shoot Apical Meristem (SAM) (Langer, 1972). Once that leaf primordium surrounds the SAM, cells in the deeper layer of the SAM start dividing on the opposite side and form a new axillary bud of the next leaf primordium (Langer, 1972). Two types of cell division starts at the base of leaf primordia, the upper layer giving rise to the leaf and the lower layer giving rise to the sheath (Langer, 1972). Cell division and expansion drives the growth of the new leaf which rises from within the folded sheaths of the more mature leaves, and this cycle continues as new leaves are formed (Langer, 1972). The oldest part of a leaf is the tip while youngest cells are located in the sheath meristem, which can continue cell division and expansion even after the tip is damaged (Langer, 1972).

1.3. Transmission, Life Cycle and Host Colonization

Until the 1980s, the genus *Epichloë* was thought to be monotypic, demonstrating only the teleomorph (sexual) stage which is known to produce symptoms on the host plants they infect (Leuchtmann et al., 2014). With the discovery of endophyte-infected asymptomatic grasses with toxicity to livestock, the anamorphic (asexual) stage of *Epichloë* came to be recognized (Leuchtmann et al., 2014). The asexual relative of *E. festucae*, *Epichloë festucae* var. *lolii* (formerly referred to as *Neotyphodium lolii*) differs in its transmission process and is only transmitted vertically, whereas *E. festucae* can be transmitted both vertically and horizontally (Leuchtmann et al, 2014).

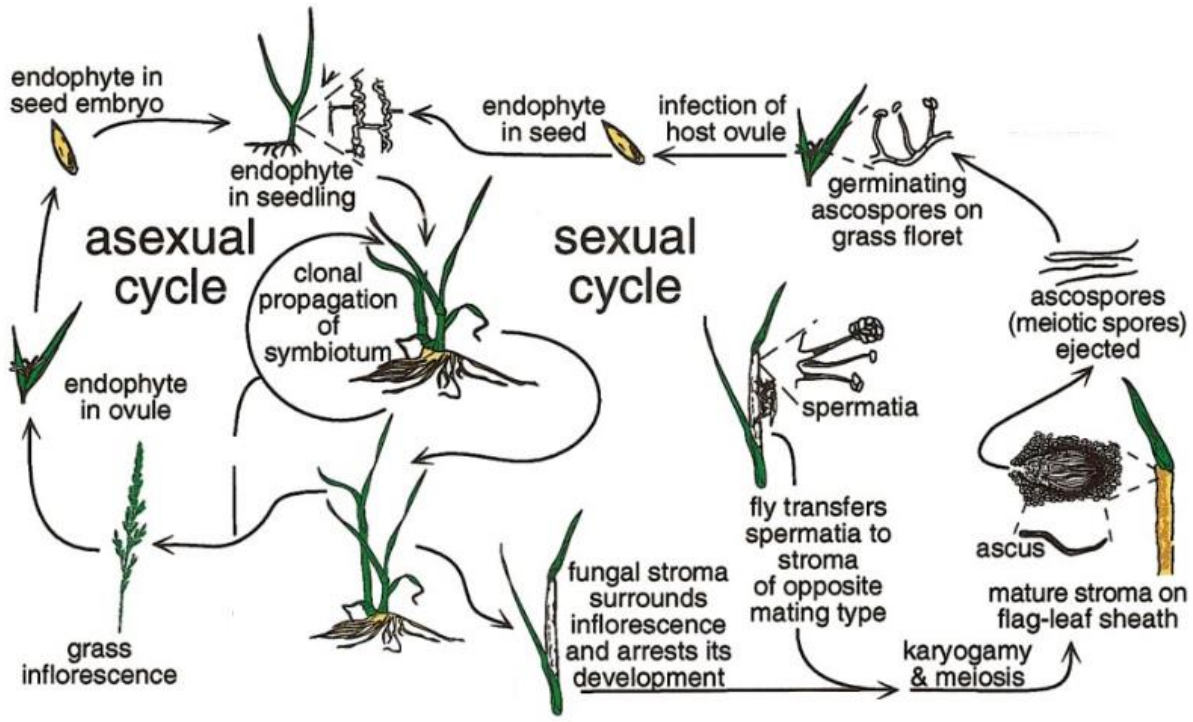

Figure 1.3 Sexual and asexual life cycles of *Epichloë* species. Adapted from Schardl, 1996.

In the vertical transmission of *E. festucae* and other *Epichloë* species, the endophyte colonizing the intercellular aerial plant tissues, including the ovules in florets, is eventually transmitted into the embryos of the seed which results in the infection of the next generation of plants (Figure 1.3) (Schardl, 1996, 2001; Scott, 2001; Tadych et al., 2014). While this mode of transmission is relatively efficient, it does reduce endophyte genetic diversity and the opportunities for adaptive change, which might be disadvantageous in the long term (Hill et al, 2013). Horizontal transmission of *E. festucae* is carried out by the production of ascospores resulting from the fertilization of female hyphae with spermatia of opposite mating types, mating type (MT) A and B (Chung and Schardl, 1997). The endophyte overgrows the inflorescence of the host plant by producing a structure called a stroma, a mycelial fruiting body structure, that stops floret development and seed production completely or partially, also known as choke disease (Figure 1.3) (Gonthier et al., 2008; Li et al., 2015; C. L. Schardl, 2001; Scott, 2001). On the stroma, spermatia and trichogynes (female hyphae) are formed and flies of *Botanophila spp* are attracted (Scott, 2012). Flies facilitate the pollination of trichogynes using spermatia, and if the fertilization of MT A and MT B is successful, resulting ascospores are ejected to invade the neighbouring grass florets, eventually infecting the seed embryo (Schardl, 2001; Scott, 2001).

In the course of its growth within the host, *E. festucae* remains in the plant intercellular spaces (Tadych et al., 2014). With the germination of endophyte infected seed, *E. festucae* hyphae start to colonize the shoot apical meristem (SAM) of the seedling (Christensen et al., 2012; Christey et al., 1986; Schardl, 1996). This enables the hyphae to colonize the developing leaf primordia. At this stage, the hyphae in the meristematic tissue grow rapidly by tip growth and are highly branched (Christensen et al., 2002;. Christensen et al., 2008; Tadych et al., 2014). As the seedling grows, and plant cells increase in number by cell division in the meristem region, and then expand in size in the region above the meristem. It is here that the hyphae become aligned parallel to the lengthwise axis of the growing leaf, become firmly attached to plant cell walls, and are much less branched (Christensen et al., 2008; Schardl, 1996; Tadych et al., 2014). The leaves are systemically colonized by hyphae during the course of plant growth. Endophyte growth occurs synchronously with host growth and colonization ceases once the plant reaches maturity and the leaves expand no more in size (Christensen et al., 2008; Harris, 2006; Li et al., 2015; Schardl, 1996; Tan et al., 2001).

1.4. Maintenance of the Symbiotic Relationship

The symbiotic relationship between fungi and their plant hosts is made possible by complex molecular interactions between the plant and the fungi, whereby fungal colonisation occurs without triggering a host immune response (Lo Presti et al, 2015). Plants are primed to recognise highly conserved microbial molecules called pathogen-associated molecular patterns (PAMPs) that bind to pattern recognition receptors (PRRs) and stimulate a defence response (Albert, 2013). This recognition activates PAMP-triggered immunity (PTI) that eventually initiates large scale transcriptional changes, resulting in rapid production of enzymes that degrade fungal cells and reinforce plant cell walls (Dodds et al., 2010). For a successful symbiotic relationship, the invading fungus must possess mechanisms that will either hide its presence from the host or suppress PTI altogether (Lo Presti et al, 2015). For this purpose, many plant invading fungi have a repertoire of proteins called effectors that can evade PTI in various ways (de Jonge et al., 2011).

Maintenance of the symbiotic relationship between ryegrass and *Epichloë* endophytes depends on the coexistence of endophyte and ryegrass, where the endophyte must maintain a growth mode restricted to the intercellular plant space and the defence mechanisms of the host is repressed by effector proteins (Eaton et al., 2011). *E. festucae* modulates PTI by reprogramming the host metabolism (Dupont et al., 2015). Transcriptomics profiles of

E. festucae-infected and non-infected *L. perenne* revealed that among 276 defence related plant genes, 95 were downregulated in infected plants compared to non-infected (Dupont et al., 2015). In contrast, plant chitinases were upregulated in infected plants compared to non-infected (Dupont et al., 2015). Chitinase is a plant defence mechanism that is used to degrade fungal cell walls (van den Burg et al., 2006). Confocal microscopy has been used to show that intercellular *E. festucae* hyphae cell walls were intact compared to epiphyllous hyphae after lectin wheat germ agglutinin that stains chitin, suggesting that they were protected from plant chitinases (Dupont et al., 2015). The results showed that *E. festucae* can cope with PTI by altering defence-related host gene expression and masking its presence from cell wall degrading enzymes (Dupont et al., 2015).

The symbiotic relationship between *E. festucae* and ryegrass not only depends on modulating PTI, but also on endophyte genes that regulate hyphal growth *in planta*. One of these regulatory genes is *sakA*, a stress-activated mitogen activated protein (MAP) kinase, a signalling pathway member, well characterized in *S. cerevisiae*, that is known to regulate fungal responses to environmental stress (Banuett et al., 1998). The fundamental and well conserved mechanism of MAP kinases is their role in signalling cascades where they respond to extracellular stimuli and activate downstream proteins in the cytoplasm through phosphorylation, which eventually alter the activity of transcription factors and induce corresponding changes in gene expression (Banuett et al, 1998). Disruption of *E. festucae sakA* resulted in decreased plant colonisation rates, a stunted plant phenotype and early death of infected plants compared to WT-infected plants (Eaton et al., 2010). Microscopic examination of tissues in the base of tillers showed that unlike WT, *E. festucae* Δ*sakA* mutants were non-uniformly distributed within the shoot apical region (Eaton et al., 2010). To determine whether a severe plant defence response was the reason of early plant deaths, blades and pseudostems were stained using lactophenol trypan blue (Eaton et al., 2010). Host colonization of wild type and mutant was also compared by aniline blue-staining of young leaf sheaths. *E. festucae* Δ*sakA* displayed a highly disorganized colonization pattern compared to wild type, and hyphae were hypherbranched (Eaton et al., 2010). Transcriptome profiles of *E. festucae* WT and Δ*sakA* infected plants revealed that 47 plant resistance genes, along with known senescence regulatory ethylene biosynthesis genes were upregulated in plants infected with mutants compared to WT infected plants (Eaton et al., 2010). These results point to the important role of *sakA* in symbiosis regulation in *E. festucae* when colonizing ryegrass (Eaton et al., 2010).

Another characterised symbiosis regulatory gene in *E. festucae* is *proA*, a fungi-unique transcription factor that possesses a Zn(II)2Cys6 binuclear cluster DNA-binding domain, known to be present in fungi transcription factors that regulate fungal growth (Tanaka et al., 2013). The discovery of *proA* and its role in regulating symbiosis was made when *Agrobacterium tumefaciens* transfer-DNA mediated *E. festucae* mutants were screened and a mutant showing abnormal growth in plants, and causing stunting phenotype in the host, was found (Tanaka et al., 2013). The T-DNA insertion was found in *proA*, and this gene was then deleted in the WT to understand its role in symbiosis (Tanaka et al., 2013). Ryegrass was infected with *E. festucae* WT and Δ*proA*, and the mutants showed disorganized and hyperbranched colonization compared to the WT (Tanaka et al., 2013). Mutants also produced significantly more conidia compared to the WT, and failed to show hyphal fusion on water agar (Tanaka et al., 2013). The findings show that *proA* is crucial for maintaining the mutualistic relationship between *E. festucae* and ryegrass (Tanaka et al., 2013).

The nicotinamide adenine dinucleotide phosphate-(NADPH) (Nox) complex in *E. festucae* has also been found to be an important regulator of the symbiotic lifestyle (Eaton et al., 2010, 2011; Tanaka et al., 2008). NADPH is a membrane-bound protein complex that generates reactive oxygen species (ROS), and mainly functions in the differentiation of cells and in host defence reactions against pathogens (Tanaka et al., 2006, 2008). In *E. festucae*, the Nox complex consists of 6 subunits (Figure 1.4).

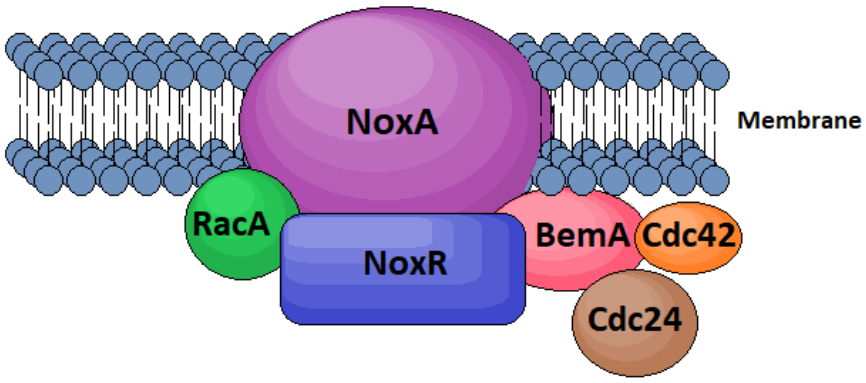

Figure 1.4 Nox complex in *E. festucae*. Reproduced from Kayano et al., 2018.

NoxA, plus the regulatory subunit NoxR and the small GTPase RacA were identified as important regulators of mutualism in *E. festucae* (Eaton et al., 2011). Deletion of *noxA* in *E. festucae* induced pathogen-like behaviour in the endophyte *in planta*, which had increased

hyphal mass and invaded the vascular bundles leading to stunted plant growth and early senescence (Tanaka et al., 2008). Understanding the complex genetic interplay between *Epichloë* and ryegrass may reveal not only the secrets to their mutualism, but also how the endophyte colonises and grows in synchronization with the plant.

1.5. Hyphal Growth

1.5.1. *E. festucae* Growth in Host Plants: Proposed Models

The vegetative growth of *Epichloë* endophytes has been studied since the beginning of the 20th century, and different growth models have been proposed in order to explain the mechanisms behind the observed morphology and localization of the endophyte in different grass tissues, and the synchronisation in growth between the symbiotic partners. Some of the earliest research conducted on endophyte growth was performed by Freeman, in which he observed growth of an unknown endophyte, subsequently identified as one of the asexual species of *Lolium temulentum* (poison grass) (Freeman, 1904). The endophyte in *L. temulentum* seed and seedlings was identified using cotton blue (aniline blue) staining that was, and is still, widely used for visualising hyphal structures within the grass tissue (Bacon & Hill, 2013; Freeman, 1904). The pattern of hyphal localization in the aleurone layer of the seed (that plays an important role in seed development by sustaining proteins, minerals and lipids) was found to be dense, strictly intercellular, not "segmented" and highly branched (Freeman, 1904). Alternatively, hyphal morphology in the developed leaf appeared to be segmented, and the hyphae appeared organized along the longitudinal leaf axis and not dispersed randomly in the aerial tissues of the developing plant (Freeman, 1904). More detailed explanations regarding the distinctive morphology of the hyphae in plant tissue came later in the 20th century. With the availability of advanced microscopy and molecular techniques it has become possible to track hyphal growth *in planta*. Several growth models have been proposed to explain the behaviour of hyphae in plant tissue using various reporter genes to visualise the localization or metabolic activities of endophyte hyphae (Tan et al., 2001).

One of the early leading hyphal growth models was suggested by Tan et al., (2001) who used *E. festucae* var. *lolii* expressing the *Escherichia coli* β-glucuronidase reporter gene to track metabolic activity, hyphal branching patterns and hyphal extension trends of the endophyte *in planta* (Tan et al., 2001). The team suggested that *E. festucae* var. *lolii* growth occurs as the

hyphae and plant cells "slide past" each other and the friction caused by this contact is sensed by mechanosensitive proteins on hyphae, regulating the apical extension rate (Tan et al., 2001). Results also showed that metabolically active hyphae were present in mature plant leaves (that have ceased growth) which suggested the uncoupling of hyphal growth and metabolism, possibly allowing hyphae to continue making bioactive alkaloids in the absence of fungal growth The authors also hypothesized that the endophyte could be responding to signalling mechanisms from the plant to regulate hyphal branching morphology in growing leaves (Tan et al., 2001). They based this hypothesis on their results showing equal numbers of hyphae in young and mature leaves and a lack of hyphal branching in leaves that had ceased growing, indicating a synchrony in growth (Tan et al., 2001).

Figure 1.5 Endophyte hyphae attachment to plant cells. A-b)TEM images of *N. lolii* flattened hyphae due to the neighbour plant cell wall attachments in young ryegrass leaves. c) Hypha of *N. coenophialum* in tall fescue leaf image obtained via frozen fracture SEM. H: hypha. Scale bars represent 1 µm. Reproduced from Christensen et al., 2008.

This model of *Epichloë* growth was later superseded when it was demonstrated that hyphae appeared attached to neighbouring plant cell walls which would prevent hyphae from sliding past growing plant tissues (Christensen et al., 2008). In their study, the research team succeeded in imaging cross sections of *E. festucae* hyphae in ryegrass tissues using

transmission electron microscopy (TEM), which revealed that hyphae are apparently attached to plant cell walls (Figure 1.5) (Christensen et al., 2008). Attached hyphae occasionally appeared to be slightly flattened, and some instances showed distortion in septal angles and asymmetric hyphal morphology suggested hyphal strands were being subjected to stretching forces in the plant expansion zone (Figure 1.5AB) (Christensen et al., 2008). As the previously proposed growth models for endophyte hyphae had proven to be insufficient, these new findings suggested a radically different understanding of vegetative hyphal growth, one in which the expansion of the host plant cells exert mechanical stretch on hyphae and carry the attached endophyte hyphae upward as the plant grows, effectively enabling the hyphae to extend, like plant tissues, by intercalary growth (Christensen et al., 2008).

1.5.2. Intercalary Growth

According to botanical terminology "intercalary" refers to the process of an insertion being made in between new cells or compartments (Merriam-Webster Online Dictionary.). In the case of fungal growth, it defines a phenomenon where fungal hyphae elongate, and new compartments are created in between existing compartments (Christensen et al., 2008; Voisey, 2010). The intercalary growth model challenges the widely held belief that vegetative hyphal growth only occurs through apical expansion, which has been shown to be the case for most filamentous fungi (Christensen et al., 2002).

Evidence for intercalary growth in fungal vegetative hyphae (*E. festucae*) was first presented by Christensen et al., 2008. First, vegetative hyphal growth rate measurements were conducted on ryegrass leave infected with *E. festucae* expressing the Enhanced Green Fluorescent Protein (EGFP) (Christensen et al., 2008). For this, hyphal lengths between selected lateral branches were measured at different time points and and hyphae in the expansion zone of the leaf shown to increase in total length over time (Figure 1.6), indicative of intercalary extension of hyphae in the leaf expansion zone. In contrast, in the mature zone of the leaf, which is no longer growing, hyphal filaments did not increase in length, confirming that hyphal growth is synchronised with host growth. Measurement of compartment lengths in hyphae at the base of the (growing) leaf to the (mature) tip showed no consistent increase in compartment size suggesting that hyphal expansion was accompanied by compartment division (Figure 1.6A) (Christensen et al., 2008). These findings led the team to conclude that *E. festucae* hyphae might be performing intercalary growth by adding compartments through mitosis and cell growth in sub-apical sections, and increasing their length in the course of plant extension (Christensen et al., 2008). Next, they

identified the position and the attachment of hyphal strands adjacent to plant cells using TEM and scanning electron microscopy (SEM). TEM imaging of hyphal positions and attachment to the plant cell walls of *E. festucae* infected cross sections of ryegrass leaves revealed that *E. festucae* hyphae became flattened or compressed between the plant cells due to tight attachment of hypha to plant cell walls (Figure 1.5AB) (Christensen et al., 2008). The firm attachment of hypha to plant was also observed in slightly damaged hyphae in cross sections due to dissection of the tissue, where hyphae remained connected with the adjacent plant cell wall despite the physical manipulation (Figure 1.5) (Christensen et al., 2008). Another finding that reinforced the idea of hyphal intercalary growth was that appearance of hyphal cross sections, which rather than perfectly circular, were asymmetric suggestive of pulling forces on the hyphal cell wall by neighbouring plant cells (Christensen et al., 2008). The findings indicated that *E. festucae* hyphae were able to undergo intercalary growth simultaneously with the expanding host cells (Christensen et al., 2008; Voisey, 2010).

Figure 1.5 Intercalary growth of *E. festucae* Fl1 vegetative hyphae in ryegrass leaves. Figure reproduced from Christensen et al., 2008. a) Hyphal compartment lengths (µm) were measured starting from the expansion zone (boxed in c) to the tip of leaves. The median values and distribution of the compartment lengths are shown white boxes. Bars show the minimum and the maximum measurements and outlier measurements are shown by asterisk. b) Intercalary expansion of *E. festucae* vegetative hyphae observed in plant expansion zone and the leaf tip. c) A representative image of a ryegrass leaf, the expansion zone is shown in the box. d) Confocal microscopy images of *E. festucae* constitutively expressing EGFP on transcription elongation factor promoter (pTEF) in the expansion zone, images taken at 0 min and 190 min apart. e) Representative diagrams of hyphal images in d.

Another interesting result supporting the intercalary growth capacity of *E. festucae* came from ultrastructure analysis of hyphae using TEM to view cross sections of ryegrass leaves (Christensen et al., 2008). The images of hyphae revealed that cytoplasmic complexity changed depending on the localization of the endophyte within the plant. Cytoplasmic content of hyphae in mature leaf sections showed additional lipid complexes and crystalloid bodies compared to hyphae in younger leaf sections (Christensen et al., 2008). Although the exact function of crystalloid bodies is unknown, it is presumed to regulate osmolarity (Mehlhorn, 2015). Cell wall thickness was also different in young versus old hyphae. Young hyphae in the expansion zone had thinner cell walls compared to older hyphae in the mature zone that had thicker cell walls, indicating that the building of hyphal walls continued even though hyphal expansion had ceased (Christensen et al., 2008). The research team concluded that *E. festucae* hyphae aged in conjunction with the plant cells, further confirming that

intercalary growth of *E. festucae* hyphae took place along with plant growth (Christensen et al., 2008).

Intercalary growth (in the form of compartment expansion) in the *Coprinus cinereus* fruiting body has also been observed during stipe formation, the fungal structure that supports the mushroom cap (Hammad et al.,1993; Kües, 2000). This growth is described as independent of the apical extension of hyphae and occurs throughout all hyphal compartments, which explains the rapid elongation of the stipe (Kües, 2000). The reason behind the adoption of intercalary expansion is thought to be the need to build this structure within a short time period, which is why cell walls of the hyphae within the stipe possess a strong, yet plastic cell wall structure, enabling them to adapt to turgor pressure changes as they extend (Kües, 2000). This type of growth differs from *E. festucae* in that it occurs predominantly through cell expansion and is not associated with significant compartment division.

Vegetative intercalary growth has also been recorded in *Allomyces macrogynus* and was described as being dependent on the oxygen concentration in the environment, in which the aquatic fungus formed thin hyphae that only demonstrated apical extension in low oxygen concentrations (Gooday et al., 1975; Moore, 1995). In contrast, at atmospheric oxygen levels, hyphae extended by intercalary growth, by increasing cell wall synthesis and rapidly adding compartments to sub apical sections resulting in hyphae that were much thicker compared to hyphae growing at the tip (Youatt et al., 1988). The mechanism driving the intercalary growth processes in these species is still unclear.

1.6. Mechanical Stretching of *E. festucae* Hyphae

It has been proposed that a mechanical stretching force, applied by rapidly expanding plant cells on attached *E. festucae* hyphae, stimulates intercalary growth (Christensen et al., 2008). This hypothesis was tested by Sameera Ariyawansa, a former PhD student, who devised an apparatus and optimised the methodology to mimic, *in vitro*, the mechanical stretch imposed by the plant on hyphae. The mechanical stretching machinery was adapted from a wool stretcher and consists of two parts, a stretching cassette and a stretching apparatus (Figure 1.7) (Ariyawansa, 2015).

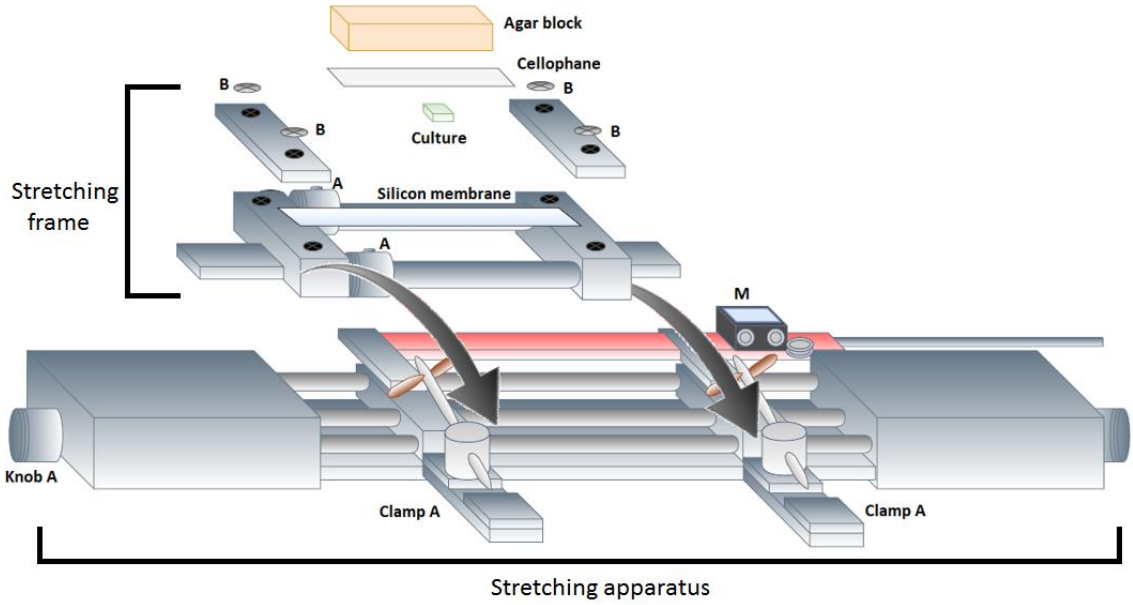

Figure 1.6 Stretching apparatus and the stretching frame used in the mechanical stretching experiments. The stretching frame is fitted on the apparatus and A clamps are turned to secure the frame. Once the frame is secure, Screws A are loosened to mobilize the stretching frame horizontally. Knob A is turned clockwise to stretch the stretching frame horizontally, which stretches silicon membrane fitted on the frame. Screws A are secured to stabilize the stretching frame and stop the silicon membrane from springing back, and the frame is released from A clamps. M: micrometer displays the amount of stretch applied to the frame in millimetres.

The endophyte culture is grown on the stretching cassette and then mounted on the stretching apparatus for mechanical stretching. The endophyte culture is grown on amino coated silicon membrane which provides attachment of hyphae to the membrane surface. On top of culture, a cellophane membrane and a PDA block is placed to provide nutrients during incubation and keep the culture from drying. When cultures are ready to stretch, the stretching cassette is mounted onto the stretching machine and the desired amount of horizontal stretching is applied, which can be tracked from the micrometre for precision (Figure 1.7). This methodology laid the groundwork for this project identifying many previously unknown aspects of *E. festucae* growth (Ariyawansa, 2015). The mechanical stretching experiments first revealed that *E. festucae* hyphae elongate proportionally to the amount of applied mechanical stretching, demonstrating the success of this methodology (Ariyawansa, 2015). When cultures are incubated after stretching, it was found that *E. festucae* hyphae not only elongate after stretching, but make new compartments in the sub apical sections, showing that they undergo intercalary growth in response to a mechanical stimulus (Ariyawansa, 2015). Further optimizations demonstrated that *E. festucae* cultures can be stretched up to 9 mm during the course of 9 h, each stretch applied in 3 mm every 3 h, almost mimicking the

growth rate of ryegrass which is presumed to be 1 cm a day (Voisey, 2010). Moreover, the compartment divisions in the stretched hyphae happened according to a hierarchy, in which longer compartments divided before the shorter compartments, suggesting a possible compartment length threshold for division (Ariyawansa, 2015). These results showed that mechanical stress is the driving force of intercalary growth in *E. festucae in vitro*.

1.7. Molecular Mechanisms that Govern Hyphal Growth in Fungi and Their Prospective Roles in Intercalary Growth of *Epichloë festucae*

Research toward understanding the regulation of hyphal growth in filamentous fungi has been focused mainly on revealing the molecular mechanisms behind polar hyphal growth, specifically the extension at the apex that requires constant delivery of essential components for rapid cell wall synthesis (Harris, 2006; Riquelme, 2013; Steinberg, 2007). To date, the functions of vital molecular mechanisms in hyphal growth such as cell wall synthesis and calcium ion channels, cytoskeletal protein activity and vesicle traffic have been studied in organisms such as *Aspergillus nidulans, Candida albicans, Neurospora crassa, Fusarium oxysporum* and *Ashbya gossypii* (Harris, 2006; Riquelme, 2013). The role of these molecular mechanisms or other pathways potentially involved in intercalary hyphal growth in *E. festucae* are still unknown.

1.7.1. Cell Wall Integrity Pathway and Sensing Mechanical Stress

The ability to adapt to rapidly changing environmental conditions is essential for the survival of organisms. Mechanisms to sense and respond to environmental cues via signal transduction pathways are widely conserved among eukaryotes. In *Saccharomyces cerevisiae*, signalling pathways that sense and act upon oxidative stress, thermal stress, osmotic stress, pH stress and mechanical stress have been identified (Hohmann & Mager, 2007). Sensing of mechanical stress in *S. cerevisiae* occurs through a number of type I transmembrane proteins Wscs 1-4, Mlt1 and Mid2 that activate the mitogen activated protein (MAP) kinase cascade, and signal the transcription of genes controlling the cell cycle and cell wall integrity (Figure 1.8) (Hohmann & Mager, 2007). When mechanical stress is exerted on the cell wall, Wsc1 activates the GTP/GDP exchange factor Rom2 with its cytoplasmic tail (Figure 1.8) (Becker et al., 2014; Verna et al., 1997). Rom2 interacts with guanine nucleotide-binding protein (GTPase protein) Rho1 to activate protein kinase C (Pkc1) (Heinisch et al., 2007; Verna et al., 1997). This leads to the activation of a mitogen activated protein kinase (MAPK) complex that includes MAP kinase kinase kinase (MAPKKK) Bck1, MAP kinase kinases

(MAPKK) Mkk1 and Mkk2, and MAP kinase MAPK Slt2. This series of kinases then stimulates the SCB Binding Factor (SBF) transcription factor complex, and Rlm1, also a transcription factor (Figure 1.8) (Jin et al., 2013; Levin et al, 2001).

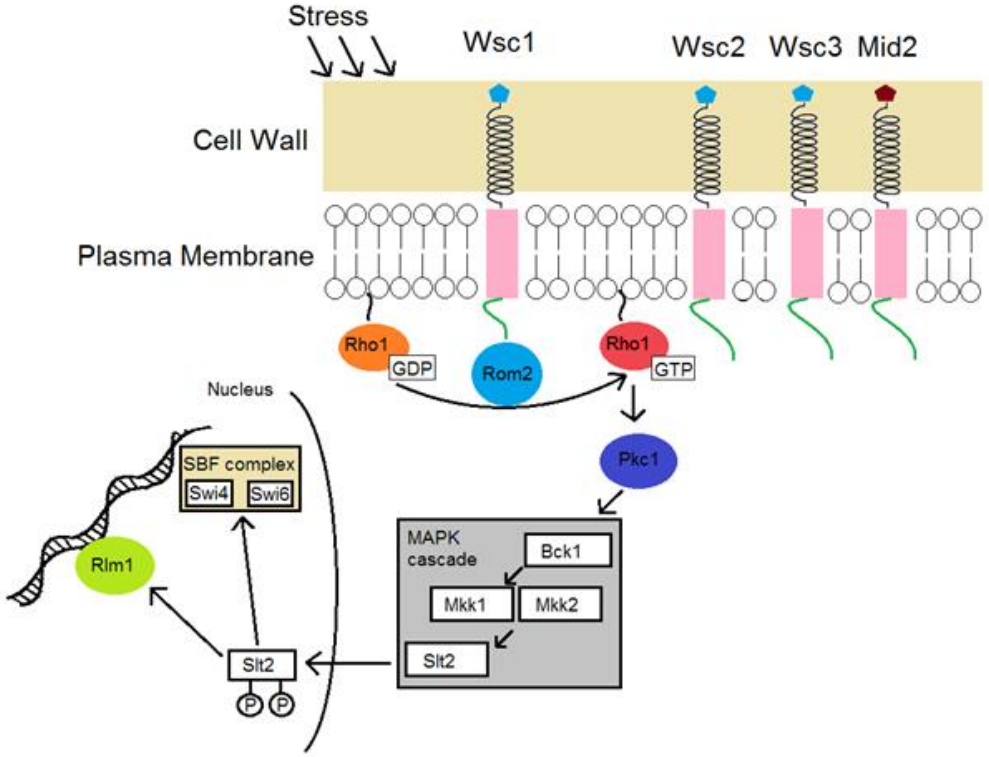

Figure 1.7 Cell Wall Integrity (CWI) signalling cascade in *S. cerevisiae*. Figure adapted from Kock et al., 2015.

1.7.1.1. The Structure of Mechanosensitive Proteins and their Mechanism of Action

In *S. cerevisiae*, there are currently four Wsc proteins identified as components of the CWI pathway (Verna et al., 1997). Among them, Wscs 1-3 are embedded in the plasma membrane, whereas Wsc4 is located on the endoplasmic reticulum membrane and is not considered to be a stress sensor protein on cell wall (Kock et al., 2015). The amino acid similarity between these proteins is 50%, and the most similar Wsc proteins are Wsc2 and Wsc3 with 61% sequence similarity (Verna et al., 1997). Domain layout analysis indicates that all of the *S. cerevisiae* Wsc proteins possess a cysteine rich domain (CRD) or wall stressor component (WSC), a serine/threonine rich region (STR), a transmembrane domain (TMD) and the cytoplasmic tail (Figure 1.9) (Verna et al., 1997). The WSC or CRD is also commonly referred to as the carbohydrate-binding domain, which is thought to be a site for glycosylation (Verna et al., 1997). The extracellular domains (WSC and STR) are thought to

be the stress sensors, whereas the TMD anchors the protein to the plasma membrane, and cytoplasmic tails is the signal conductor.

Figure 1.8 Type I transmembrane proteins of Cell Wall Integrity (CWI) in *S. cerevisiae*. Figure reproduced from Kock et al., 2015. Mxe: maximum possible extension. Cle: computed live-cell extension. PM: Plasma membrane.

The CRD, also referred to as the carbohydrate binding domain or wall stressor component (WSC), is thought to be the site for glycosylation (Verna et al., 1997). There are 8 cysteine residues that make up a conserved Wsc cysteine motif which is thought to be essential for interactions between this domain and cell wall components (Verna et al., 1997). Cysteine-rich motifs are found widely in receptor proteins, and because of their ability to interact with the glucans in the cell wall, WSC domains can be found in 80 different protein types in almost all organisms (Jendretzki et al., 2011). The adjacent extracellular domain, STR, is heavily *O*-mannosylated and provides rigidity to proteins upon glycosylation (Straede & Heinisch, 2007). The spring-like structure of the STR allows it to sense stress which alters the

localization of lipids and polysaccharides of the cell wall, and this tilt is conducted to the cytoplasmic tail and changes its conformation (Figure 1.10) (Jendretzki et al., 2011).

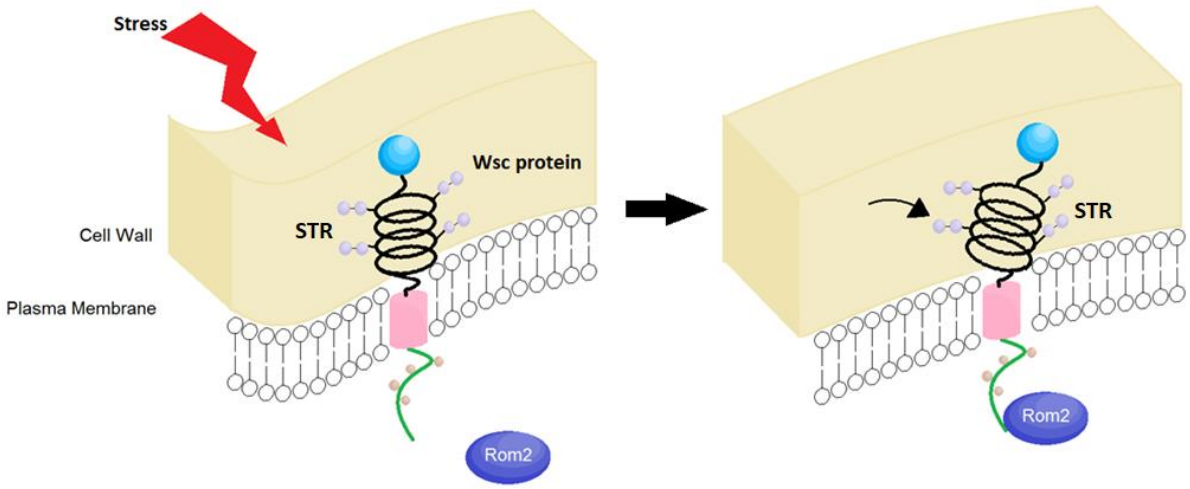

Figure 1.9 Conformational change in the serine/threonine rich (STR) region of a Wsc protein upon cell wall stress. Figure reproduced from Jendretzki et al., 2011.

The change in the conformation of the cytoplasmic tail is thought to trigger an interaction with Rom2 and initiate the MAPK cascade (Jendretzki et al., 2011). The length of the STR is variable among Wsc proteins with Wsc4 possessing the longest STR sequence (Verna et al., 1997). The TMD anchors the protein into the plasma membrane and attaches the extracellular regions to the cytoplasmic tail (Verna et al., 1997). The cytoplasmic tail also varies in length between Wsc proteins, again with Wsc4 possessing the longest cytoplasmic tail, and the highest divergence of amino acid sequence among Wsc proteins domains (Verna et al., 1997).

1.7.1.2. Cellular Localization and Distribution of Wsc Proteins

The cellular location of Wsc proteins was initially discovered in *S. cerevisiae* through transcriptional fusions to Green Fluorescent Protein (GFP). The Wsc1 and Wsc2 were found to be localized on the cell wall and distributed evenly throughout the periphery of the cell (Verna et al., 1997). Recent studies using Atomic Force Microscopy have demonstrated that *Sc*Wsc1 is distributed in the cell surface in patches that are approximately 200 nm in diameter (Heinisch et al., 2010). Heat shock and osmotic stress increased the size of the Wsc1 patches and their density, presenting another line of evidence that the CWI pathway is responsive to external stress factors (Heinisch et al., 2010). The localization and the clustering of the Wsc1 proteins on the cell was linked to the presence of functional WSC, specifically the conserved

cysteine motif, since the mutants lacking this motif failed to localize and form patches on the cell (Heinisch et al., 2010). It is proposed that upon stress on the cell wall, the WSC undergoes conformational changes that lead to sensor clustering in that region and formation of the "Wsc1 sensosome" that increases CWI signalling efficiency (Heinisch et al., 2010).

1.7.1.3. Functions of Wsc Proteins in Fungi

Functional analysis of *S. cerevisiae* Wsc proteins has demonstrated that they are crucial for maintaining the cell wall integrity against many stress factors, and also for the long term growth and survival of the organism. Deletion of *wsc1* in *S. cerevisiae* results in cell wall defects, temperature-specific growth defects and a degree of sensitivity to the phosphodiesterase inhibitor, caffeine (Verna et al., 1997). The *wsc1* mutant could grow on Yeast Peptone Dextrose (YPD) at 28˚C but not at 37˚C, suggesting that Wsc1 might be important in regulation of heat stress (Verna et al., 1997). The *wsc1* mutant also showed sensitivity staurosporine (Verna et al., 1997). Caffeine is a purine analogue that causes cell death via unknown mechanisms and staurosporine is a drug known to induce programmed cell death (Kuranda et al., 2006; Fernandes et al., 2011). Deletion of *wsc2* or *wsc3* alone, or together, did not cause phenotypic change compared to wild type, however when either of them were deleted in the *wsc1* mutant, it exacerbated the Δ*wsc1* phenotype, which suggested that Wsc proteins might be redundant in function (Verna et al., 1997). Although Δ*wsc2* did not display significant phenotypic differences, a growth competition assay using yeast extract peptone dextrose (YEPD) medium demonstrated that the fitness of Δ*wsc2* is reduced relative to wild type, indicating the important role Wsc2 plays in the growth of *S. cerevisiae* (Wilk et al., 2010). The double mutant *wsc1wsc2*Δ showed further temperature dependent growth defects, failed to grow on YPD media at 28˚C and had increased sensitivity to caffeine (Verna et al., 1997). Furthermore, both *wsc1wsc2*Δ and *wsc1wsc3*Δ showed sensitivity to the kinase inhibitor staurosporine (Verna et al., 1997;). The triple mutant *wsc1wsc2wsc3*Δ could only grow on Synthetic Complete (SC) media at 28˚C and showed severe glycogen accumulation defects and increased sensitivity to staurosporine (Table 1.1) (Verna et al., 1997). These results showed the crucial role of Wsc proteins and their functional redundancy in maintaining cell wall integrity during heat shock and exposure to cell wall perturbing agents in *S. cerevisiae* (Verna et al., 1997).

Table 1.1 Phenotypic changes caused by the *wsc* mutations. Table reproduced from Verna et al., 1997.

Genotype	Growth on YPD 28°C	Growth on YPD 37°C	Growth on SC 28°C	Growth on SC 37°C	Caffeine sensitivity SC 28°C	Staurosporine sensitivity SC 28°C
Wild type	+	+	+	+	-	-
wsc1Δ	+	-	+	+	-	-
wsc1wsc3Δ	+	-	+	-	+	±
wsc1wsc2Δ	-	-	+	-	+	±
wsc1wsc2wsc3Δ	-	-	+	-	+	+

The temperature dependent growth defects could be partially restored by exposing the *wsc1wsc2wsc3*Δ strain to higher temperatures gradually, however their tolerance to heat was still much reduced compared to WT, suggesting that Wsc proteins are important regulators of heat shock in *S. cerevisiae* (Verna et al., 1997). The redundancy between the Wsc proteins was then demonstrated by overexpressing each *wsc* gene in a double or triple mutant and observing the phenotypic changes (Verna et al., 1997). The reduced growth rate of *wsc1wsc3*Δ was successfully rescued by overexpression of *wsc1, wsc2* or *wsc3* (Verna et al., 1997). The growth defect resulting from a weak cell wall in Δ*wsc1wsc3* was also successfully restored by the overexpression of *wsc1* (Verna et al., 1997). This indicates that *Sc*Wsc 1-3 proteins could be redundant in function during growth and maintenance of cell wall integrity (Verna et al., 1997).

The CWI pathway is also crucial for biosynthesis and maintenance of the cell wall in other fungi. So far, CWI pathway proteins have been identified and functionally characterized in *A. fumigatus, C. albicans, N. crassa* and *Kluyveromyces lactis* (Dichtl et al, 2012; Norice et al., 2007; Maddi et al., 2012; Heinisch et al., 2008).

Using *S. cerevisiae* Wsc1-3 proteins as reference sequences, the *A. fumigatus* genome was searched for homologues (Dichtl et al, 2012). Candidate Wsc1-3 proteins contained a CRD in the N-terminal, followed by a single STR, TMH, and cytoplasmic tail domain (Dichtl et al, 2012). Only the Wsc2 candidate in *A. fumigatus* appeared to lack a cytoplasmic tail and possessed an incomplete TMH (Dichtl et al, 2012). The localization of GFP tagged Wsc1-3 proteins in *A. fumigatus* mostly accumulated in the cell wall and septa (Dichtl et al, 2012). Similar to what has been observed in *S. cerevisiae*, *A. fumigatus* Δ*wsc2* or Δ*wsc3* strains did not show a phenotypic change compared to wild type (Dichtl et al, 2012). In contrast, in *A. fumigatus* Δ*wsc1* radial growth rate was slightly decreased compared to wild type (Dichtl et al, 2012). In the double mutant Δ*wsc1*Δ*wsc3* radial growth decreased compared to Δ*wsc1*,

but deleting *wsc2* in Δ*wsc1* or in Δ*wsc1*Δ*wsc3* strains did not reduce the growth rate or affect the colony morphology beyond that of the Δ*wsc1*Δ*wsc3* double mutant (Dichtl et al, 2012). When *wsc1* was complemented in Δ*wsc1*Δ*wsc3,* the growth rate returned to wild type levels (Dichtl et al., 2012). Contrary to *S. cerevisiae wsc* mutants, none of the *A. fumigatus wsc* mutants (single, double or triple) were sensitive to cell wall perturbing agents such as calcofluor white (CW) and Congo red (CR), and these mutants were also resistant to heat shock, surviving in temperatures of up to 48˚C (Dichtl et al., 2012). *A. fumigatus* Δ*wsc1* was sensitive to the β-1,3 glucanase inhibitor, echinocandin (Caspofungin), but not to the azole group of antifungals, and deletion of *wsc2* or *wsc3* in *A. funigatus* Δ*wsc1* did not increase the sensitivity (Dichtl et al., 2012). These results showed that unlike *S. cerevisiae, A. fumigatus* Wsc proteins did not participate in heat stress regulation, however they were important in growth regulation (Dichtl et al., 2012).

The maintenance of the cell wall of milk yeast *K. lactis*, a close relative of *S. cerevisiae*, is also regulated by the CWI pathway (Heinisch et al., 2008). In the *K. lactis* genome, 2 genes encode proteins homologous to ScWsc protein sequences (Heinisch et al., 2008). One of the candidate proteins, *Kl*Wsc1, has 39% amino acid sequence identity with *Sc*Wsc1 (with), whereas the other candidate was similar to both *Sc*Wsc2 (with 35% amino acid sequence identity) and *Sc*Wsc3 (with 32% amino acid sequence identity), and is therefore referred to as *Kl*Wsc2/3 (Heinisch et al., 2008). The putative *Kl*Wsc1 protein possessed CRD, STR and TMH domains and a cytoplasmic tail, which are necessary components of Wsc proteins (Rodicio et al., 2008). However, putative *Kl*Wsc1 contained an extra 32 amino acids on the N terminal that prevents the automated annotation of this signal peptide region, and a shorter STR (35 amino acids less) and a longer cytoplasmic tail (39 amino acids more) compared to *Sc*Wsc1 (Rodicio et al., 2008). The putative *Kl*Wsc2/3 also possessed all the domains that are normally found in Wsc proteins, however its STR was nearly 70 amino acids shorter than the *Sc*Wsc2 and *Sc*Wsc3 (Rodicio et al., 2008). The localization of *Kl*Wsc1 and *Kl*Wsc2/3 were mostly distributed on the cell wall in patches (Rodicio et al., 2008). However, *Kl*Wsc1 distribution was more dynamic concentrating on the emerging buds during cell cycle, while *Kl*Wsc2/3 distribution was stable throughout (Heinisch et al., 2008). *Kl*Wsc1 localization was later observed to be concentrated on the bud necks and emerging buds of the cells undergoing cytokinesis, consistent with the previous observations made on the *Sc*Wsc1 localization (Verna et al., 1997; Heinisch et al., 2008). Deletion mutants of *Kl*Wsc1 or *Kl*Wsc2/3 did not show different phenotypes compared to wild type, however the *K. lactis* Δ*wsc2/3* strain

showed increased sensitivity to temperature, the cell wall perturbing agent CR, and also phosphodiesterase inhibitor caffeine compared to wild type and Δ*wsc1 K. lactis* (Heinisch et al., 2008). In a yeast complementation assay using *S. cerevisiae,* it was demonstrated that *K. lactis* Wsc2/3 could complement the defective phenotype of the *S. cerevisiae* Δ*wsc1*Δ*mid2* double mutant, which was chosen because of its severe CR and caffeine sensitivity, and heat sensitive growth pattern (Heinisch et al., 2008). Either *Kl*Wsc1 or *Kl*Wsc2/3 could rescue the caffeine and CW sensitivity and heat sensitive growth of *S. cerevisiae wsc1mid2* double mutant (Heinisch et al., 2008). However, overexpressing *Kl*Wsc1 in *S. cerevisiae* improved the cell wall sensitivity phenotype of the *S. cerevisiae wsc1mid2* strain (Heinisch et al., 2008). These findings indicate that *K. lactis* Wsc1 and 2/3 proteins are cell surface sensors that participate in regulating stress response, however distinctive roles for *Kl*Wsc1 and *Kl*Wsc2/3 in the CWI pathway have not yet been found (Heinisch et al., 2008).

In *N. crassa*, putative CWI pathway proteins were identified using a broader approach involving a large scale proteomics analysis on cell wall protein extracts, detecting the proteins with Glycosylphosphatidylinositol (GPI) anchors using liquid chromatography and mass spectrometry (LC-MS) and searching for homologues of CWI proteins in *N. crassa* genome using *S. cerevisiae, Schizosaccharmyces pombe, C. albicans* and *Aspergillus* spp. CWI pathway proteins sequences as reference (Maddi et al., 2012). Candidate CWI pathway proteins in *N. crassa* were searched in the single gene deletion library constructed within the *N. crassa* genome project, which limited the candidate list to 65 proteins (Maddi et al., 2012). The identified deletion mutants from the single deletion library were exposed to cell wall stresses such as heat shock, osmotic stress, pH, and cell wall perturbing agents, and 3 mutants showed distinctive phenotype changes under the different conditions, one of them being identified as putative *N. crassa* Δ*wsc1* (Maddi et al., 2012). *N. crassa* Wsc1 showed a similar domain layout to ScWsc1, and was also similar to *Sc*Wsc1-3 in terms of amino acid sequence. Although serine and threonine residues could be observed after the CRD, a distinct STR could not be annotated (Maddi et al., 2012). The highest sequence identity between *Nc*Wsc1 and *Sc*Wsc1 was observed in the cytoplasmic tail amino acid sequence, which is thought to initiate CWI signalling through Rho1 (Maddi et al., 2012). Bioinformatics analyses revealed another putative Wsc in *N. crassa*, named putative Wsc2 which showed the same domain layout, with a clearly annotated STR (Maddi et al., 2012). Functional analyses of *N. crassa* Δ*wsc1* showed significantly reduced radial growth rate, sensitivity to Caspofungin and CW, poor hyphae formation and an unability to form conidia compared to

wild type (Maddi et al., 2012). In contrast, the *N. crassa* Δ*wsc2* phenotype was similar to wild type, only showing a slight decrease in the growth rate (Maddi et al., 2012). The phenotypes of *N. crassa* Δ*wsc1* and *N. crassa* Δ*wsc1*Δ*wsc2* were similar, indicating that putative *Nc*Wsc1 was the main regulator of the cell wall stress sensing in CWI pathway (Maddi et al., 2012). No yeast complementation tests were conducted using putative *Ncwsc1* and *wsc2*, therefore their orthology to *S. cerevisiae* Wsc1 and Wsc2 could not be established for certain (Maddi et al., 2012).

In *C. albicans*, putative CWI pathway proteins were identified by a similar approach used for *N. crassa* putative CWI proteins identification, by creating homozygous insertion mutations in putative cell wall maintaining genes and selecting the mutants according to their phenotypes under cell wall stress (Norice et al., 2007). One of the mutants with deletion in putative CaWsc1, demonstrated sensitivity to Caspofungin and CR, and decreased biofilm formation (Norice et al., 2007). No localization or yeast complementation analysis has been carried out for CaWsc1, therefore its extensive role in CWI pathway is yet to be understood.

1.7.1.4. Functions of Wsc Proteins in *Epichloë festucae*

The Cell Wall Integrity (CWI) pathway is hypothesised to be important during intercalary growth of *E. festucae* , since mechanical strain (which induces intercalary growth) is expected to place stress on cell walls. Among the many proteins that participate in the *S. cerevisiae* CWI pathway, the Wsc1 protein has been shown in other species to play an important role in sensing mechanical stress on cell walls, due to its spring-like function (see Section 1.7.1.1).

A preliminary bioinformatics analysis and annotation of the Wsc1 and Wsc2 proteins in *E. festucae* has been carried out previously by Sameera Ariyawansa (Ariyawansa, 2015). Using *Sc*Wsc1 (also referred to as Slg1) (NP_014650.1), *Sc*Wsc2 (NP_014116.1), *Sc*Wsc3 (NP_014536.1), *Sc*Wsc4 (NP_011835.1) and *Af*Wsc1 (XP_751464.1) proteins sequences as references. Among the candidates obtained, *E. festucae* Wsc1 (referred to as WscA herein) with lowest E-value (3e-06) and highest amino acid identity (21%) to *Sc*Wsc1 was selected for further analysis (Ariyawansa, 2015). The *E. festucae wscA* gene encodes a predicted protein of 306 amino acids with a conserved WSC domain and a TMH domain, along with a signal peptide and a cytoplasmic tail (Ariyawansa, 2015). Functional analyses of *E. festucae wscA* deletion mutants showed they had substantially reduced colony radial growth rates and abnormal hyphal morphology compared to WT (Ariyawansa, 2015). The abnormal morphology of *E. festucae wscA* was rescued by sorbitol, which is an osmotic stabilizer,

suggesting defects in the cell wall of this mutant (Ariyawansa, 2015). The mutant showed increased sensitivity to CW compared to wild type, and addition of sorbitol in the medium rescued the sensitive morphology, further pointing to the defective cell wall in the mutant (Ariyawansa, 2015). To understand the colonization pattern of mutant and compare to colonization of WT, ryegrass seedlings were inoculated with *E. festucae* Δ*wsc* and WT (Ariyawansa, 2015). The plant colonization pattern of the mutant did not differ significantly from WT (Ariyawansa, 2015). This suggested a possible redundancy of function between *E. festucae* Wsc proteins (Ariyawansa, 2015), or alternatively that Wsc1 is not involved in sensing and/or stimulating intercalary growth *in planta*. In previous bioinformatics analyses, the presence of other putative Wsc or Wsc like proteins in *E. festucae* has been reported but not investigated to confirm their potential involvement in the CWI pathway (Ariyawansa, 2015).

1.7.2. Mechanosensitive Ion Channels and Regulation of Calcium Ions in Hyphae

The sensing of mechanical stimuli and activation of cellular responses is necessary for organisms to interact with their environment (Kocer, 2015). In fungi, mechanical impulse sensing is thought to be mediated by mechanosensitive ion channels, G protein coupled receptors (GPCR) and mechano-receptors that sense environmental stress and regulatedifferentiation and pathogenicity (Kumamoto, 2008). Among these sensors, mechanosensitive ion channels are another widely studied mechano-sensing mechanism, membrane proteins that are shown to mediate influx of ions in response to mechanical stimuli on the cell wall (Heinisch et al., 2011; Kocer, 2015; Kumamoto, 2008). In *S. cerevisiae*, the mechanosensitive ion channel encoding gene *mid1* is shown to regulate hyphal growth and mating via calcium influx through the associated channel Cch1 (Lew et al., 2011; Iida et al., 1994; Wang et al., 2012).

Calcium ions regulate many eukaryotic processes such as protein modification, apoptosis, cell cycle regulation and gene expression (Jackson et al., 1993; Regaladot, 1998). In *S. cerevisiae*, intracellular Ca^{2+} concentration is regulated by two different systems: the High Affinity Calcium Uptake System (HACS) and Low Affinity Calcium Influx System (LACS), in which the different ion channels take up different concentrations of Ca^{2+} ions according to environmental stimuli and the requirements of the organism (Verna et al., 1997; Zhang et al., 2014). Mechanical stretch-activated Mid1, voltage activated Cch1 and Ecm7 proteins are three Ca^{2+} uptake proteins identified as a part of the HACS, which function when

extracellular Ca^{2+} concentration is low (Figure 1.11) (Jin et al., 2013). Whereas in the LACS, the Fig1 protein is responsible for Ca^{2+} uptake from high extracellular Ca^{2+} concentration into low intracellular Ca^{2+} during mating and cell wall synthesis in *S. cerevisiae* (Cavinder & Trail, 2012).

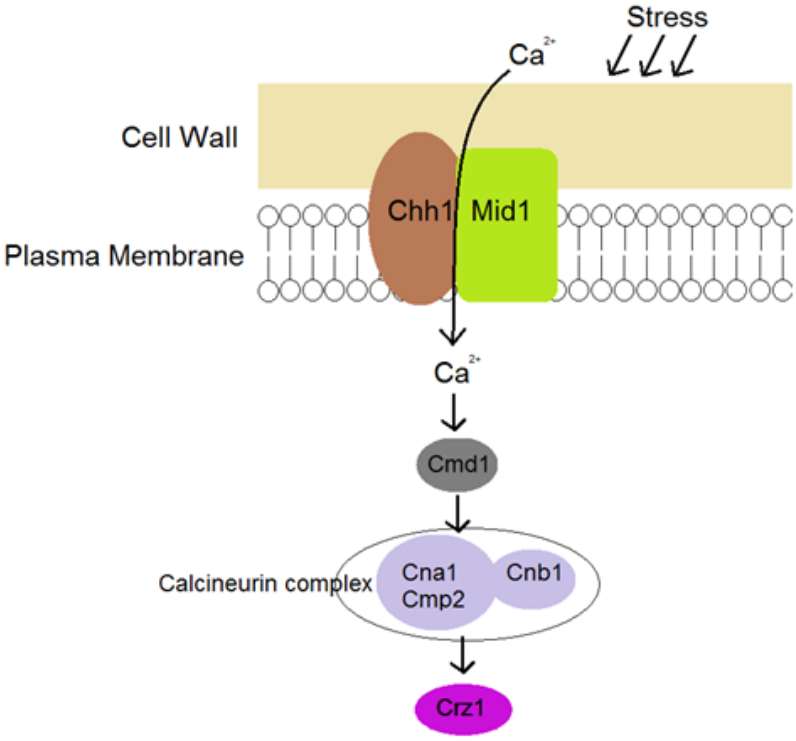

Figure 1.10 High Affinity Calcium Uptake System (HACS) in *S. cerevisiae*. Reproduced from Jin et al., 2013.

Homologues of Mid1 and Fig1 have been identified in several filamentous fungi including *A. nidulans* and *F. graminearum* (Brand et al., 2007; Cavinder et al., 2011; Lew et al., 2008; Zhang et al., 2014). The role of Mid1 in hyphal growth of filamentous fungi has been addressed in many studies and found to be important in tip growth, mediating a high cytosolic Ca^{2+} concentration at the hyphal tip (Steinberg, 2007).

1.7.2.1. The Structure of Mechanosensitive Ion Channel Protein and its Mechanism of Action

In *S. cerevisiae*, Mid1 is described as an *N*-glycosylated integral membrane protein that consists of four hydrophobic domains (H1- H4) in the N- terminus and two cysteine rich domains (C1 and C2) in the C- terminus (Figure 1.12) (Iida et al., 1994).

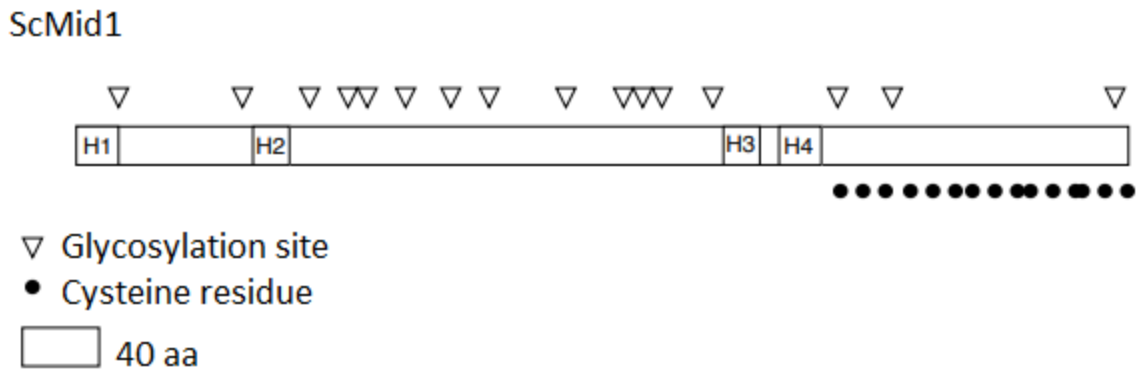

Figure 1.11 Domain layout of *S. cerevisiae* Mid1 protein reproduced from Sokabe et al., 2005. H1-H4: hydrophobic domains 1-4.

Mid1 shows very low similarity to either Cch1 or Ecm7 in terms of amino acid sequence or domain layout (Kanzaki et al., 1999). The C- terminus of Mid1 has been reported to be crucial for calcium uptake by *in vitro* site-directed mutagenesis of amino acid residues in this region (Maruoka et al., 2002). Another functionally important domain in Mid1 is the hydrophobic region in the N-terminus, the H2 domain. This was found to harbour a glycine residue that is crucial for the viability of *S. cerevisiae* cells (Maruoka et al., 2002). Previously, glycine residues in *S. cerevisiae* Cch1 have been reported to be highly conserved and important for the activity of the channel. Glycine residues in *Sc*Cch1 were changed to glutamine in the transmembrane linker domains of the protein and this resulted in complete loss of function (Iida et al., 2007).

1.7.2.2. Cellular Localization and Distribution of Mid1 Protein

Due to their mechanosensitive nature, stretch-activated ion channels are presumed to be localized on the plasma membrane where they can sense the mechanical stress applied on the cell and signal to downstream signalling pathways. In *S. cerevisiae*, localization of Mid1 was detected using polyclonal rabbit antibodies targeting the C- terminus of the protein via indirect immunofluorescence (Yoshimura et al., 2004). A *mid1* mutant was transformed with a plasmid harbouring multiple copies of *mid1* to overcome the detection difficulty arising from the low expression of Mid1 in wild type *S. cerevisiae* (Yoshimura et al., 2004). Mid1 was observed on the plasma membrane and the ER membrane of the complemented *mid1* mutant, whereas there was no fluorescence detected on control cells transformed with empty vector (Yoshimura et al., 2004). The same cells were treated with α-factor to see if Mid1 localization and distribution changed on the plasma membrane or ER membrane during rapid calcium uptake in mating (Yoshimura et al., 2004). α-Factor is a mating pheromone in

S. cerevisiae that is known to activate Mid1 to take up calcium during later stages of mating, specifically during plasma membrane and cell wall reorganization to accommodate the polarized growth of the cells (Iida et al., 1990) There was no significant difference in neither localization nor distribution of Mid1 during polarized growth of *S. cerevisiae* upon α-factor treatment (Yoshimura et al., 2004). Moreover, the amount of Mid1 did not change before and after α-factor treatments (Yoshimura et al., 2004).

A homolog of Mid1 has been characterized in *B. cinerea* and its cellular localization was determined by expressing a Mid1 GFP fusion in both the wild type and *mid1* mutant (Tudzynski et al., 2013). Unlike *S. cerevisiae*, Mid1 was found to be localized around nuclei (Tudzynski et al., 2013). Other Mid1 homologs in filamentous fungi have not been studied for their localization to date.

1.7.2.3. Function of Mid1 in Fungi

Mid1 has been functionally characterized in *S. cerevisiae* and in several filamentous fungi, and found to be crucial for maintenance of metabolism and growth due to the universal importance of calcium in many signalling pathways (Goldman et al., 2014).

When discovered in *S. cerevisiae*, *mid1* was named after the mating pheromone-induced death (MID) phenotype, since *mid1* mutants showed decreased viability after exposure to α-factor in the absence of calcium, and the phenotype was rescued when supplemented exclusively with calcium (Iida et al., 1994). Therefore, the mutation was speculated to be on a gene that was responsible of calcium uptake during polarized growth. The calcium uptake capacity of both wild type and mutants was tested using radioactively-labelled $CaCl_2$ and calcium uptake in *mid1* mutants was significantly reduced compared to wild type (Iida et al., 1994). Mating between *MAT*α and *MAT*a *mid1* mutants was also significantly impaired compared to wild type *MAT*α and *MAT*a strains, but again rescued with large concentrations of calcium in the medium (Iida et al., 1994). These findings showed the essential role of Mid1 in *S. cerevisiae* in calcium uptake and mating.

Homologs of *mid1* has been characterized in a number of filamentous fungi such as *A. fumigatus, C. purpurea, A. nidulans, C. albicans* and *G. zeae*. In *A. fumigatus*, the Mid1 homolog MidA was identified in the genome by identity to *S. cerevisiae mid1* and protein domain layout (Goldman et al., 2014). Compared to wild type, the *A. fumigatus midA* mutant demonstrated reduced radial growth which was partially rescued by supplemental $CaCl_2$ (25-200 mM) (Goldman et al., 2014). Compared to wild type, *Af*Δ*midA* was no more sensitive than wild type to CW or CR, osmotic stress from sorbitol or salt, high temperature, or

membrane perturbation from SDS (Goldman et al., 2014). Aside from these stressors, Δ*midA* was more sensitive to the oxidative stress inducer paraquat compared to wild type (Goldman et al., 2014). The amount of calcium taken up by cells on media containing $CaCl_2$ in the range of 25-200 mM was measured using a fluorescent dye (Fluo-3) and *Af*Δ*midA* had significantly lower intracellular calcium concentrations compared to wild type, the largest difference observed at 200 mM (Goldman et al., 2014). The virulence of Δ*midA* has also been compared to wild type using a murine model of invasive pulmonary aspergillosis (Goldman et al., 2014). The mortality rates of mice infected with *A. fumigatus* Δ*midA* was significantly reduced compared to wild type, along with reduced fungal biomass in the infected lungs and pulmonary epithelium (Goldman et al., 2014). These results point to the importance of MidA in *A. fumigatus* during *in vitro* vegetative growth, calcium uptake and virulence in a mouse model.

In *A. nidulans,* the Mid1 homolog MidA was identified and characterized in a similar way and found to be essential for conidiation, polarized hyphal growth and cell wall composition (Wang et al., 2012). *An*Δ*midA* formed smaller colonies compare to wild type on minimal or enriched media, and did not form any conidia on minimal media, contrary to wild type (Wang et al., 2012). Microscopic analysis of mutants showed that loss of *midA* function caused abnormal phialide and metulae formation in existing conidia, showing the importance of *AnmidA* in conidiation (Wang et al., 2012). As expected, the abnormal conidiation phenotype of Δ*midA* was successfully rescued by addition of extracellular $CaCl_2$ (Wang et al., 2012). To test whether the calcium uptake is dependent on HACS, calcineurin, a component of HACS was blocked by the FK506 calcineurin inhibitor in a minimal medium. The wild type and Δ*midA* could not sporulate on the medium containing FK506, and supplemental $CaCl_2$ did not rescue the non-sporulation phenotype in wild type, confirming the role of HACS in regulating conidiation (Wang et al., 2012). The Δ*midA* also failed to produce apically-dominant hyphae, and were hyper-branched and irregular in hyphal thickness (Wang et al., 2012). Furthermore CW staining showed that *An*Δ*midA* mutants had an uneven distribution of chitin along the hyphal cell wall, in contrast to the wild type which had an even chitin distribution, only increasing towards the hyphal tip (Wang et al., 2012). This suggested that MidA played a regulatory role in chitin distribution along the cell wall (Wang et al., 2012). The chitin and β-1, 3 glucan content of the cell wall in the Δ*midA* mutants was significantly increased compared to wild type, showing that the cell wall underwent a compositional change in the absence of MidA (Wang et al., 2012). Together, these findings suggest that

MidA plays a crucial regulatory role in conidiation, hyphal polarity and cell wall composition of *A. nidulans* (Wang et al., 2012).

Characterization of the Mid1 homolog in *B. cinerea,* a pathogenic plant fungus, showed that Mid1 apparently has a limited function in this organism (Tudzynski et al., 2013). Compared to wild type, no difference in either spore germination or virulence during plant infection was observed in Δ*mid1* (Tudzynski et al., 2013). When grown on axenic culture, Δ*mid1* showed significant growth reduction compared to wild type, however no difference in growth was observed in response to CR, CCW, SDS or antifungal agent fluconazole (Tudzynski et al., 2013). Fungal biomass in Δ*mid1* was reduced significantly compared to wild type and restored by addition of 50 mM extracellular $CaCl_2$ to the medium, indicating that *B. cinerea* Mid1 functions as a part of the HACS (Tudzynski et al., 2013). Additionally, presence of EGTA and BAPTA, both Ca^{2+} chelating agents, in the medium resulted in significant growth reduction and complete failure in growth of Δ*mid1* (Tudzynski et al., 2013). The cytosolic calcium concentration of wild type and Δ*mid1* was compared by expressing aequorin, a calcium activated photoprotein that has bioluminescence activity, and found that although Δ*mid1* showed decreased growth, the cytosolic calcium concentration did not differ from wild type (Tudzynski et al., 2013).

In *C. albicans*, a human pathogenic fungus, a Mid1 homolog has been identified and characterized as a part of the HACS and found that it had a regulatory role in hyphal polarization (Brand et al., 2007). The growth rate of *C. albicans* Δ*mid1* was reduced compared to wild type, and hyphal tropic growth was abnormal compared to wild type (Ganguly & Mitchell 2014). The tropic growth of hyphae was assessed by growing cultures on a special quartz slide with obstacles (Ganguly & Mitchell 2014). Upon coming to contact with the ridges, 60% of wild type hyphae changed the direction of growth, whereas only 30% of Δ*mid1* redirected their hyphal growth, indicating the role of Mid1 as a mechanically-activated channel in thigmotropic growth (Ganguly & Mitchell 2014). In *C. purpurea,* the *mid1* homolog has been characterized as a mechanically activated calcium channel and its role in regulating hyphal morphology, development and pathogenicity in host tissue has been shown (Tudzynski et al., 2009). The *mid1* homolog was replaced with phleomycin resistance cassette via homologous recombination (Tudzynski et al., 2009). The resulting Δ*mid1* showed reduced growth rate compared to wild type and could not be rescued with additional extracellular $CaCl_2$ (Tudzynski et al., 2009). Cell wall stressors CR and CW were used to test cell wall sensitivity, CW and both compounds reduced the growth rate of Δ*mid1* significantly

compared to wild type (Tudzynski et al., 2009). Moreover, confocal microscopy revealed that after incubation with CW, Δ*mid1* hyphae appeared to have irregular distribution of polysaccharides in cell wall and thickened septa compared to wild type (Tudzynski et al., 2009). To assess the role of Mid1 in pathogenicity, two tissue types of rye were infected with wild type or Δ*mid1*, using spores or a mycelia suspension (Tudzynski et al., 2009). In both rye florets and ovary tissues Δ*mid1* infection could not be established with either spores or mycelial suspension injections (Tudzynski et al., 2009). The tissues were imaged using scanning electron microscopy (SEM) and found that Δ*mid1* formed a hyperbranched hyphal accumulation resembling an appressorium, growing in multiple directions on the tissue surface but unable to colonize intercellular tissue (Tudzynski et al., 2009). These findings revealed that Mid1 regulates pathogenicity, *in vitro* hyphal growth and cell wall stress sensing in *C. purpurea* (Tudzynski et al., 2009).

In *G. zeae*, the Mid1 homolog has been characterized and found to play an important role in ascospore morphology and discharge, and growth rate (Cavinder et al., 2011). Compared to wild type, Δ*mid1* grew at a significantly slower rate on carrot agar and failed to grown on calcium-limited media that included 1 mM BAPTA, which was partially rescued by the addition of the extracellular Calcium Ionophore A23187 (Cavinder et al., 2011). Ascospores of Δ*mid1* mutants produced abnormal two-celled ascospores which were constricted in their central septum and sometimes split in two, whereas the wild type produced intact ascospores with four cells (Cavinder et al., 2011). Ascospore discharge in the wild type and Δ*mid1* was compared on agar and the mutants discharged significantly fewer ascospores compared to wild type. This was only partially restored by extracellular $CaCl_2$ (Cavinder et al.,2011). To understand the role of Mid1 in pathogenicity of *G. zeae*, wheat was inoculated with macroconidia of wild type or Δ*mid1*, however there was no difference in the infection rate or symptoms on kernels (Cavinder et al., 2011). The findings showed that Mid1 is involved in the regulation of ascospore discharge and morphology as well as vegetative growth in *G. zeae* but is not required for pathogenicity (Cavinder et al., 2011).

1.7.2.4. Function of Mid1 in *Epichloë festucae*

The High Affinity Calcium Uptake System (HACS) is potentially another important pathway for sensing mechanical stress in *E. festucae* and mediating intercalary growth, due to the fact that Mid1 is a mechanically-activated calcium channel that regulates hyphal growth and cell wall integrity in several other filamentous fungi.

In *E. festucae* , a Mid1 homolog has previously been annotated and functionally characterized to understand its role in regulating intercalary growth. For this, Mid1 protein sequences from *S. cerevisiae* (SGD ID- S000005235), *G. zeae* (ESU13681) and *C. purpurea* (CAU66903.1) were used as queries (31%, 46% and 66% identity scores, respectively) (Ariyawansa, 2015). *E. festucae* Mid1 was named MidA according to *E. festucae* gene nomenclature (Schardl 2012). *E. festucae midA* encodes a predicted protein of 638 amino acids that is recognized as a Mid1 family protein (IPR024338) by InterProScan (Ariyawansa, 2015). The domain layout of MidA consists of a signal peptide at the N-terminus, 4 hydrophobic regions (H1-H4) followed by nine *N*-glycosylation sites and a cysteine rich region including 10 conserved cysteine residues (Ariyawansa, 2015). Functional characterization of *E. festucae midA* has been carried out to understand its role in calcium uptake, hyphal growth and plant colonization (Ariyawansa, 2015). Using the split marker method, *midA* was replaced by a hygromycin resistance cassette (Ariyawansa, 2015). The resulting *Ef*Δ*midA* strains were assessed for growth rate on Potato Dextrose Agar (PDA) and radial colony growth rate was significantly reduced compared to wild type. The colony growth rate could be restored by the addition of 50 mM $CaCl_2$ to the medium (Ariyawansa, 2015). The presence of calcium chelating agent EGTA in the medium had a greater impact on Δ*midA* growth than the wild type, suggesting that MidA is required for calcium uptake (Ariyawansa, 2015). To understand the role of MidA in cell wall integrity, the cell wall perturbing agents CR and CW were added to media (0.1 and 0.15 mg/mL, and 0.25 and 0.5 mg/mL respectively). The addition of cell wall perturbing agents further reduced the growth rate of both wild type and mutants, mutants being affected more severely (Ariyawansa, 2015). The reduction in growth rate was restored by sorbitol which is an osmotic stabilizer, and also chemically complemented by extracellular $CaIC_2$ (Ariyawansa, 2015), which was likely taken up through the functional LAC system. To understand the role of MidA in plant colonization, *L. perenne* seedlings were inoculated using mycelial plugs of the wild type or Δ*midA* mutants expressing enhanced green fluorescent protein (EGFP), and colonization patterns were examined by confocal microscopy (Ariyawansa, 2015). Cross sections of meristems, tillers and leaves were colonized by the wild type as typically observed. This involved extensive colonisation of the basal grass shoot apex (primarily by hyphal tips) and then synchronous colonisation of developing leaves to produce the long straight hyphae that are characteristically found in the leaf expansion zone undergoing intercalary growth. In contrast, hyphae of the Δ*midA* mutants, while apparently able to fully colonise the shoot apex (by tip growth), were much

less abundant in developing and mature leaves, consistent with an inability to undergo intercalary growth (Ariyawansa, 2015). There was no difference in the phenotypes of plants infected with either the wild type or Δ*midA* strains (Ariyawansa, 2015). The role of *Ef*MidA in calcium uptake has been further evaluated by live imaging of cytoplasmic calcium in mutant and wild type *E. festucae* compartments in culture through confocal microscopy. This was achieved through the ectopic integration of plasmid GCaMP5 that expresses a calcium sensor protein consisting of fusion between a circular permuted green fluorescent protein (cpGFP) and calmodulin (CaM). The protein becomes fluorescent upon binding by calcium and enables the localisation periodicity of calcium to be visually recorded (Akerboom et al., 2012). Rapid calcium oscillations in growing *E. festucae* hyphal tips wereobserved, plus a lower amplitude oscillation in sub-apical sections (Ariyawansa, 2015). Addition of calcium chelating agent EGTA inhibited these pulses in the WT, suggesting that the influx of calcium is from external sources (Ariyawansa, 2015). In the Δ*midA* mutant, pulses were observed approximately every five min, indicating that an alternative calcium channel (possibly the LAC system) was also responsible for the calcium influx into hyphae (Ariyawansa, 2015). These findings point to the role of MidA in vegetative growth, cell wall integrity, plant colonization and calcium uptake in *E. festucae*.

Aims and Objectives

In this PhD project, three hypotheses were developed in order to expand on our understanding of the mechanisms used by *E. festucae* to perform intercalary growth by sensing mechanical stress.

Hypothesis 1: Intercalary growth and plant colonization in *E. festucae* is mediated through mechanical stretch sensor MidA, a regulator of the High Affinity Calcium Uptake System (HACS), and calcium uptake is required for cell wall expansion and hyphal compartmentalisation.

Hypothesis 2: Mechanical stretch stimulates a programme of gene expression in *E. festucae*, consistent with processes involved in primary metabolism immediately after stretching, and cell wall synthesis, growth and maintainance of hyphal integrity as a later response to mechanical stress.

Hypothesis 3: Mechanical stretch imposed on *E. festucae* by host cell expansion is also sensed through membrane-bound Wsc proteins that stimulate cell wall growth through the Cell Wall Integrity (CWI) signaling pathway.

Aim 1: To investigate the role of MidA in plant colonization as well as mechanical stretching.

Objectives:

a) Plant inoculation using *E. festucae* Δ*midA* to observe plant phenotype and hyphal biomass in order to determine the role of MidA during colonization of different tissue types.
b) Mechanical stretching of *E. festucae* Δ*midA* to investigate the role of MidA in cell wall plasticity and intercalary growth.

Aim 2: To identify immediate and later responses of *E. festucae* genes to mechanical stretching.

Objectives:

a) Mechanical stretching of *E. festucae* cultures to capture the immediate and later responses to mechanical stretch by RNA sequencing.
b) Annotation and analysis of differentially expressed genes to reveal the molecular mechanisms controlling responses to mechanical stretch.

Aim 3: To investigate homologs of mechanosensitive Wsc proteins, which are sensors of the Cell Wall Integrity (CWI) pathway, in *E. festucae* using bioinformatics tools.

Objectives:

a) Identify potential Wsc homologs in the *E. festucae* genome and conduct a phylogenetic analysis.

b) Functionally characterize an additional Wsc protein homolog in *E. festucae* and determine its role in culture.

2. Materials and Methods

2.1. Biological Materials and Strains

The founder strain used in this study was *Epichloe festucae* Fl1, originally isolated from *Festuca trachyphylla* (Leuchtmann et al., 2014) and provided by AgResearch, Palmerston North, New Zealand. A list of the other strains used, and their origins are given in Table 2.1. Seeds of *Lolium perenne* (accession number A11104), that were free from endophytes, were provided by AgResearch, Palmerston North, New Zealand. When not in use, seeds were kept at 4°C.

Table 2.1 Organisms used in this study.

Organism	Genotype	Source
***E. festucae* Fl1**	Wild type	AgResearch
***E. festucae* Δ*mid*-20**	Fl1/Δ*midA*::P*gpdA-hph*-T*trpC,* HygR	Ariyawansa, 2015
***E. festucae* Δ*mid*-36**	Fl1/Δ*midA*::P*gpdA-hph*-T*trpC,* HygR	Ariyawansa, 2015
***E. festucae* Δ*mid*-43**	Fl1/Δ*midA*::P*gpdA-hph*-T*trpC,* HygR	Ariyawansa, 2015
***E. festucae* Δ*mid*-comp-20**	Δ*midA/midA*::P*trpC-nptII*-T*trpC,* HygR, GenR	Ariyawansa, 2015
***E. festucae* Δ*mid*-comp-36**	Δ*midA/midA*::P*trpC-nptII*-T*trpC,* HygR, GenR	Ariyawansa, 2015
***E. festucae* pYH2A-6**	Fl1/P*gpd:hh2A:eyfp*:T*trpc*,HygR	Ariyawansa, 2015
***E. festucae* pYH2A-7**	Fl1/P*gpd:hh2A:eyfp*:T*trpc*,HygR	Ariyawansa, 2015
***E. festucae* pYH2A-9**	Fl1/P*gpd:hh2A:eyfp*:T*trpc*,HygR	Ariyawansa, 2015
***L. perenne* (Accession A11104)**	Wild type, cultivated variety "Samson"	AgResearch

2.2. Preparation of Media

All culture media were prepared using deionized water from the Milli-Q Integral Water Purification System (Merck Millipore, Darmstadt, Germany) and sterilised for 15 min at 121˚C. For Potato Dextrose Broth (PDB), 24 g of PDB (Difco™, USA) was dissolved in 1 L of water and sterilized. For Potato Dextose Agar (PDA), 39 g of PDA (Difco™) was dissolved in water and sterilized as described above. For PDA supplemented with calcium,

sterile 1 M $CaCl_2$ was added to sterile melted PDA to a desired final concentration prior to pouring into Petri dishes.

2.2.1. Culturing and Storage of Microbes

All culturing procedures were carried out using aseptic techniques in a Class II laminar flow cabinet. *E. festucae* Fl1 was grown on 2.4% (w/v) PDA, LePont De Claix, France). The *E. festucae* Δ*midA* strains were grown on PDA supplemented with 100 µg/mL of hygromycin B (Gibco®, USA). For long term storage of cultures at -80˚C, approximately 50 mg of the mycelia from 7-8 day old cultures grown on PDA were trimmed of excess media and homogenized in 1 ml of PDB. Then 500 µL of the homogenate was mixed with 500 µL of 60% (v/v) glycerol (99.5% AnalaR® grade, BDH, VWR International, Australia), and the mixture was stored at -80˚C. For revival of cultures from storage, 100 µL of the macerated mycelium were spread on a PDA plate supplemented with the appropriate antibiotic. The cultures were then incubated in a growth chamber at 22˚C under a 16 h light, 8 h dark cycle for 4-5 d. A 2 mm^2 plug from the edge of each freshly-grown colony was then transferred to a new PDA plate and the cultures were incubated as before.

2.3. Radial Colony Growth Measurement

For radial growth colony measurements, plugs of approximately 5 mm in diameter were taken from corresponding cultures using the back of sterile pipette tips. The plugs were placed on desired petri plates. For each *E. festucae* strain, three culture plugs were inoculated on each plate. Colony pictures were taken using Canon D500 DRLS digital camera and radial growth of the colonies was measured using Image J software. The measurement on each colony was repeated every five d for three times throughout the incubation, until the mycelia reached the edges of the medium plate. The diameter of the colonies were measured at four equidistant points in millimetres using a micrometre.

2.3.1. Determination of Colony Morphology

The colony morphology was first determined by examining the cultures under a dissecting microscope Olympus SZX12, equipped with Olympus DP20 digital camera. Then, a 1 mm^2 plug of culture was taken from the leading edge of the colony and placed on the microscope slide. Approximately 10 µL of sterile water was dropped on the culture plug, and a cover slip was gently placed onto the culture. The culture morphology was examined under an Olympus BX50 Epifluorescence light microscope using Olympus UPlanFL N 20X (20X/0.5NA,

∞/0.17/FN26.5) and 40X (40X/0.75NA, ∞/0.17/FN26.5) objective lenses, equipped with digital microscope camera Leica DFC3000 G (Leica Microsystems©). The images were captured and analysed using Leica Application Suite X (LAS X) software core offline version (Leica Microsystems©).

2.4. Genomic DNA Extraction and Storage

For high molecular weight genomic DNA extraction from endophytes, autoclave sterilized cellophane membranes (Waugh Rubber Bands, New Zealand) were sterilized for 15 min at 121˚C and placed onto PDA plates. Homogenates of the desired culture were prepared by removing 5 mm^2 from the leading edge of a freshly grown colony and disrupting it in 1 ml of PDB in a sterile 1.5 mL tube using an Omni Bead Ruptor-24 (Omni International), at 4 m/s for 15 s. Of the resulting homogenate, 250 µl was spread onto the cellophane membrane and the cultures were incubated at 22˚C as described in Section 2.2.1. Freshly grown cultures were then scraped from the cellophane using a sterile small metal spatula and weighed. Approximately 0.75-1 g wet weight of mycelium from each culture was crushed into a fine powder in liquid N_2 using a sterile mortar and a pestle. DNA was extracted using the Zymo Research Fungal/Bacterial DNA extraction kit according to the manufacturer's manual (Zymo Research Corporation, CA, USA). The quality and the quantity of genomic DNA was assessed using a NanoDrop 2000 UV-Vis Spectrophotometer. For more precise measurements and further confirmation of the DNA concentration, an Invitrogen Qubit Fluorometer (CA, USA) was used according to the manufacturer's instructions.

For high molecular weight genomic DNA extraction from plants, the plant tissues were ground in liquid N_2 and the DNA extraction was carried out using the Zymo Research Plant/Seed DNA extraction kit (Qiagen, USA), following the manufacturer's instructions. The DNA was quantified using the Qubit™ 4 Fluorometer (ThermoFisher Scientific).

2.5. PCR Amplification

Standard PCR was carried out using Platinum® Taq DNA Polymerase (InvitrogenTM). Reactions contained 5 µL of 10X PCR buffer (minus Mg^{2+}), 1.5 µL of $MgCl_2$ (50 mM), 0.6 µL of dNTP (25 mM), forward and reverse primers (10 µM each), genomic DNA (20 ng) or plasmid DNA (approximately 50 ng), 0.4 µL Platinum® Taq DNA polymerase (10 U/µL) and deionised water to complete the reaction volume to 50 µL. Cycle conditions were set to the following: 1 cycle at 94°C for 5 min, 29 cycles of 94°C for 30 sec, 54-58°C for 30 sec, 72°C for 1 min/1 kb. Final incubation temperature was 4°C.

For vector construction PCR, Platinum™ SuperFi™ PCR Master Mix (Thermo Fisher, USA) was used. This polymerase was preferred for its high fidelity and proof reading exonuclease activity to minimize errors during amplification of gene flanks for targeted deletion. Reactions were prepared in 25 /µL total volume which included 12.5 µL Platinum™ SuperFi™ PCR Master Mix, forward and reverse primers (10 µM each) and genomic DNA (5-50 ng) or plasmid DNA (1pg-10 ng). Cycle conditions were set to the following: 1 cycle at 98°C for 30 sec, 29 cycles of 98°C for 10 sec, 54-58°C for 30 sec, 72°C for 30 sec/1 kb. Final extension temperature was 72°C for 5 min. Final incubation temperature was 4°C. Positive and negative controls were used in each PCR reaction. The primers used in this study are given in the Appendix 3.

2.6. Agarose Gel Electrophoresis of Genomic DNA

Agarose gel electrophoresis was carried out in either 0.8% or 1% (w/v) agarose (UltraPure™, Invitrogen™) gels in Tris-Acetate-EDTA (TAE) (Tris base 40 mM, EDTA 1 mM, pH 8.0) buffer. DNA samples were mixed with 6X loading dye containing bromophenol blue (0.25%) and xylene cyanol (0.25%) (Appendix 2). DNA fragment size was estimated relative to the 1Kb plus DNA ladder (Invitrogen™, USA). The agarose gel was run for between 60 and 80 min at 80 to 90 volts. The DNA was stained with TAE buffer containing 0.5 µg/mL ethidium bromide (UltraPure™, Invitrogen™). The DNA was visualised under a UV light at 302 nm wavelength (Gel Doc™, Bio-Rad, CA, USA).

2.7. Mechanical Stretching of *Epichloë festucae* Hyphae

This novel technique to test the effects of mechanical strain on *Epichloë festucae* hyphae *in vitro* was developed and optimised by Sameera Ariyawansa (Ariyawansa, 2015) as described below.

2.7.1. Hyphal Stretching

The stretching machinery used in this study was adapted from a mechanism originally developed to observe the impact of physical stretch on wool fibres (unpublished). The concept involved growing *E. festucae* hyphae on a sterile amino-coated silicone membrane mounted on a stretching frame, and the culture was then subjected to a specific amount of mechanical strain at defined time points. Bright field and fluorescent microscopy techniques were used to capture images of the hyphae before and after each stretching period. The amount of stretching applied, the time interval between each stretch, and the best conditions

for *E. festucae* growth and attachment to the silicon membrane were optimised previously by Sameera Ariyawansa (Ariyawansa, 2015). In those experiments he was also able to show that the device stretched hyphae uniformly along their length, and that compartment length increased proportionally with the amount of stretch applied (Ariyawansa, 2015).

Where possible, hyphal stretching experiments were performed with *E. festucae* Fl1 strains transformed with pYH2A (Table 2.1) containing the yellow fluorescent protein (YFP) gene fused to the C terminus of histone protein H2A coding gene, driven by the *A. nidulans gpd* promoter (Rech et al, 2007). Since the H2A::YFP fusion protein localized to the nuclei, and *E. festucae* compartments are largely mono-nucleate, fluorescent nuclei were one of the criteria used to identify individual compartments.

The stretching experiments were conducted in a laminar flow cabinet using aseptic techniques. The stretching frame consists of two parts (Figure 2.1), one that clamps onto the silicon membrane using B Screws and the other that enables the stretching of the silicon membrane using A Screws.

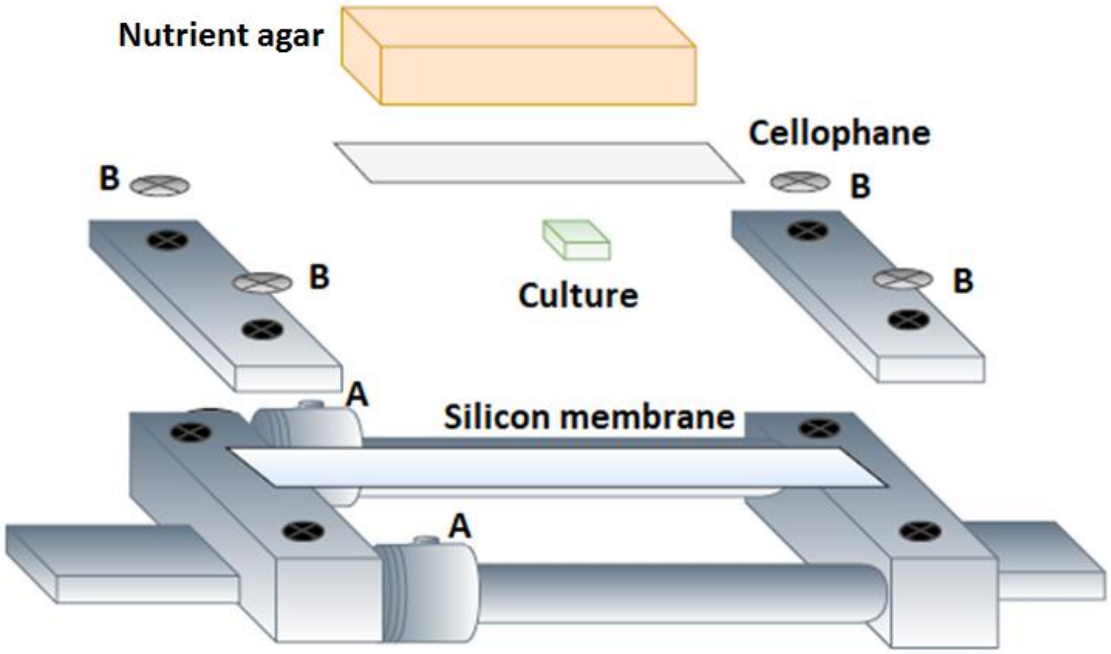

Figure 2.1 Stretcher frame used to grow and stretch the endophyte culture *in vitro*. Screws A clamp the silicon membrane on either side of the stretching frame and screws B are loosened to allow stretch to be applied to the membrane and then are tightened to retain the desired tension. The silicone membrane is amino coated to facilitate attachment of hyphae.

Sterile amino-coated silicon membranes (Flexercell, Burlington, USA, Silicon Membrane Amino Coated) were cut to 4.5 cm x 0.5 cm dimensions, the metal parts under Screw A were removed, and the membrane placed into the cavity using sterile forceps. The metal parts were then clamped onto the silicon membrane, and the B Screws firmly tightened. The silicon membrane was tightened lightly to create sufficient tension to enable the membrane to support the endophyte culture and the nutrient agar block without sagging, and A Screws were tightened to maintain the tension. A small square (approximately 1 mm^2) of mycelium from the edge of a freshly-grown culture of the desired *E. festucae* strain was cut using a sterile razor blade, the agar removed using sterile tweezers and the culture placed in the middle of the silicon membrane. Nutrition was provided by placing a block of PDB supplemented with 4% (w/v) agar on the culture with a sterile cellophane membrane between the culture and the agar block. The PDA was supplemented with $CaCl_2$ or other compounds as necessary. The agar block was cut to similar dimensions as the silicon membrane to prevent the membrane and the culture from drying out during the incubation. For stretching of *E. festucae* Δ*midA* and pYH2A strains, agar block was also supplemented with 100 µg/mL of hygromycin B to prevent contamination during manipulation of the stretching frame for the stretching procedures. For stretching experiments using *E. festucae* WT the hygromycin B in the agar block was omitted. The air bubbles between the silicon membrane and the agar block were eliminated by rolling a sterile glass rod gently over the agar block. Once assembled, the stretching frames were placed in a sterile plastic container and the box was wrapped in plastic wrap to prevent drying during incubation. The stretching frames in the plastic container were incubated in a growth chamber at 22˚C under a cycle of 16 h light and 8 h dark for 3 d. After the incubation, cultures with single, clearly visible, hyphae were selected for stretching experiments. For the stretching procedure, the stretching frames, prepared as described above, were placed into the frame stage (Figure 2.2).

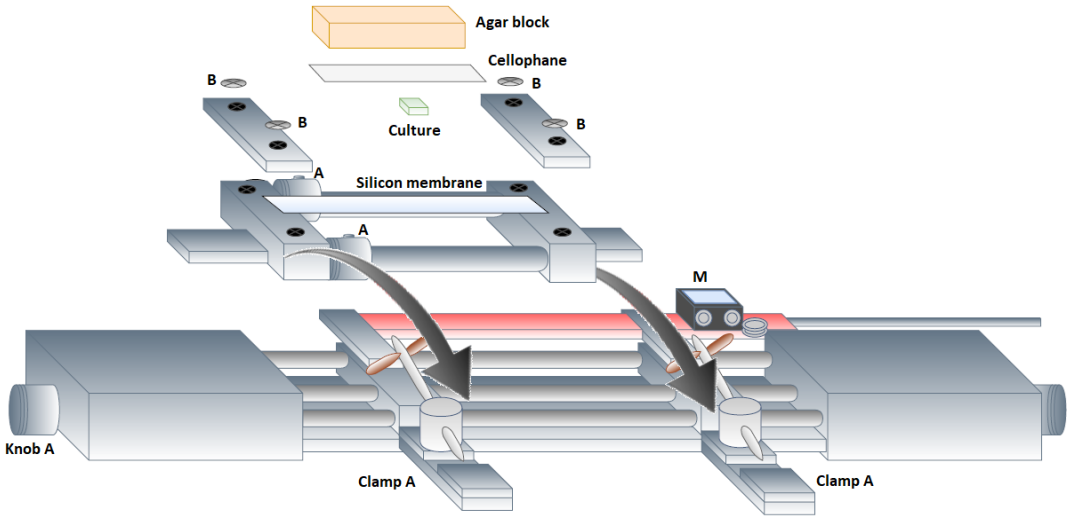

Figure 2.2 Stretching apparatus used to stretch the stretching frames. The stretching frame is fitted on the apparatus and A clamps are turned to secure the frame. Once the frame is secure, Screws A are loosened to mobilize the stretching frame horizontally. When Knob A is turned clockwise, the frame stretches the silicon membrane. Screws A are secured to stabilize the stretching frame and stop the silicon membrane from springing back, and the frame is released from A clamps. M: micrometer displays the amount of stretch applied to the frame in millimetres.

After setting the stretching frame into the apparatus, the stretching frame was tightly secured with Clamps A (Figure 2.2). In order to apply stretch, Screws B were loosened after the frame was tightly secured on the apparatus. The nutrient agar block was slowly lifted halfway to expose the culture using sterile forceps. This was done to ensure full delivery of mechanical stretch to hyphae, as the PDA block and cellophane can cling to hyphae and inhibit mechanical stretch. Knobs were turned clockwise to stretch the frame and the amount of stretch applied to the frame was tracked using the micrometer. Once the desired amount of stretch was applied, the agar block was slowly lowered onto the culture, and Screws B were tightened again to secure the silicon membrane. Clamps A were loosened to remove the frame from the apparatus so that it could be returned to the humidity chamber for continued incubation as described above.

Previous experimentation demonstrated that the optimal degree of stretching for *E. festucae* YH2A was 3 mm every 3 h, 3 times per day. In total, the 4.5 cm membrane was therefore subjected to 9 mm of stretch over 9 h. This is roughly equivalent with the growth rate of *L. perenne* leaves, which can grow at approximately 1 cm per day over the expansion zone (MacAdam et al., 1989). And it is estimated that an individual grass epidermal cell has the potential to elongate from 12-20 µm up to 100-1000 µm (Schnyder et al., 1990; Schäufele et

al., 2000). The candidate hyphae for tracking the course of mechanical stretching was selected according to few criteria. The hyphae were required to be individual and straight, as well as horizontally grown. The compartments up to 11th (excluding the first compartment, which is hyphal apex) were required to be visible for measurements before and after each stretch. The tracked hyphae were imaged using bright field and fluorescence microscopy. The locations of tracked hyphae were noted by the position on the stretching frame (ie left bottom of culture) and by comparing the visible frames to previously captured images. The control group did not receive any stretching; however their agar blocks were still lifted for experimental consistency.

In order to record the elasticity and growth of hyphae in the control and the treatment groups, the number of septa and nuclei in each hypha before and after each stretching period was recorded. The length of each compartment was also measured before and after each stretching procedure. At least three hyphae per strain were subjected to stretching for each control and treatment group. The increase in the number of compartments per 100 µm of hyphae from the first compartment behind the tip was recorded. The compartments were counted starting from the 2nd (compartment behind the apical tip) up to 11th towards culture centre. After the 11th, the compartments became difficult to visualize due to the hyphal density.

The numbers of septa and lengths of hyphal compartments were analysed and compared using unpaired t tests of the null hypothesis of no difference between control and stretched treatments, with two degrees of freedom.

2.8. Microscopy Techniques

Bright field and fluorescence imaging of *E. festucae* hyphae was conducted using an Olympus BX50 Epifluorescence light microscope using an Olympus UPlanFL N 40X objective lens, and equipped with a digital microscope camera (Leica DFC3000 G, Leica Microsystems©). The images were analyzed using Leica Application Suite (LAS) and ImageJ software. For fluorescence imaging, the U-MWG fluorescence cube was used to visualise YFP-tagged nuclei in hyphae of *E. festucae* pYH2a strain (Tale 2.1). UV light exposure to the endophyte was kept to a minimum during the fluorescence microscopy to prevent any damage to the cultures. The slide holder and specimen clips were removed from the microscope stage to accommodate the stretcher frames, with the specimen inverted and the silicon membrane closest to the objective lens (Figure 2.3).

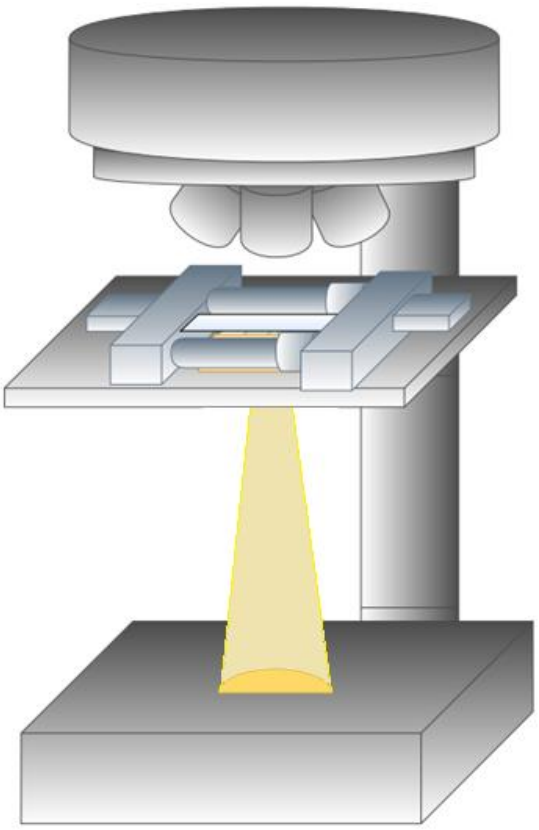

Figure 2.3 Positioning of the stretcher frame on the microscope stage. The specimen holder and clips were removed for easy manipulation of the frame during imaging (Ariyawansa, 2015).

2.9. Transcriptomics

Transcriptomics techniques were employed to identify the early and late gene responses in *E. festucae* hyphae to mechanical stress. For each technical replicate, the stretcher frames were divided into three treatment groups, each group harbouring six stretcher frames, therefore 18 stretcher frames were prepared in total for one technical replication. The frames were numbered and randomly assigned to a treatment to account for any structural differences that may have influenced the results. Each two stretcher frames in each treatment group were set up using three biological replicates, *E. festucae* pYH2a-6, 7, and 9 as described in the Section 2.7, separately. The incubation time was increased from 3 d to 4 d to yield more endophyte culture for tissue collection. The cultures in the control group did not receive any mechanical stretching to establish a basal gene expression profile for the endophyte, however their agar blocks were still lifted before the microscopy imaging to capture any impact of air exposure or mechanical disturbance in the transcriptome profile. The cultures in the early response group were subjected to mechanical stretching of 3 mm then their mycelia were harvested immediately and stored. The cultures in the late group were

also subjected to mechanical stretching of 3 mm but then incubated for 3 h at 22˚C prior to harvesting and storage. All the cultures were imaged before and after mechanical stretching to ensure the hyphae were correctly stretched by observing the hyphal positions (for early response) and new compartmentalization (in late response). The imaging was carried out using an Olympus BX50 Epifluorescence light microscope using an Olympus UPlanFL N 20X and 40X objective lens, equipped with a digital microscope camera (Leica DFC3000 G, Leica Microsystems©). Prior to tissue harvesting, nuclease-free sterile 1.5 mL tubes (Eppendorf, USA) were pre-cooled in liquid nitrogen. To ensure that the bulk of the sample used for the transcriptomics was obtained from horizontally-stretched hyphae, a vertical cut was made through the colony on either side of the centre and hyphae growing perpendicular to the axis of the stretch were excluded from the harvest (Figure 2.4). Liquid nitrogen was then poured directly onto the cut cultures on the silicon membrane, and snap frozen mycelia to the left and right of the cuts was scraped from the membrane into the pre-cooled tubes using a sterile scalpel blade. The cut samples were stored at -80˚C.

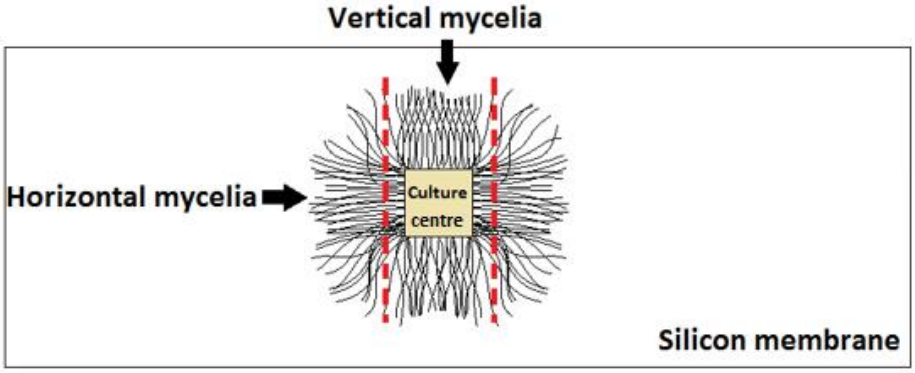

Figure 2.4 A representative diagram of the tissue collected from *E. festucae* cultures growing on a silicon membrane. The mechanical stretching is applied in horizontal direction. Red dotted lines show the incisions made to separate the horizontal mycelia from the rest of the culture. The mycelia remaining in vertical direction and the culture centre were discarded. Only mycelia from the left and the right of the incisions were taken for RNA extraction and transcriptomics.

To ensure sufficient mycelial yield for total RNA extraction, the 18 stretcher frame experiment was replicated 6 times (each on a different day) (Figure 2.5). For each *E. festucae* pYH2a strain, 2x18 frames were set up for three treatment groups (6x18 frames for all *E. festucae* pYH2a strains in total). In each technical replication, one treatment group consisted of cultures collected from 6 frames in total. To prevent potential differences in the gene expression profiles due to circadian rhythm changes, each cycle of 18 stretcher frames

was set up and processed within the same time limit each day throughout the course of the experiments.

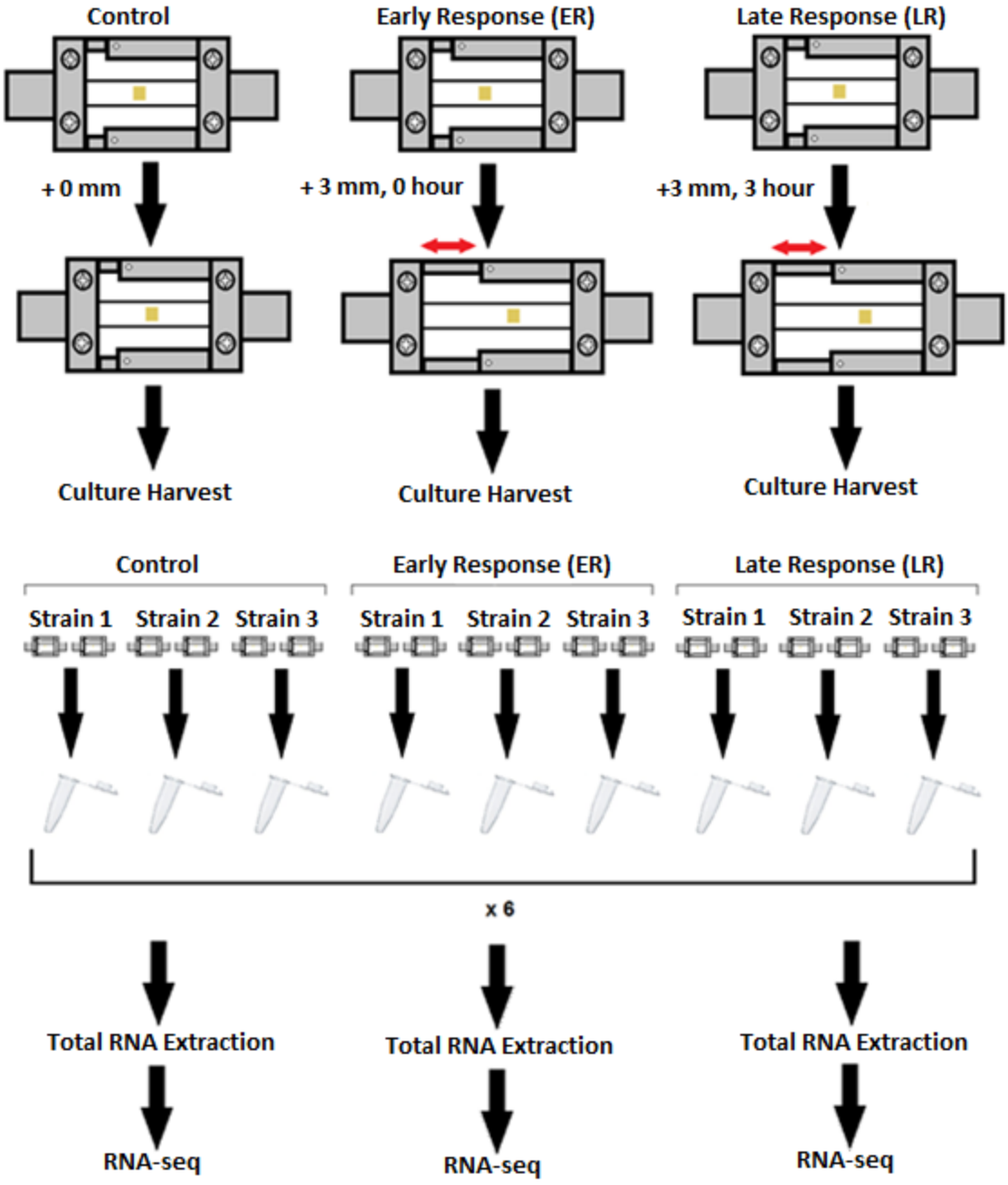

Figure 2.5 The strategy for sample pooling for total RNA extraction. The stretching frames were set up with silicone membrane and *E. festucae* cultures were inoculated on for 4 d. Mycelia from each two stretcher frames that were set up with each *E. festucae* pYH2a strain were subjected to treatment, collected in individual sterile tubes and stored for further steps after each cycle. Strain 1: *E. festucae* pYH2a-6, Strain 2: *E. festucae* pYH2a-7, Strain 3: *E. festucae* pYH2a-9.

2.10. Total RNA Extraction and Storage

Total RNA was extracted from the tissue samples in a ribonuclease (RNase)-deduced environment by wiping down the workplace using 3% (v/v) Trigene (Ceva Animal Health Pty Ltd, Australia), using RNase free reagents and filter pipette tips throughout the extraction process.

RNA from the collected mycelia was extracted using the Qiagen RNeasy® MinElute® Cleanup Kit (Qiagen, USA) according to the manufacturer's instructions. For each sample, 500 µL of TRIzol® Reagent (Thermo Fisher Scientific) was pre-heated in nuclease-free sterile 1.5 ml tubes (Thermo Fisher Scientific, USA) on a heat block at 40˚C for 5 min. The columns from the Qiagen RNeasy® MinElute® Cleanup Kit were taken out from 4˚C and pre-warmed to room temperature.

In order to prevent RNA degradation, the tubes that contained the mycelia were kept in liquid nitrogen. Approximately 200 µL of liquid nitrogen was poured into each tube to pre-cool the mycelia. The autoclave sterilized micro-pestles were cooled down similarly and mycelia were ground into a powder by hand. After the samples were ground, 500 µL of TRIzol® Reagent was added to each tube and the samples mixed thoroughly. The mixed samples were incubated at room temperature for between 5 to 10 min. The samples were then incubated at -20˚C overnight.

After the incubation, the RNA extraction was carried out according to manufacturer's protocol. The quality and quantity of the RNA samples (1.5 µL) were initially assessed using the NanoDrop 2000 UV-Vis Spectrophotometer. The RNA samples were then stored at -80˚C for further experiments. The samples with 2.0≥260/280 ratio were considered as sufficiently pure RNA for RNA Integrity Number (RIN) analysis.

2.10.1. Analysis of RNA Integrity

The RNA integrity number (RIN) of the total RNA samples was analysed using the Agilent 2100 Bioanalyzer (Agilent Technologies©, USA) by the Massey University Genome Service (MGS), Palmerston North, New Zealand. For each sample, 5 µL of total RNA was loaded onto the RNA 6000 Nano LabChip (Agilent Technologies©, USA) according to manufacturer's instructions. The RIN for each total RNA samples was interpreted using Agilent 2100 Expert Software (Agilent Technologies©, USA). Those samples with RIN≥8 were considered suitable for sequencing.

2.10.2. RNA Sequencing

Library preparation and sequencing of total RNA samples were carried out by the Beijing Genomics Institute (BGI Tech Solutions Hong Kong Co., Ltd.). Strand specific libraries were constructed using the Illumina TruSeq Stranded Total RNA Library Prep Kit (Illumina©). The sequencing was carried out on an Illumina HiSeq4000 PE101 system using two lanes (Illumina, USA). For each treatment group, three bulked biological replicates were sequenced (see Section 2.9).

2.10.3. RNA Sequencing Data Analysis Pipeline

Data analysis was conducted by Paul Maclean (AgResearch, Palmerston North, New Zealand). The quality of the reads was determined using FastQC (Anders, 2014). Low quality ($q < 20$) regions and sequencing artefacts were removed using FlexBar (Dodt, 2012).

The adapter sequences were trimmed from the 100 bp reads using Flexbar 2.7 algorithm (Dodt et al, 2012). The trimmed reads were mapped against the *E. festucae* Fl1 genome found on Kentucky University Genome Database using STAR (Dobin, 2013), which also enumerated the read pairs at the gene level (http://www.endophyte.uky.edu/, *E. festucae* FL1, 2011-03-01 assembly, version 2). Differential expression of the read pair counts for each gene was calculated between all three treatments using DEGseq (Wang et al., 2010). Annotation of the gene products was processed using BLAST (Camacho, 2009), InterProScan (Jones, 2014) and the Massey *Epichloë* Database (Cox and DuPont, 2017). Gene ontology assignment and significance testing was performed using Blast2GO (Conesa, 2005).

2.11. Statistical Analysis

Minitab 17 statistical analysis tool was used to determine the she statistical significant difference ($p<0.05$) between two or more groups using the student's t-test or one way analysis of variance (ANOVA).

2.12. Bioinformatics Analysis and Annotation of *E. festucae wsc* Genes

Saccharomyces cerevisiae Wsc protein sequences were retrieved from the SGD (*Saccharomyces* Genome Database, http://www.yeastgenome.org/). Functionally characterized and uncharacterized Wsc protein sequences from other fungi were retrieved from the JGI MycoCosm database (Joint Genome Institute Fungal Genomic Resource, http://genome.jgi.doe.gov/). Putative *E. festucae* Wsc protein sequences were obtained from

the Massey University *Epichloë* Database using the Blastx (Basic Local Alignment Search Tool) algorithm (Eaton et al., 2014). The translation and annotation of candidate *wsc1* genes in *E. festucae* were obtained from the Gbrowse tool in http://www.endophyte.uky.edu/, *E. festucae* Fl1, 2011-03 assembly, version 2 using MAKER and FGeneSH gene and protein prediction algorithms of this database (Schardl et al., 2013). Protein domains were predicted by Dr Pierre-Yves Dupont using the InterProScan domain analysis tool (Zdobnov et al., 2001) with the Geneious InterProScan extension (Quevillon et al., 2005).

Wsc protein sequences were aligned using the MAFFT E-NS-i alignment algorithm (Katoh et al., 2002) on Geneious (Biomatters©). For alignment of a small group of amino acid sequences (28 sequences), phylogenetic trees were constructed using the Maximum Likelihood method (PhyML software) with 1000 Bootstrap replicates (Guindon et al., 2010). The Generalized Time Reversible (GTR)+I(Inversion)+G (Gamma) protein evolution model was used in the PhyML software to estimate the probability of changes between the amino acids (Lanave et al., 1984). The best evolution model was predicted by the ProtTest algorithm (Abascal et al., 2005).

2.13. Deletion of *wsc* Genes in *E. festucae*

E. festucae genes were deleted by targeted gene replacement using the split marker method (Fairhead et al., 1996, Rahnama et al, 2017). This was done based on the homologous recombination technique using MultiSite Gateway® technology (Invitrogen) by constructing vectors that are able to replace the entire coding region of the targeted gene. For this, 3' and 5' flanking sequences of the target gene were amplified using Platinum™ SuperFi™ PCR Master Mix (Thermo Fisher, USA) via PCR as described in Section 2.5. These PCR products were then purified and cloned into donor plasmids pDONR-SMR and pDONR-SML (Invitrogen™) using BP clonase. Competent *E. coli* cells (Invitrogen One Shot® TOP10) were transformed using these constructs. Plasmids isolated from *E. coli* were screened using PCR to confirm the correct sizes of cloned products. Confirmed vectors were later transformed into *E. festucae* Fl1 protoplasts (Fairhead et al., 1996, Rahnama et al, 2017).

2.14. Inoculation of Ryegrass Seedlings

L. perenne seeds (accession number A11104) were sourced from Margo Forde Germplasm Centre, AgResearch Grasslands. They were stored at 0°C and 30% humidity for optimal seed viability prior to use. Approximately 2 grams of seeds were surface sterilized by immersion in 30 ml of 50% (v/v) sulphuric acid (BDH ARISTAR® PLUS, VWR International, England) for 15 min and washing with sterile water at least three times. Next, the seeds were immersed in 30 ml of 10% (v/v) domestic bleach (Janola, NaOCl≤10%before dilution) for a further 15 min and washed again with sterile water three times. Washed seeds were air-dried on sterile Whatman papers placed in petri dish for 3 h to overnight inside a laminar flow hood.

Surface sterilized seeds were grown upright in the dark on 4% (w/v) water agar for one week as the seedlings start to germinate after first week and do not require light for photosynthesis. For this, 10 seeds per plates were planted to face the same direction, also to enable downwards root growth and upwards seedling growth. The petri dishes were placed perpendicular to the surface. *E. festucae* colonies were first cultured for 4 d on PDA without antifungal supplementation. Presence of antifungals in the inoculated endophyte cultures inhibit successful infection. Approximately 25 seedlings per stain were inoculated *in situ* by insertion of a trace amount of fungal hyphae from the leading edge of the colony into a small incision in the shoot apex using sterile scalpel blades according to the method of Latch and Christensen (1985). After inoculation the seedlings were incubated upright for one week at 22°C in the dark followed by another week at 22°C under 16 h light. Seedlings were then transplanted into soil using standard potting mixture and standard pots (7.5 x 10 cm) and grown for a further 8 wks in PC2 glasshouse conditions. Plants were screened for endophyte infection when seedlings were approximately 7 wks old (6 wks post infection) (see below).

2.15. Detection of Endophyte in Plants via Tissue Print Immunoassay

Endophyte infection in plants was confirmed by tissue print immunoassay as described by Hahn et al (2003). Tillers were cut from the crown of the plants and the dead tissue was removed. Plants that had previously been confirmed to be endophyte positive were used as positive controls, and plants that had been confirmed to be free of endophytes were used as negative controls. The cut ends of tillers were pressed onto a nitrocellulose membrane (Thermo Fisher, USA) and the membrane was soaked in 0.5% (w/v) non-fat milk powder (Anchor, New Zealand) dissolved in blocking solution (20 mM Tris (hydroxymethyl)

methylamine, 50 mM NaCl) for at least 1 h at room temperature on orbital shaker (Total Lab Systems, New Zealand) at 60 rpm. After blocking, membranes were rinsed with the blocking solution three times and then incubated in fresh blocking solution containing Endophyte specific rabbit polyclonal primary antibody (1:1000 dilution) in room temperature overnight with shaking as before. The membranes were rinsed with blocking solution three times the next day and incubated in fresh blocking solution containing goat anti-rabbit IgG-AP secondary antibody (Santa Cruz Biotechnology, USA) in room temperature for 4 h on a shaker. The membranes were washed with blocking solution to wash off excess antibodies and soaked in a chromogenic development solution (20 mM Tris (hydroxymethyl) methylamine, 0.1% napthol as-mx phosphate, 0.1% Fast Red, pH 8.2) for 15 min in room temperature on an orbital shaker at 60 rpm. Once the development was sufficient, the membrane was rinsed in RO water to halt the chromogenic reaction.

2.16. Evaluation of Plant Morphology

The infected plants at 10 wks post inoculation were evaluated for the phenotypes of infection rate, number of tillers and tiller lengths. The number of tillers on each plant were counted. The 3 longest tillers from each plant were measured using a ruler. One way ANOVA was done using R Software (R Core Team, 2013) to compare tiller numbers and lengths of *E. festucae* WT to Δ*midA* and complement infected plants. A natural log transformation was used to meet the ANOVA assumptions of normality and homogeneity.

2.17. Plant Tissue Collection

For hyphal biomass analysis, nine tillers per plant were harvested from three plants per inoculated strain at 10 wks after inoculation. The harvested tillers were divided into two tissue types, the SA concentrated tissue and the leaf blade/leaf sheath tissue surrounding and above the SA. To do this, a 5 mm section was cut from the ryegrass pseudostem with the lowest cut made below the shoot apex through the stem immediately above the adventitious roots of the tiller base. (Figure 2.6).

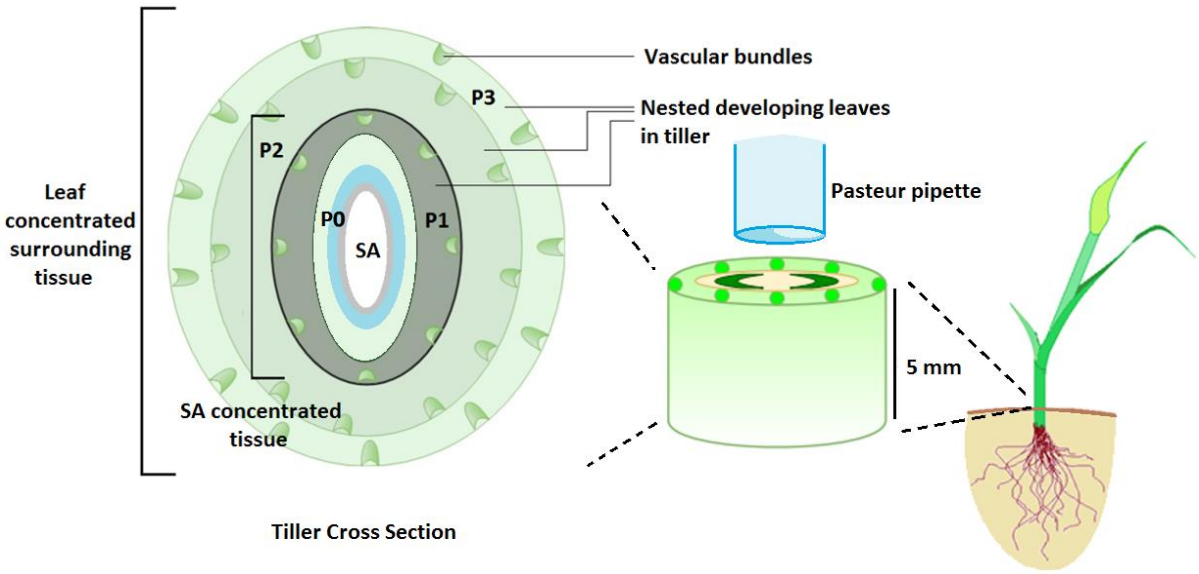

Figure 2.6 Schematic representation of plant tissue dissection for hyphal biomass analysis. SA: shoot apical. M: Meristem. P0 through P3 represents each emerging leaf encircling meristem.

Shoot apex enriched tissues were taken from the section as a core through the centre of the pseudostem using the tip of a sterile glass Pasteur pipette (Figure 2.6). The pipette tip containing the SA-enriched tissue was broken off using the back of a scalpel and immediately frozen in liquid nitrogen. The remaining tissues, comprised of developing blades and developing and mature leaf sheaths, was snap frozen in liquid nitrogen separately. For each plant, nine tillers were harvested and from these three SA and three pseudostem tissues were pooled due to small size of the tissues. For each biological replicate three technical replicates were carried out as shown in Figure 2.7.

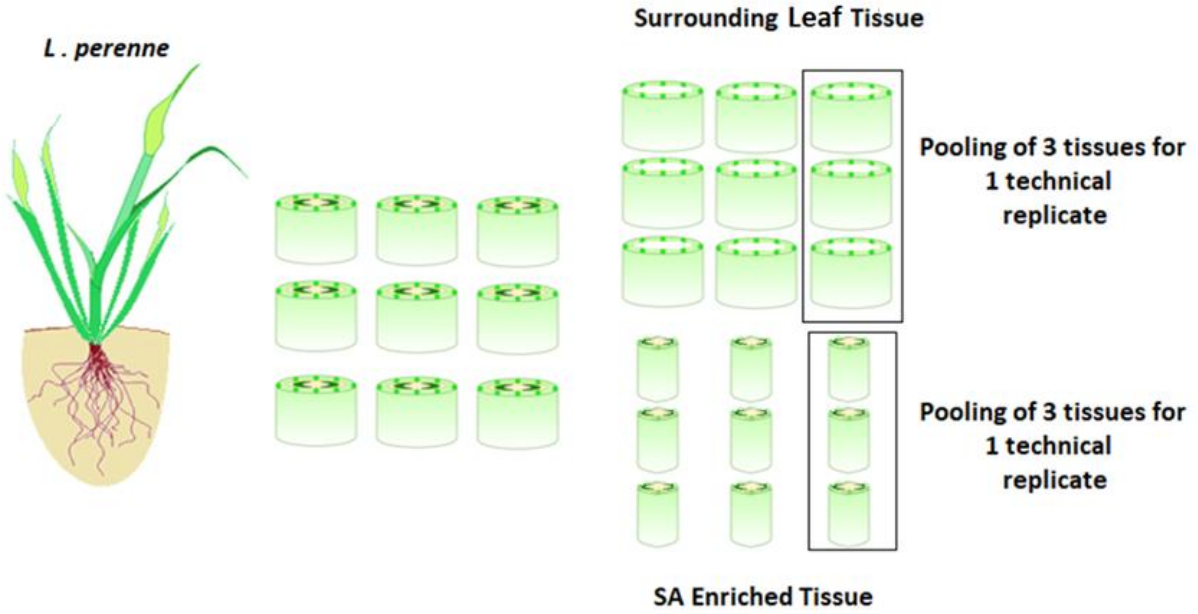

Figure 2.7 Schematic representation of technical replication and pooling of shoot apical (SA) enriched and surrounding mature tissue samples after plant tissue dissection for hyphal biomass analysis. This procedure was carried out for three biological replicates separately.

2.18. Hyphal Biomass Analysis using qPCR

For hyphal biomass analysis, genomic DNA (gDNA) from *E. festucae* Fl1 and uninfected wild type *L. perenne* was extracted as described in Section 2.17 and used to generate standard curves for endophyte and plant with concentration ranges of 0.00032-25 ng/ul and 0.000256-20 ng/µl, respectively. For endophyte, primers amplified a 153 bp sequence of an endophyte-specific non-ribosomal peptide synthetase-1 (*NRPS*-1) gene (NRPS-1F: gtccgatcattccaagctcgtt, NRPS-1R: tggtgggaagttccctgcac), and the plant primers (Lp-EF1a-RT-F2/3: caccacgagtctatgct, Lp-EF1a-RT-R2: gacctgggcaacaaagc) amplified a 74 bp sequence from the elongation factor-1 alpha (*EF*-1) gene (Rasmussen 2007, Zhou, 2010). Amplifications were processed in Lightcycler 480 (Roche) using KAPA SYBR® FAST qPCR Master Mix (2X) Kit (Kapa Biosystems©) in 10 µl reactions consisting of 2 µl DNA, and 8 µl of Master Mix containing 50 nM of each corresponding primer pairs. For each biological replicate, three technical replicates were processed. Standard curves were created using the logarithmic values of eight time serial dilutions of plant and endophyte gDNA against the cycle threshold (Ct) values, which is the first cycle that fluorescence can be detected from the background. The data were analyzed using One Way ANOVA, with Fisher's Least Significant Difference used to compare individual hyphal biomass percentages.

3. The Requirement for Calcium in Host Colonisation and Intercalary Growth in *E. festucae*

3.1. The Role of MidA in Plant Colonization by *E. festucae*

Mechanosensitive ion channels are crucial for organisms to sense mechanical stimuli and respond to their environment by regulating the influx of ions accordingly (Kocer, 2015). Mid1 in *S. cerevisiae*, and its homologs in several filamentous fungi, have been shown to regulate intracellular Ca^{2+} concentrations and thus to regulate various metabolic activities such as mating, vegetative hyphal growth and sometimes pathogenicity (Iida et al., 1994, Wang et al., 2012, Tudzynski et al., 2009 & 2013). In *E. festucae*, a Mid1 homolog, MidA, has been functionally characterized and found to play a role in regulation of vegetative growth, cell wall integrity, plant colonization and calcium uptake (Ariyawansa, 2015).

The ability of *E. festucae* Δ*midA* mutants to colonize different ryegrass tissues such as the meristem and leaves of infected tillers was also investigated in Δ*midA* mutants expressing enhanced green fluorescent protein (EGFP) (Ariyawansa, 2015). Compared to the WT, cross sections of tillers infected with *E. festucae* Δ*midA* showed normal colonization in meristems but reduced colonization in young leaves (i.e. the intercalary growth zone), in which hyphal density appeared to be substantially reduced (Ariyawansa, 2015). However, hyphal biomass, infection frequency and plant phenotype effects were not determined in that study. In order to understand the role of MidA in colonization of the intercalary zone in plants, I infected *L. perenne* seedlings with *E. festucae* WT, Δ*midA* and *mid1*-complemented strains, and calculated their host infection rates and effects on plant phenotype. I also analysed hyphal biomass (hyphal DNA concentration) in different tissues using qPCR. Next, to understand the role of calcium in intercalary growth, I subjected *E. festucae* WT, Δ*midA* and *mid1*-complemented strains to mechanical stretching *in vitro* to assess and compare their capacity to undergo intercalary extension and compartment division.

3.1.1. Deletion of *E. festucae midA* has No Effect on Plant Phenotype

For plant phenotype assessments, one week old *L. perenne* seedlings were inoculated *in situ* with a trace amount of fungal hyphae from the leading edge of an *E. festucae* colony into a small incision in the shoot apex using sterile razor blades according to the method of Latch and Christensen (1985). After inoculation, the seedlings were incubated in a growth chamber for two wks and then transplanted into soil and maintained in a glass house. The surviving

L. perenne plants were subjected to tissue print immunoassay to confirm the presence of endophyte at 8 wks (Table 3.1).

Table 3.1 Number of *L. perenne* seedlings post inoculation for each *E. festucae* strain.

Seedling numbers	**WT**	***midA*-20**	***midA*-36**	***midA*-43**	**Comp-20**	**Comp-36**
Pre-inoculation	26	28	32	30	39	27
Post inoculation	18	26	20	21	30	18
Planted	13	23	12	17	24	17
Survived (8 wks)	9	13	9	16	7	6

The three Δ*midA* strains used in this study are independent replacement mutants harbouring the hygromycin cassette (Ariyawansa, 2015). The two *mid1*-complemented strains were individually transformed with a functional copy of the *E. festucae midA* gene (Ariyawansa, 2015). Comp-20 and Comp-36 were made from *midA*-20 and *midA*-36 mutants respectively.
For tissue print immunoassay, 4 tillers from each plant were cut transversely from the plant at the crown and the cut end manually printed onto nitrocellulose membrane (Figure 3.1).
Multiple tillers were tested as previous findings suggested that *E. festucae* Δ*midA* strains may not colonise all tillers, resulting in plants with negative and positive tillers. Plants were classified as positive if they had one or more infected tillers (Ariyawansa, 2015). The infection percentages were calculated as by ratios of infected surviving plants against number of seedlings post inoculation. *E. festucae* WT was able to infect 50% of plants, whereas Δ*midA*-20, 36 and 43strains resulted in 50%, 45% and 76.1% infection percentages, respectively. Comp-20 and Comp-36 strains were able to infect 23.3% and 33.3% of the inoculated seedlings, respectively.

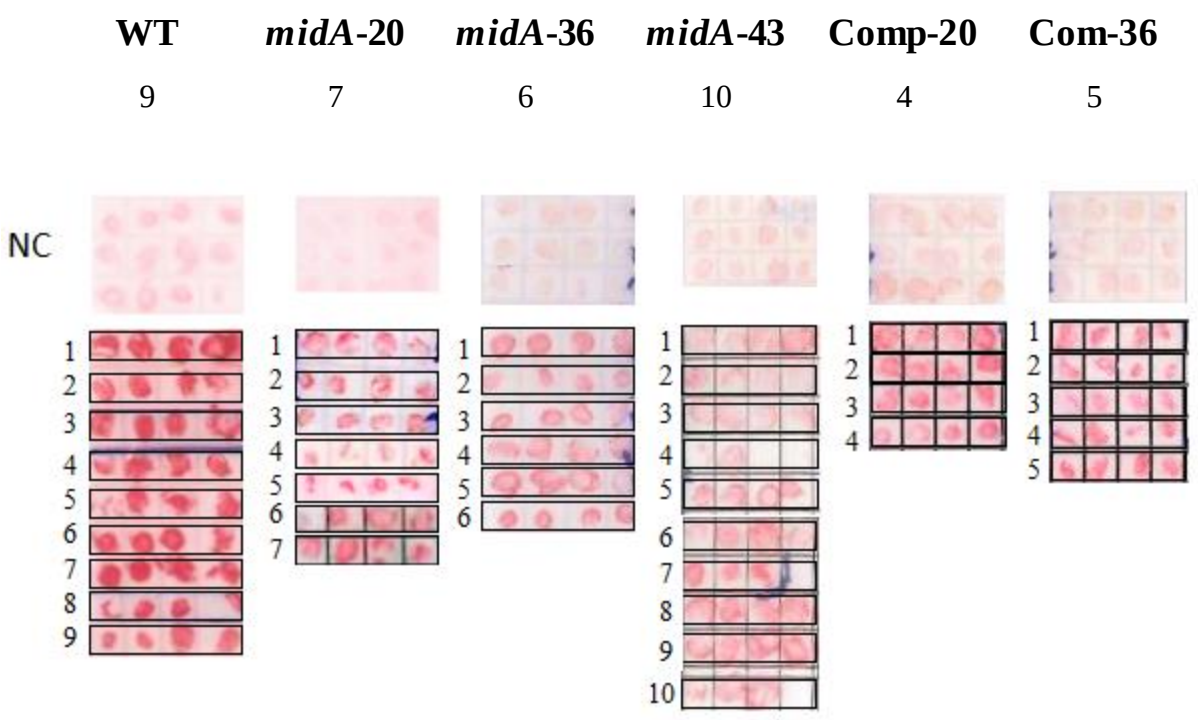

Figure 3.1 Tissue print immunoassay results of positive and negative *L. perenne* tillers. For confirmation of endophyte presence, four tillers from each infected *L. perenne* plants were printed on nitrocellulose membrane and developed as described in Section 2.15. The plants which tested positive for endophytes are numbered and the four tillers tested are enclosed by black rectangles. NC: tissue print immunoassay results of negative control plants that were not inoculated with endophyte. The top row of numbers show positively infected plants with corresponding strain.

Endophyte positive *L. perenne* plants were assessed for their phenotypes by comparing tiller numbers and lengths, as well as general appearance, with plants infected with *E. festucae* WT, Δ*midA* and *mid1*-complemented strains (Figure 3.1). Plants infected with *E. festucae* WT, Δ*midA* and complement strains did not show any consistent visual differences (Figure 3.2). To confirm visual observations, the number of tillers on each *L. perenne* plant successfully infected with WT, Δ*midA* and complement strains were counted. The averages of tiller numbers were then compared between WT, mutants and complements using a one way ANOVA test. Tiller numbers between different plant genotypes were quite variable and no significant differences in tiller number was observed between plants infected with *E. festucae* WT and the Δ*midA* mutant strains. However, only the plants infected with *E. festucae* Comp-20 produced significantly more tillers compared to plants infected with the other strains (p=0.02) (Figure 3.3A).

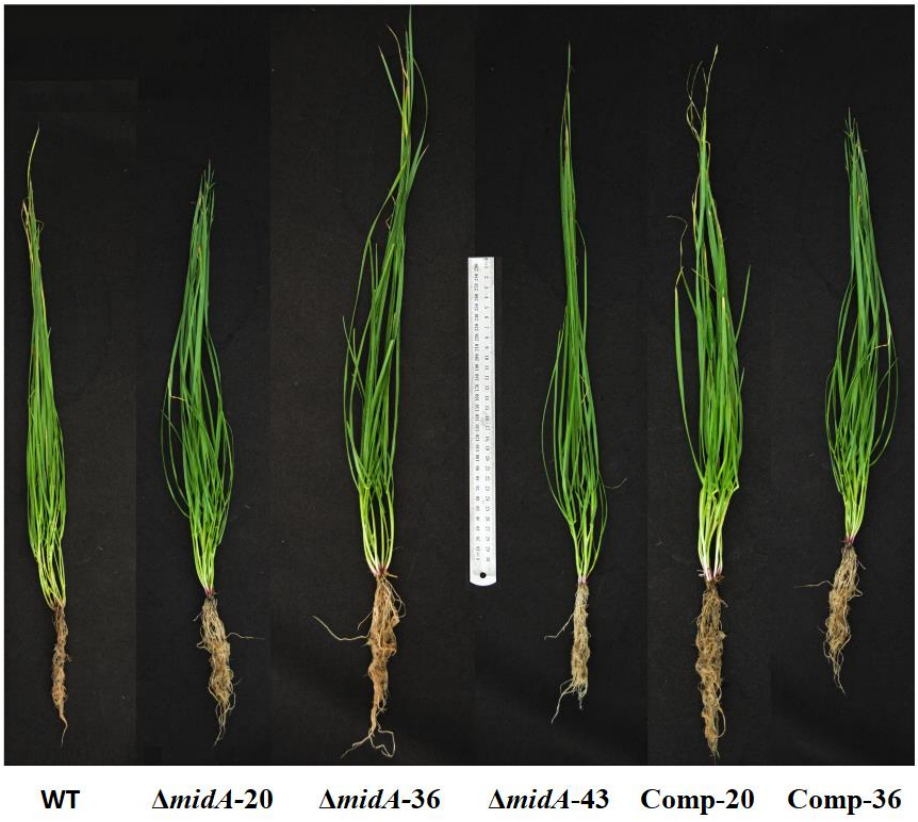

Figure 3.2 Effects of *E. festucae* WT, Δ*midA* and complement strains on the phenotype of *L. perenne*. WT is representative of 9, Δ*midA* strains are representatives of 23 and complements are of 9 plants each. The plants shown were 10 wks post inoculation. The scale shows 30 cm.

To determine whether there were any difference in tiller lengths between plants infected with the different strains, the three tallest tillers from each *L. perenne* plant infected with WT, Δ*midA* and complement strains was measured. The average of tiller lengths of plants inoculated with *E. festucae* WT were compared to average tiller lengths of plants inoculated with *E. festucae* Δ*midA* strains and complements using the one way ANOVA test. Tiller lengths of *L. perenne* infected with *E. festucae* WT were significantly higher than the plants inoculated with Δ*midA* mutants and complements ($p<0.05$), however no significant difference between tiller lengths of Δ*midA* strains and complement strains was observed (Figure 3.3B). The results suggest that shorter tiller lengths in plants infected with E. *festucae* Δ*midA* mutants may not be due to loss of *midA* function, as plants with *E. festucae* complement-strain infections did not restore average tiller lengths in their hosts (Figure 3.3B).

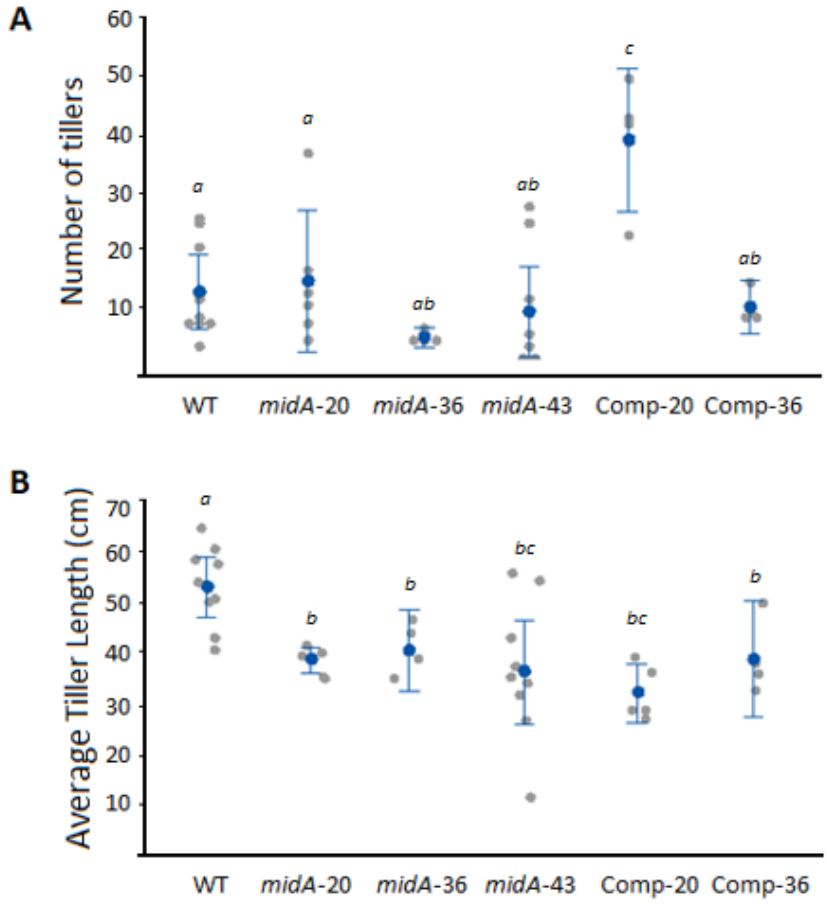

Figure 3.3 Phenotype comparisons of A) Numbers of tillers and B) Tiller lengths (cm) of *L. perenne* infected with *E. festucae* WT, Δ*midA*-20, Δ*midA*-36, Δ*midA*-43, Δ*midA*-20 complement (Comp-20) and Δ*midA*-36 complement (Comp-36) strains. The averages of tiller numbers and tiller lengths of *E. festucae* WT, Δ*midA* and *mid1*-complemented strains were compared using a one way ANOVA test within each phenotype. Treatments with the same letter are not different at the 5% level as determined by Fisher's protected least significant difference test.

3.1.2. Deletion of *E. festucae midA* Reduces Hyphal Biomass in the Intercalary Zone in Plants

To understand the role of *midA* in plant colonization by *E. festucae*, the biomass analysis of *E. festucae* WT, Δ*midA* or complement strains was analysed in plants 10 wks after inoculation. Tillers were dissected at the base of the plant to attempt to distinguish the biomass in the shoot apex (SA) enriched-tissue from that in the surrounding more mature leaf tissues, where intercalary growth is required for colonisation (Figure 2.6). For this, a section of approximately 5 mm from the base of the tiller was cut using a scalpel and the younger tissue in the centre of this section was extracted using the tip of a sterile glass Pasteur pipette. For each strain of *E. festucae*, three plants were used for hyphal biomass analysis. Due to the

very small sizes of tissues, sections of young tissues and mature tissues from six tillers were pooled together from each plant and DNA extraction was performed.

Hyphal biomass was estimated using qPCR. Genomic DNA extracted from *E. festucae* Fl1 grown in culture, and from un-infected *L. perenne* tissues, was used to generate standard curves for endophyte and plant DNA respectively. The endophyte primers amplified a 153 bp sequence of an endophyte-specific non-ribosomal peptide synthetase-1 (*NRPS*-1) gene (NRPS-1F: gtccgatcattccaagctcgtt, NRPS-1R: tggtgggaagttccctgcac), and the plant primers (Lp-EF1a-RT-F2/3: caccacgagtctatgct, Lp-EF1a-RT-R2: gacctgggcaacaaagc) amplified a 74 bp sequence from the elongation factor-1 alpha (*EF*-1) gene (Rasmussen 2007, Zhou, 2010). The endophyte to plant biomass ratio was estimated by comparing the amplification of target genes from the endophyte and the plant (see Section 2.18).

DNA from *E. festucae* Δ*midA*-20 was not detectable in these experiments, possibly because endophyte biomass was too low, or the endophyte had failed to infect all the tillers. In the SA-enriched tissue, the results of the biomass analyses for the remaining mutants were conflicting. The relative biomass of Δ*midA*-36 was lower compared to the wild type strain ($p<0.05$), while no significant differences were detected between WT and Δ*midA*-43 (Figure 3.4A). Furthermore, the relative biomass of both the *mid1*-complemented strains was significantly higher than WT implying that calcium uptake is a limiting factor for endophyte colonisation of the SA-enriched tissues ($p<0.05$), however this needs to be tested with larger numbers of plants and strains (Figure 3.4A). Conversely, in the leaf tissues surrounding the SA, which is a mixture of young and old tissues, the biomass of Δ*midA*-36 and Δ*midA*-43 was significantly lower than the ($p<0.05$) than wild type (Figure 3.4B). No difference in biomass was detected between WT and complement strains in leaf tissues (Figure 3.4B). The relative biomass of the WT and *mid1*-complemented strains was 10 fold higher in leaf compared to the SA-enriched tissues.

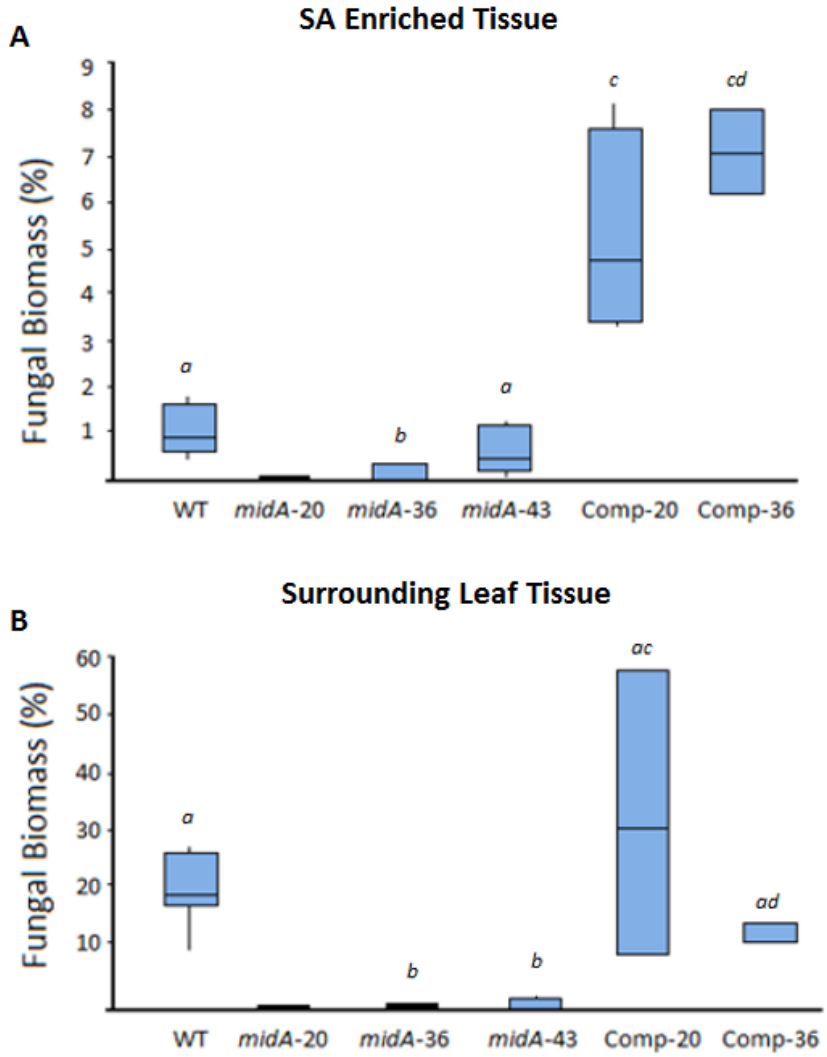

Figure 3.4 Hyphal biomass of *E. festucae* WT, Δ*midA*-20, Δ*midA*-36, Δ*midA*-43, Δ*midA*-20 complement (Comp-20) and Δ*midA*-36 complement (Comp-36) in *L. perenne*. Fungal biomass was calculated by quantifying the copy number of an endophyte and plant gene via qPCR, and presenting hyphal DNA copy number relative to plant DNA copy number. A) Shoot apex (SA) - enriched tissues and B) Surrounding leaf tissues. The replicates within each strain were analysed using the One-Way ANOVA test, the differences between biomass means of each strain was assessed using Fisher's Least Significant Difference test at the 5% level and strains that were assigned the same letter were not significantly different ($p \leq 0.05$). *E. festucae* Δ*midA*-20 hyphal biomass was below the detection levels, therefore was not included in the analysis.

The results confirmed that deletion of *midA* caused a marked failure of colonization in the leaf tissues surrounding the host SAM, where hyphae become aligned parallel to the leaf growth axis and extend by intercalary growth in synchronization with growing plant cells, and also to some extent in the SA enriched tissues. There was also some evidence for a reduction in colonisation in the SA- enriched region, however this was not consistent between the strains and remains unresolved.

3.2. Role of Calcium in *E. festucae* Reponses to Mechanical Stretch

In *E. festucae*, the first evidence for intercalary growth was shown using EGFP-expressing *E. festucae*, where vegetative hyphal growth rate measurements in plants infected with this strain showed consistent hyphal length extensions with plant growth without an increase in average compartment length (Christensen et al., 2008). The same study presented Transmission Electron Microscopy (TEM) images of *E. festucae* hyphae becoming flattened or compressed between the plant cells due to tight attachment of hyphae to plant cell walls, indicating that *E. festucae* hyphae underwent intercalary growth simultaneously with the growing plant cells (Christensen et al., 2008). These findings led to the hypothesis that mechanical stretching force, applied by rapidly growing plant cells to *E. festucae* hyphae, induced intercalary growth through the formation of new compartments (Christensen et al., 2008). To test this hypothesis, a wool fibre stretching apparatus was modified to stretch hyphae *in vitro* to mimic the mechanical stretch force imposed by plant cells (Ariyawansa, 2015). Mechanically stretched *E. festucae* hyphae elongate proportionally to the amount of stretching applied, and hyphal compartments divide according to a hierarchy, in which longer compartments divide before the shorter ones, suggesting a possible length threshold for division (Ariyawansa, 2015).

To replicate the results obtained by Ariyawansa 2015, stretching experiments were first conducted on WT strains using the mechanical stretching machinery described in Section 2.7.1. Compartment numbers and lengths were compared between un-stretched and stretched *E. festucae* cultures, as well as rate of compartmentalization of hyphae over 9 h. For this, compartment numbers and lengths of un-stretched and stretched hyphae were traced and measured using ImageJ software. For stretching, three independent *E. festucae* strains expressing YFP fused to Histone 2A protein were used as biological replicates (see Table 2.1). Each strain was grown on a silicon membrane under PDA supplemented with 50 mM of $CaCl_2$. After 3 d of incubation, single and straight hyphae were selected and tracked throughout the course of the experiment. Each tracked hypha was visualised from the 2nd compartment (the first compartment behind the tip) up to the 11th compartment. The number of compartments measured was limited by an increase in lateral hyphal branches nearer the colony centre which obscured the filament. The 1st compartment, which is the apex of the hypha, was not monitored as this compartment undergoes polar extension in culture independently of the forces applied by the mechanical stretcher. Intercalary extension is marginal in *E. festucae* sub-apical regions in the absence of applied mechanical stretch

(Ariyawansa 2015). Monitoring the same number of compartments in each hypha enabled comparison of total length differences and compartment number increases in control and stretched hyphae. Since each hypha differed in initial length, compartment number and compartment size, a formula was used to normalize the values by taking these initial differences into account as shown below. This compartmentalization formula enabled comparisons to be made between different stretched cultures and was used to calculate the compartmentalization.

$$\text{Number of newly formed compartments within a given time per 100 µm of initial hyphal length (hyphal length at T=0)} = \left[\frac{\text{Number of newly formed compartments within the given time}}{\text{Cumulative length of all 10 compartments of hypha at T=0}}\right] \times 100$$

When no stretch was applied, no change in the length of compartments was observed over the 9 h tracking period. However, on average one additional intercalary compartment per 100 µm of hyphae average was detected in that time (Figure 3.5, Figure 3.7, Table 3.2). However, when 3 mm of stretch was applied 3 times, 3 h apart, hyphae increased in length in proportion to the amount of stretch applied as shown in Table 3.3. The stretched hyphae also responded by increasing the compartmentalisation, which was an average of 2.1, a significantly increase ($p \leq 0.05$) compared to un-stretched hyphae over the 9 h treatment (Figure 3.5, Figure 3.7, Table 3.3). This result confirmed the previous finding that mechanical stretch stimulates intercalary growth in *E. festucae* hyphae *in vitro* by increasing compartment length and rates of division (Ariyawansa, 2015).

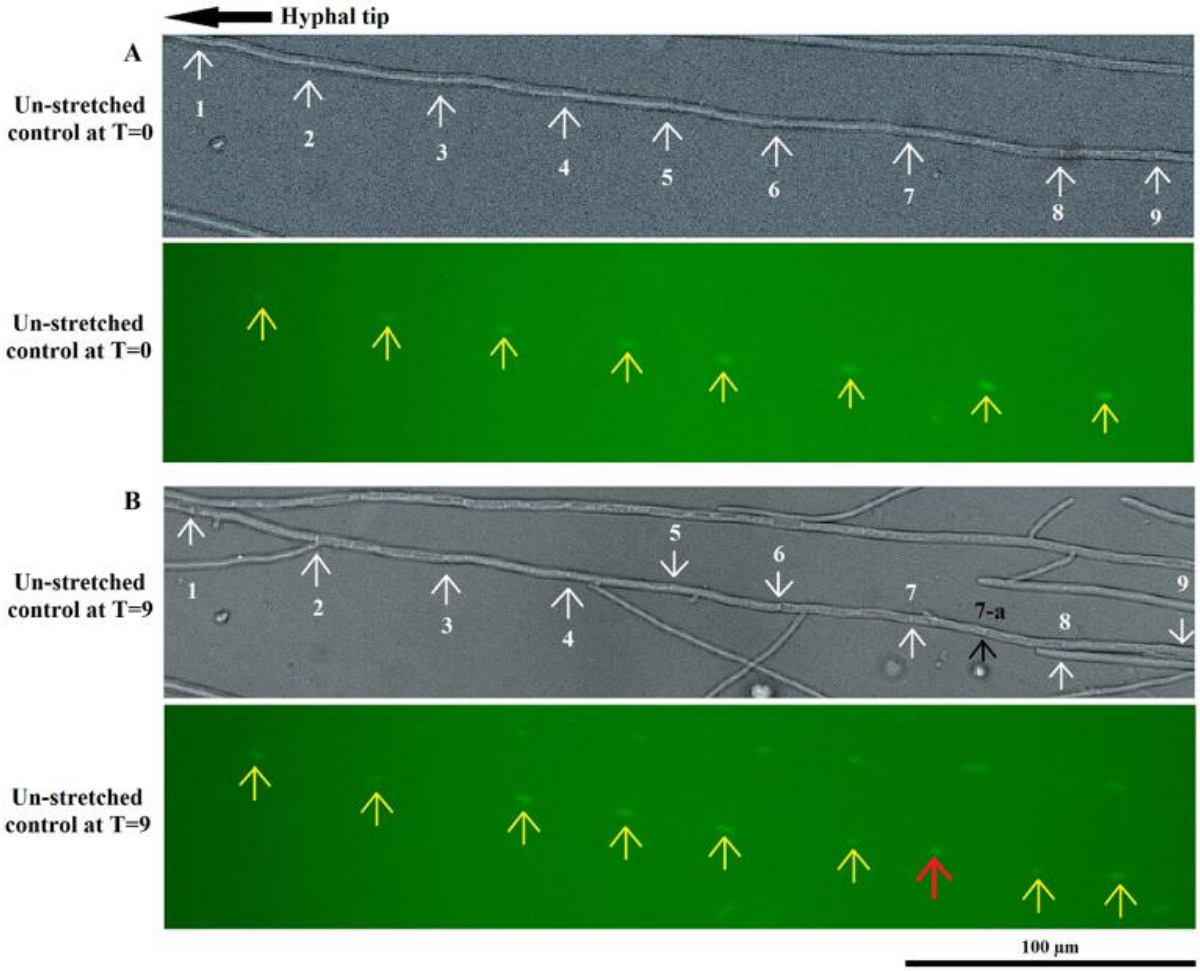

Figure 3.5 Position of septa and nuclei over time in an un-stretched *E. festucae* pYH2A-6 hypha grown under PDA supplemented with 50 mM $CaCl_2$. A: Sub-apical section of un-stretched hypha at T=0. Bright field (above) and fluorescence microscopy (below) images show a representative sub-apical hypha expressing YFP fused to Histone 2A protein. T indicates h. B: The same hyphal section after 9 h of incubation showing one new septum and one additional nucleus. White and yellow arrows show the septa and nuclei respectively, present at T=0 as well as T=9. The red arrow marks a new nucleus after 9 h of incubation. The black arrow shows a new septum that formed after 9 h of incubation.

Table 3.2 A representative un-stretched *E. festucae* pYH2A-6 hypha showing compartment sizes and division over time (not the same hypha as shown in Figure 3.6) in µm. The colony was grown on a silicon membrane suspended in a stretching device (but no stretch was applied) under PDA supplemented with 50 mM $CaCl_2$.To closely mimic the procedure used when hyphae are stretched, compartments were first measured (labelled "before"), and the stretcher was then handled and manipulated as it would be to apply stretch, but no stretching force was applied, and then the same compartments were measured again (labelled "after"). Therefore, the imaging and compartment measurements were carried out twice at T=0, 3 and 6 even though the cultures did not receive any stretching. At T=9, the imaging and measurement was carried out only once due to time limitations over the course of experiment. The table shows representative measurements of compartment division and lengths (µm) of one *E. festucae* wild type hypha expressing YFP fused to Histone 2A protein and measured after 0, 3, 6 and 9 h of incubation. T indicates h of observation. The hypha was monitored from the second (C-2) to the eleventh compartment (C-11). The first compartment (hyphal tip) was excluded from the measurement. C: Compartment.

Time	Imaging	C-2					C-3	C-4			C-5	C-6	C-7		C-8	C-9		C-10	C-11
T=0	Before	244.0					41.7	106.3			49.2	25.5	53.2		24.6	65.6		40.5	39.4
	After	245.2					41.7	106.6			49.7	25.5	54.1		24.7	65.5		40.7	39.4
T=3	Before	110.3		135			41.9	38.5	71.8		49.8	25.5	54.2		24.6	66.7		40.7	39.4
	After	110.4		134.8			41.9	38.5	71.9		49.7	25.4	55.5		24.6	66.8		40.8	39.5
T=6	Before	58.6	51.9	49.9	75		41.8	38.1	34.7	37.1	49.7	25.5	54.9		24.8	66.7		41	39.4
	After	58.9	52	49.9	76.8		41.9	38.2	34.8	37	50.8	25.6	56.9		24.8	66.7		41.1	39.5
T=9		58.9	51.9	49.8	37.6	38.8	41.8	38.1	34.7	37.2	50.7	25.5	32.1	25	25.1	34.8	31.3	41.1	39.5

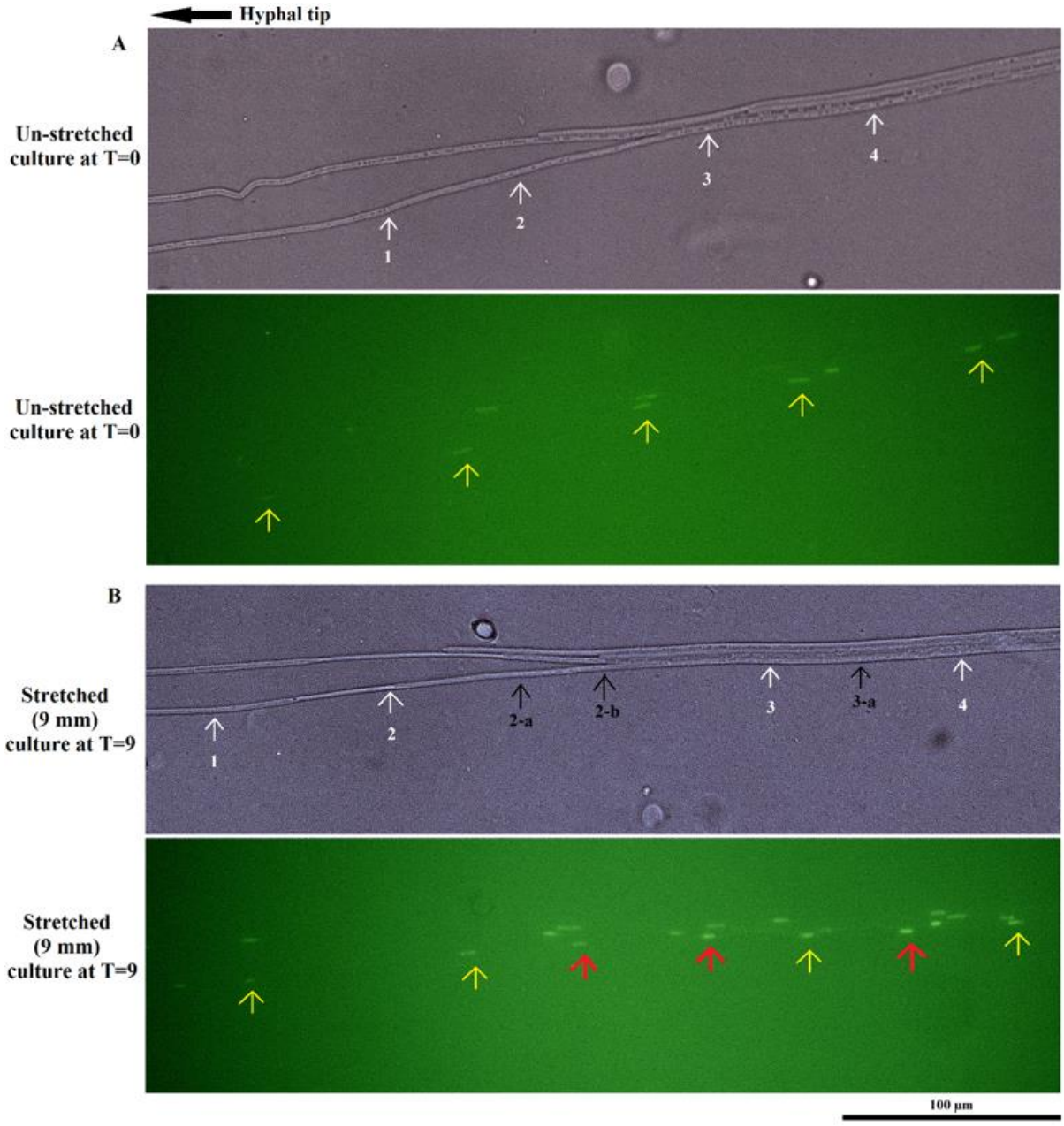

Figure 3.6 Position of septa and nuclei over time in a stretched *E. festucae* pYH2A-6 hypha grown under PDA supplemented with 50 mM $CaCl_2$. A: Sub-apical section of un-stretched hypha at T=0. Bright field (above) and fluorescence microscopy (below) images show a representative sub-apical hypha expressing YFP fused to Histone 2A protein. T indicates hour. B: The same hyphal section after 9 h of incubation showing three new septa and three additional nuclei. White and yellow arrows show the septa and nuclei respectively, present at T=0 as well as T=9. Red arrow marks the new nuclei after mechanical stretching. The black arrow shows new septa after mechanical stretching.

Table 3.3 A representative stretched *E. festucae* pYH2A-6 hypha (not the same as Figure 3.7) showing of expansion and division in µm**.** The colony was grown on a silicon membrane suspended in a stretching device under PDA supplemented with 50 mM $CaCl_2$.The hypha was stretched 3 mm at T=0, T=3 and T=6. At T=9; the imaging and measurement was carried out only once due to time limitations over the course of experiment. T indicates h of observation. The hypha was monitored from the second (C-2) to the eleventh compartment (C-11). The first compartment (hyphal tip) was excluded from the measurement. C: Compartment.

Time	Imaging	C-2								C-3		C-4			
T=0	Before	270.2								47.1		121.7			
	After	291.7								50.9		131.6			
T=3	Before	116.6				174.8				51		131.4			
	After	126.4				191				54.8		144.1			
T=6	Before	31.6	62.9		32	38.2	34.9	60.8	56.9	54.5		70.4		74.3	
	After	34.2	68.5		34.9	41.6	37.5	65.6	60.7	60.2		76.1		80.6	
T=9		34	35.6	33.1	34.6	41.1	37.3	36	29.8	60.2	32.4	28.1	41.4	34.6	33.1	47.6

C-5		C-6	C-7		C-8	C-9		C-10		C-11	
54.5		28.4	59.2		27.4	70.8		45.2		44.8	
58.3		30.8	63.8		30.6	76.4		49		48.1	
58.1		30.5	63.4		30.7	76.2		48.8		48	
63.2		33.2	69		33.9	82.1		52.1		52.5	
63.1		33.4	36.4	32.7	34	43.4	38.6	52.2		52.2	
68.9		37.2	39.9	37.2	36.8	47.1	41.5	56.5		56.8	
35.6	33.1	36.9	39.6	37	36.6	39.9	41.4	29.2	27	30.4	26.3

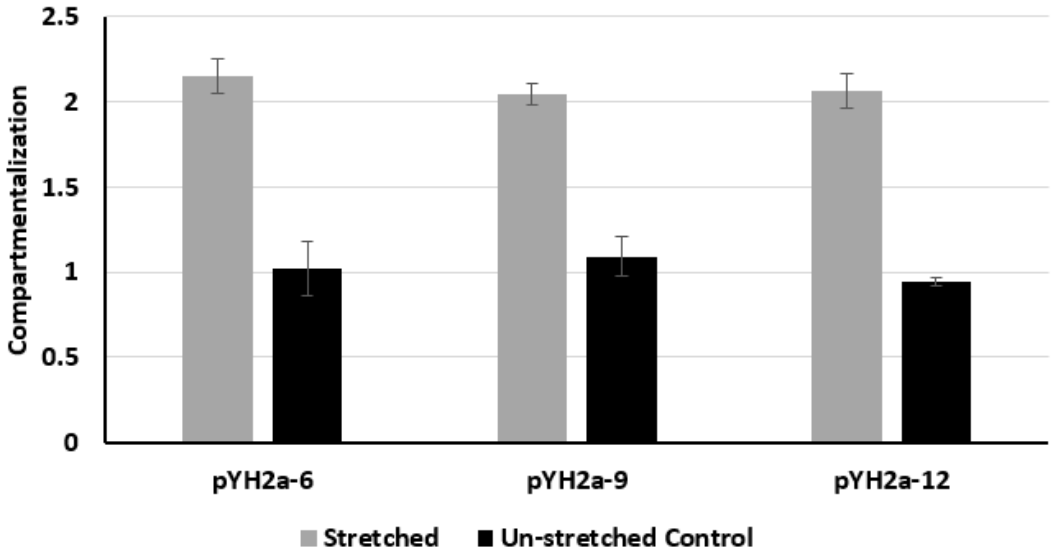

Figure 3.7 Comparison of compartmentalization of mechanically-stretched versus un-stretched controls in three independent *E. festucae* pYH2A cultures expressing YFP fused to Histone 2A protein (see Section 2.1). The cultures were grown under PDA supplemented with 50 mM $CaCl_2$ and incubated for 3 d prior to stretching. For each strain, one hypha from three independent single colonies for each strain growing on randomized individual stretching cassettes were tracked. The compartmentalization was calculated by using the formula presented in Section 3.3. The number of newly formed compartments at the end of the 9 h experiment was divided by initial hyphal lengths and multiplied by 100 to normalize the different hyphal lengths and calculate the compartmentalization.

3.2.1. Determining the Role of Calcium in the Plasticity of Wild Type *E. festucae* Hyphae after Stretch

The amount of mechanical stretching that *E. festucae* hyphae can tolerate has not been investigated in detail, however a previous study found that 5 mm of mechanical stretching applied over the 4.5 cm silicon membrane (an 18% increase in length) at one time resulted in hyphal cell wall damage (Ariyawansa, 2015). Therefore, to better define the plasticity of the cell wall, and determine whether calcium plays a role in cell wall plasticity, wild type *E. festucae* cultures were grown on stretching cassettes under PDA with or without supplemental calcium and increasing amounts of stretching was applied in intervals to determine the elastomeric potential of *E. festucae* hyphae *in vitro*.

For this, WT *E. festucae* cultures were grown on silicon membranes fitted onto stretching frames, under PDA or PDA plus 50 mM $CaCl_2$ and incubated for three d. Nine technical replicates were prepared, each culture inoculated individually onto membranes as described previously (Section 2.7.1). For control, WT cultures were grown and handled separately under identical conditions but were not mechanically stretched. After incubation, three separate hyphae from each colony, growing horizontal to the stretching plane, were selected

for observation. The cultures were mechanically stretched in increments as described in Section 2.7.1. The hyphae were examined by bright field microscopy for cell wall breakage between each incremental stretch, and the elastomeric potential of hyphae recorded as the percentage of cumulative stretch sustained without visible hyphal breakage in any of the three hyphae examined in one culture. In *E. festucae* WT growing on PDA alone, Of the nine cultures subjected to 3 mm of mechanical stretching (i.e. 6.6% of the 4.5 cm silicon membrane) three hyphae of seven cultures showed consistent breakages. This contrasts with wild type *E. festucae* cultures grown under PDA supplemented with 50 mM $CaCl_2$, where no hyphal breakages were observed after 3 mm of stretching delivered in one go. To determine the exact amount of mechanical stretching where hyphae start to break, wild type *E. festucae* cultures were grown under PDA without $CaCl_2$ supplementation and subjected to 1 mm of mechanical stretching sequentially three times. Out of nine cultures, hyphae of eight cultures showed consistent breakages after the full 3 mm of mechanical stretching (Figure 3.8), whereas no apparent breakages were observed in hyphae from the other culture.

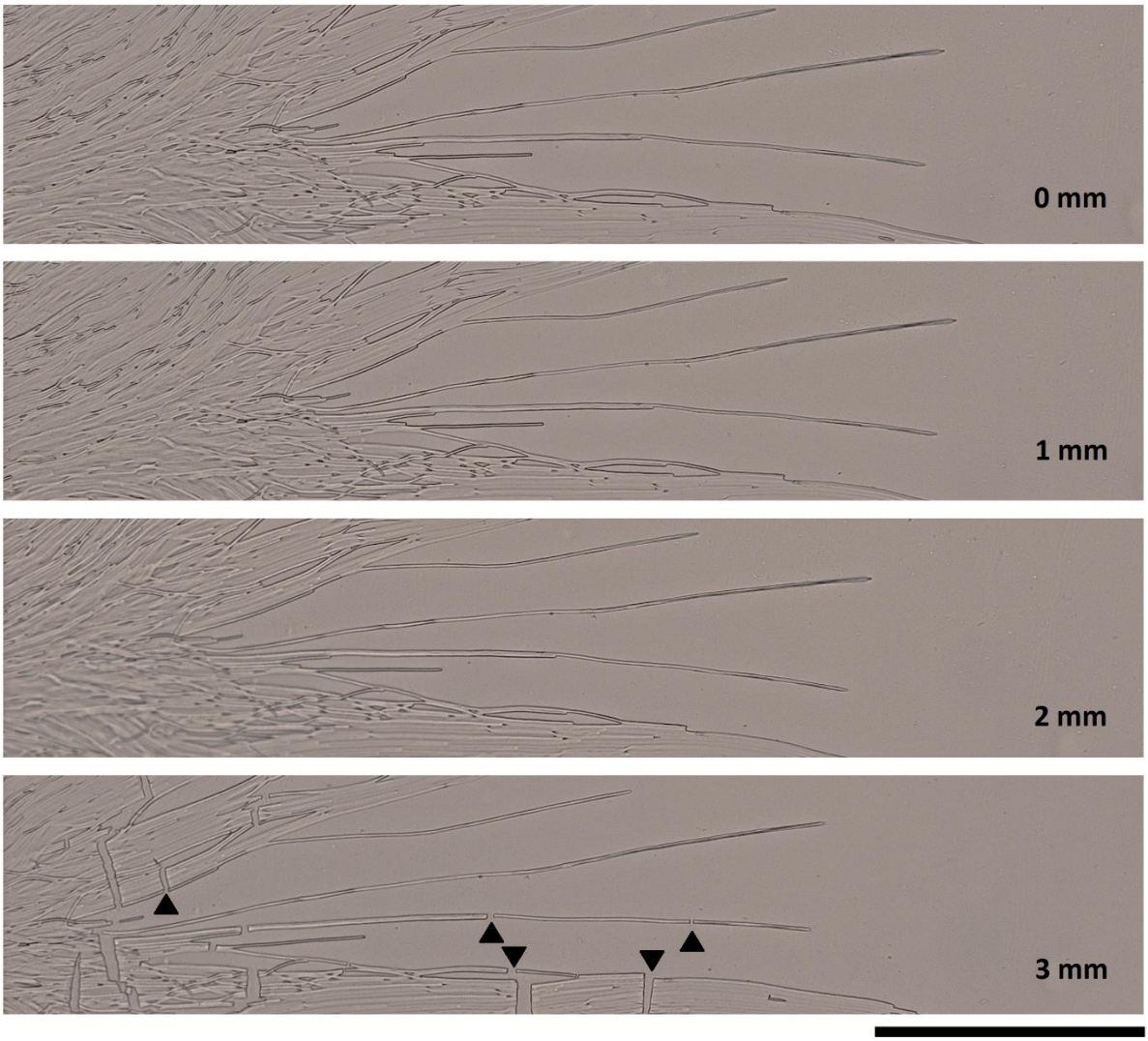

Figure 3.8 A representative example of hyphal breakage after mechanical stretch in *E. festucae* WT grown under PDA without $CaCl_2$ supplementation. The colony was grown on a silicon membrane and subjected sequential challenges of 1 mm of mechanical stretch over the 4.5 cm membrane. The first evidence of hyphal breakage was observed between 2 and 3 mm of stretch. The black arrows indicate breakage sites on hyphae. Images were obtained using Olympus bright field microscopy with a 20X objective lens. The scale bar shows 200 µm. Images are representative of 9 individual treatments.

Mechanical stretching experiments so far demonstrated that wild type *E. festucae* cultures grown under PDA with 50 mM $CaCl_2$ supplement can be stretched by 9 mm on 4.5 cm silicon membrane over the course of 9 h in 3 h intervals (see Section 3.3). To observe the extend of cell wall plasticity in the presence of $CaCl_2$, wild type *E. festucae* cultures were grown under PDA with 50 mM $CaCl_2$ and were first subjected to 3 mm of sequential mechanical stretching up to the point of hyphal breakage. The wild type *E. festucae* hyphae were able to undergo a maximum total of 12 mm of mechanical stretching, applied as four consecutive 3 mm stretches (Figure 3.9). When stretched for another 1 mm, hyphal breakage

was observed (Figure 3.9). Consistent hyphal breakage at 12 mm was observed in seven out of nine technical replicate cultures, the remaining two cultures showed hyphal breakages after 13 mm of stretching (Table 3.4).

Table 3.4 Hyphal breakage points in *E. festucae* wild type cultures grown on PDA or PDA plus 50 mM $CaCl_2$. The cultures grown under PDA were stretched in 1 mm increments, whereas cultures grown under PDA plus 50 mM $CaCl_2$ were stretched in 3 mm increments until 12 mm, and thereafter in 1 mm increments. From each culture, three single, straight horizontal hyphae were selected and examined. For evidence of consistent hyphal wall breakage, all three hyphae were observed to be broken at least in one location. Imaging was done between each stretching interval using an Olympus BX50 microscope with a 40X objective. "-" indicates unsuccessful stretching of hyphae up to 3 mm in the 7th replicate culture.

Replicate ID	Maximum stretch (mm)	
	PDA	PDA + 50 mM $CaCl_2$
1	3	12
2	3	13
3	3	12
4	3	12
5	3	12
6	3	12
7	-	13
8	3	12
9	3	12

The results indicated that supplementation of PDA with 50 mM $CaCl_2$ markedly increased cell wall plasticity in *E. festucae* wild type hyphae, and thus the amount of mechanical stretching that could be sustained by compartment walls before breakage.

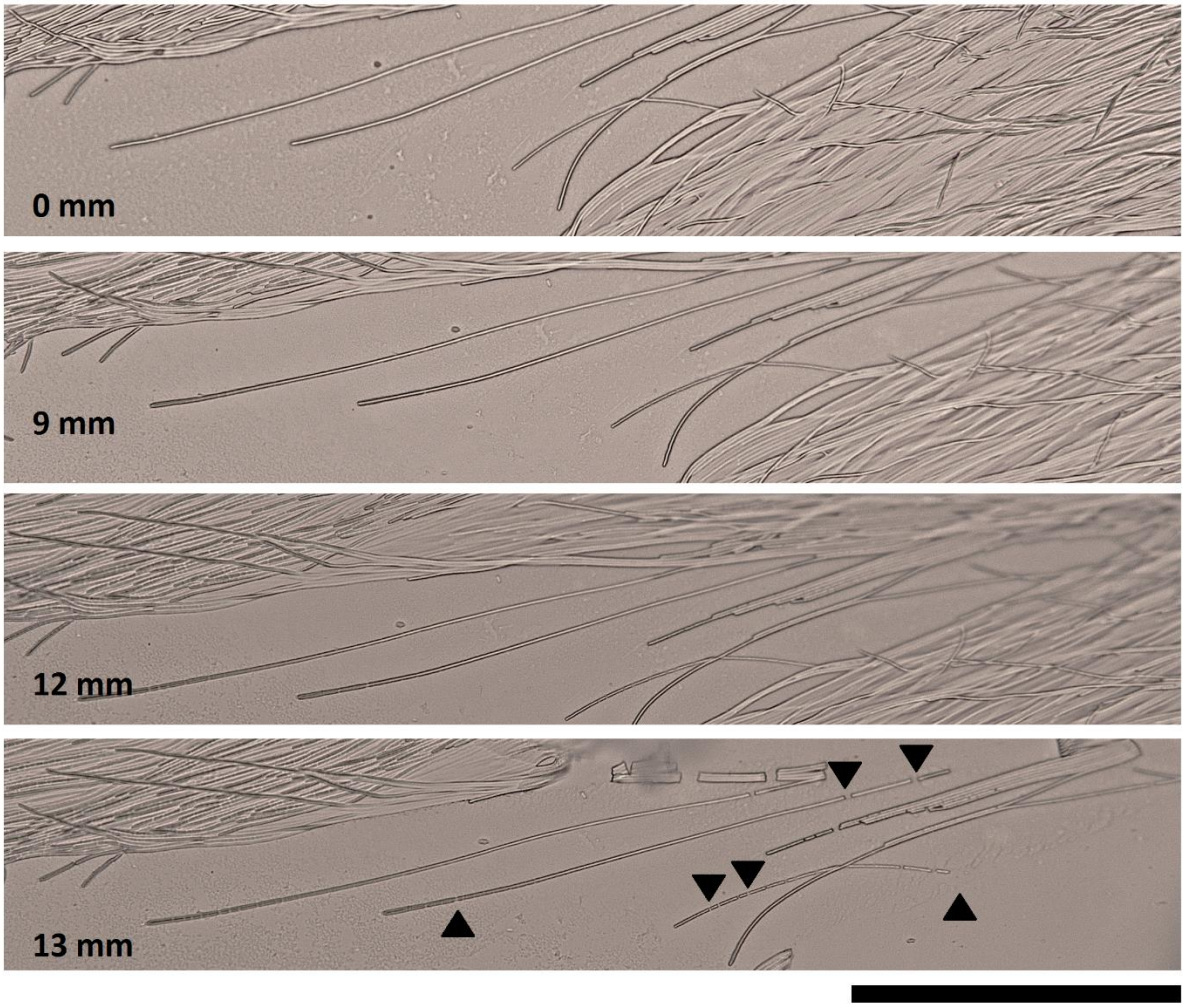

Figure 3.9 A representative example of hyphal breakage after mechanical stretch of an *E. festucae* WT culture grown under PDA supplemented with 50 mM $CaCl_2$. The colony was grown on a silicon membrane and subjected sequential challenges of 3 mm of mechanical stretch over the 4.5 cm membrane. They hyphae appeared to be able to tolerate at least 12 mm of stretch over a short period of time. The first evidence of hyphal breakage was observed between 12 and 13 mm of stretch. The black arrows indicate breakage sites on hyphae. Images were obtained using bright field microscopy on a BX50 Olympus microscopy fitted with a 20X objective lens. The scale bar shows 200 µm.

3.2.2. The Effect of MidA Deletion on *E. festucae* Intercalary Growth after Mechanical Stretch

The mechanical stretch-activated Mid1 protein in *S. cerevisiae*, and its homologs in several filamentous fungi, have been shown to be responsible for calcium uptake, hyphal growth and sensing of stress on cell walls (Iida et al., 1994, Tudzynski et al., 2009, 2013). In *E. festucae*, *midA* was found to regulate colony growth rate, morphology and cell wall stress responses in culture (Ariyawansa, 2015). In particular, deletion of *midA* resulted in reduced colony growth

rate and denser morphology compared to WT, which was rescued by addition of $CaCl_2$ or sorbitol to the Potato Dextrose Agar (PDA) medium (Ariyawansa, 2015). Moreover, the slow growth rate and dense morphology in culture were exacerbated by addition of the calcium chelating agent ethylene glycol-bis (β-aminoethyl ether)-N,N,N′,N′-tetraacetic acid (EGTA), indicating that MidA is responsible for extracellular calcium uptake by *E. festucae* (Ariyawansa, 2015). The *E. festucae* Δ*midA* strains were also found to be sensitive to cell wall perturbing agents Congo red (CR) and Calcofluor white (CW), suggesting that MidA has a role in sensing cell wall stress (Ariyawansa, 2015). However, the roles of MidA and extracellular calcium in sensing mechanical stretching and mediating intercalary growth in culture have not yet been studied. Therefore, to understand the function of MidA and importance of calcium during intercalary growth, the media were optimised to facilitate mechanical stretching of *E. festucae* Δ*midA*. The custom-designed mechanical stretching machinery (see Section 2.7.1) was then used to quantify changes in the length and division of intercalary compartments of Δ*midA*, WT and complement strains in the presence or absence of extracellular calcium *in vitro*.

3.2.2.1. Optimization of a Suitable Medium for Mechanical Stretching of *E. festucae* Δ*midA* mutants

Previously, hyphae of *E. festucae* Δ*midA* have been shown to have cell wall aberrations and grow at a slower rate compared to WT on PDA, and these traits were rescued by additional extracellular $CaCl_2$ (Ariyawansa, 2015). The slow colony growth rate and difficulty in identifying septa by bright field microscopy meant that stretching of *midA* deletion strains to quantify effects on compartment length and division was not possible. Therefore, the growth medium was first supplemented with calcium, to chemically complement the strains and determine whether differences between wild type and *midA* mutants could be detected. To optimize a suitable medium that would yield hyphae with minimum branching and sufficient length, I grew *E. festucae* Δ*midA*, as well as WT and complement strains on PDA with $CaCl_2$ ranging from 25 to 100 mM (Figure 3.10). For each strain, colony disks of the same size were grown in triplicate on PDA supplemented with different calcium concentrations for 5 d. The resulting colony sizes were used to determine the radial growth rate (mm) per day.

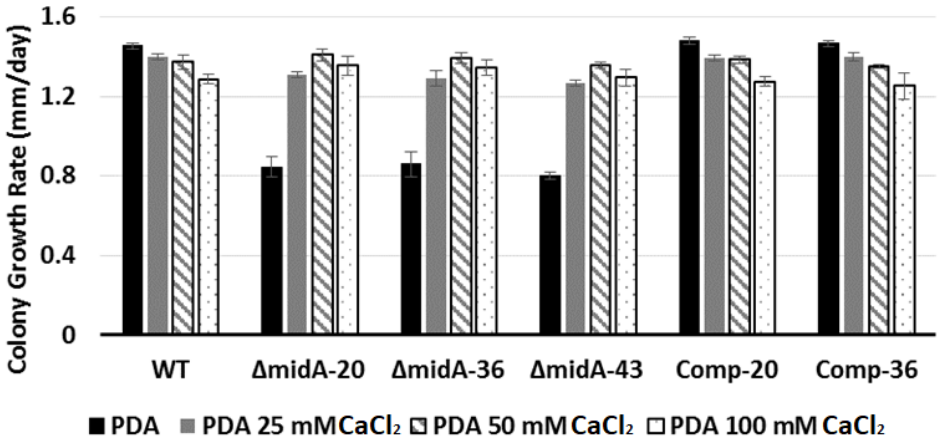

Figure 3.10 Mean radial colony growth rates of *E. festucae* WT, Δ*midA*-20, Δ*midA*-36, Δ*midA*-43, Δ*midA*-20 complement (Comp-20) and Δ*midA*-36 complement (Comp-36) on PDA supplemented with $CaCl_2$ concentrations of 25 mM, 50 mM and 100 mM. From each strain, three colony plugs were inoculated onto nutrient media as described in Section 2.7.1 and the colony radial growth (measured at four equidistant points on the colony) compared using the Student's t test. Bars indicate the standard deviation of the mean.

The addition of increasing amounts of calcium to the growth medium caused a small reduction in the growth rates of WT and complement colonies however this was not significant between colonies growing on different calcium concentrations, whereas all the calcium concentrations tested rescued the reduced radial growth rates of Δ*midA* strains (Figure 3.11) to a similar extent. The optimal growth rate of Δ*midA* strains was achieved with 50 mM $CaCl_2$ addition, and no significant increase in growth rate in mutants were observed in100 mM $CaCl_2$ (Figure 3.10).

To observe hyphal morphology, and assess its suitability for mechanical stretching, *E. festucae* Δ*midA*, WT and *mid1*-complemented strains were grown on silicon membranes and incubated under blocks of PDA supplemented with the same range of calcium concentrations as in the radial growth rate experiment discussed above. The cultures were established on hyphal stretcher frames as described in Section 2.7.1 and incubated for 3 d prior to imaging using an Olympus DIC microscope with a 40X objective lens. Hyphae of Δ*midA* strains growing on PDA appeared thinner and more vacuolated compared to hyphae growing on PDA with calcium supplementation. These features made it more difficult to trace septa and assess changes in compartmentalization in the absence of $CaCl_2$ in PDA (Figure 3.11). The Δ*midA* strains grown on PDA alone also produced shorter mycelia compared to Δ*midA* grown on PDA with calcium (after 3 d of incubation), which also made them unusable for mechanical stretching. However, supplemental calcium rescued these hyphal aberrations (Figure 3.11), and since the optimal medium growing Δ*midA* strains was

PDA supplemented with 50 mM $CaCl_2$, this medium was used in the mechanical stretching experiments throughout.

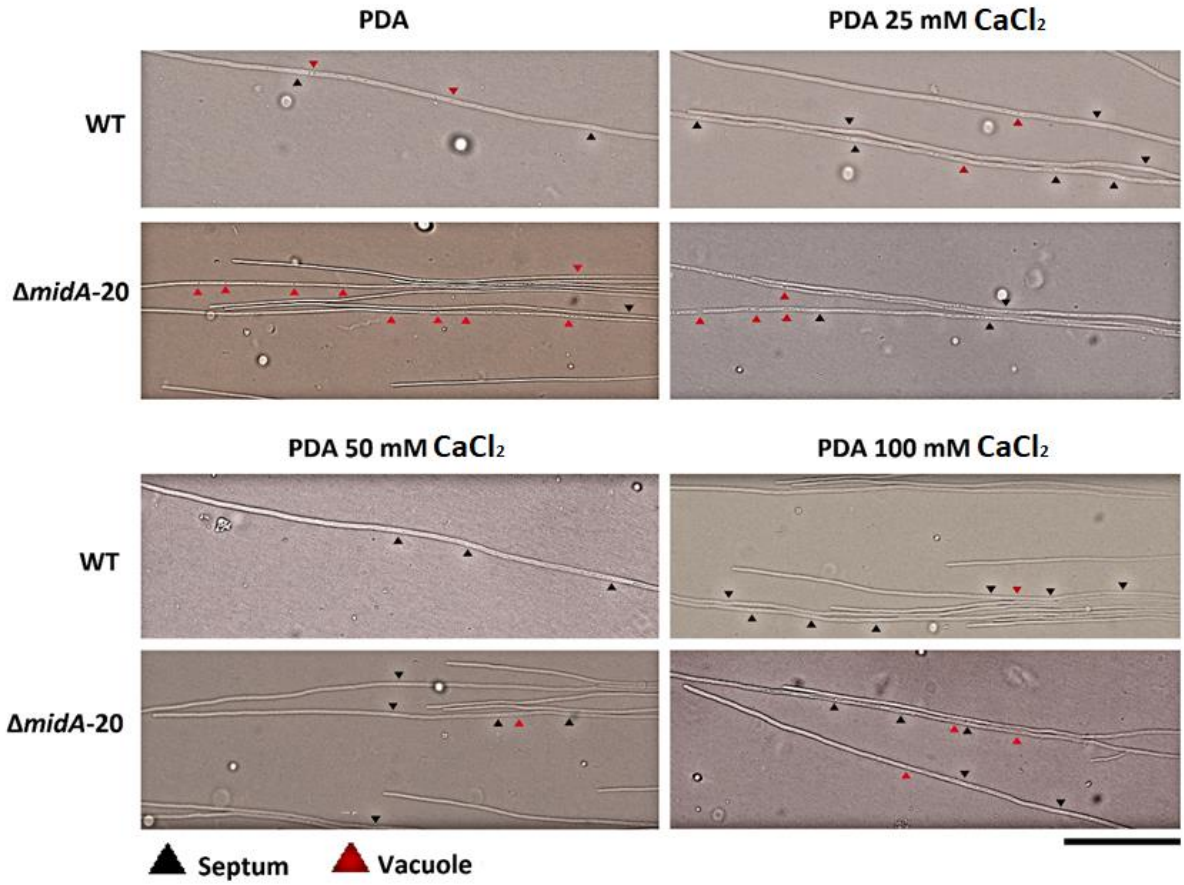

Figure 3.11 Morphology of *E. festucae* WT and Δ*midA*-20 hyphae after growth on silicon membranes under a PDA block supplemented with $CaCl_2$ ranging from 25 mM to 100 mM. The DIC microscopy images were obtained using a 40X objective lens. The scale bar represents 100 µm.

3.2.3. The Role of MidA in Plasticity of *E. festucae* Hyphae after Stretch

As shown above, growth of WT hyphae under PDA supplemented with 50 mM of $CaCl_2$ enhanced the resilience of hyphae to stretch when compared to growth under PDA alone, which showed that extracellular calcium affects cell wall plasticity during mechanical stretch. Next, to investigate the role of *midA* in response to mechanical stretching and in cell wall plasticity, three *E. festucae* Δ*midA* strains were subjected to mechanical stretch under PDA with and without 50 mM $CaCl_2$. *E. festucae* Δ*midA*-20, 36 and 40 strains were grown on silicon membranes fitted on stretching cassettes and incubated for three d as described previously. Each culture was grown in triplicate on individual stretching cassettes. The cultures were subjected to mechanical stretching in increments of 1 mm. Hyphal breakages in

three hyphae per culture were recorded to assess the plasticity of cell walls in each treatment as described previously.

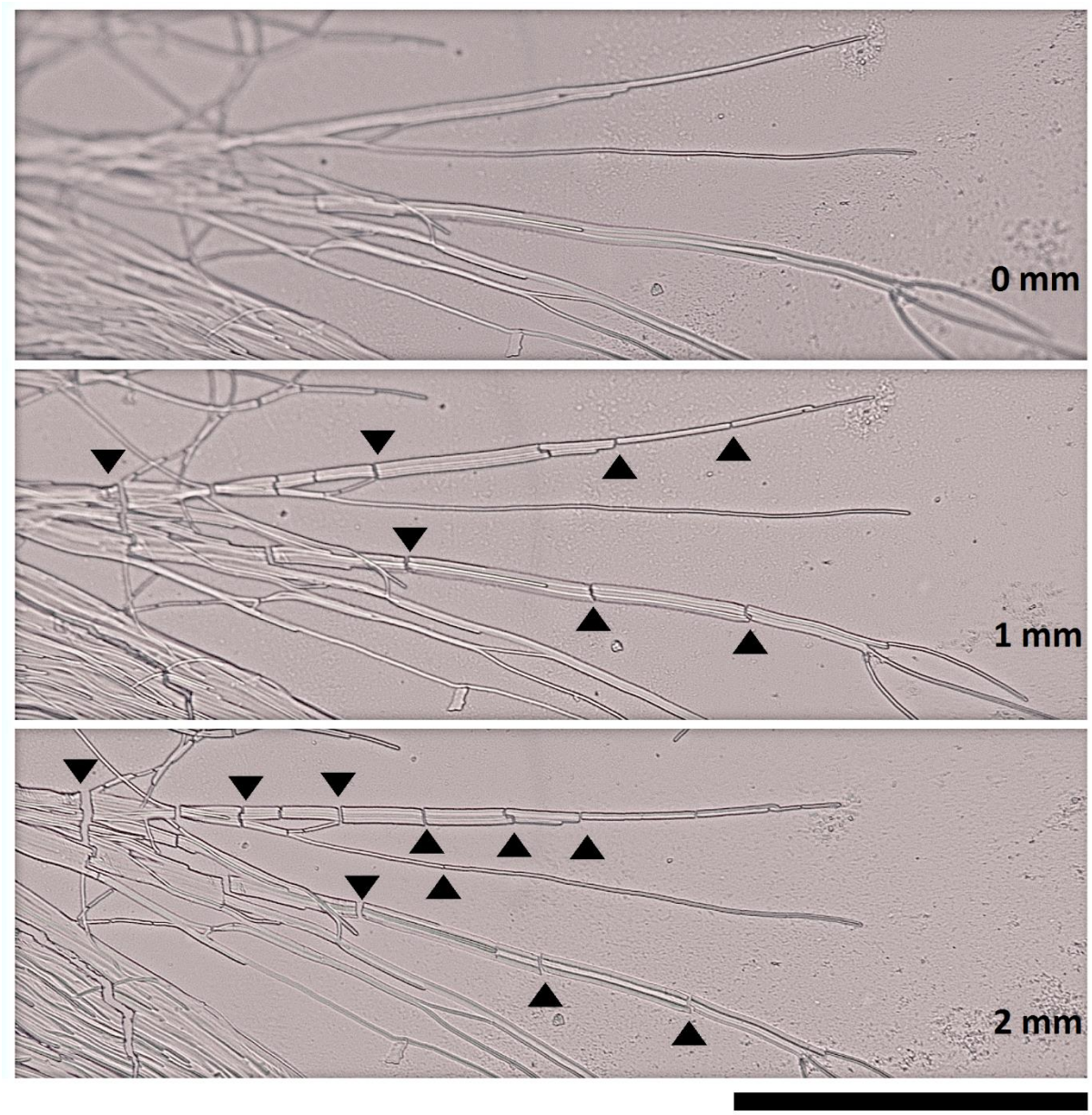

Figure 3.12 A representative example of hyphal breakage after mechanical stretch in *E. festucae* Δ*midA*-20 grown on PDA without calcium supplementation. The colony was grown on a silicon membrane and subjected to sequential challenges of 1 mm of mechanical stretch over the 4.5 cm membrane. Hyphal breakage was observed after 1 mm of stretching. The black arrows indicate breakage sites on hyphae. Images were obtained using Olympus bright field microscopy fitted with a 20X objective lens. The scale bar shows 200 µm. Images are representative of three biological and three technical replicates grown on individual stretching frames. The scale bar shows 200 µm.

The three independent *E. festucae* Δ*midA* strains grown under PDA without supplemented calcium all showed consistent hyphal breakages after 1 mm of mechanical stretching (Figure 3.12). The same Δ*midA* strains were grown under PDA with 50 mM $CaCl_2$ and were subjected to consecutive mechanical stretching in 1 mm increments until hyphal breakage was observed. All triplicate cultures of three *E. festucae* Δ*midA* strains grown under PDA without supplement were able to undergo 1 mm of mechanical stretching in total without hyphal breakage. The hyphal breakage of *E. festucae* Δ*midA* cultures was observed at 4 mm of mechanical stretching. All triplicate cultures of three *E. festucae* Δ*midA* strains grown under PDA with 50 mM $CaCl_2$ showed consistent hyphal breakages after 4 mm of mechanical stretching (Figure 3.13). The hyphal breakage points of three *E. festucae* Δ*midA* strains are given in the Table 3.5 below.

Table 3.5 Hyphal breakage points in *E. festucae* Δ*midA* cultures grown on PDA or PDA plus 50 mM $CaCl_2$. All cultures were stretched in 1 mm increments. From each culture, three single, straight horizontal hyphae were selected and examined. For evidence of consistent hyphal wall breakage, all three hyphae were observed to be broken at least in one location. Imaging was done between each stretching interval using an Olympus BX50 microscope with a 40X objective.

Replicate ID	Maximum stretch (mm)	
	PDA	PDA + 50 mM $CaCl_2$
1-Δ*midA*-20	1	3
2-Δ*midA*-20	1	3
3-Δ*midA*-20	1	3
1-Δ*midA*-36	1	3
2-Δ*midA*-36	1	3
3-Δ*midA*-36	1	3
1-Δ*midA*-43	1	3
2-Δ*midA*-43	1	3
3-Δ*midA*-43	1	3

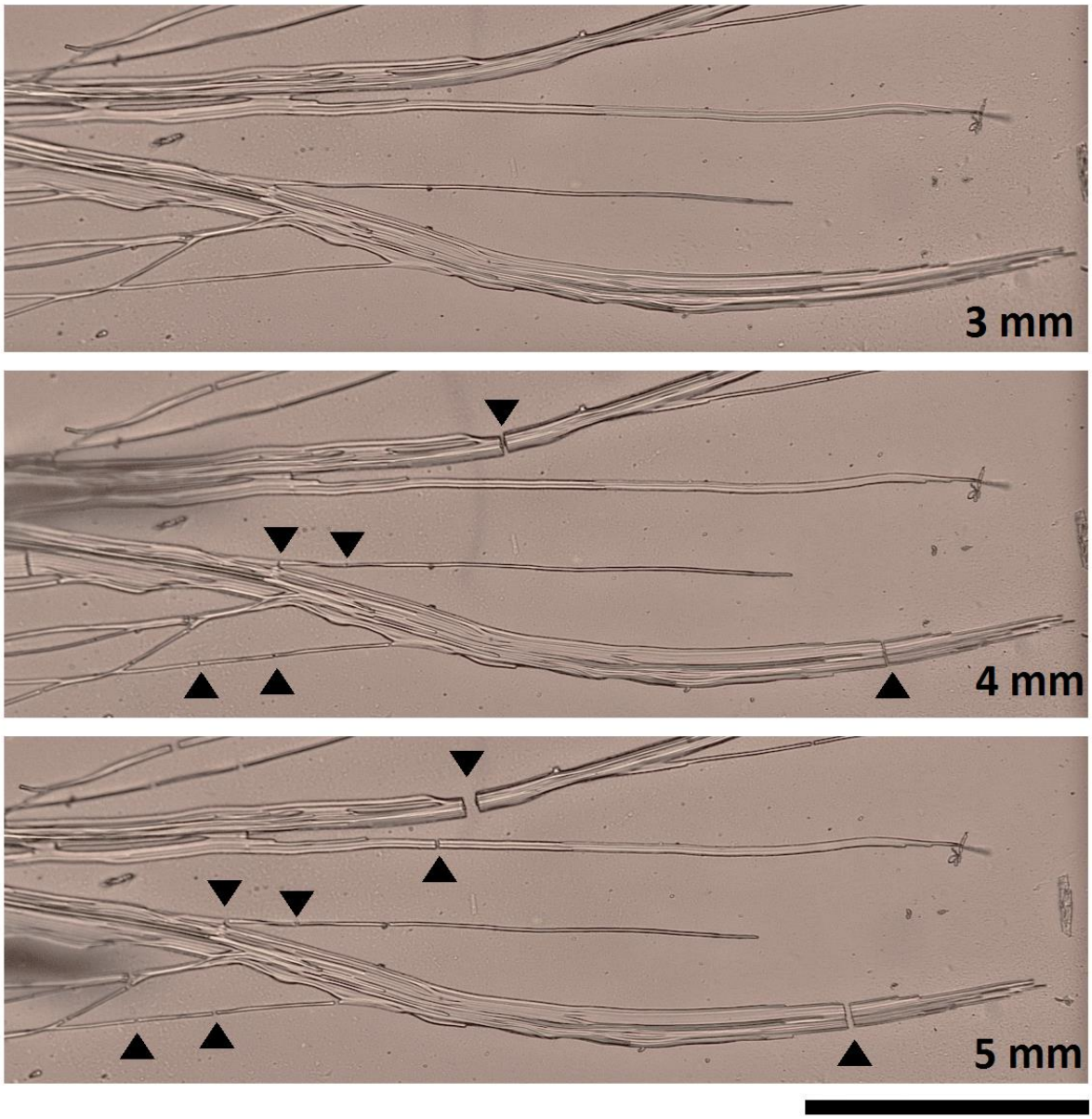

Figure 3.13 A representative example of hyphal breakage after mechanical stretch in *E. festucae* Δ*midA*-20 grown on PDA with 50 mM $CaCl_2$. The colony was grown on a silicon membrane and subjected sequential challenges of 1 mm of mechanical stretch over the 4.5 cm membrane. The first evidence of hyphal breakage was observed after 4 mm of stretching. The black arrows indicate breakage sites on hyphae. Images were obtained using Olympus bright field microscopy with a 20X objective lens. The scale bar shows 200 µm. Images are representative of three biological and three technical replicates grown on individual stretching frames. The scale bar shows 200 µm.

E. festucae Δ*midA* complement strains Comp-20 and Comp-36 were also subjected to mechanical stretching in the presence or absence of calcium to confirm the complementation of *midA* in mutants and thus restoration of cell wall plasticity while under mechanical stress. The complement strains were grown in triplicate on individual stretching frames using either

PDA with and without 50 mM $CaCl_2$ supplementation. The cultures grown under no calcium supplementation were mechanically stretched 1 mm each time until hyphal breakage was observed, whereas cultures grown under PDA with 50 mM $CaCl_2$ were stretched 3 mm each time until hyphal breakage was noted. The *midA* complement strains exhibited the same plasticity under mechanical stretch as the wild type. Hyphae of cultures grown under PDA consistently broke after 3 mm of mechanical stretch, whereas hyphae of cultures grown under PDA with 50 mM $CaCl_2$ broke beyond 12 mm or 13 mm of mechanical stretch. The hyphal breakage points of *midA* complement strains are given in Table 3.6.

Table 3.6 Hyphal breakage points in *E. festucae* Δ*midA* complemented strains Comp-20 and Comp-36 grown on PDA or PDA plus 50 mM $CaCl_2$. The cultures grown under PDA were stretched in 1 mm increments, whereas cultures grown under PDA plus 50 mM $CaCl_2$ were stretched in 3 mm increments until 12 mm, and thereafter in 1 mm increments. From each culture, three single, straight horizontal hyphae were selected and examined. For evidence of consistent hyphal wall breakage, all three hyphae were observed to be broken at least in one location. Imaging was done between each stretching interval using an Olympus BX50 microscope with a 40X objective.

Replicate ID	Maximum stretch (mm)	
	PDA	PDA + 50 mM $CaCl_2$
Comp-20	3	12
Comp-20	3	13
Comp-20	4	13
Comp-36	3	13
Comp-36	3	13
Comp-36	3	13

3.2.4. The Role of MidA in Compartment Division in of *E. festucae* Hyphae after Stretch

In the previous section (see Section 3.4.1) I investigated the radial growth rates (mm per day) of *E. festucae* WT, Δ*midA* and *mid1*-complemented strains to understand the role of extracellular calcium in mycelial growth in culture. The results showed that while the addition of increasing amounts of $CaCl_2$ in PDA caused a small reduction in the growth rates of WT and complement colonies, all $CaCl_2$ concentrations tested restored the reduced radial growth rates of Δ*midA* strains, where optimal growth rate for Δ*midA* strains was achieved

with 50 mM $CaCl_2$ in PDA (Figure 3.10). These findings indicated that calcium played an important role in regulating mycelial growth of *E. festucae*, however its role in hyphal compartmentalization is not known. To understand the effect of extracellular calcium in hyphal compartmentalization, *E. festucae* WT, Δ*midA* and complement strains, the same strains were grown on stretching frames under either PDA or PDA with 50 mM $CaCl_2$, and hyphal compartment division compared between strains. For this, cultures of each strain were grown on three individual stretching frames and incubated for three d prior to imaging and from each culture, three hyphae were examined for compartment numbers. On each hypha, the compartment numbers were counted along the first 500 µm of each hypha and compared, which is approximately 200 µm shorter than the hyphae tracked in *E. festucae* WT grown on PDA with 50 mM $CaCl_2$. This was due to short hyphal lengths of *E. festucae* Δ*midA* cultures grown under PDA with no supplement. None of the cultures received mechanical stretching. There were no significant differences in hyphal compartment numbers between WT and *mid1*-complemented strains that were grown under PDA or PDA with 50 mM $CaCl_2$ (Figure 3.14). In contrast, in *E. festucae* Δ*midA* strains there was a trend suggesting that compartment numbers slightly increased in cultures grown under PDA with 50 mM $CaCl_2$ when compared with the same strains growing on PDA alone, however this was not statistically significant (Figure 3.14).

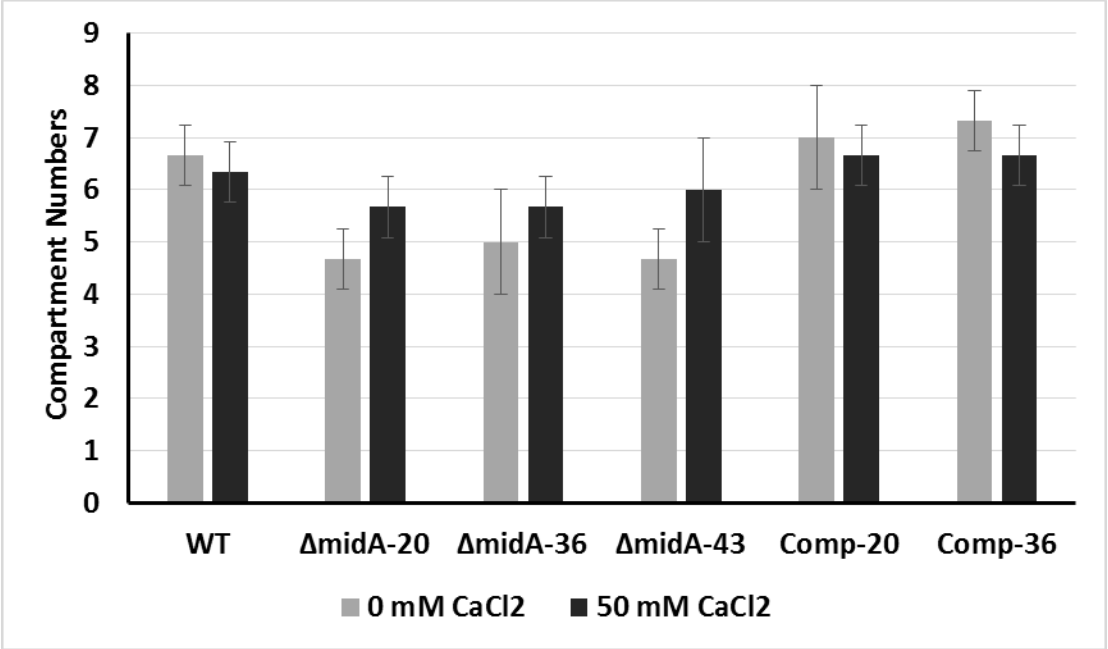

Figure 3.14 Comparison of compartment numbers in the first 500 µm of hyphae in cultures of *E. festucae* WT, Δ*midA*-20, Δ*midA*-36, Δ*midA*-43, Δ*midA*-20 complement (Comp-20) and Δ*midA*-36 complement (Comp-36). The cultures were grown on randomized individual stretching frames using either PDA or PDA with 50 mM $CaCl_2$ and incubated for three d. For each strain, three hyphae were examined. Error bars indicate the standard deviations.

The result showed that presence of additional $CaCl_2$ in PDA did not change the compartment numbers in *E. festucae* WT, Δ*midA* or complement hyphae under no mechanical stretching.

3.2.5. The Effects of Supplemental Calcium on Division of Intercalary Compartments in *E. festucae* WT and Δ*midA* Mutants

My results showed that 50 mM $CaCl_2$ in PDA rescued the reduced radial growth rates of *E. festucae* Δ*midA* cultures and increased the elastomeric potential of WT, Δ*midA* and complement hyphae under mechanical stretching. Next, to determine the impact of MidA on responses to mechanical stretching and thus intercalary growth in *E. festucae*, WT, Δ*midA* and complement strains were grown on stretching frames using either PDA with no supplement or PDA with 50 mM $CaCl_2$, and then subjected to mechanical stretching as described in Section 2.7.1 to see their intercalary growth capacity. However, due to the more fragile hyphal morphology observed in all strains in the absence of extracellular calcium, the mechanical stretching was applied 2 times over 6 h, in 3 mm amounts each time to observe effects on the compartmentalization of hyphae.

The cultures of the same strains of *E. festucae* WT, Δ*midA* and complements used in the elastomeric potential assessment were grown on stretching frames under either PDA or PDA with 50 mM $CaCl_2$ and incubated for three d. For each strain, two stretching frames were set up with cultures and from each culture, one hypha was tracked for compartmentalization. The initial length of tracked hypha was measured until the C-6 compartment. The hyphae were not tracked to the 11^{th} compartment as before, since Δ*midA* strains produced shorter hyphae in the absence of extracellular calcium that could not be tracked beyond compartment 6. After the mechanical stretching, new compartments were recorded, and compartmentalization was calculated using the formula described in Section 3.3. The compartmentalization rate of strains in the presence or absence of 50 mM $CaCl_2$ were compared to understand the effect of extracellular calcium on formation of new compartments in hyphae in response to mechanical stress.

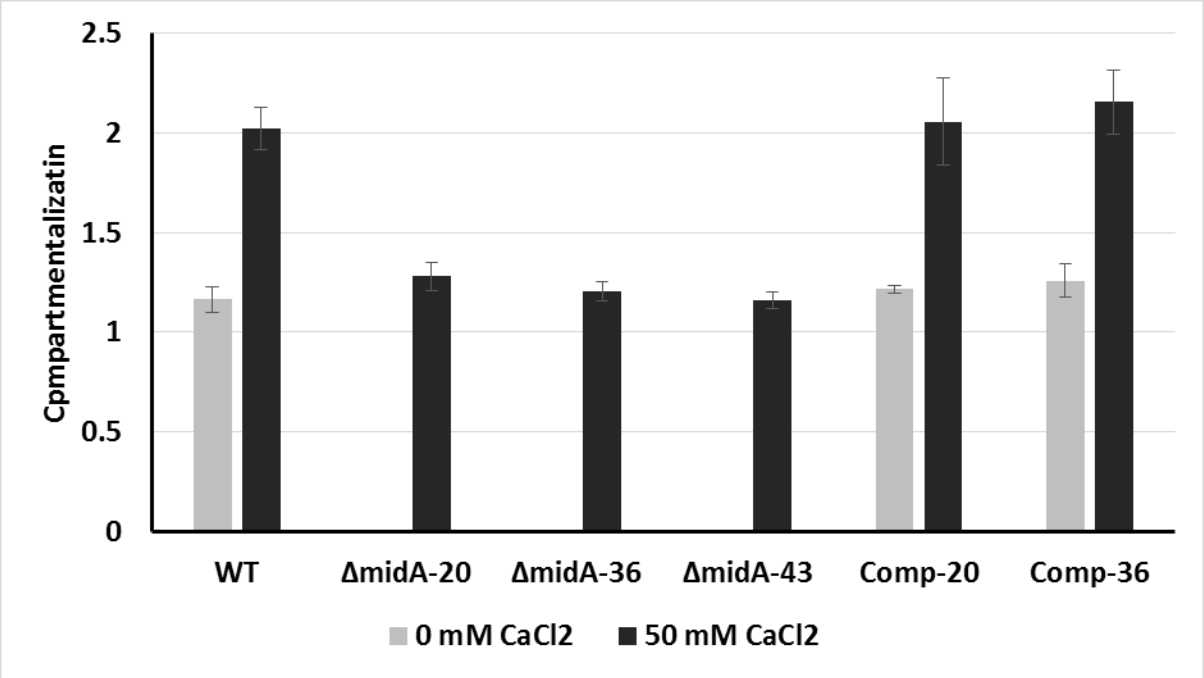

Figure 3.15 Comparison of hyphal compartmentalization in cultures of *E. festucae* WT, Δ*midA*-20, Δ*midA*-36, Δ*midA*-43, Δ*midA*-20 complement (Comp-20) and Δ*midA*-36 complement (Comp-36). The cultures were grown on randomized individual stretching frames using either PDA or PDA with 50 mM $CaCl_2$ and incubated for three d. For each strain, two cultures were prepared, and one hypha was tracked on each culture. The cultures were subjected to 6 mm of mechanical stretching, applied in 3 mm amounts every 3 h. Compartmentalization was calculated using the formula described in Section 3.3. Error bars indicate the standard deviations. The compartmentalization data of Δ*midA* strains could not be obtained due to very fragile hyphae in the absence of 50 mM $CaCl_2$ in PDA.

As shown in *E. festucae* WT, the presence of 50 mM $CaCl_2$ during incubation increased hyphal compartmentalization after mechanical stretching compared to cultures grown on PDA alone (Figure 3.15). In the absence of supplemental calcium, although the tracked hyphae remained intact in both WT cultures, several other hyphae showed breakages after the first and the second mechanical stretching, supporting our previous findings on *E. festucae* WT hyphal elastomeric potential in the absence of $CaCl_2$ (Figure 3.8). However, addition of 50 mM $CaCl_2$ in PDA restored their intercalary growth ability, since they were able to undergo 6 mm of stretching, applied in 3 mm amounts every 3 h. In the absence of 50 mM $CaCl_2$, *E. festucae* Δ*mid*A strains could not be mechanically stretched to 3 mm without snapping, therefore their compartmentalization could not be calculated. In the presence of 50 mM $CaCl_2$ in PDA, compartment formation in *E. festucae* Δ*midA* hyphae was the same as WT growing without supplemental calcium, and significantly lower than WT undergoing stretch in the presence of calcium. There were no differences between WT and *mid1*-complemented strains in the presence or absence of supplemental calcium. These data

confirm that extracellular calcium is critical for compartmentalisation in *E. festucae* in response to mechanical stretch and that MidA is required for this response.

3.3. Discussion

A major gap in our understanding of *E. festucae* colonisation of grasses is how the endophyte switches from tip growth in the host shoot apex to intercalary growth in developing leaves. Previous experiments conducted *in vitro* indicate that the stimulus may be mechanical stretch, which extends hyphal length and induces intercalary compartment division (Ariyawansa, 2015). Identification of the mechanisms through which mechanical forces are sensed, and intercalary growth induced, will provide further insight into *E. festucae* plant colonisation processes and a better understanding of this important symbiosis.

Previous research conducted on *E. festucae midA* deletion mutants suggested a role for MidA in polar growth in culture and intercalary growth in plants. The current hypothesis is that *E. festucae* MidA, a homolog of the *S. cerevisiae* Mid1 stretch activated calcium permeable channel, senses mechanical stretch in the membrane and regulates calcium influx through the HAC to enable compartment division and cell wall synthesis to occur. In this chapter, the infectivity of *E. festucae* MidA mutants, and their ability to colonise the shoot apex and intercalary growth zone of *L. perenne* was characterised. I also investigated the impact of MidA function and supplemental calcium on intercalary compartment division and cell wall plasticity in response to mechanical stress *in vitro*.

3.3.1. Deletion of *midA* in *E. festucae* did not Affect the Infection Frequency of *L. perenne*

Ariyawansa had previously reported that *E. festucae* Δ*midA* strains colonise the shoot apex similarly to wild type, but were poor colonisers of the host leaf expansion zone (Ariyawansa, 2015). On the basis of his findings, I elected to quantify host infection rates by testing inoculated plants using tillers cut through the crown of the plant which included the shoot apex. The results of this study showed that there were no differences between *E. festucae* WT, Δ*midA* and complementation strains with respect to host infection rate, indicating that the MidA is not essential for host invasion when artificially inoculated into seedlings. This involved inserting mycelium from cultures grown in axenic culture into an incision in the shoot apex of ryegrass seedlings (Latch and Christensen, 1985). Hyphae grow predominantly at the tip in the host shoot apex (Christensen et al.,2008), and this suggests that tip growth in the Δ*midA* mutants, although impaired in culture (Ariyawansa, 2015), is nevertheless adequate for endophyte colonisation of the host shoot apex. This outcome was different to the results of Ariyawansa (2015), who found that the Δ*midA* deletion mutants were not as

infectious as the other strains. The reason for the difference may be due to the host tissues selected for analysis the two studies. I used tillers cut through the crown (containing the shoot apex) and he used tillers cut 0.5 cm above the shoot apex in the leaf expansion zone. Endophyte testing of this tissue likely underestimated the number of infected plants in the Δ*midA* mutants.

The function of Mid1 homologues in other filamentous fungi during host colonization has been studied. In the maize pathogen *G. zeae* although *mid1* mutants were slower to infect the host, loss of *mid1* did not affect the wheat colonization pattern compared to WT (Cavinder et al., 2011). Whereas in *C. purpurea,* loss of *mid1* resulted in failure to infect rye florets and unusual hypherbanching in the rye ovaries, where the inoculation took place, suggesting that *C. purpurea* Mid1 is required for tissue invasion (Bormann et al., 2009). In contrast, *B. cinerea mid1* functional studies showed that infection rates of mutants were similar to WT in bean plants even though *mid1* mutants showed reduced growth rates in culture (Tudzynski et al., 2013). These findings suggest that Mid1 is involved in host infection in some, but not all, filamentous fungi. In *E. festucae,* current findings indicate that MidA does not directly regulate the plant infection rates but does regulate which tissues can be invaded. The difference in findings related to Mid1 function during host colonization of filamentous fungi might be arising from the type of tissues investigated in the studies, where some tissues grow more rapidly than others, requiring more calcium influx during fungal colonization.

3.3.2. Deletion of *midA* in *E. festucae* did not Affect the Plant Phenotype of *L. perenne*

Next, to understand the role of MidA on the phenotype of the symbiotum, *L. perenne* plants infected with *E. festucae* WT, Δ*midA* or *mid1*-complemented strains were evaluated for their phenotypes by comparing tiller numbers and lengths. Tiller numbers did not show a consistent difference across the plants infected with *E. festucae* WT or the Δ*midA* strains (Figure 3.3). Although difficult to quantify, in plants infected with Δ*midA* strains, the tillers consistently appeared to be more thin and fragile, and were easily squashed when pressed against the nitrocellulose membranes for tissue print immunoassay. This phenotype was not investigated further due to time constraints, but warrants further study as it implies that the mutant endophytes altered host architecture to some degree. The effect was not seen in wild type or complemented strains. In the previous study, no phenotype differences in plants infected with *E. festucae* WT, Δ*midA* and complement strains were reported (Ariyawansa,

2015). Similarly in *B. cinerea*, the *mid1* deletion did not show any difference in bean plant phenotypes, forming very similar lesions on beans compared to WT (Tudzynski et al., 2013). The fragile tiller phenotype may be a result of altered lignin content in these tillers, which is a complex polymer of plant cell walls that provides rigidity and defence against pathogen infections (Schenk, 2015). In the future, lignin quantification could be carried out in plant tillers infected with *E. festucae* WT, Δ*midA* and complement strains to understand the effect of MidA loss on plant phenotype in more depth. Another reason for the thin tiller phenotype could be the result of hyphal colonization in the SAM that is defective in moving into developing leaves and possibly hindering plant cell differentiation and expansion in this region. Abnormal colonization patterns of *E. festucae* hyphae in *L. perenne* has been reported to affect the plant phenotype previously. In *E. festucae*, disruption of stress-activated mitogen activated protein (MAP) kinase (*sakA*) has been shown to result in decreased hyphal colonization in plants, stunted plant phenotype and eventually early death of hosts (Eaton et al., 2010). Host stunting due to hyperbranching and increased biomass was reported when *E. festucae proA*, a fungi-unique transcription factor encoding gene, was mutated (Tanaka et al., 2013). However, phenotypic changes due to decreased leaf colonization has not been specifically reported for *E. festucae* and *L. perenne* symbiosis.

3.3.3. Deletion of *midA* in *E. festucae* Reduced Hyphal Biomass in *L. perenne*

A major finding in *E. festucae* Δ*midA* infected grasses is that hyphae are relatively numerous in the SA, but are very sparse in the intercalary growth zone of leaves compared to the wild type (Ariyawansa, 2015). To confirm these results, SA-enriched and leaf-enriched samples were dissected (Figure 2.7) and hyphal DNA relative to plant DNA concentration determined by qPCR in *L. perenne* infected with WT, Δ*midA* and *mid1*-complemented strains. DNA from Δ*midA-20* was not detected in either tissue from any plants suggesting that the plants had lost the endophyte or hyphae were below the levels of detection. In SA enriched tissues, *E. festucae* Δ*midA*-43 DNA concentration was similar to the WT and *mid1*-complemented strains, however tissue infected with Δ*midA*-36 contained statistically less hyphal DNA (Figure 3.4A). This inconsistency could be due to the method used to separate SA-enriched tissues from the surrounding leaves. This involved taking a core of SA-enriched tissues from the centre of the crown using a glass Pasteur pipette, however since some tillers were smaller than the others, it is possible that the core taken included more of the surrounding leaf tissues in some plants than others, which may have affected the hyphal biomass findings. Due to the inconsistency between strains in these results, I was not able to draw a firm conclusion on the

effects of *midA* deletion on hyphal density in the SA or to compare the results with the previous non-quantitative confocal microscopy study that suggested that *midA* deletion mutants had similar hyphal density to the wild type in the SA. (Ariyawansa, 2015). In the future, inconsistencies between samples could be overcome by dissecting SA enriched region from the surrounding leaf tissues by using a laser microtome method before the flowering, to avoid the surrounding leaf tissue as much as possible. For this, EGFP expressing *E. festucae* strains could be used to confirm colonization in different parts of tissues and successful dissection. The samples could be pooled together as was done in this study to ensure sufficient genomic DNA.

Conversely, the hyphal DNA concentration of Δ*midA* strains in the leaf tissues surrounding the crown was more uniform and *E. festucae* Δ*midA*-36 and Δ*midA*-43 DNA concentration was markedly reduced compared to WT (Figure 3.4B). Relative hyphal DNA concentration measurements nevertheless confirmed the visual observations of Ariyawansa (2015) and suggested that colonisation by Δ*midA* hyphae was very low in the intercalary growth zone. DNA levels were so low in Δ*midA*-36 that they were below detectable levels, suggesting that there were very few or no hyphae in these tissues. This result provides further evidence that MidA is required for colonizing the intercalary growth zone of the grass host, and that calcium import is important for intercalary hyphal growth.

The reduced *E. festucae* Δ*midA* hyphal biomass could also be the result of the fewer nuclei in the mutant hyphae, which are shorter and less compartmentalized even when supplemented with extracellular calcium, compared to WT. Therefore, it is possible that the hyphal biomass of Δ*midA* strains was underestimated. Nevertheless, the fact that surrounding leaf tissue is still colonized by *E. festucae* Δ*midA* (even though colonization is reduced) implies that *E. festucae* Δ*midA* is still able to perform intercalary growth to a limited extent. This is supported by the previous study, where several intact *E. festucae* Δ*midA* hyphae were observed in the longitudinal tiller sections, along with broken hyphae and empty spaces in this tissue (Ariyawansa, 2015).

Potential factors underlying this pattern of colonization could be the presence of osmotic stabilizers in apoplastic fluid, such as sugars and amino acids, plus ions such as K^+, $Fe^{2/3+}$, and most importantly, Ca^{2+}, that may act as an extracellular supplement for *E. festucae* Δ*midA* that enables it to perform intercalary growth in plants (O'Leary et al., 2014). Sucrose is an osmotic stabilizer that is used to supplement media to create a hypertonic environment for cells with sensitive cell walls (Martinez, 1979). Amino acids are known to regulate the

osmotic balance inside the cells to protect proteins from denaturing (Arakawa, 1985). High-performance liquid chromatography (HPLC) analysis of apoplastic fluids of several plants showed amino acid concentrations ranging from 2 mM (*Zea mays*) to 10 mM (*Vicia faba*), and sugar molecules such as sucrose and hexose concentrations between 0.2 mM to 5.2 mM (Lohaus, 2001). In *Phaseolus vulgaris*, apoplastic fluid was found to contain sucrose (between 100-150 µM) and several amino acids (between 100-200 µM) (O'Leary et al., 2016).

Calcium concentration in the apoplastic fluid of several plant species has been investigated previously and approximately 200 ppm of Ca^{2+} concentration was reported in *P. vulgaris* (O'Leary et al, 2016), 0.7 mM in *V. faba*, 2.3 mM in *H. vulgare* and 0.6 mM in *Z. mays* (Lohaus, 2001). In the future, *L. perenne* apoplastic fluid content could be investigated for sugar, amino acid and ion concentrations to understand its potential as osmotic stabilizer and to provide sufficient extracellular calcium concentrations for intercalary growth of *E. festucae*. In this study, extracellular supplementation using $CaCl_2$ was shown to restore reduced growth rates of *E. festucae* Δ*midA* (Figure 3.10), and same finding was reported in the previous study along with the finding that the osmotic stabilizer Sorbitol could rescue reduced growth rates of *E. festucae* Δ*midA* (Ariyawansa, 2015). In the future, the role of MidA during colonization of intercalary growth zones in plants should be addressed by deleting the *S. cerevisiae cch1* homolog together with *midA*, as Cch1 is part of a HACS complex responsible of calcium uptake in yeast (Locke et al., 2000). Together, these findings indicate that *E. festucae* MidA is required for colonizing the host intercalary growth zone.

The main limination during the investigation of hyphal biomass was the separation of SA-enriched tissues from surrounding leaf tissues, which proved to be difficult and sometimes introduced inconsistency between tillers. The obtained samples were very small and difficult to handle, also during the extraction using Pasteur pipette tips, small amounts of tissues were lost or damaged. The differences in tiller sizes across plants introduced size differences in SA-enriched and surrounding leaf tissues. The Pasteur pipette tip extraction method was preferred because it made rapid tissue extraction possible and practical. Alternatively, each tiller could be dissected under microscope to enable better distinction of SA-enriched and surrounding leaf tissues. However, given the number of samples to be handled this would prove non-practical and time consuming.

3.3.4. Extracellular $CaCl_2$ Suppelementation Increased the Elastomeric Potential of *E. festucae* WT

In the next part of my study, I investigated the elastomeric potential of *E. festucae* WT hyphae under mechanical stress using PDA with or without $CaCl_2$ supplementation, to understand the impact of extracellular calcium on hyphal cell wall plasticity. For this, *E. festucae* WT cultures were grown on stretching frames under PDA or PDA with 50 mM $CaCl_2$ prior to stretching. The cultures grown without calcium were hypothesized to be more fragile and were stretched in smaller increments (1 mm as opposed to 3 mm increments). *E. festucae* WT grown on PDA were able to undergo 1 mm of stretching 2 times consecutively, and showed consistent hyphal breakage at 3 mm of stretching in total, where three separate hyphae of same culture growing horizontal to the stretching plane were broken in at least one location (Figure 3.8). Whereas *E. festucae* WT grown with 50 mM $CaCl_2$ were able to undergo 3 mm of mechanical stretching 4 times sequentially, showing consistent hyphal breakage at 13 mm (Figure 3.9). These findings showed that extracellular calcium is crucial for cell wall plasticity of *E. festucae* during mechanical stretching. In the previous study (Ariyawansa 2015), the amount of mechanical stretching that *E. festucae* hyphae can tolerate has been shown to be no more than 5 mm applied over the 4.5 cm silicon membrane at one time, as this amount damaged the cell membranes (as shown by FM4-64 staining), and 8 mm of mechanical stretching at one time was found to cause cell wall damage in hyphae (Ariyawansa, 2015). However, the effects of extracellular calcium on the elastomeric properties of hyphae has not been tested in *E. festucae* to date. Calcium is a crucial signal molecule in eukaryotes for regulating many molecular pathways. The effect of extracellular calcium on the cell wall has been studied in *B. cinerea*, where cultures were grown in the presence of different extracellular $CaCl_2$ concentrations to observe the changes in cell wall weight and cell wall composition (Chardonnet et al., 1999). It was found that although the extracellular $CaCl_2$ did not affect the growth rates of cultures significantly, cell wall dry weights increased exponentially with the increasing concentrations of $CaCl_2$ (Chardonnet et al., 1999). Moreover, extracellular $CaCl_2$ was found to change the composition of the *B. cinerea* cell wall, where decreases in neutral sugars and cell wall proteins were observed with increasing $CaCl_2$ (Chardonnet et al., 1999). This was thought to be due to effects of Ca^{2+} on cell wall remodelling enzymes such as β-glucan synthases (Chardonnet et al., 1999). In a study conducted on *C. albicans*, expression of two cell wall remodelling enzyme encoding genes, *utr2* and *crh11*, was found to be regulated by Ca^{2+}-calmodulin-dependent

serine/threonine protein phosphatase (Cna1) (Ene, 2015). Moreover, when *C. albicans* wild type and *cna1* mutants were exposed to osmotic stress in medium rich in lactate, the wild type cells showed resistance to osmotic stress by surviving over time, however Δ*cna1* cells produced much fewer colonies compared to WT (Ene, 2015). It was stated that in *C. albicans*, cell wall plasticity during osmotic shock was controlled by the calcineurin pathway, however the effects of extracellular calcium on cell wall elasticity have not been tested (Ene, 2015). Therefore, mechanisms in which extracellular Ca^{2+} regulates cell wall synthesis or remodelling enzymes in fungi are still unknown. In the future, to understand the role of Ca^{2+} on cell wall plasticity, and to uncover the molecular mechanisms controlled by this ion, a transcriptomics study using *E. festucae* cultures grown under different $CaCl_2$ concentrations and subjected to mechanical stretching could be conducted.

3.3.5. Extracellular $CaCl_2$ Increased The Elastomeric Potential of *E. festucae* Δ*midA*

Following the *E. festucae* WT mechanical stretching, the elastomeric potential of *E. festucae* Δ*midA* hyphae was investigated under mechanical stress using PDA with or without $CaCl_2$ supplementation, to understand the impact of the putative MidA calcium channel regulator on hyphal cell wall plasticity. For this, *E. festucae* Δ*midA* cultures were grown on stretching frames under PDA or PDA with 50 mM $CaCl_2$ prior to stretching. All cultures, regardless of incubation with or without $CaCl_2$ supplementation, were subjected to 1 mm of mechanical stretching at one time. Since loss of *midA* was hypothesized to result in more fragile hyphae compared to WT even in the presence of 50 mM $CaCl_2$,calcium uptake would be presumably facilitated by LACS instead of HACS, which does not possess a stress activated calcium channel (Cavinder et al., 2012). *E. festucae* Δ*midA* cultures grown on PDA were not able to tolerate even 1 mm of stretch without hyphal breakage (Figure 3.12). Whereas *E. festucae* Δ*midA* cultures grown on PDA with 50 mM $CaCl_2$ were able to tolerate a total 3 mm of mechanical stretch, showing consistent hyphal breakage at 4 mm (Figure 3.13) These results showed that 50 mM of extracellular calcium was able to only partially complement the cell wall plasticity of *E. festucae* Δ*midA* mutants. This suggests that in *E. festucae*, cell wall integrity during mechanical stress largely relies on calcium uptake regulated by MidA, which is likely to be functioning as a part of the HACS to facilitate calcium uptake with a Cch1 calcium influx channel homolog. In the future, presence of HACS proteins Cch1, Cmd1, Crz1, and calcineurin complex in *E. festucae* should be confirmed using *S. cerevisiae* and several filamentous fungi homologs as queries in bioinformatics annotations. Increases in

E. festucae Δ*midA* cell wall plasticity with 50 mM $CaCl_2$ supplementation of the growth medium may be through a further calcium uptake pathway such as the Fig1 channel of the LACS, which imports calcium across fungal cell walls from a high (external) to low (internal) concentration gradient (Locke et al., 2001). In *E. festucae*, the influx of extracellular calcium into hyphae has been studied previously in *E. festucae* WT and Δ*midA* mutants growing on PDA plus 50 mM $CaCl_2$ using the calcium sensor GCaMP5 (Ariyawansa, 2015). In the WT, rapid calcium oscillations were detected in the hyphal tips in culture, whereas in *E. festucae* Δ*midA*, the pulses at the hyphal tips were infrequent, and larger in signal amplitude (Ariyawansa, 2015). One hypothesis is that the additional calcium signature is from calcium import through the *E. festucae* FigA homolog of the LACS, which is presumably still functional in the absence of MidA (Ariyawansa, 2015). In *S. cerevisiae*, the LACS protein Fig1 has been found to regulate calcium influx and membrane fusion during mating (Aguilar et al., 2007). In *A. nidulans*, HACS and LACS are thought to function together during vegetative hyphal growth and sexual development, along with regulation of cell wall morphology in culture (Zhang et al., 2013). It was found that growth retardations in *A. nidulans* Δ*fig1*Δ*cch1* and Δ*fig1*Δ*mid1* are much more severe compared to *A. nidulans* Δ*fig1*, suggesting that these systems work together during vegetative growth (Zhang et al., 2013). In the case of HACS and LACS functioning together, in *E. festucae* loss of function in MidA may affect LACS function, which could be one explanation for the partial restoration of cell wall plasticity in *E. festucae* Δ*midA* cultures grown in 50 mM $CaCl_2$ during mechanical stretching. Another explanation for the partial cell wall plasticity restoration in *E. festucae* Δ*midA* cultures could be that the LACS calcium influx channel Fig1, not being a stress activated influx protein, may not facilitate sufficient calcium uptake to sustain cell wall remodelling during mechanical stress. In the future studies, the role of Fig1 during mechanical stretching should be addressed to better understand its contribution and its interaction with the HACS during mechanical stress, and in the cell wall plasticity of *E. festucae*.

3.3.6. Extracellular $CaCl_2$ Increases Compartmentalization in *E. festucae* Hyphae

Following the investigation of elastomeric potential of *E. festucae* hyphae in the presence or absence of extracellular calcium, the intercalary growth ability of *E. festucae* was studied, again, in the presence or absence of $CaCl_2$ to understand the effect of calcium in creation of new compartments after exposure to mechanical stress. For this, *E. festucae* WT, Δ*midA* and

complement strains were cultured on stretching frames and grown under either non-supplemented PDA or PDA with 50 mM $CaCl_2$ and subjected to mechanical stretching. The mechanical stretching was applied twice (3 mm each time) over 6 h, since cell wall plasticity has been observed to decrease in the absence of calcium in all strains. Moreover, hyphae were tracked up to 5th compartment (C-6) to normalize the shorter hyphal lengths observed in the absence of 50 mM $CaCl_2$. The 50 mM $CaCl_2$ supplementation in PDA significantly increased compartmentalization in all strains (Figure 3.15). The compartmentalization of *E. festucae* Δ*midA* strains could not be assessed in the absence of extracellular calcium, since their hyphae showed consistent breakage after 3mm of mechanical stretching, thus the experiment could not be carried out further. However, addition of 50 mM $CaCl_2$ in PDA increased their elastomeric potential and compartmentalization was observed after 6 mm of mechanical stretching, applied in 3 mm each 3 h (Figure 3.15). However, the finding that compartmentalization of *E. festucae* Δ*midA* not being restored to WT levels even in the presence of 50 mM $CaCl_2$ suggested that MidA is crucial for the intercalary growth ability of *E. festucae*. During this experiment, WT hyphae showed hyphal breakages in two cultures observed, however the intercalary growth ability was assessed on intact hypha tracked on each culture. The previous findings on elastomeric potential of *E. festucae* WT have shown that after 3 mm of mechanical stretching, eight cultures out of nine showed consistent hyphal breakages in the absence of extracellular calcium. In the investigation of intercalary growth capacity, two cultures set up using *E. festucae* WT has shown hyphal breakages after 3 mm of mechanical stretching, however the compartmentalization was tracked on intact hyphae. Overall, these findings pointed to the role of extracellular calcium in intercalary growth capacity of *E. festucae* hyphae. Although intercellular calcium concentrations in host plants during endophyte infection have not been investigated, a study conducted on *Pseudomonas syringae* showed that pathogen infection altered the apoplastic calcium concentrations in *P. vulgaris* leaves (O'Leary et al., 2016). Comparison of apoplastic washing fluid extractions of uninfected and infected *P. vulgaris* leaves showed that calcium concentration in the fluid increased upon *P. syringae* infection, and continued to increase over time (O'Leary et al., 2016). Influx of ions like calcium from apoplastic fluid into the cytosolic space in plants during pathogenic infection is thought to be one of the defence mechanisms against infection (Grant, 2000), however, a reverse influx of calcium into the intracellular tissue suggests suppression of plant defence (O'Leary et al., 2016). In the future, the signalling mechanisms in *E. festucae* triggering the influx of calcium into plant

intercellular spaces could be investigated. Since controlling ion influx is one of the defence mechanisms in host plants, suppression of this mechanism might be regulated by a set of *E. festucae* effector proteins. Deletion of candidate effector genes and analysis of *L. perenne* apoplastic fluid during early and late stages of colonization could shed light on plant endophyte interactions, and investigation of colonization patterns in plants could further point to the role of calcium in intercalary growth.

Another limitation in this project concerned the intricacies of the mechanical stretching machinery. Although this apparatus enabled *in vitro* mechanical stretching of *E. festucae* cultures and imaging under a microscope, it presented several difficulties. For a successful mechanical stretching experiment, single and horizontally straight hyphae are required for imaging convenience and tracking of hyphal compartments. However, finding hyphae that fit these criteria was often difficult, as hyphae tended to grow in multiple directions and became tangled during incubation. To minimize this, the incubation period was set to three d to avoid over-crowding of mycelia. However, the decreased incubation period, in turn, resulted in shorter hyphae where the 11^{th} compartment was close to the culture centre and these were difficult to image under the microscope. Multiple stretching frames were prepared for each mechanical stretching experiment, and had to be processed within a short time frame to avoid introducing differences in the way the cultures are handled, such as exposure to air. Moreover, the tracked hyphae, before and after mechanical stretching, had to be identified correctly by comparing the hyphae with the microscopy images taken at the previous stretch step. The moisture level of supporting PDA blocks had to be sufficiently high to keep the cultures viable, but not too high to allow the hyphae to shift on the silicon membrane.

In the future, experiments the test the effects of calcium chelating agents (such EGTA), and calcium ion channel inhibitors (such as gadolinium chloride), on the cell wall plasticity of *E. festucae* are needed to confirm the role of extracellular calcium in cell wall plasticity. Furthermore, upregulation of cell wall remodelling enzymes by calcium supplementation of media, and during mechanical stretch, will also be informative. Moreover, imaging using Calcofluor white and FM4-64 are also needed to determine when cell wall architecture and the plasma membrane of *E. festucae* respectively, are damaged by mechanical stretching.

3.3.7. Conclusions and Major Impact

This study has attempted to shed light on the importance of calcium, and role of the putative mechanically-activated calcium channel complex protein MidA in *E. festucae* during intercalary growth in plants and cell wall plasticity in culture. The findings suggest that MidA

is required for colonizing the intercalary growth zones in grass leaves, and that extracellular calcium is necessary for cell wall plasticity and compartmentalization in *E. festucae* under mechanical stress. The work has profound implications for how fungal cell walls grow. Calcium is essential for hyphal growth and has long been shown to be present in hyphae in a tip-high gradient, effectively present at highest concentrations at the region of tip extension. This study suggests that cell wall plasticity is mediated by calcium. This may occur directly, or through another mechanism such as the rapid upregulation of cell wall remodelling enzymes. As the tip extends, and the calcium concentration reduces, the nascent wall presumably becomes less plastic and is able to strengthen. When considering the role of calcium in cell wall plasticity and intercalary growth after mechanical stretch, the simplest explanation is that mechanical stretch stimulates calcium influx along the length of the hypha. This has not yet been tested but a pilot study conducted by Ariyawansa (2015) has shown that mechanical disturbance of an *E. festucae* culture expressing the Ca^{2+}sensor gCAMP5 (by squashing the culture under the cover slip) resulted in calcium pulses along the length of filaments, suggesting that this is a plausible explanation. Assuming this is correct, then all the processes of hyphal growth normally observed at the tip may be invoked by mechanical stretch, including cell wall plasticity during host cell expansion in the absence of light, followed by cell wall strengthening during phases of rest under daylight. To develop these findings further, *E. festucae* expressing calcium sensor GCaMP5 could be subjected to mechanical stretching to observe the role of calcium in regulating cell wall plasticity during mechanical stress. To my knowledge this is the first time that the role of MidA and extracellular calcium on cell wall plasticity of *E. festucae* in fungi under mechanical stress has been studied.

4. Gene Expression Responses of *Epichloë festucae* Hyphae to Mechanical Stretch in Culture *via* Transcriptomics

The molecular mechanisms that are involved in polar vegetative hyphal growth in filamentous fungi are known to some extent (Steinberg, 2007, Requelme, 2018). It is thought that hyphal tip growth is mediated by rapid trafficking of vesicles that transport cell wall components to the growing tip and that polarity is determined by the Spitzenkörper complex and turgor pressure (Steinberg, 2007).

Although the Cell Wall Integrity (CWI) pathway and High Affinity Calcium Uptake System (HACS) are thought to be involved in regulation of intercalary growth in *E. festucae* (Ariyawansa, 2015), other molecular mechanisms that respond to mechanical stress and initiate intercalary growth are yet to be discovered. The objectives of this research were to understand the molecular mechanisms that are responsive to mechanical stretch, including those that mediate intercalary growth in *E. festucae in vitro*.

To gain this understanding, *E. festucae* cultures were grown, the hyphae mechanically stretched using the stretching machinery, and these hyphae collected at different time points to determine the early (immediate) and late gene responses to mechanical stress. To do this, wild type *E. festucae* Fl1 cultures were grown *in vitro* on amino-coated silicon membranes suspended in a customised hyphal stretching frame as described in Section 2.7.1. Nutrients were supplied to the growing culture from above using a PDA block supplemented with 50 mM $CaCl_2$. Additional calcium was supplied as I previously showed that this was essential for induction of intercalary growth in *E. festucae* after mechanical stretch (Section 3.3). After 3 d of growth, each culture was examined by microscopy (Section 2.7.1) to confirm that mechanical stretch had increased the length of the compartments as expected. Three hyphal stretching treatments were examined. In the first, hyphae were harvested immediately after stretch (approximately 10 min) to determine early responses (ER) to mechanical stretch. In the second, hyphae were stretched, and the colonies incubated for 3 h to identify genes involved in initiating intercalary growth (late response [LT]). The third was the control where all the sample handling of the test treatments was replicated, excluding the stretching. As *E. festucae* hyphae are mostly orientated in the direction of leaf growth, only those hyphae growing parallel to the length of the silicon membrane were used in the transcriptomics experiments (see Section 2.7.1).

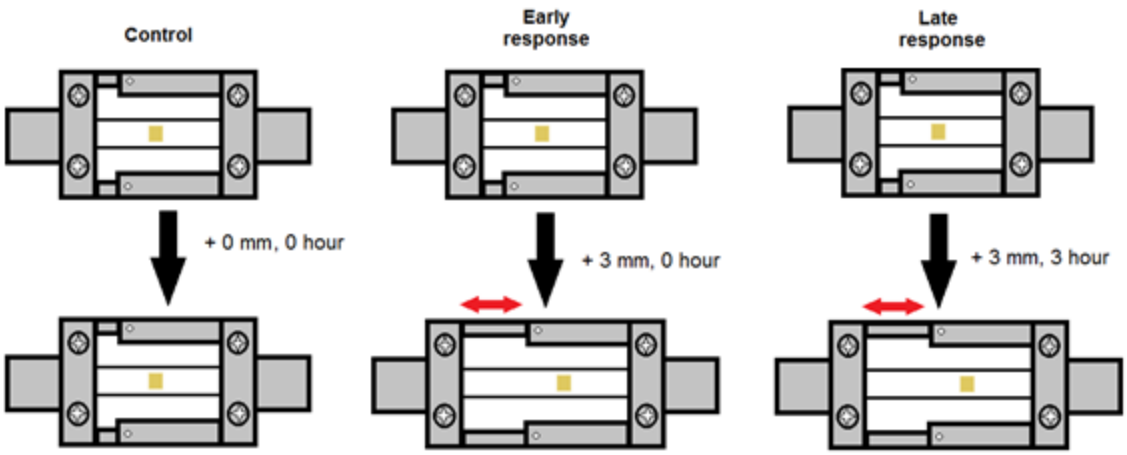

Figure 4.1 Schematic diagram showing the experimental design for investigation of gene expression profiles in *E. festucae* hyphae in response to mechanical stretch. There were 3 pseudo-replicates for each treatment group (control, early and late responses). Each pseudo-replicate consisted of 12 pooled technical replicates (Section 3.7). Each technical replicate was from one colony growing individually on a stretching frame. The stretching frames were numbered and, prior to inoculation, each frame was randomly allocated to a treatment to avoid any frame bias. The amount of stretch applied (mm) and the incubation time after stretch (h) is shown for each treatment (black arrows). The red arrows show where stretch was applied.

The three treatment groups were represented equally in each experiment by cultures on two stretching frames. After the treatments were applied, the cultures were harvested and snap frozen for later total RNA extraction. This was repeated six times and the cultures from six repeats were pooled to create each pseudo-replicate as described in Section 3.7 (Figure 4.1). The total RNA was extracted as described in Section 2.10. Strand-specific libraries were constructed, and the sequencing was carried out on an Illumina HiSeq4000 PE101 system using two lanes (Illumina, USA) by Beijing Genomics Institute (BGI Tech Solutions Hong Kong Co., Ltd.). The RNA-sequencing data were put through quality control analysis, the adapter sequences trimmed, and the reads mapped to the *E. festucae* Fl1 genome assembly (version) 2011-03 on the Kentucky University *E. festucae* genome project database (Schardl et al, 2013) as described in Section 2.9 (Table 4.1). A total of 797, 289, 048 reads were obtained and 796, 898, 882 were mapped against the reference *E. festucae* Fl1 genome. The percentage of mapped reads is given in Table 4.1.

Table 4.1 Average RNA reads, before and after read trimming, from 3 pseudo-replicates in the control, early and late response treatments, and the percentages of reads that mapped to the *E. festucae* FL1 reference genome.

	Number of reads	Number of trimmed reads	Mapped reads (%)
Control	247, 173, 893	247, 064, 741	88
Early Response	252, 154, 704	252, 030, 390	87
Late Response	297, 960, 451	297, 803, 751	88

To investigate the early and late hyphal responses to mechanical stretch, expression of *E. festucae* genes between the control versus the early group, and the control versus the late group, were compared. The threshold for assigning a gene as differentially regulated was an expression fold change of $\geq \pm 1.5$ and a $p \leq 0.05$. The fold changes in this study were not converted to logarithmic scale as the range of gene expression fold change was only between +9 and -3. Using these criteria, 105 (63 up-regulated, 42 down- regulated) genes were differentially regulated in the early response compared to control. In the late response, a larger number of genes (403; 352 up regulated, 51 down regulated) were differentially expressed compared to the control (Figure 4.2A). Far more genes were upregulated in the late response that the early response. Among the differentially expressed genes in the early response, nine genes appeared to be *Epichloë*-unique, and in the late response, 18 were *Epichloë*-unique (Figure 4.2B). Among the differentially expressed genes that were common to both early and late responses, 45 were up-regulated whilst only 13 were down-regulated (Figure 4.2C).

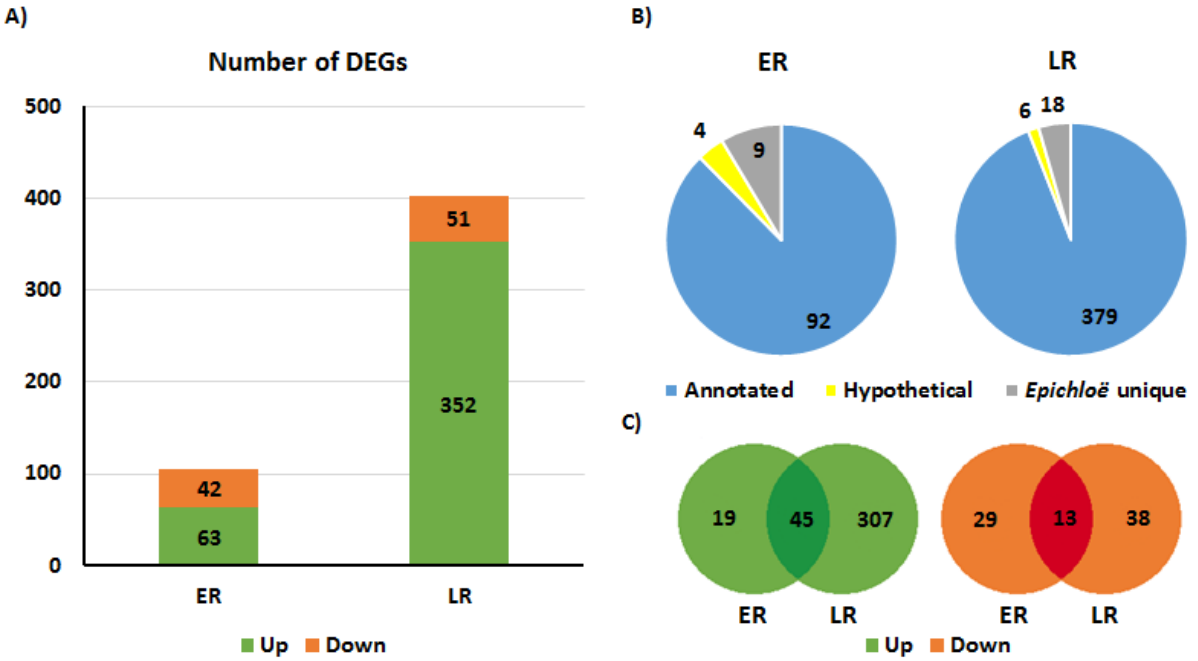

Figure 4.2 RNA-seq results of early (immediate) and late (3 h incubation) responses to mechanical stretch compared to the un-stretched control. A) Numbers of differentially expressed genes (DEG) in both early and late responses compared to control. B) The numbers of annotated, hypothetical and *Epichloë*-unique genes in early and late responses compared to control. C) Upregulated or downregulated genes in common between early vs late responses compared to control. The fold change threshold is $\geq \pm 1.5$, and significance level is $p \leq 0.05$. ER: Early response, LR: Late response. Up: Up-regulated genes, Down: Down-regulated genes.

4.1. Gene Ontology Enrichment Analysis of Differentially Expressed *E. festucae* Genes during Early and Late Responses

To understand overall changes in the metabolism of *E. festucae* on molecular, cellular and biological levels in response to mechanical stretching, differentially expressed genes were analysed using the Gene Ontology (GO) Enrichment Tool (see Section 2.12). The analysis revealed that 22 GO categories were enriched in the early response (Figure 4.3) and 46 GO categories in the late response (Figure 4.4) compared to the control ($p \leq 0.05$). Among them, 13 GO categories were enriched in common to both responses.

4.1.1. Commonly Enriched GO Categories of *E. festucae* in Response to Mechanical Stretch

Both the early and late responses to mechanical stretch were enriched for Nitrate and Nitrite transport (GO:0015706, GO:0015707), Nitrate reductase (GO:0008940) and Nitrate Assimilation (GO:0042128) categories, that are related to nitrogen metabolism. In filamentous fungi and many other organisms, nitrogen metabolism is crucial for growth,

reproduction, secondary metabolism and development (Davis and Wong, 2010; Tudzynski et al., 2014). Another enriched category in both responses, Heme Binding (GO:0020037), is important for respiration, as well as synthesis of amino acids and lipids in fungi, since heme proteins such as cytochromes carry out electron transfer (Philpott, 2006; Poulos 2007). A further category, D-Serine Metabolism (GO:0070178), is thought to be responsible for growth, development and cAMP signalling in soil amoeba *Dictyostelium discoideum* (Ito, 2018). The Molybdopterin Cofactor Binding (GO:0043546) category encompasses proteins that act as cofactors of reactive oxygen species-producing enzymes such as xanthine oxidases (Cultrone, 2005). The Extracellular Region (GO:0005576) category contains proteins involved in structural changes in the outermost layer of the cells, mainly cell wall, as well as interactions with environment such as host tissues, apoplast or surfaces (Prag, 2007).

4.1.2. Uniquely Enriched GO categories in ER to Mechanical Stretch of *E. festucae* Hyphae

In addition to the common early-late GO categories described above, nine further enriched GO categories were unique to the early response (Figure 4.3). Amongst these, Cutinase Activity (GO:0050525) is linked to host colonization in pathogenic fungi such as *Fusarium solani* and *Pyrenopeziza brassicae* (Davies, 2000, Skamnioti 2008, Morid 2009), and Plasma Membrane Fusion during Cytogamy (GO:0032220) category relates to changes in the lipid membrane bilayer during mating or differentiation (Heiman 2000). Related to the enrichment in nitrogen metabolism mentioned above as being common to both early and late responses, the unique early responses also showed enrichment for urea metabolism (GO:0009039, GO:0043419) (Newcomb 2002, Kinghorn 1984). Nickel Ion Binding (GO:0016151) and Molybdenum Ion Binding (GO:0030151) enrichment further suggested regulation of urea and nitrite/nitrate metabolism, as these categories co-occur in GO assessments (GO Consortium, 2017).

In total, 24 *E. festucae* genes with functional predictions were included in the early response under the 22 enriched GO categories (Figure4.4), and all of them were up-regulated after stretching. The differentially regulated genes within each enriched GO category in the early response compared to the control are shown in Figure 4.4. Ten up-regulated genes were listed in both Biological Process and Molecular Function GO categories, so are only shown once in Figure 4.4.

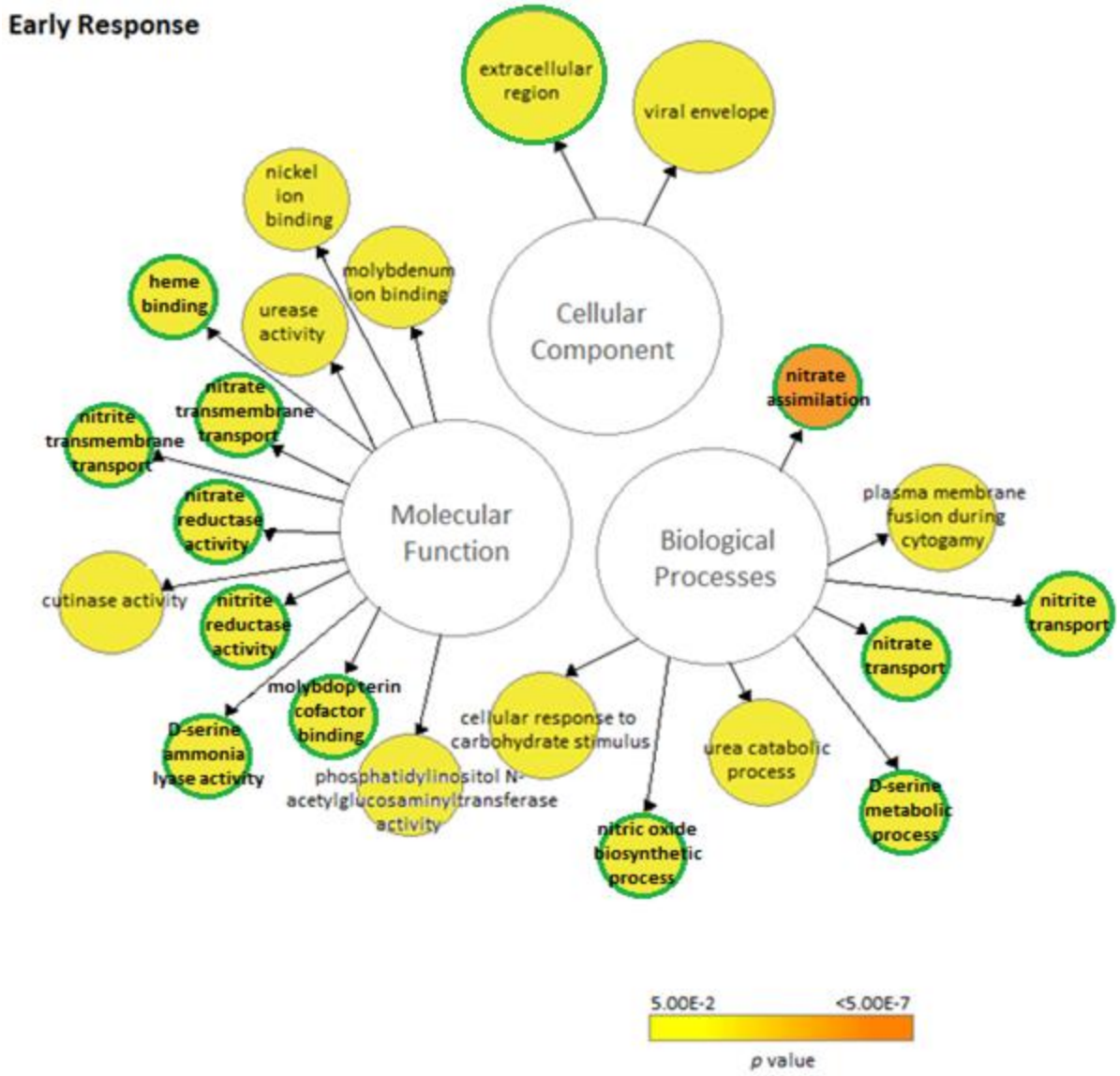

Figure 4.3 Gene Ontology (GO) Enrichment Analysis of genes differentially regulated in the early response to mechanical stretch in *E. festucae* compared to control ($p \leq 0.05$). The categories that were enriched in both early and late responses are circled in green. The circle sizes are arbitrary.

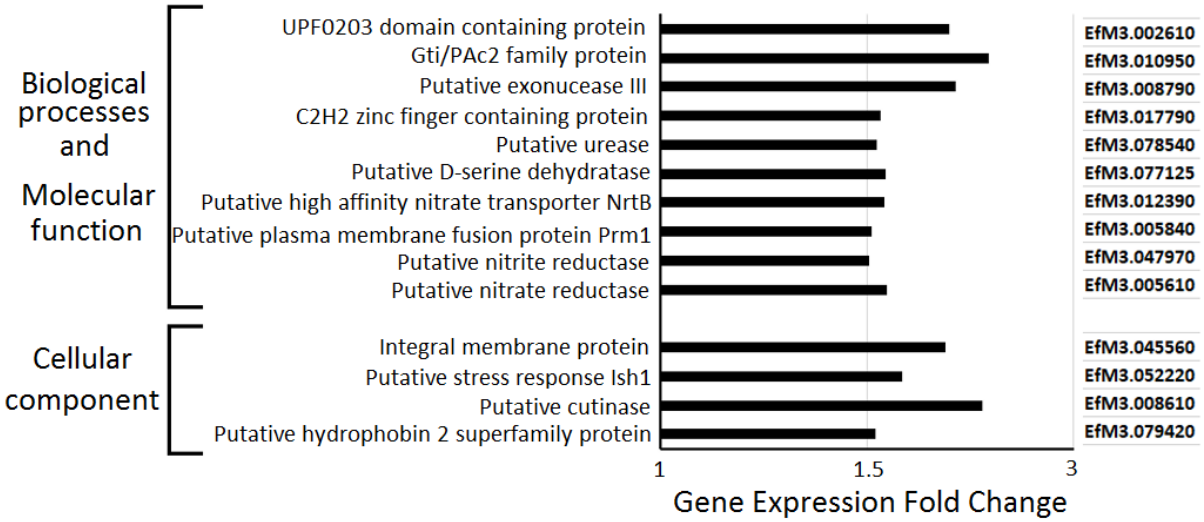

Figure 4.4 *E. festucae* DEGs in each enriched GO category in the early response of hyphae to mechanical stretch ($p \leq 0.05$). The fold change threshold for DEGs is ±1.5. In Biological Processes and Molecular Function categories, 10 genes are up-regulated in common therefore only shown once. GO categories are shown on the left and gene model numbers on the right.

4.1.2.1. Uniquely Enriched GO categories in the Late Response to Mechanical Stretch of *E. festucae* Hyphae

In the late response to mechanical stretch, in addition to 13 enriched GO categories shared with early response, 33 unique GO categories were enriched. These unique categories included 2 in Cellular Components, 12 in Biological Processes and 18 in Molecular Function (Figure 4.5).

Protein and carbohydrate metabolism, citric acid cycle and ammonium transport were among the enriched primary metabolic activities, indicative of growth, reproduction and development in filamentous fungi (Davis and Wong, 2010). Protein metabolism was found to be enriched through Peptide Cross-Linking (GO:0018149) and Serine Type Endopeptidase Activity (GO:0004252). Peptide Cross-Linking Activity refers to the process of protein modification via covalent cross-linking proteins to one another or to sugar molecules to form polymers (Gow et al., 2017). In filamentous fungi, peptide cross linking is crucial for the structural integrity of the cell wall, since glucan branches are cross linked to chitin, which provides rigidity to the cell wall (Iorio, 2008). Serine Type Endopeptidase Activity is a part of protein catabolic metabolism and is responsible for degradation of peptide bonds via the serine residues that serve as nucleophiles at the active site of the enzyme (Hedstrom, 2002). In fungi, serine peptidases are known to regulate symbiotic or pathogenic fungal host interactions, where serine peptidases function to degrade host chitinases or to utilise the

protein sources available in host tissues (Langner, 2016, Muszewska, 2017). Aside from the protein metabolism enrichment, carbohydrate metabolism enrichment was observed through Fructan Catabolic Process (GO:0010147), Raffinose Catabolic Process (GO:0034484), Alpha Amylase Activity (GO:0004556), Beta-Fructofuranosidase Activity (GO:0004564) and Inulinase Activity (GO:0051670). All of these refer to process of polysaccharide breakdown in cells. Among these, Fructan and Raffinose Catabolic Processes, Inulinase and Beta-Fructofuranosidase Activities co-occur in GO assessments (GO Consortium, 2017).

Other than primary metabolism, enrichment in categories indicating hyphal growth and changes in the cell wall were observed in late response to mechanical stretching. Cellular Component contained genes involved in Hyphal Cell Wall (GO:0030446), and Biological Processes showed enrichment in Hyphal Growth (GO:0030448). Hyphal Cell Wall Category refers to the changes in the cell wall or cell surface proteins such as hydrophobins that facilitate host colonization of filamentous fungi, while Hyphal Growth Category refers to filamentous growth (Urban 2003; Castillo; 2008, Puttikamonkul 2010; Zaragoza, 2009). Further, enrichment in Ribonuclease T1 Activity (GO:0046589), plus Spermine and its precursor Putrescine metabolism (GO:0046208, GO:0000296, GO:0015847), pointed to changes in RNA metabolism and DNA replication (Katagiri, 1998; Gerashchenko, 2017). Enrichment in Oxidoreductase Activity (GO:0016491), Oxidation Reduction Process (GO:0055114) and Polyamine Oxidase Activity (GO:0046592) pointed to changes in the rates of redox reactions within cells (Johanson, 2007).

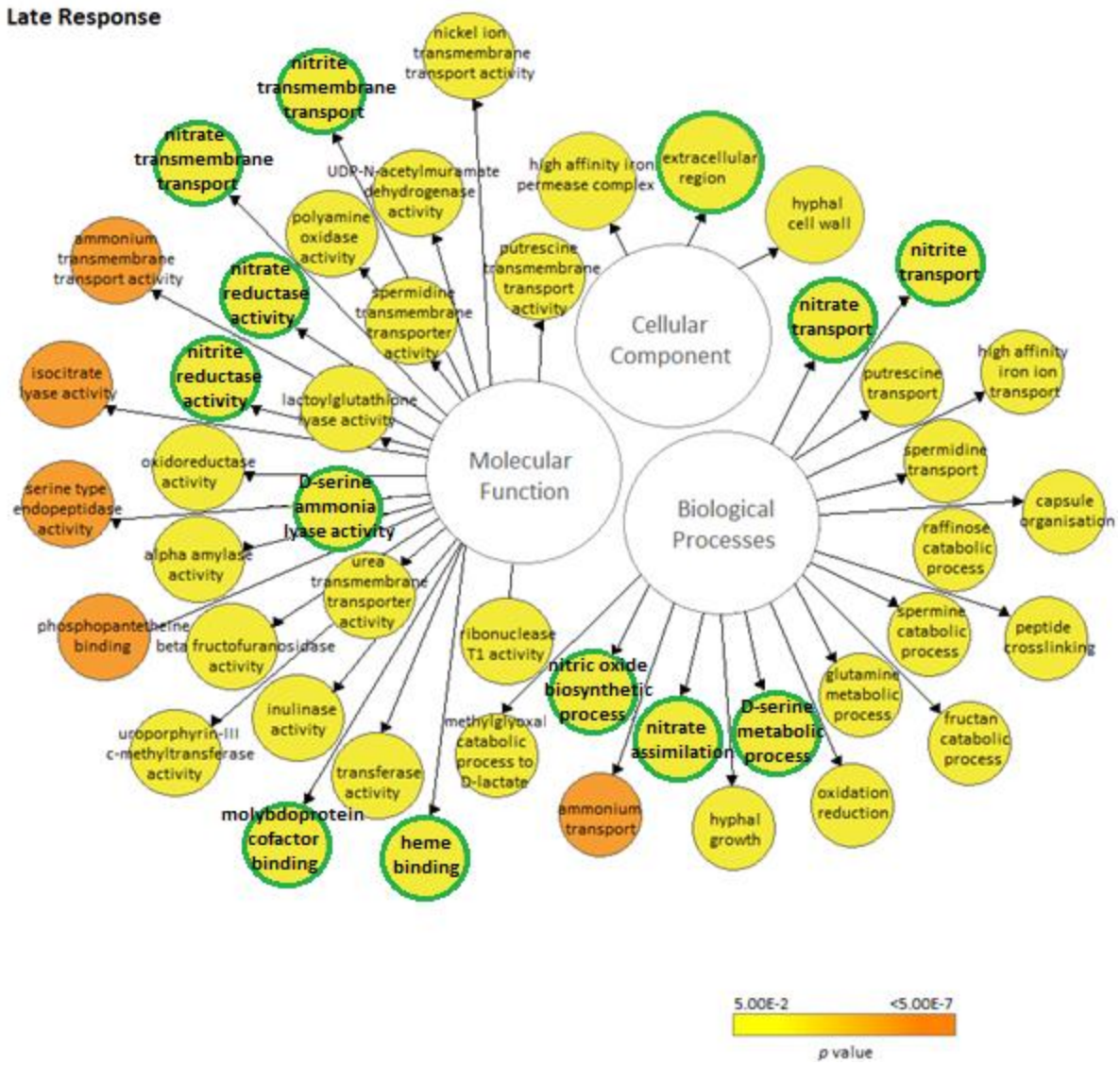

Figure 4.5 Gene Ontology (GO) Enrichment Analysis of genes differentially regulated in the late response to mechanical stretch in *E. festucae* compared to control ($p \leq 0.05$). The categories that are enriched in both early and late responses are circled in green. The circle sizes are arbitrary.

In total, 57 *E. festucae* differentially-expressed genes (DEGs) were represented in 46 enriched GO categories. Among them, 6 were differentially-expressed within Cellular Component (Figure 4.6), 29 within the Biological Processes (Figure 4.7) and 22 within the Molecular Function category (Figure 4.8). There were 7 genes (all up-regulated) in common between Biological Processes and Molecular Function (Figure 4.8).

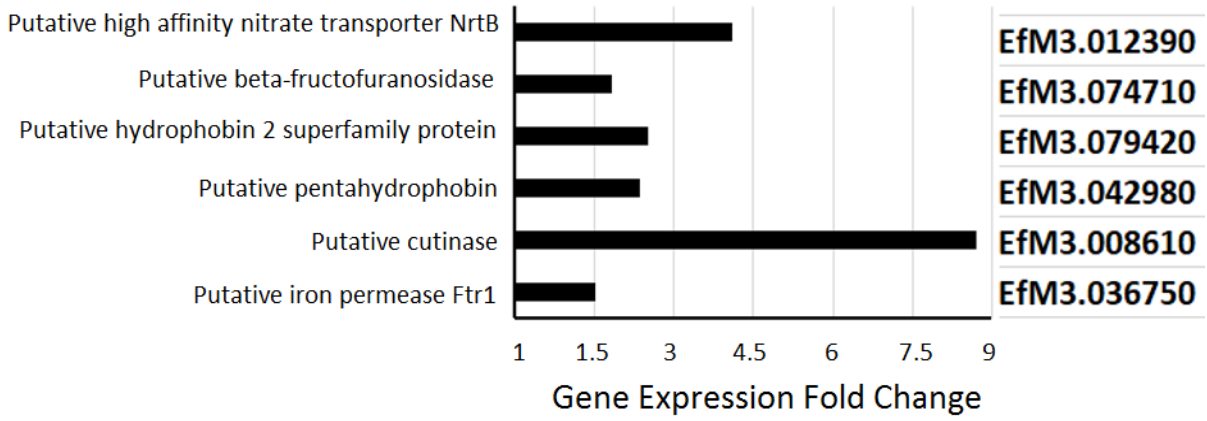

Figure 4.6 *E. festucae* DEGs in the GO Cellular Component category in late responses of hyphae to mechanical stretch ($p \leq 0.05$). The fold change threshold for DEGs is ±1.5. GO categories are shown on the left and gene model numbers on the right.

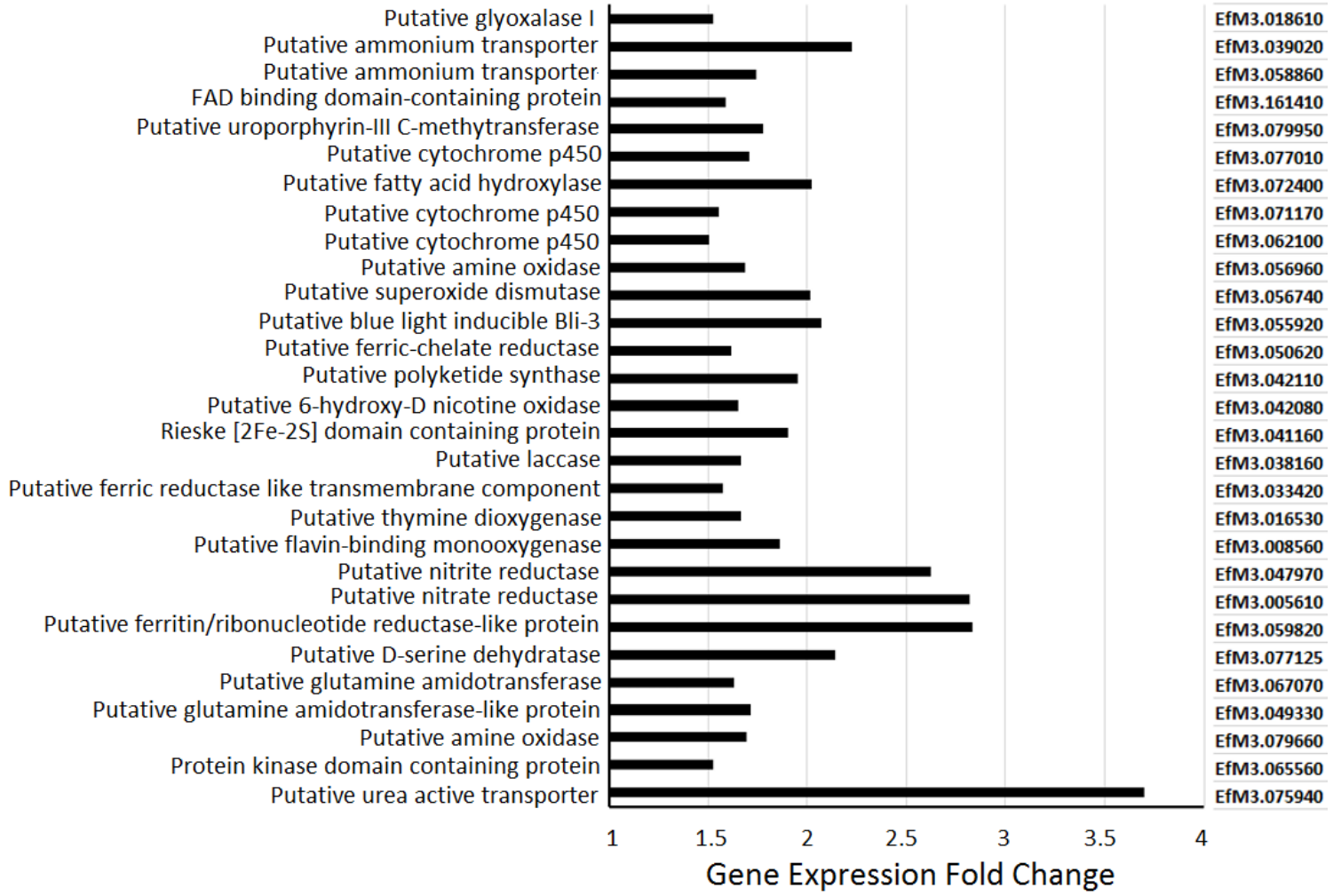

Figure 4.7 *E. festucae* DEGs in the GO Biological Processes category in late response compared to un-stretched control cultures ($p \leq 0.05$). The fold change threshold for DEGs is ±1.5. GO categories are shown on the left and gene model numbers on the right.

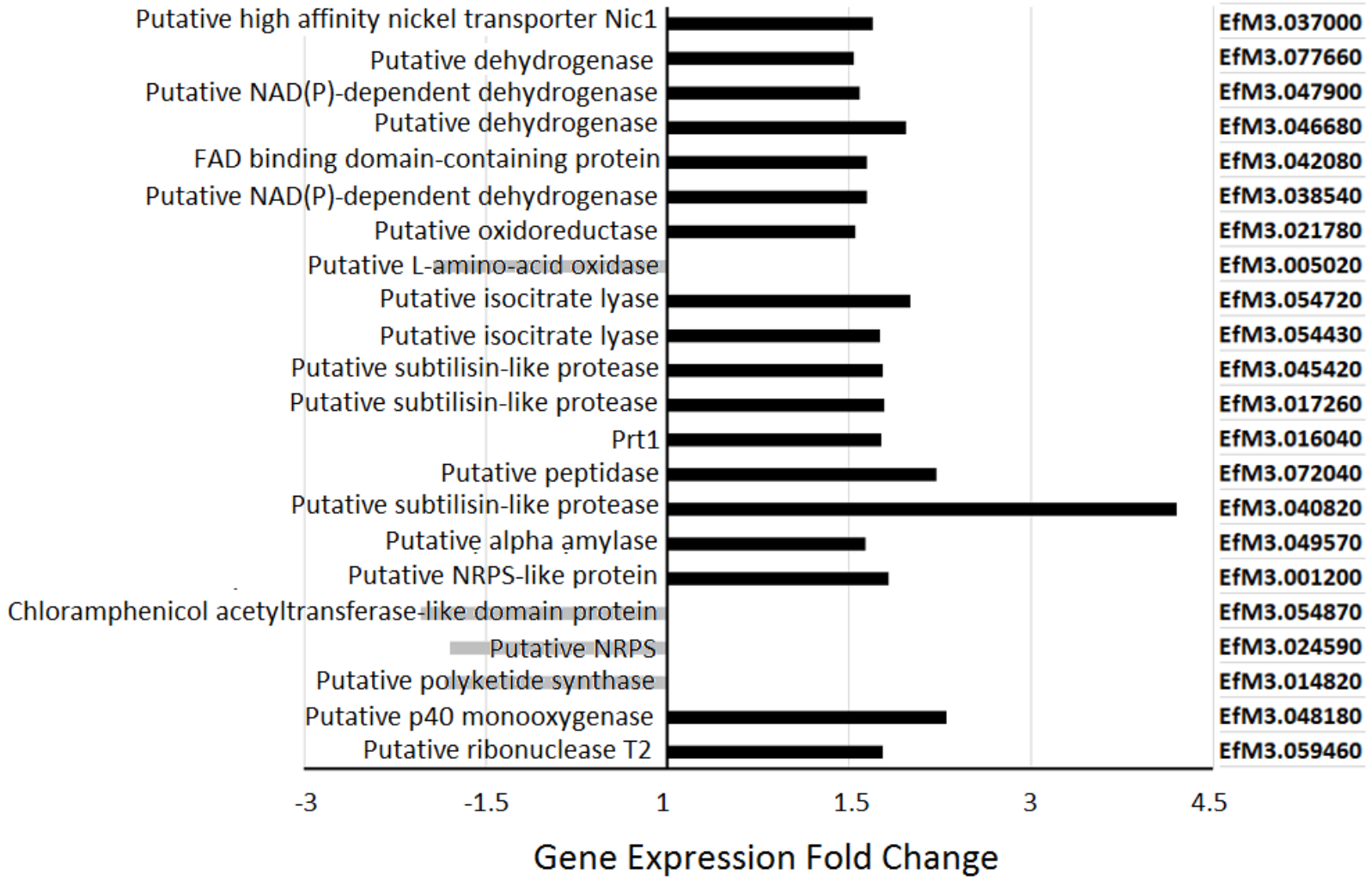

Figure 4.8 *E. festucae* DEGs in the GO molecular function category in late response compared to un-stretched control cultures ($p \leq 0.05$). The fold change threshold for DEGs is ±1.5. GO categories are shown on the left and gene model numbers on the right.

4.2. Differential Expression of Candidate Fungal Growth and Cell Wall Remodelling Genes in *E. festucae* Hyphae in Response to Mechanical Stretch

Due to poorly annotated GO IDs for the *E. festucae* Fl1 genome, 88 DEGs in the early response and 346 DEGs in the late response could not be included in the GO analysis. However, the most highly up-regulated genes in each response compared to control showed genes that might be related to hyphal growth and cell wall remodelling, stress response, transcription regulation and symbiosis regulation (Table 4.2, Table 4.3). To further understand the early and late responses of hyphae to mechanical stretch, DEGs in each response were analysed by computational annotation and categorised according to their possible functions under the categories of fungal growth and cell wall remodelling, transcriptional regulation, and plant and endophyte signalling.

Table 4.2 Most highly up-regulated genes in the early response compared to un-stretched control. RPKM: Reads Per Kilobase per Million. The EfM3 gene models were obtained from *E. festucae* Fl1 genome assembly (version) 2011-03 on Kentucky University *E. festucae* genome project database (Schardl et al, 2013) as described in Section 2.9. The green rows indicate the commonly up-regulated genes in both early and late response.

ID	Annotation	Fold Change	Control RPKM	Early Response RPKM
EfM3.008610	Putative cutinase	2.34	162	374
EfM3.080330	Putative transmembrane protein	2.22	1477	3279
EfM3.028430	Hypothetical	2.20	58	129
CUFF.4927	Hypothetical	2.15	2453	5316
EfM3.008790	Putative exonuclease III	2.14	1139	2381
EfM3.045560	Putative integral membrane protein	2.07	246	513
EfM3.113700	Hypothetical	1.95	307	607
EfM3.039990	PAS domain containing protein	1.95	13859	27380
EfM3.055920	Putative blue light inducible Bli-3	1.93	1658	3229
EfM3.033270	Hypothetical	1.93	4637	9038
EfM3.036880	Putative protein kinase	1.88	27	51
EfM3.120460	Hypothetical	1.82	3634	6663
EfM3.000680	Hypothetical	1.82	170	313
EfM3.060350	Hypothetical	1.81	2825	5157
EfM3.006290	Putative uracil permease	1.81	5158	9319
EfM3.052220	Putative stress response protein Ish1	1.76	2355	4179
EfM3.056730	Hypothetical	1.76	1258	2211
EfM3.061970	Hypothetical	1.76	28	50
EfM3.010610	Putative hydrophobic surface binding protein	1.75	3202	5534
EfM3.105390	Glycoside hydrolase family 61 protein	1.74	233	409

Table 4.3 Most highly up-regulated genes in the late response compared to un-stretched control. RPKM: Reads Per Kilobase per Million. The EfM3 gene models were obtained from *E. festucae* Fl1 genome assembly (version) 2011-03 on Kentucky University *E. festucae* genome project database (Schardl et al, 2013) as described in Section 2.9. The green rows indicate the commonly up-regulated genes in both early and late response.

ID	Annotation	Fold Change	Control RPKM	Late Response RPKM
EfM3.008610	Putative cutinase	8.69	162	1308
CUFF.4927	Hypothetical	6.75	2453	15712
EfM3.028430	Hypothetical	6.68	58	369
EfM3.008790	Putative exonuclease III	5.92	1139	6186
EfM3.033270	Hypothetical	5.04	4637	22226
EfM3.068210	Hypothetical	4.86	1758	8099
EfM3.060350	Hypothetical	4.63	2825	12462
EfM3.110490	Hypothetical	4.61	408	1805
EfM3.120460	Hypothetical	4.47	3634	15444
EfM3.006290	Putative uracil permease	4.33	5158	21063
EfM3.010610	Putative hydrophobic surface binding protein	4.33	3202	12983
EfM3.040820	Putative subtilisin-like protease	4.20	3802	15053
EfM3.045110	Putative hydrophobic surface binding protein	4.13	2504	9780
EfM3.012390	Putative high affinity nitrate transporter NrtB	4.09	2525	9684
EfM3.124560	Hypothetical	4.05	2645	10235
EfM3.066800	Putative malate dehydrogenase	3.94	7321	27473
CUFF.4266	Hypothetical	3.86	1630	6003
EfM3.105390	Glycoside hydrolase family 61 protein	3.81	233	843
EfM3.017790	C2H2 zinc finger containing protein	3.78	252	916
EfM3.075940	Putative urea active transporter	3.70	9921	34780

Hyphal elongation and compartment division during intercalary growth in *E. festucae* requires cell wall plasticity and rapid growth while maintaining cell wall integrity. Therefore, fungal growth and cell wall remodelling-related genes are hypothesised to take part in regulating these processes. Cell wall plasticity for rapid hyphal growth is provided by carbohydrate remodelling enzymes such as chitin synthases, β-1, 3 glucosyltransferases, glycoside hydrolase family enzymes and transglycosylases (Mouyna, 2013; Taylor, 2015). To determine whether putative homologs of fungal genes involved in cell wall remodelling and fungal growth were regulated by mechanical stretch in *E. festucae*, these genes were recovered from the transcriptomics data and their expression profiles examined. For this,

DEGs in both the early and late responses were recovered using protein BLAST (blastp) and their homology to characterized cell wall-related genes in fungi determined.

A total of 15 *E. festucae* genes with putative roles in hyphal growth and cell wall remodelling were differentially expressed in late responses to mechanical stretch, and two of them were differentially expressed in the early response to mechanical stretch (Table 4.4). Among them, five were putative cell wall remodelling enzymes, seven were putative cell wall structural proteins and three were putative cytoskeleton proteins (Table 4.4). Cell wall integrity MAP kinases MpkA, MkkA and protein kinase C (PkcA) were not differentially expressed in either the early or late response to mechanical stretch.

Putative membrane and cell wall remodelling enzymes that were up-regulated in late responses compared to the control were homologous to endo-1,3-β-glucanase, exo-1,3-β-glucanase, glucan-1,3-β-glucosidase, glycosyl transferase and omega-6 fatty acid desaturase (Table 4.4). In contrast, a putative chitinase, also a cell wall remodelling enzyme was found to be down-regulated in the late response (Table 4.4). Chitinases hydrolase glycosidic bonds in chitin, a polymer of β-(1,4) linked *N*-acetylglucosamines, to provide elasticity to the cell wall (Jollès, 1999). Two classes have been defined for chitinases, endochitinases that randomly cleave chitin into multimers, and exochitinases that breakdown chitin into dimers or *N*-acetylglucoseamine monomers (Sahai, 1993). In fungi, exochitinases function to regulate hyphal growth and autolysis, whereas endochitinases are linked to nutrition acquisition from host tissues, virulence and morphogenesis (Hartl, 2012).

The five membrane or cell wall structural proteins, and three cytoskeleton proteins, found to be up-regulated in response to mechanical stretch, showed homology to glycine-rich cell wall structural proteins, proteolipids and the endoplasmic reticulum (ER) membrane protein Pro41 (Table 4.4). The putative cytoskeleton proteins were homologous to α-tubulin, centromere or microtubule binding protein Cbf5 and the actin filament organization protein App1-like (Table 4.4).

The increased expression of putative glucan modifying enzymes, cell wall or membrane component proteins and cytoskeletal proteins indicated that mechanical stretching induced genes involved in cell wall plasticity and cell wall remodelling in *E. festucae*.

Table 4.4 Heat map showing the induction of putative hyphal growth and/or cell wall remodelling-related genes in *E. festucae* during early (ER) and late (LR) responses to mechanical stretch. Up-regulated genes are shown in yellow and down-regulated genes are shown in blue. RPKM values of significantly differentially expressed genes ($p \leq 0.05$) compared to the control are shown with bold numbers.

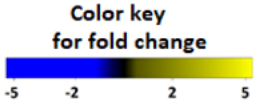

ID	Transcript Length	Annotation	Control RPKM	Early Response RPKM	Late Response RPKM	ER	LR
EfM3.06800	1689	Exo-beta-1,3-glucanase	2913	3853	**5541**		
EfM3.001210	1350	Omega-6 fatty acid desaturase	43185	54949	**82020**		
EfM3.071540	917	Glycine-rich cell wall structural protein 1	919	1121	**1664**		
EfM3.050650	1463	Putative α-tubulin	8755	11516	**14772**		
EfM3.059140	1344	Sphingolipid long chain base-responsive protein PIL1	6424	8623	**10719**		
EfM3.000730	1922	Microtubule binding protein Cbf5	2755	3280	**4472**		
EfM3.036790	2352	Glucan 1,3 beta glucosidase	2464	2581	**3955**		
EfM3.005930	2311	Actin filament organization App1-like protein	2634	2834	**3947**		
EfM3.028450	277	Plasma membrane proteolipid 3	11362	16502	**16904**		
EfM3.009370	441	Pro41 membrane protein	1365	1665	**2733**		
EfM3.037810	1284	Chitin binding domain 3 containing protein	4040	4543	**8523**		
EfM3.005840	2830	Putative membrane protein	2037	3176	**5926**		
EfM3.020020	1207	Putative membrane protein	5307	**6510**	**12375**		
EfM3.046410	1886	Putative Chitinase	761	1097	**436**		
EfM3.068210	1119	Endo-beta-1,4-glucanase D	1758	**2697**	**8099**		

4.2.1. Differential Expression of Putative Symbiosis-Related Genes in *E. festucae* hyphae in Response to Mechanical Stretch

Regulation of symbiosis between pathogenic fungi and their hosts depends on a complex network of signalling pathways involving masking the presence of the fungi from the host and/or suppression of plant responses (Lo Presti et al, 2015). In the case of *E. festucae* host colonization, the importance of symbiosis regulatory genes such as *sakA*, *proA* and the Nox protein complex during ryegrass colonisation has been shown previously (Eaton et al., 2010; Tanaka et al 2013; Tanaka et al., 2008). However, the role of mechanical stretching in symbiosis regulation is unknown. To identify the role of mechanical stretching in this process, the expression of known symbiosis related genes was examined along with known host colonization, pathogenicity and surface attachment-related genes in fungi (Table 4.5). The genes identified in this category are listed in Table 4.5.

Table 4.5 Heat map showing eight putative symbiosis related genes in *E. festucae* that are DE during early (ER) and late (LR) responses to mechanical stretch. Up-regulated genes are shown in yellow and down-regulated genes are shown in blue. RPKM values of significantly differentially expressed genes ($p \leq 0.05$) compared to the control are shown with bold numbers. The functionally characterized *E. festucae* genes are shown in asterisk.

ID	Transcript Length	Annotation	Control RPKM	Early Response RPKM	Late Response RPKM	Fold Change
EfM3.060970	2268	ProA*	12679	14014	**21033**	
EfM3.121200	474	Soft*	2194	2405	**3488**	
EfM3.021490	2354	Adhesin-like protein 1	12133	13673	**18286**	
EfM3.009370	441	NoxD*	1365	1655	**2733**	
EfM3.048730	531	AcyA*	106	159	**168**	
EfM3.050940	747	Putative HsbA	36335	49310	**60997**	
EfM3.032780	267	CFEM domain containing protein	292	**387**	**439**	
EfM3.069290	1820	SymC*	17895	22806	**34274**	
EfM3.042980	1275	Pentahydrophobin	1026	1264	**2316**	
EfM3.055470	691	Putative HsbA	979	1456	**2116**	
EfM3.079420	270	Hydrophobin	522	**830**	**1268**	
EfM3.010610	788	Hydrophobin	3202	**5534**	**12983**	
EfM3.045110	728	Putative HsbA	2504	3710	**9780**	

Five characterized and eight putative symbiosis related genes that were differentially expressed in early and/or late responses to mechanical stretching in *E. festucae* were found (Table 4.5). *E. festucae* symbiosis and host colonization regulatory genes *proA, soft, symC, noxD* and *acyA* were found to be up-regulated compared to control cultures (Table 4.5). In *E. festucae proA*, a fungal unique transcription factor, has been shown to be an important regulator of the mutualistic relationship between the endophyte and its host (Tanaka et al., 2013). My data showed that *proA* was significantly up-regulated (+1.73 fold) in the late response to mechanical stretching, compared to control cultures (Table 4.5). Another important *E. festucae* symbiosis regulatory gene is *soft*, an ortholog of the *N. crassa so* gene that regulates hyphal anastomosis in this organism (Fleissner 2005; Charlton 2012). Similar to *proA*, *soft* was up-regulated (+1.64 fold) in the late response, compared to control cultures (Table 4.5). *E. festucae* membrane proteins SymB and SymC are also known to regulate symbiosis with the host plant (Green, 2016). In my data, *symC* (but not *symB*) was found to be up-regulated (+1.99 fold), again, in the late response to mechanical stretching compared to the control (Table 4.5). A further well known symbiosis regulator is the nicotinamide adenine dinucleotide phosphate-(NADPH) (Nox) complex, which has been shown to be important in the maintenance of mutualism between *E. festucae* and ryegrass (Eaton et al., 2010, 2011; Tanaka et al., 2008). The characterised subunits of Nox in the *E. festucae* complex are NoxA, NoxD, NoxR, RacA, BemA, Cdc24 and Cdc42 (Scott, 2007, Ozaki et al., 2015; Becker et al., 2016; Kanayno 2018). My data showed that among the Nox complex proteins, only *noxD* was up-regulated (+2.09 fold) in the late response compared to control (Table 4.5). Another symbiosis regulatory mechanism in *E. festucae* is adenosine 3′, 5′-cyclic monophosphate (cAMP)-dependent signalling, which has a regulatory role in a broad range of metabolic activities. This signalling pathway is often essential for maintenance of some host pathogen interactions and regulation of hyphal biomass in the host (D'Souza and Heitman 2011, Voisey 2016). My data showed up-regulation (+1.64 fold) in *E. festucae* adenylate cyclase gene *acyA* in late response, compared to control (Table 4.5). The up-regulation of important symbiosis related genes in *E. festucae* in response to mechanical stretching points to the possible role of mechanical stress in regulating symbiotic interactions of endophyte and plant during intercalary growth.

The eight putative fungal host interaction related genes that were up-regulated in early and late responses compared to control cultures were all putative surface attachment proteins (Table 4.5). We found three putative hydrophobic surface binding protein A (HsbA) genes,

three putative hydrophobins, one putative adhesin-like protein 1 homolog and a CFEM domain containing protein (Table 4.5). The roles of these types of proteins in plant endophyte mutualistic interactions have not been studied so far, however their role in pathogenic interactions between fungi and their hosts has been reported previously. HsbA and hydrophobins in pathogenic fungi are small secreted proteins which facilitate attachment to synthetic or organic surfaces such as the cuticle on plant cell walls), and can recruit lytic enzymes to extracellular spaces (Gurr 2007; Muszewska 2018). These findings may suggest a role for mechanical stretching in surface attachment of hyphae to the host plant, potentially via Hsb and hydrophobins.

4.2.2. Differential Expression of Transcription Related Genes in *E. festucae* hyphae in response to Mechanical Stretch

Transcriptional regulation in *Epichloë*-grass symbioses appears to be affected by host tissue type (Schmid 2017; Nagabhyru et al., 2018). In the association between *Brachypodium sylvaticum* with *E. sylvatica,* 422 endophyte DEGs were found in ovaries compared to vegetative pseudostems, and eight of the DEGs were transcription factors (Nagabhyru et al., 2018). To determine the transcription factors and epigenetic regulators that are responsive to mechanical stretching, and presumably differentially regulated in intercalary zone, the expression of known transcription factors (TF) in fungi were recovered from the transcriptomics data (Table 4.6).

Table 4.6 Heat map showing the expression 13 of putative transcriptional regulatory genes in *E. festucae* during early (ER) and late (LR) responses to mechanical stretch. Up-regulated genes are shown in yellow and down-regulated genes are shown in blue. RPKM values of significantly differentially expressed genes ($p \leq 0.05$) compared to the control are shown with bold numbers.

ID	Transcript Length	Annotation	Control RPKM	Early Response RPKM	Late Response RPKM	ER	LR
EfM3.059960	2679	Zn(2)-C6 fungal transcription factor	4591	5191	**7665**		
EfM3.069640	1416	CCHC-type Zinc finger domain containing protein	1032	1102	**1671**		
EfM3.041170	2166	Zn(2)-C6 fungal transcription factor	6235	6511	**10886**		
EfM3.035780	651	CAMK family protein	9017	10873	**15575**		
EfM3.059400	1062	HLH transcription factor	357	439	**598**		
EfM3.040180	907	Putative bzip transcription factor Atf2	175	158	**260**		
EfM3.037810	1284	OB-fold Nucleic acid binding domain containing protein	4040	4543	**8523**		
EfM3.053400	1053	Myb family protein	1139	1520	**3569**		
EfM3.020010	404	CTF NFI domain containing protein	1497	2044	**3956**		
EfM3.017790	1440	Putative transcription factor Azf1	252	**410**	**916**		
EfM3.030390	1218	GAL4-like Zn(II)2Cys6 (or C6 zinc) binuclear cluster DNA-binding domain containing protein	762	762	**1282**		
EfM3.016420	250	CCHC-type Zinc finger domain containing protein	36	50	**54**		
EfM3.022120	1899	BED zinc finger DNA binding protein	3002	**4581**	2354		

Thirteen putative fungal TFs that were differentially expressed in early and/or late responses to mechanical stretch were identified as DE (Table 4.6). Among them, six were zinc finger domain-containing putative fungal TFs, two were putative Helix loop helix (HLH) TFs and the remainder contained Myb-like DNA binding domains, basic leucine zipper (bZIP), a Forkhead associated domain (FHA) and CCAAT box-binding domain (CTF) (Table 4.6).
Except for the BED zinc finger DNA binding domain containing protein, all these putative TFs were up-regulated in late response to mechanical stretching compared to control (Table 4.6). A putative homolog of zinc finger domain-containing *S. cerevisiae* TF Gal4, that regulates galactose metabolism, and CCHC-type Azf1, that controls glucose metabolism, growth and cell wall integrity, were up-regulated in the late response to mechanical stretching compared to control (MacPherson, 2006; Slattery et al., 2006). Myb-like TFs Myb1, 2, and 3 have been characterized in *Fusarium graminearum* and shown to regulate mating, vegetative growth and pathogenicity (Kim et al., 2014). Myb TFs can also form complexes with HLH TFs to regulate stress response, cell wall biosynthesis, metabolite production and cell death in plants (Pireye et al., 2015).

In fungi, bZIP TFs are known to mainly regulate cellular response to reactive oxygen species (ROS) (Roze, 2011; Wee et al., 2017). Forkhead associated domain (FHA) TFs are conserved eukaryotic TFs that are known to regulate cell cycle, pathogenicity and cellular responses to stress in fungi (Wang et al., 2015, Park et al.,2014). CTFs are proteins that bind to CCAAT sequences upstream of transcription start sites in target genes and are widely found in eukaryotic promoters (Romier, 2014). In filamentous fungi, several CTFs have been characterized and used in industries to facilitate production of cellulose enzymes and penicillin (Kato, 2005). The up-regulation of putative TFs in late response to mechanical stretching is evidence that *E. festucae* transcriptional regulation is affected by mechanical stress.

4.2.3. Differential expression of Stress Response Genes in *E. festucae* Hyphae after Mechanical Stretch

In the symbiotic association of *E. coenophiala* with tall fescue, several stress related genes were differentially expressed in different tissues of the host plant (Nagabhyru et al., 2018). To understand the role of mechanical stretch in invoking a stress response, the expression of known stress response genes were recovered from the transcriptomics data (Table 4.7).

Table 4.7 Heat map showing the expression of 11 putative stress response or related genes in *E. festucae* during early (ER) and late (LR) responses to mechanical stretch. Up-regulated genes are shown in yellow and down-regulated genes are shown in blue. RPKM values that are significantly ($p \leq 0.05$) upregulated compared to the control are shown with bold numbers.

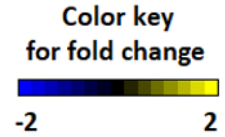

ID	Transcript Length	Annotation	Control RPKM	Early Response RPKM	Late Response RPKM	Fold Change
EfM3.055640	1773	N2227-like protein	7400	8960	**13233**	
EfM3.055920	709	Protein Bli-3	1658	**3229**	**3297**	
EfM3.011760	3422	Heat shock protein 70	893	673	**581**	
EfM3.068620	1734	Heat shock protein Sti1	34911	31828	29554	
EfM3.082260	1971	Heat shock protein 70-2	248220	193122	182612	
EfM3.046980	2161	Heat shock protein 60	64970	56408	47372	
EfM3.005640	2169	Heat shock protein Hsp88	54286	45680	44083	
EfM3.045500	618	Heat shock protein 30	10601	10605	9366	
EfM3.008720	1283	Heat shock protein DnaJ	5528	5659	5645	
EfM3.052650	1881	Putative inhibitor of apoptosis protein (IAP)-like protein (Ilp-2)	414	620	**1253**	
EfM3.003110	1462	Putative DDR48 heatshock protein	32279	39537	**53278**	

The data revealed that among 11 putative *E. festucae* heat shock (HSPs) and other chaperone proteins (including cochaperones and chaperonins), only two were differentially regulated in late response to mechanical stretching compared to control (Table 4.7). HSPs are highly conserved eukaryotic proteins that are synthesized in response to various environmental stresses such as heat, and they function to protect other proteins from unfolding (Verghese et al., 2012). Aside from HSPs, my data revealed up-regulation of a putative N2227-like protein in late response to mechanical stretching (Table 4.7). In *S. cerevisiae*, this protein is known to participate in the regulation of meiosis and stress responses, however, further studies are needed to confirm its exact function (Garcia-Cantalejoa et al., 1995). My dataset also revealed up-regulation of a putative inhibitor of apoptosis protein (IAP)-like protein (Ilp-2), which is an IAP family protein widely found in eukaryotes (O'Riordan 2008). In mammals, this family of proteins shows inhibitory effects towards apoptotic caspases that degrade organelles and other cellular components, and in yeast an IAP-like protein was found to regulate spindle fiber formation during mitosis (Yoon et al., 1999, Li, 2000). Up-regulation of a putative Blue light inducible 3 (Bli-3) protein was also observed in early and late response to mechanical stretching (Table 4.7). Light inducible genes were first characterized in *N. crassa*, in which their expression levels were responsive to light and they controlled 79% of genes in this organism, mostly related to metabolism and antioxidant production (Wu et al., 2014). (Owsianowski et al., 2008). My results indicate that moderate mechanical stretch (6%) does not induce a significant stress response at the transcriptional level in *E. festucae* hyphae.

4.3. Discussion

Evidence for the role of mechanical stretch in stimulating intercalary hyphal growth has been limited to observations of intercalary compartment extension and division in *E. festucae,* and there is currently no supporting information concerning molecular responses of hyphae to this stimulus. My hypothesis is that mechanical stretch induces a molecular programme that results in cell wall remodelling and synthesis, and compartment division. I also propose that, assuming the stimulus is not overwhelming, it will induce a minimal amount of hyphal stress. In this chapter, a transcriptomics approach was used to determine the responses of *E. festucae* hyphae to mechanical stretching to shed light on the early and later molecular mechanisms that sense and respond to mechanical stress respectively. To do this *E. festucae* cultures were subjected to a physiologically relevant amount of stretch (6% over the length of membrane), and mycelia harvested immediately after, and 3 h after stretching. The data were analysed to identify differentially-expressed genes, and Gene Ontology (GO) assessment used to reveal which GO categories that were significantly enriched in early vs late responses, and which were common to both. DE genes were also interrogated to identify genes putatively involved in fungal growth and cell wall remodelling, transcriptional regulation, symbiosis and stress, to determine how they responded to this mechanical stimulus. The data showed that mechanical stretching invoked changes in the nitrogen and carbohydrate metabolism of *E. festucae*, as well as elevated expression of genes related to cell wall plasticity, hyphal growth, symbiosis regulation and transcription.

4.3.1. Mechanical Stretching Induces Metabolic Changes in *E. festucae*

GO assessments showed that changes in nitrogen metabolism (in the categories Nitrate/Nitrite Reductase, Nitrate/Nitrite Transport and Transmembrane Transport, Nitric Oxide Biosynthetic Process, Nitrate Assimilation) were in common to both early and late responses, as well as Heme binding, D-serine metabolism, Molybdopterin Cofactor Binding and Extracellular Region (Figure 4.3).

Enrichment in nitrogen metabolism-related categories in the GO analysis in early and late responses to mechanical stretching showed that mechanical stretching may increase the requirement for nitrogen metabolism in *E. festucae* (Figure 4.3). In filamentous fungi, as well as many other organisms, nitrogen metabolism is essential for growth, reproduction, secondary metabolism, development and sometimes pathogenicity (Davis and Wong, 2010, Cox, 2000, Tudzynski et al., 2014). Many filamentous fungi prefer glutamine or ammonium

as nitrogen source but may also be able to utilize urea or uric acid, nitrate, amines or amides, and purines or pyrimidines (Wong, 2008). My data showed up-regulation of putative nitrite/nitrate reductases, putative nitrate transporter *nrtB* and putative urease genes in both responses, as well as up-regulation of two putative ammonium transporters, amine oxidase and urea active transporter genes in the late response to mechanical stretch compared to the control.

Although these genes have not been characterized in *E. festucae*, several studies have showed their critical function in the nitrogen metabolism of other fungi such as *S. cerevisiae*, *N. crassa* and *A. nidulans*. In *N. crassa* and *A. nidulans*, mutations in nitrate/nitrite reductases cause failures in growth due to an inability to utilize nitrogen sources in the media (Marzluf et al., 1997). In *A. nidulans*, the nitrate transporter NrtB is responsible for nitrite and nitrate uptake (Unkles, 2004). Ureases, the enzymes that break down urea into ammonia and carbon dioxide, have been linked to pathogenicity in *C. ablicans* and *C. neoformans* (Milne, 2015, Cox, 2000, Klengel, 2005, Navarathna, 2010). As well as nitrogen metabolism related GO categories, Molybdopterin Cofactor Binding and Heme-Binding categories were enriched in early and late response to mechanical stretching. These categories are known to be important for respiration as well as synthesis of amino acids and lipids in fungi (Philpott et al., 2006). Heme binding activity has also been shown to regulate nitrogen metabolism in fungi, since nitrate reductases are known to possess a heme binding domain (Campbell, 1990; Kelley, 2017). In *N. crassa*, mutation of histidine residues in the heme binding domain of nitrate reductase abolished the function of this enzyme (Okamoto, 1993).

Another enrichment found in both responses was D-Serine Metabolic Process, which refers to serine amino acid synthesis and hydrolysis. In fungi, D-serine can be used as a nitrogen or carbon source and, in some pathogenic fungi, it has been shown to regulate host colonization (Pollegioni, 2007). For example, in *Staphylococcus saprophyticus*, a bacterial pathogen of the urinary tract, mutation of D-serine-deaminase *dsdA* was found to cause failure in breaking down D-serine to pyruvate, and significantly decreased colonization of murine models compared to WT (Korte-Berwanger et al., 2013). The enrichment in D-serine metabolic process in early and late responses is a further line of evidence that mechanical stretching induced the requirement for nitrogen and carbon sources in *E. festucae* hyphae. Nitrogen and amino acid concentrations in plant apoplastic fluids have been found to be modified in response to fungal infections (O'Leary et al., 2014). Infection of *Phaseolus vulgaris* (common bean) by pathogenic *Pseudomonas syringae* was reported to increase amino acid concentrations in the apoplastic fluid of bean leaves (O'Leary et al., 2016). Similarly,

infection of tomato leaves by the tomato leaf mould *Cladosporium fulvum* resulted in an increase in the nitrogen and amino acid concentrations (ranging between 0.1 and 0.7 mM) in the infected leaves compared to non-infected plants (Solomon, 2014). As nitrogen metabolism has a wide range of roles in fungi, its specific function in sensing mechanical stretching and mediating intercalary growth should be investigated in the future. A putative urease, nitrate/nitrite reductases or the nitrate transporter NrtB could be deleted in *E. festucae* and mutants subjected to mechanical stretching to observe cell wall extension, synthesis and compartmentalization in hyphae.

Enrichment of DE genes in the Extracellular Region GO category in both early and late response to mechanical stretching indicated that mechanical stretching may influence hyphae and cell surface interactions. Under this category, up-regulation in a putative cutinase in both responses was detected. Cutinases are enzymes that degrade cutin polymers that surround plant tissues (Di Pietro, 2009). In *E. festucae*, two putative cutinases have been found to be up-regulated in *E. festucae* mutants Δ*proA*, Δ*sakA* and Δ*noxA* during colonisation of plants (Eaton et al., 2015). One of these cutinases (EfM3.008610), a potential homolog of *M. oryzae* cutinase gene *cut2*, was up-regulated by mechanical stretch in both early and late responses (Table 4.2, 3.9). In *M. oryzae, cut2* was found to be crucial for surface sensing, cutin degradation and pathogenicity on plant hosts (Skamnioti and Gurr, 2007). In the soil fungus *Fusarium solani,* cutinase activity was detected spectrophotometrically and found to be significantly increased in pathogenic isolates compared to non-pathogenic isolates, where cutinase activity was barely detected (Morid, 2009). The role of cutinases in *E. festucae* are yet to be studied, however it is possible to speculate that its role may be in surface sensing and cuticle degrading for better hyphal attachment to plant cells during intercalary growth. The putative cutinase (EfM3.008610), which is up-regulated in response to mechanical stretch in this study, possesses a signal peptide which makes it a good candidate for future characterization, since fungal cutinases are usually secreted to extracellular space for cutin degradation (Guo et al., 1996). Functional characterization studies on this putative cutinase, including gene replacement, would shed further light on its role in intercalary growth and colonization of host plants.

4.3.2. Mechanical Stretching Induces Unique Enrichments in Early and Late Responses in *E. festucae*

Although several GO categories were enriched commonly in both responses, some were unique to each mechanical stretch response. In the early response only, nine further enriched GO categories were observed (Figure 4.3). Amongst these were Cutinase Activity (GO:0050525) and Plasma Membrane Fusion during Cytogamy (GO:0032220) which are linked to host colonization in pathogenic fungi and changes in the lipid membrane bilayer during mating or differentiation (Heiman et al., 2000; Davies et al., 2000; Skamnioti et al., 2008; Morid et al., 2009). Unique early responses also showed enrichment for urea metabolism (GO:0009039, GO:0043419), Nickel Ion Binding (GO:0016151) and Molybdenum Ion Binding (GO:0030151), which further suggested regulation of urea and nitrite/nitrate metabolism, as these categories co-occur in GO assessments (GO Consortium, 2017). Altogether, these finding showed that mechanical stretching triggers requirement for nitrogen and boosts urea and carbohydrate metabolism, as well as changes in the plasma membrane of *E. festucae* hyphae.

In the late response to mechanical stretching, in addition to 13 commonly enriched GO categories, 33 unique GO categories were enriched, a much larger response compared to ER (Figure 4.4). The uniquely enriched categories in late response pointed to an increase in protein and carbohydrate metabolism, hyphal growth and cell wall building, nucleic acid metabolism and oxidation/reduction, indicating that during the incubation period after stretching, *E. festucae* hyphae were exhibiting growth.

Protein metabolism enrichment was observed through Peptide Cross-Linking (GO:0018149) and Serine Type Endopeptidase Activity (GO:0004252), which are necessary for the structural integrity of the cell wall and degradation of peptides (Hedstrom, 2002, Iorio, 2008). Serine peptidases are important during the symbiotic or pathogenic fungal host interactions, since serine peptidases function to degrade host chitinases or utilizing the protein sources available in the host (Langner, 2016; Muszewska, 2017). These findings suggest that *E. festucae* hyphae might require more proteins for growth after mechanical stimulation.

Other than primary metabolism changes, enrichment in Hyphal Cell Wall (GO:0030446) and Hyphal Growth (GO:0030448) were observed uniquely in LR, suggesting that mechanical stretching acted as a stimulus for changes in *E. festucae* cell walls and promoted filamentous growth (Urban et al., 2003; Castillo et al., 2008; Puttikamonkul et al., 2010; Zaragoza et al., 2009). Moreover, Ribonuclease T1 Activity (GO:0046589), Spermine and its precursor

Putrescine metabolism (GO:0046208, GO:0000296, GO:0015847) enrichments pointed to an increase in RNA and DNA metabolism, which altogether confirms the previous findings that mechanical stretching of *E. festucae* facilitates intercalary growth in hyphae by increasing compartment numbers and sizes, as well as the formation of new nuclei (Ariyawansa, 2015). Moreover, enrichment in redox related categories such as Oxidoreductase Activity (GO:0016491), Oxidation Reduction Process (GO:0055114) and Polyamine Oxidase Activity (GO:0046592) were observed, indicating that later response to mechanical stretching leads to an increase in reactive oxygen species (ROS) (Johanson, 2007). ROS in fungi has functions in signalling, cell differentiation and fungal host interactions (Breitenbach, 2015). In *E. festucae*, the NADPH complex (Nox) has been identified and found to be crucial for the symbiotic plant endophyte interactions (Tanaka et al., 2008, Eaton et al., 2011). In the pathogenic fungus *Magnaporthe oryzae*, NoxA and NoxB are necessary for plant tissue penetration (Egan, 2007). Although CW and FM4-64 staining has been carried out in mechanically stretched *E. festucae* hyphae, the ROS production before, immediately after and later mechanical stretching has not been carried out before. To understand the role of mechanical stretching in ROS production, propidium iodide staining could be carried out to determine the amount of ROS in hyphae. The findings would bring us closer to understanding the role of oxidative stress as a response to mechanical stretching in hyphae during endophyte plant interactions though.

In our GO analysis, we were able to include 5749 *E. festucae* genes that were associated with one or more GO IDs. The remaining 3333 *E. festucae* genes could not be included due to lack of GO ID annotations. From the 509 DEGs of early and late responses, only 83 of them were detected by GO analysis. We have investigated the remaining DEGs to find out their putative functions. For this, we first focused on the most highly expressed 20 DEGs in both responses compared to un-stretched controls to determine the categories of functions of interest. In both responses, the 20 most highly up-regulated DEGs showed putative functions in filamentous growth and cell wall remodelling, symbiosis or host endophyte signalling, and finally transcriptional regulation (Table 4.2, 4.3).

4.3.3. Mechanical Stretching Induces Expressions of Genes Related to Filamentous Growth and Cell Wall Remodelling in *E. festucae*

New hyphal compartment formation and hyphal growth in *E. festucae* presumably requires cell wall plasticity and rapid growth while maintaining the integrity of the cell wall. I found 15 putative fungal growth and cell wall remodelling related DEGs in early and late responses

compared to un-stretched control cultures (Table 4.4). The putative cell wall remodelling enzymes that were up-regulated in early and late responses to mechanical stretching showed homology to endo-1, 4-β glucanase, exo-1, 3-β glucanase, glucan-1, 3 β glucosidase, glycosyl transferase and Omega-6 fatty acid desaturase (Table 4.4). Glucanases are known to degrade, rearrange and cross-link 1, 3-β glucans, the abundant fungal cell wall component, during growth and sporulation in fungi (Baladro´n et al., 2002). For example, in *S. cerevisiae*, multiple endo-1, 3-β glucanase and exo-1, 3-β glucanases have been characterized and found to play a role during budding, vegetative growth and maintenance of normal morphology (Adams et al., 2004).

Similar to β-glucanases, β-glucosidases are thought to be involved in cell wall remodelling in fungi (Adams et al., 2004). In *Coccidioides immitis*, a pathogenic fungus in soil, deletion of a β-glucosidase-encoding gene leads to decreases in pathogenicity and hyphal growth rate, as well as a decrease in virulence in mice (Hung et al., 2001). Since these enzymes are upregulated in *E. festucae* within 10 min of mechanical stretch, and remain elevated for at least 3 h, it is tempting to speculate that they may be involved in loosening the intercalary cell wall to enable the hyphae to stretch without sustaining cell wall fractures. If this were the case, this would mimic the situation at the hyphal tip where cell wall remodelling enzymes are proposed to loosen the cell wall, allowing turgor pressure (a mechanical force) to push the tip forward (Gow et al., 2017). These findings show the effect of mechanical stretching in evoking a cell wall remodelling response in *E. festucae* hyphae.

Fatty acid desaturases are important enzymes in the synthesis of essential unsaturated fatty acids, which are incorporated in cell membrane structures (Li et al., 2016). These enzymes enable a more fluid membrane structure by removing two hydrogen atoms from fatty acids to make carbon-carbon double bonds during environmental stress (Alberts, 2015). Although they have been extensively studied in bacteria and plants, their role in the membranes of filamentous fungi is not clear. The up-regulation in putative Omega-6- fatty acid desaturase in late response to mechanical stretching might indicate that plasma membranes of *E. festucae* hyphae require more fluidity in response to mechanical stretch to enable intercalary growth. Cell wall integrity MAP kinases MpkA, MkkA and protein kinase C (PkcA) were not differentially expressed in early or late responses to mechanical stretching (Table 4.4).

The up-regulation in putative cell wall remodelling enzymes and plasma membrane desaturases, as well as membrane proteins point to a structural change in the cell wall and plasma membrane in response to mechanical stretching, presumably, to maintain the integrity

of the cell wall and the plasma membrane under mechanical stimulus. Therefore, it is possible to speculate that mechanical stretching could trigger cell wall remodelling in *E. festucae* hyphae, which is essential for intercalary growth.

In my study a putative chitinase was found to be down-regulated in response to mechanical stretching (Table 4.4). Chitinases, which belong to the glycoside hydrolase 18 (GH18) enzyme family are known to carry out chitin hydrolysis and contribute to cell wall remodelling in fungi (Hartl 2011). In *A. fumigatus*, deletion of chitinase encoding *chiA* resulted in decreased hyphal growth and spore germination rate (Takaya et al., 1998). Glycosyl transferases are responsible for cell wall biosynthesis by attaching oligosaccharides to cell wall proteins, and cross-linking them to the cell wall (Bowman and Free, 2006). Similar to other cell wall remodelling enzymes, there have been multiple glycosyl transferases found in the *S. cerevisiae* genome and they are linked to maintenance of cell wall integrity, normal growth rate and survival (Bowman and Free, 2006). Chitinases are also known to be associated with autolysis, as well as nutrition acquisition from host tissues, virulence and morphogenesis of fungi (Hartl, 2012). The putative *E. festucae* chitinase is slightly but not significantly up-regulated in the early response, and significantly down-regulated in the late response to mechanical stretching (Table 4.4). This might indicate that chitin degradation is required during the first response to mechanical stretching to achieve cell wall plasticity quickly, and later down-regulated in the absence of mechanical stimulus to strengthen the cell wall. Another possible explanation for chitinase down-regulation could be that *E. festucae* hyphae may reduce chitin content during mechanical stretching to avoid exposure to athogen-associated molecular pattern (PAMP)-triggered immunity (PAMPS). Previous research has shown that chitin in endophytic *E. festucae* hyphae is only detectable in the septa, however epiphyllous *E. festucae* cell wall seem to contain abundant chitin (Becker et al., 2016). This could be either due to low levels of chitin in the cell walls of endophytic hyphae, or alternatively, masked chitin in plants (Becker et al., 2016). In either case, chitin content in *E. festucae* seems to be playing a role in maintaining symbiosis and mechanical stretching might be a trigger for remodelling the chitin in cell wall.

4.3.4. Mechanical Stretching Induces Expressions of Genes Related to Symbiosis in *E. festucae*

A further group of 13 genes that were upregulated in both early and late responses to mechanical stretch have been shown to be important in symbiotic associations between *E. festucae* and perennial ryegrass. Genes that regulate *E. festucae* host colonization such as

sakA, *proA* and Nox protein complex has been studied previously, however the role of mechanical stretching in this process has not been addressed (Eaton et al., 2010; Tanaka et al., 2008, Tanaka et al., 2013). Therefore, we examined the expressions of known symbiosis and host colonization, pathogenicity and surface attachment related genes in fungi (Table 4.5). My results showed 13 DEGs in both responses that could potentially be involved in symbiosis regulation (Table 4.5).

We found that the functionally characterized *E. festucae* symbiosis regulatory genes *proA*, *soft*, *symC*, *noxD* and *acyA* were up-regulated compared to control un-stretched cultures. In *E. festucae*, *proA*, a fungi-unique transcription factor has been found to be an important regulator of the mutualistic relationship between *E. festucae* and perennial ryegrass (Tanaka et al., 2013). The finding that *proA* has been up-regulated in the late response to mechanical stretching points to the possibility that mechanical stretch has a role in mediating symbiosis through *proA* transcriptional regulation in *E. festucae*. Another important symbiosis regulatory gene is *soft*, an ortholog of *N. crassa so,* that regulates hyphal anastomosis by encoding the So protein that localizes in septal plugs during hyphal damage (Fleissner et al., 2005; Charlton et al., 2012). Disruption of the *soft* gene in *E. festucae* resulted in impaired hyphal anastomosis in culture, and plants infected with mutants were severely stunted and died earlier than plants infected with WT indicating that the *soft* gene is crucial for maintaining a mutualistic relationship between *E. festucae* and the host plant (Charlton et al., 2012). Up-regulation of the *soft* gene in the late response to mechanical stretching again points to the role of mechanical stretching in maintaining symbiosis between endophyte and the plant host. In *E. festucae*, membrane proteins SymB and SymC, homologs of fruiting body development signalling in *Podospora anserina* Idc2 and Idc3 proteins, were found to be regulators of symbiosis (Green, 2016). Deletion of *symB* and *symC* reduced hyphal fusion in culture, and caused excessive colonization in the pseudostem compared to WT, resulting in stunting and early deaths in plants upon infection (Green, 2016). Both SymB and SymC were shown to have putative binding sites for *proA* transcription factor, and a transcriptomics study showed that both genes were down-regulated in *E. festucae* Δ*proA* compared to WT (Eaton et al., 2015). Simultaneous up-regulation in *proA* and *symC* in the late response support these findings and might indicate that mechanical stretching controls the symbiosis of *E. festucae* and plant through *proA* and *symC*.

In *E. festucae*, nicotinamide adenine dinucleotide phosphate-(NADPH) (Nox) complex has been shown to be an important regulator of mutualistic relationship between the endophyte and host plant (Eaton et al., 2010, 2011; Tanaka et al., 2008). The Nox complex is

responsible for producing reactive oxygen species (ROS) that regulates hyphal growth in plants and maintains symbiotic interactions (Kayano et al., 2018). So far, six subunits of the Nox complex (NoxA, NoxR, RacA, BemA, Cdc24 and Cdc42) have been identified in *E. festucae* (Kanayno 2018). None of them were found to be differentially expressed in response to mechanical stretching except NoxD, which is a newly identified subunit that interacts with NoxA in Nox complex (Ozaki et al., 2015). NoxD has been shown to be crucial for maintaining symbiosis between *E. festucae* and host plant (Ozaki et al., 2015). The fact that only NoxD was up-regulated in response to mechanical stretching indicates that this component might be the only protein in Nox complex to be influenced by mechanical stretching.

In *E. festucae*, adenosine 3′, 5′-cyclic monophosphate (cAMP)-dependent signalling, which has a regulatory role in broad range of metabolic activities was found to be crucial for maintaining symbiosis between endophyte and host plant (D'Souza and Heitman 2011, Voisey, 2016). Deletion of the adenylate cyclase gene (*acyA*) in *E. festucae* resulted in a decreased radial growth rate and hyper-branching of hyphae in cultures *in vitro*, and elevated hyphal biomass in infected plants compared to WT (Voisey, 2016). Up-regulation of *acyA* in response to mechanical stretching might indicate that mechanical stretching controls hyphal branching and tip growth through cAMP-dependent signalling.

The eight putative fungal host interaction related genes that were differentially expressed in responses compared to un-stretched control cultures were putative surface attachment proteins (Table 4.5). Among them, only two hydrophobins and a CFEM domain containing proteins were up-regulated in early response, and all eight of them were up-regulated in the late response to mechanical stretching (Table 4.5). We found three putative hydrophobic surface binding protein A (HsbA), three putative hydrophobins, one putative adhesin-like protein 1 homolog and a CFEM domain containing protein that were up-regulated in late response to mechanical stretching (Table 4.5). The roles of these types of proteins in plant endophyte mutualistic interactions have not been studied so far, however their role in pathogenic interactions between fungi and their host have been reported previously. HsbA and hydrophobins in pathogenic fungi are small secreted proteins which are known to facilitate attachment to surfaces and recruitment of lysis enzymes to extracellular spaces (Muszewska et al., 2018). A homolog of HsbA in *M. anisopliae* has been found to be expressed during colonization of the insect cuticle (Ohtaki et al., 2006). In *A. oryzae*, HsbA was found to be required for adherence to a synthetic surface and recruitment of cutinase 1 (CutL1) to degrade it (Ohtaki et al., 2006). Also in the same organism, hydrophobin RolA

was found to be highly expressed in a medium containing synthetic degradable material, and CutL1 production was also increased (Takahashi et al., 2005). RolA was found to be directly interacting with CutL1 via immunostaining (Takahashi et al., 2005). Therefore, Hsb and hydrophobins are thought to be important surface attachment proteins that can recruit enzymes such as cutinases to the insect cuticle or plant cell wall that is to be colonized or infected by pathogenic fungi (Takahashi 2005). As mentioned above, I found a putative *E. festucae* cutinase that was highly transcribed in early and late responses to mechanical stretching compare to control cultures (Table 4.2, 4.3). Also, in *M. oryzae*, nitrogen-utilizing enzymes encoded by *npr1* and *npr2* were also found to control pathogenicity and expression of the hydrophobin-encoding gene *mpg1* (Froeliger, 1996). Combined with my GO assessment showing DEG enrichment in categories associated with nitrogen utilization in response to mechanical stretching, the expression of hydrophobins might indicate co-regulation of nitrogen utilization and hydrophobin expression in *E. festucae*. My findings so far indicate that mechanical stretching might promote increase in surface attachment of hyphae via Hsb and hydrophobins, which in turn might result in recruitment of cutinase to facilitate better hyphal attachment to surfaces. Collectively, the up-regulation of important symbiosis related genes in *E. festucae* in response to mechanical stretching points to the possible role of mechanical stress in symbiosis and host colonization.

4.3.5. Mechanical Stretching Induces Expressions of Genes Related to Transcription in *E. festucae*

To understand the role of mechanical stretching in transcriptional regulation, we have examined the expression of known transcription factors (TF) in fungi (Figure 3.19). My results revealed 13 putative TFs that were differentially regulated in early and late responses to mechanical stretching (Table 4.6). Among them, we have found 6 putative zinc finger domain containing TFs, 2 putative Helix loop helix (HLH) TFs 1 Myb-like DNA binding domain containing TF, 1 basic leucine zipper (bZIP), 1 Forkhead associated domain (FHA) containing and 1 CCAAT box-binding TF (CTF) (Table 4.6). Four TF families have been defined as fungal-specific TFs and the Zn(2)-C6 DNA binding domain containing TF family is one of them, recognized by their conserved cysteine motif (Shelest et al., 2017). There are 55 estimated zinc cluster TFs in *S. cerevisiae* and their characterization has revealed their diverse roles from regulating sugar metabolism to stress responses (MacPherson, 2006). In my data, a putative homolog of the *S. cerevisiae* Gal4 TF was up-regulated in response to mechanical stretching (Table 4.6). Gal4 TF in *S. cerevisiae* is one of the well-studied TFs in

yeast that is known to regulate galactose metabolism by a complex mechanism of action involving phosphorylation, DNA binding or recruiting chromatin remodelling proteins to promoters (Breunig et al., 2000). In *A. nidulans*, a Gal4 like TF with a Zn(2)-C6 domain was identified and found to regulate nitrate metabolism (Burger et al., 1991). If the putative Gal4 like TF in *E. festucae* is also responsible for nitrate metabolism, its up-regulation in response to mechanical stretching supports my findings from the GO analysis, where nitrate metabolism was enriched in response to mechanical stretching (Figure 4.3). We also found another putative TF homolog of *S. cerevisiae*, Azf1, with zinc finger domain that was up-regulated in early and late response to stretch compare to controls (Table 4.6). *S. cerevisiae* TF Azf1 is known to regulate glucose metabolism and growth, as well as cell wall integrity (Slattery et al., 2006). Deletion of *azf1* resulted in cell wall defects and increased susceptibility to caffeine and SDS compared to WT (Slattery et al., 2006). If putative *E. festucae* Azf1 is regulating glucose metabolism, growth and cell wall integrity similar to *S. cerevisiae* Azf1, this would support my GO analysis findings where carbohydrate metabolism and hyphal growth related categories were enriched in response to mechanical stress (Figure 4.5). Therefore, a connection can be made on the influence of mechanical stretch on transcriptional regulation of these metabolic activities via Azf1. We found 2 putative HLH TF up-regulated in response to mechanical stress (Table 4.6). In yeast, HLH domain containing TF are involved in regulation of biosynthesis of phospholipids and uptake of phosphates (Berben, 1990). Functions of HLH transcription factors have not been extensively studied in filamentous fungi. My result showed a putative Myb-like TF was up-regulated in response to mechanical stretching (Table 4.6). Myb-like TFs have been studied more extensively in plants and found to participate in regulation of drought resistance, growth, cell cycle and cell differentiation (Rawat et al., 2009; Hirai et al., 1996; Shin et al., 2011; Kirik et al., 2004). In *F. graminearum*, Myb-like TFs Myt1, Myt2 and Myt3 have been characterized (Kim et al., 2014). Myt1 and Myt2 were found to control sexual development, while Myt3 controlled vegetative growth in culture and pathogenicity during wheat infection (Kim et al., 2014). Another finding in my data was of a bZIP TF putative that was differentially regulated in response to mechanical stretch (Table 4.6). A recently characterized bZIP TF AtfB in *A. parasiticus* was found to regulate aflatoxin synthesis and formation of conidiospores (Wee et al., 2017). Moreover, RNA sequencing of *atfb* mutants showed that this TF controlled 40 genes putatively associated with virulence (Wee et al., 2017). A putative Forkhead domain-containing TF was also up-regulated in my data (Table 4.6). In *M. oryzae*, 2 Forkhead domain carrying TFs Fkh1 and Hcm1 have been characterized

(Park et al., 2014). Both Fkh1 and Hcm1 deletion caused hyphal growth impairment and conidiation defects, Fkh1 deletion further caused abnormal septal formation and hyphal morphology, also decreased pathogenicity on rice presenting as smaller lesions compared to WT (Park et al., 2014). Due to a lack of information on the exact role of these putative TFs, a conclusion cannot be drawn on the role of mechanical stretching in transcriptional regulation of certain pathways. Characterization of these TFs in the future will lead to a better understanding of the pathways that are influenced by mechanical stretching in *E. festucae*.

4.3.6. Mechanical Stretching does not Induce Expressions of Stress Related Genes in *E. festucae*

Finally, I looked at the expression of stress-related genes in response to mechanical stretching to determine whether mechanical stretch induced a stress response. We have found 2 differentially regulated Heath Shock Proteins (HSP) among 20 known *E. festucae* HSP. HSPs are highly conserved eukaryotic proteins that are synthesized in response to various environmental stresses, mainly heat, to protect other proteins from unfolding or facilitate refolding (Verghese et al., 2012). In *S. cerevisiae*, heat stress induces activation of three pathways; Cell Wall Integrity (CWI), Heat Shock Response (HSR) and Environmental Stress Response (ESR) (Verghese et al., 2012). Upon exposure to stress, the cell cycle is halted and metabolites such as trehalose are synthesized to increase tolerance to heat, and membrane and cell wall structures are modified to become richer in lipid-derived components (Dickson et al., 2002; Verghese et al., 2012). None of the putative *E. festucae* apoptosis genes were among the DEGs in my datasets, however a putative homolog of Inhibitor of apoptosis protein (IAP)-like protein (Ilp-2) in *M. brunneum* was up-regulated in the late response to mechanical stretching compared to control (Table 4.7). Apoptosis is a tightly controlled cell death program that is necessary part of cellular development and the life course of an organism (Ligr et al., 1998). Apoptosis inhibitors function to prevent apoptosis by facilitating the ubiquitination of caspases, which are responsible of cleaving crucial cellular structures (Owsianowski et al., 2008). An IAP family protein, Bir1, in *S. cerevisiae* has been characterized and found that deletion of *bir1* resulted in cells more susceptible to apoptosis by oxidative stress compared to WT, and overexpression of *bir1* in aging cells delayed apoptosis significantly (Walter et al., 2006). This implies that the *E. festucae ilp-2*-like gene may protect hyphae from damage caused by mechanical stress. However, none of the putative *E. festucae* Cn/Zn superoxide dismutases were differentially regulated, as well as putative trehalose biosynthesis genes, chloride channel genes and copper metallothionein genes that

have been associated with stress response in endophytes (Nagabhyru et al., 2018). We have also found that putative N2227-like protein and Blue light inducible 3 (Bli-3) proteins were up-regulated in late response to mechanical stretching (Table 4.7). None of these proteins have been characterized in *E. festucae* previously, and studies on other fungi are limited to *S. cerevisiae* (for N2227 protein) and *N. crassa* (for Bli proteins). The limited literature on N2227 indicates that this protein is involved in meiosis and stress response in *S. cerevisiae*, and its role in filamentous fungi is yet to be studied (Garcia-Cantalejoa et al., 1995). Bli proteins have been studied in *N. crassa* and known to regulate many gene expressions in response to light exposure, however their role in endophytic fungi is not known (Wu et al., 2014). The expression levels of stress related genes in early and late responses so far did not indicate a strong stress reaction in *E. festucae* hyphae during mechanical stretching, therefore we concluded that 6% of mechanical stretching along the stretchable silicon membrane was not a significant stress-inducing stimulus for *E. festucae*.

4.3.7. Conclusion and Major Impact

This transcriptomics study was the first attempt in the literature to show the gene expression changes in *E. festucae* solely in response to *in vitro* mechanical stretching. In immediate responses to mechanical stimuli, *E. festucae* hyphae showed changes in the nitrogen metabolism and cutinase activity, whereas in the later response to mechanical stimuli, a greater response was observed overall, mainly in carbohydrate metabolism, hyphal growth and cell wall and oxidoreductase activities. Moreover, up-regulation of fungal growth and cell wall remodelling, symbiosis and transcription regulatory genes showed that mechanical stretching acted as a stimulus to promote hyphal growth and revealed its possible role in the regulation of symbiosis. Lack of consistent up-regulation in stress-related genes indicated that mechanical stretching applied to the cultures in this study (3 mm in total, 6% of the whole silicon membrane) functioned as a stimulus rather than a stressor. These findings supported the previous studies on intercalary growth and mechanical stimuli by showing the gene expression profiles of un-stretched and stretched hyphae.

Several limitations were encountered throughout the study that hindered a more thorough analysis of DEGs in *E. festucae* in response to mechanical stretching. Due to small culture sizes and dissection of horizontal hyphae that made the sample sizes even smaller, samples of the same treatments had to be pooled together to yield sufficient total RNA for sequencing. This required many replications of culturing, stretching and culture harvesting that forced me to reduce my treatment conditions to only the control, early and late, in which early and late

cultures were subjected to 3 mm of stretching only once. Therefore, we were not able to observe the DEGs after a full course of stretching, which usually takes place over 9 h and cultures are stretched 9 mm in total. Therefore, my DEGs list might have only captured a fraction of reactions to mechanical stimuli, or gene expression fold changes might have been in the smaller range compared to cultures hypothetically stretched for 9 mm over 9 h. Nevertheless, because the study had a lot of technical replication, I was able to detect even slight changes in gene expression, and was able to set the fold change threshold to ±1.5. In the future, it would be useful to validate the data by qPCR and by examining gene expression in cultures stretched over longer time periods, and also in samples from the leaf expansion zone where hyphae are presumably being subjected to mechanical stretch as the plant cells expand. Another limitation of this study was that the GO category IDs of *E. festucae* genes are poorly annotated. In total, 88 DEGs in the early response and 346 DEGs in late response were not detected in the GO analysis process, which we have overcome by computationally annotating the remaining DEGs to attempt to understand their functions in *E. festucae*.

While the transcriptomics approach was useful in determining the effects of mechanical stretch on *E. festucae* gene expression, the findings will not reflect all the changes that occur in response to stretch. For example, stress sensing pathways may be contitutively expressed and activated through other mechanicsms such as phosphorylation or changes in protein conformation. In future, these changes could be observed with additional methodologies, such as phosphylation assays. Immunofluorescence techniques could also be used to visualize the localisation of mechanosensor proteins in response to mechanical stretch. In summary, this transcriptomics study has paved the way for future characterization studies in *E. festucae* to understand the genes that sense and respond to mechanical stretching, and hopefully translate the *in vitro* findings to better understand the plant endophyte interactions.

5. Investigation of the Role of Putative Wsc Proteins in *Epichloë festucae*

The Cell Wall Integrity (CWI) pathway is considered likely to be important in intercalary growth of *E. festucae*, since mechanical strain is expected to place stress on cell walls. The CWI pathway is able to sense cell wall disturbance and appropriate molecular responses are initiated to strengthen the wall (Jin et al., 2013; Ketela et al., 1999; Heinisch et al, 2007). As one of the aims of this project, the identification of potential Wsc proteins linked to the CWI pathway in *E. festucae* was carried out for better understanding of how intercalary growth is regulated. For this, functionally characterized Wsc proteins from other fungi were used as queries to retrieve homologous sequences from the *E. festucae* genome, and these candidate Wsc proteins were subjected to domain analysis, and then evolutionary relationships between these candidate proteins and functional Wsc proteins were assessed.

5.1. *In silico* Identification of Putative *E. festucae* Wsc proteins

In the well-characterised CWI pathway of *S. cerevisiae*, Wsc1 protein is known to play an important role in sensing mechanical stress imposed on the cell wall due to its spring like function (Jendretzki et al., 2011). *S. cerevisiae* Wsc1 contains an N-terminal signal peptide (SP), an extracellular carbohydrate binding domain or wall stressor component (WSC), a region rich in serine/threonine residues in the N terminal (STR) and a transmembrane domain (TMH) for embedding Wsc1 into the cell membrane, and finally a C-terminal cytoplasmic domain (CT) for molecular signalling in the cytoplasm (Straede & Heinisch, 2007). Most of the homolog Wsc proteins from other organisms share the same domain layout by carrying SP, WSC, STR, THM and CT (Dichtl et al., 2016). Functionally characterized Wsc homologs in fungi to date are shown in Table 5.1.

Table 5.1 Wsc proteins that have been characterized as a functional component of CWI in other fungal species.

Species	Protein	Reference
Saccharomyces cerevisiae	Wsc1 (NP_014650), Wsc2 (KZV08342), Wsc3 (KZV07773), Wsc4 (KZV10689)	Verna et al., 1997, Rodicio et al., 2010
Aspergillus fumigatus	Wsc1 (AFUA_4G13670), Wsc2 (AFUA_3G07050), Wsc3 (AFUA_5G09020)	Dichtl et al, 2012
Candida albicans	Wsc1/3 (AOW28444)	Norice et al., 2007, Zucchi et al., 2011
Neurospora crassa	Wsc1 (JQ520130), Wsc2 (JQ520133)	Maddi et al., 2012
Kluyveromyces lactis	Wsc1 (KLLA0D14377), Wsc2/3 (KLLA0E00771)	Heinisch et al., 2008, Rodicio et al., 2008
Candida glabrata	Slg1 (Wsc1) (KTB22651)	Rosenwald et al., 2016
Pichia pastoris	Wsc1 (CCA39535)	Ohsawa et al., 2017

The bioinformatics analyses for retrieving Wsc proteins from *E. festucae* was carried out under the supervision of bioinformatician Dr Pierre Yves-Dupont. *E. festucae* Wsc candidate proteins were retrieved from two sources. First, *E. festucae* model protein sequences containing WSC domains were retrieved from the *Epichloë* database of Massey University by searching the *E. festucae* Fl1M3 Gene Models for computationally annotated WSC domains, using WSC as the keyword. In addition, the *E. festucae* Fl1 genome was interrogated using tBLASTn (Basic Local Alignment Search Tool) (Altschul et al., 1990) using known functionally characterized Wsc protein sequences in Table 5.1 as queries. The retrieved proteins with score bits lower than 40 were filtered out from the candidate list. The previously annotated *E. festucae* WscA (Ariyawansa, 2015) was included in the candidate Wsc proteins retrieved through these methods. *Sc*Wsc4 and Wsc4 homologs from other fungi were not included since they are located in the ER membrane rather than the plasma membrane adjacent to the cell wall, and also do not appear to have a direct role in sensing cell wall stress in other fungi (Kock et al., 2015).

The retrieved proteins were subjected to domain analysis using the InterProScan tool (Zdobnov et al., 2001) and their domains used to refine the putative *E. festucae* Wsc homolog list further. Proteins containing a WSC domain and a TMH domain, along with the presence of STR and CT domains, were considered as strong candidates. Other putative *E. festucae* Wsc protein homologs that lacked WSC, SP, CT and/or TMH domains were not included in further analyses, since Wsc proteins are expected to have these domains to function as a cell wall stress sensor (Verna et al., 1997). As a result, two candidate Wsc proteins from

E. festucae (including the previously characterized WscA) were analysed further. Wsc proteins that have been functionally characterized in other fungi (Table 5.1) were retrieved from JGI (The Fungal Genomic Resource, http://genome.jgi.doe.gov/) for use in the protein sequence alignments and phylogenetic trees. The domains of the retrieved Wsc proteins were analysed and annotated using the InterProScan extension in Geneious, as described above. The amino acid sequences of the candidate Wsc proteins from *E. festucae*, and functionally characterized Wsc proteins from the other fungi, a total of 16 sequences, were aligned to assess similarities between the proteins (Figure 5.1).

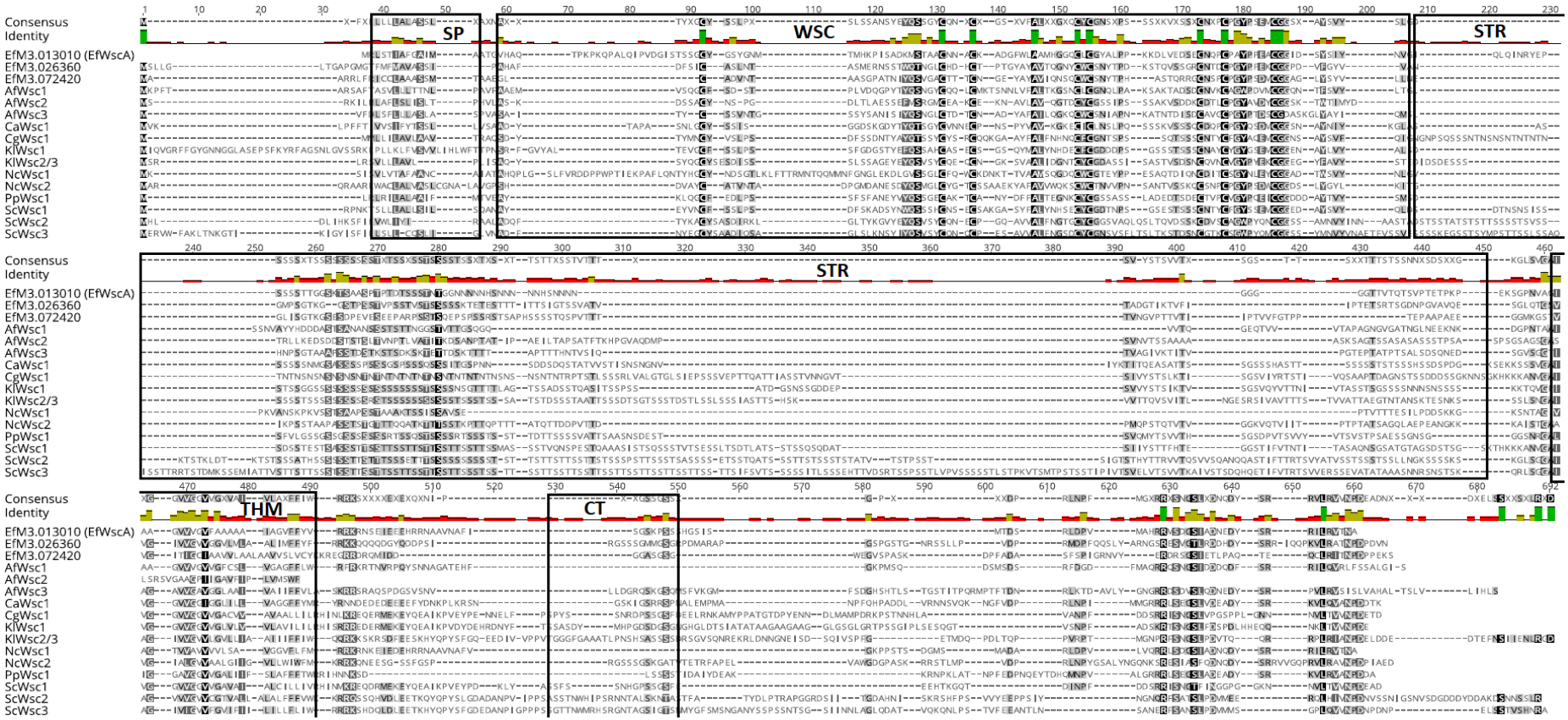

Figure 5.1 Protein sequence alignment of *E. festucae* Wsc candidates (EfM3.026360 and EfM3.072420) and *Ef*WscA (EfM3.013010) with other functionally characterized fungal Wsc proteins. Amino acid similarity to consensus is indicated by grey and black boxes along the sequences, grey showing similar amino acids and black showing the same amino acids throughout the sequences. Af: *A. fumigatus*, Ca: *C. albicans*, Cg: *C. glabrata*, Ef: *E. festucae*, Kl: *K. lactis*, Nc: *N. crassa*, Pp: *P. pastoris*, Sc: *S. cerevisiae.* Accessions numbers for each characterized protein are given in Table 5.1. Protein domains are shown in black squares. SP: Signal peptide, WSC: Wsc domain, STR: Serine/threonine rich region, THM: Transmembrane domain, CT: Cytoplasmic tail.

Table 5.2 Matrix of amino acid identity scores of *E. festucae* Wsc candidates (EfM3.026360 and EfM3.072420) and *Ef*WscA (EfM3.013010) aligned with other functionally characterized Wsc proteins. The highest identity scores between *E. festucae* proteins and Wsc proteins from other fungi are shown in red squares. Af: *A. fumigatus*, Ca: *C. albicans*, Cg: *C. glabrata*, Ef: *E. festucae*, Kl: *K. lactis*, Nc: *N. crassa*, Pp: *P. pastoris*, Sc: *S. cerevisiae*. Accessions numbers for each protein are given in Table 5.1.

	AfWsc1	AfWsc2	AfWsc3	CaWsc1	CgWsc1	EfM3.013010	EfM3.026360	EfM3.072420	KlWsc1	KlWsc2/3	NcWsc1	NcWsc2	PpWsc1	ScWsc1	ScWsc2	ScWsc3
AfWsc1		16.7%	20.3%	20.7%	14.1%	23.5%	17.3%	15.1%	15.3%	18.2%	24.2%	15.8%	20.1%	17.3%	14.5%	14.1%
AfWsc2	16.7%		19.7%	21.2%	15.2%	15.6%	19.5%	14.8%	14.0%	16.7%	13.7%	17.0%	21.3%	17.3%	15.8%	14.6%
AfWsc3	20.3%	19.7%		20.2%	15.1%	20.1%	27.3%	22.2%	15.7%	17.7%	19.3%	29.4%	21.4%	15.5%	13.6%	13.5%
CaWsc1	20.7%	21.2%	20.2%		20.4%	22.6%	22.7%	16.5%	24.3%	23.4%	19.4%	21.7%	28.8%	25.2%	20.2%	17.9%
CgWsc1	14.1%	15.2%	15.1%	20.4%		14.8%	13.4%	13.5%	32.8%	20.8%	12.5%	15.5%	21.2%	43.9%	18.1%	17.7%
EfM3.013010 (EfWscA)	23.5%	15.6%	20.1%	22.6%	14.8%		19.6%	14.7%	14.4%	15.6%	30.4%	17.4%	18.9%	16.5%	11.5%	11.3%
EfM3.026360	17.3%	19.5%	27.3%	22.7%	13.4%	19.6%		25.1%	16.7%	17.8%	18.9%	33.5%	24.4%	16.6%	13.9%	14.1%
EfM3.072420	15.1%	14.8%	22.2%	16.5%	13.5%	14.7%	25.1%		14.0%	16.3%	14.9%	24.2%	18.1%	16.8%	10.7%	12.2%
KlWsc1	15.3%	14.0%	15.7%	24.3%	32.8%	14.4%	16.7%	14.0%		24.1%	14.6%	15.5%	24.2%	36.9%	20.1%	19.9%
KlWsc2/3	18.2%	16.7%	17.7%	23.4%	20.8%	15.6%	17.8%	16.3%	24.1%		15.2%	16.3%	27.3%	25.5%	31.6%	30.9%
NcWsc1	24.2%	13.7%	19.3%	19.4%	12.5%	30.4%	18.9%	14.9%	14.6%	15.2%		15.9%	16.4%	13.5%	12.6%	11.2%
NcWsc2	15.8%	17.0%	29.4%	21.7%	15.5%	17.4%	33.5%	24.2%	15.5%	16.3%	15.9%		20.6%	17.3%	13.8%	13.9%
PpWsc1	20.1%	21.3%	21.4%	28.8%	21.2%	18.9%	24.4%	18.1%	24.2%	27.3%	16.4%	20.6%		26.1%	19.0%	17.6%
ScWsc1	17.3%	17.3%	15.5%	25.2%	43.9%	16.5%	16.6%	16.8%	36.9%	25.5%	13.5%	17.3%	26.1%		22.6%	22.2%
ScWsc2	14.5%	15.8%	13.6%	20.2%	18.1%	11.5%	13.9%	10.7%	20.1%	31.6%	12.6%	13.8%	19.0%	22.6%		42.1%
ScWsc3	14.1%	14.6%	13.5%	17.9%	17.7%	11.3%	14.1%	12.2%	19.9%	30.9%	11.2%	13.9%	17.6%	22.2%	42.1%	

The alignment of Wsc proteins showed an overall low similarity between the *E. festucae* Wsc proteins and others, the highest sequence identity between *E. festucae* proteins and others was between *Nc*Wsc2 and EfM3.026360 as 33.5% identity score (Table 5.2). The lowest identity was observed between *Sc*Wsc2 and EfM3.072420 (10.7%), and the highest identity was observed between *Sc*Wsc1 and *Cg*Wsc1 (43.9%) (Table 5.2).

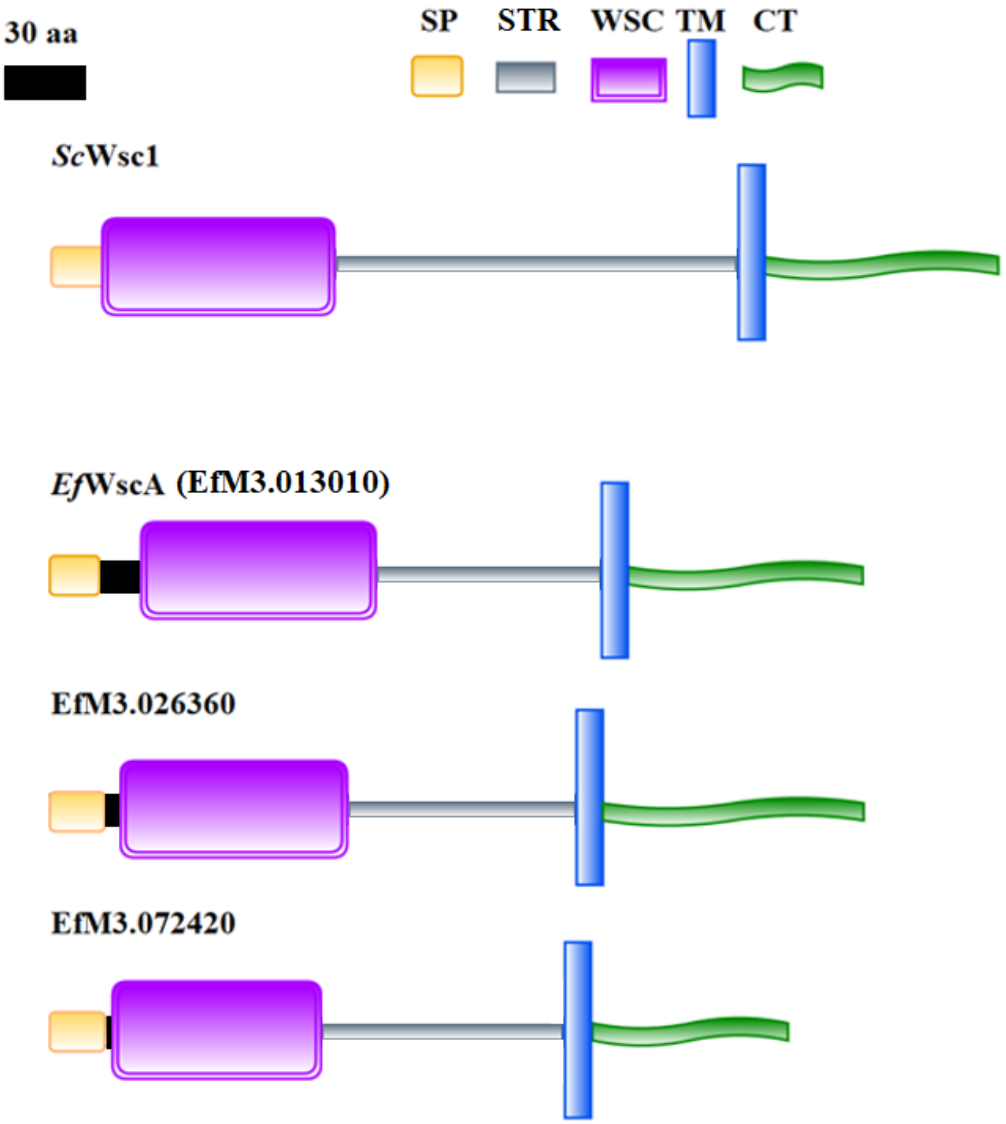

Figure 5.2 Two *E. festucae* candidate Wsc proteins, *Ef*WscA and *Sc*Wsc1 (NP_014650) with their annotated domains drawn approximately to scale. SP: Signal peptide, WSC: Cysteine rich domain, STR: Serine/threonine rich region, TM: Transmembrane domain, CT: Cytoplasmic tail. Black shows non-homologous regions.

The Wsc domains of the three *E. festucae* proteins had the eight conserved cysteine residues (Figure 5.3) characteristic of cysteine motifs in WSC domains which are thought to be essential for the function of the Wsc proteins during interactions with cell wall components (Verna et al., 1997).

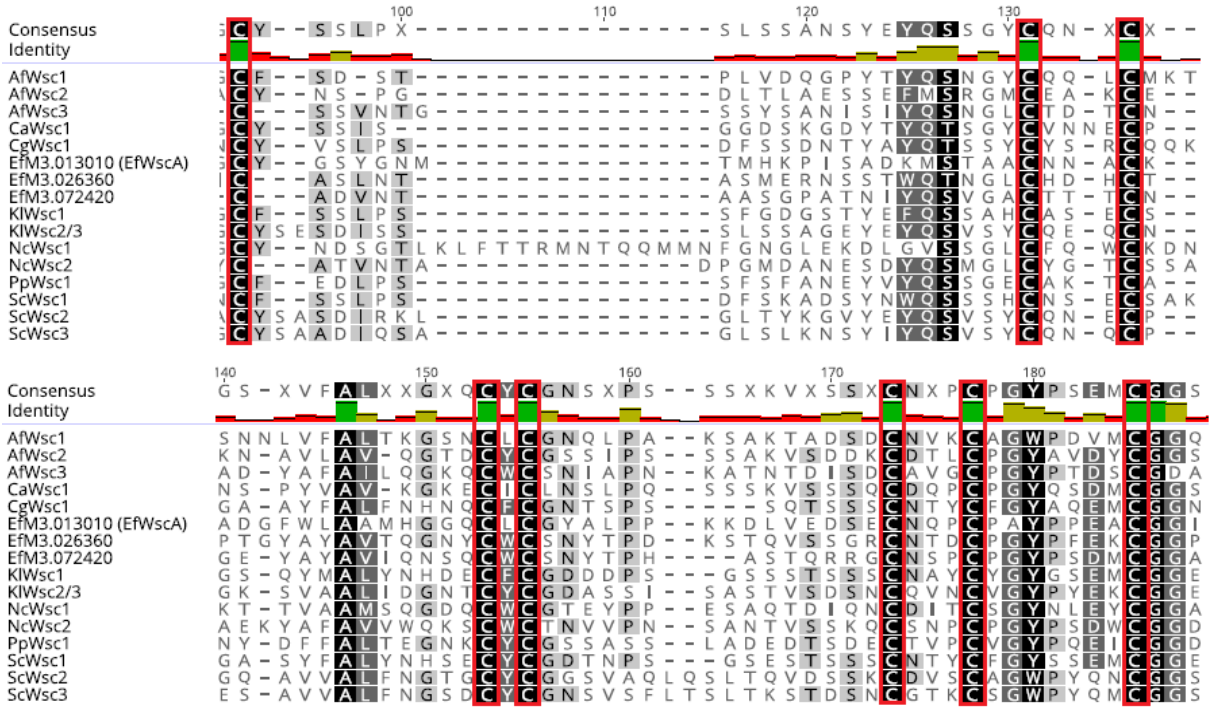

Figure 5.3 Alignment of WSC domains in Wsc protein sequences. The eight conserved cysteine residues are marked with red squares throughout the domain. Af: *A. fumigatus*, Ca: *C. albicans*, Cg: *C. glabrata*, Ef: *E. festucae*, Kl: *K. lactis*, Nc: *N. crassa*, Pp: *P. pastoris*, Sc: *S. cerevisiae*. Accessions numbers for each protein are given in Table 5.1.

Following the WSC domain, a serine threonine rich region (STR) was observed in all proteins in the alignment (Figure 5.2). The STR domain strengthens the evidence that *E. festucae* Wsc candidates (EfM3.026360 and EfM3.072420) and *Ef*WscA (EfM3.013010) Wsc proteins, since the function of STR is to sense mechanical stress through the *O*-linked glycosylation of serine and threonine residues in *Sc*Wsc1 (Verna et al., 1997).

In order to assess the evolutionary relationship between candidate *E. festucae* and the other fungal proteins, a phylogenetic tree was constructed using the protein alignment using the MAFFT E-INS-i alignment algorithm and Maximum Likelihood from PhyML software with 1000 Bootstrap replicates in Geneious. (Figure 5.4).

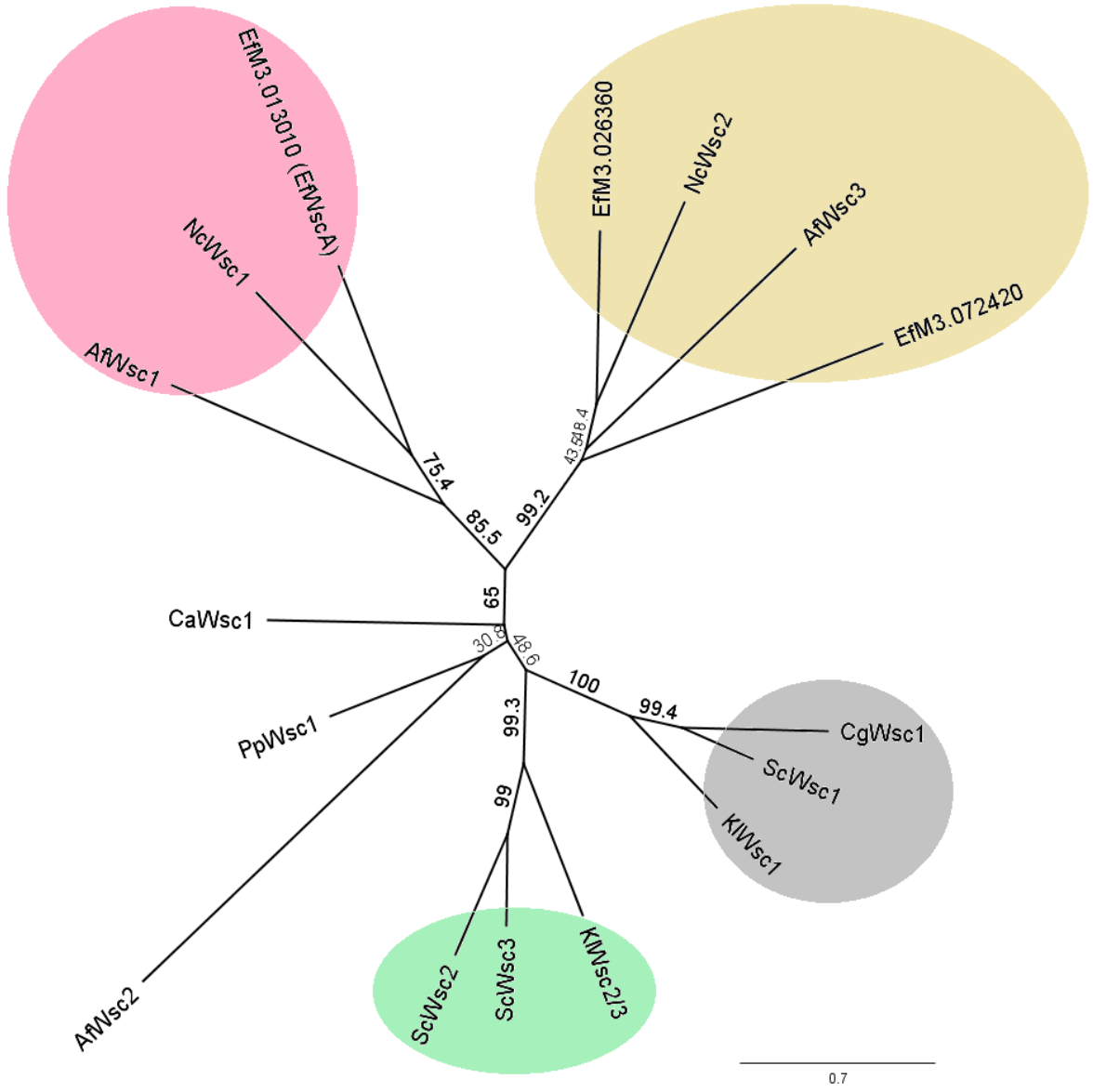

Figure 5.4 Phylogenetic relationship of Wsc proteins constructed using the MAFFT E-INS-i alignment algorithm and Maximum Likelihood from PhyML software with 1000 Bootstrap replicates. The organisms are labelled using their initials. : Filamentous WscA group, : Filamentous WscB or WscC group, : Yeast Wsc1 group, : Yeast Wsc2 or Wsc3 group. Af: *A. fumigatus*, Ca: *C. albicans*, Cg: *C. glabrata*, Ef: *E. festucae*, Kl: *K. lactis*, Nc: *N. crassa*, Pp: *P. pastoris*, Sc: *S. cerevisiae*. Accessions numbers for each protein are given in Table 5.1.

The phylogenetic tree revealed that the previously functionally characterized *E. festucae* WscA (EfM3.013010) showed closest similarity to NcWsc1 and AfWsc1 highlighted in pink (Figure 5.4). Also, EfM3.026360 and EfM3.07240 were grouped with NcWsc2 and AfWsc3, indicating that these two proteins could be potential Wsc2 or Wsc3 homologs (highlighted in yellow). The phylogenetic tree demonstrated that candidate *E. festucae* Wsc proteins and the functionally characterized *Ef*WscA are more likely to be similar to Wsc proteins from other

filamentous fungi (*N. crassa* or *A. fumigatus*) than to the *C. glabrata*, *K. lactis* and *S. cerevisiae* Wsc proteins.

5.2. Expression of *E. festucae* CWI Genes in Response to Mechanical Stretch

In *S. cerevisiae*, expression of genes in the CWI pathway and in cell wall biogenesis have been studied (Jung et al., 2002). Mitogen-activated protein kinase (MpkA), that activates the CWI pathway, was overexpressed in *S. cerevisiae* and a transcriptomic analysis was conducted to identify the genes regulated by MpkA (Jung et al., 2002). Although genes for several cell wall protein, stress sensors and cell wall remodelling enzymes were differentially regulated, there was no evidence of differential regulation of the Wsc genes (Jung et al., 2002). In my transcriptomics data, several *E. festucae* cell wall proteins and remodelling enzymes were differentially expressed in response to mechanical stretching compared to control (Chapter 4.2). Therefore, in order to understand if *E. festucae* putative wsc genes were expressed differently in response to mechanical stretching in a similar way, transcriptomics data was interrogated using candidate *Ef*Wsc gene models (as described in Chapter 2.12). Transcriptomic data was searched using the gene models EfM3.013010, EfM3.026360 and EfM3.072420. The criteria used for selecting DE genes was a fold change in expression of ±1.5 between the un-stretched control and the early or late mechanically-stretched hyphae, and a significance difference of $p<0.05$. Using these criteria, none of the candidate *E. festucae* Wsc genes were differentially expressed in hyphae growing on PDA supplemented with 50 mM $CaCl_2$, in either the early or late responses to mechanical stress (Table 5.3).

Table 5.3 The expression of *E. festucae* candidate Wsc genes in early and late responses to mechanical stress, compared to control un-stretched hyphae. ER: early response immediately after stretching, LR: late response 3 h after stretching. RPKM: Reads Per Kilobase Million.

Gene Model	Control	Early	Late	Fold Change	
	RPKM	RPKM	RPKM	ER	LR
EfM3.013010	65794	72522	68702	1.09	1.08
EfM3.026360	1411	1177	1183	-1.2	-1.15
EfM3.072420	4479	5268	5357	1.15	1.23

This result shows that expression of the putative Wsc genes did not alter up to 3 h after mechanical stretch (when the late harvest was taken). It is possible that gene responses may occur later than 3h and thus would not have been detected in this experiment. However, previous research on *Sc*Wsc proteins has shown that *Sc*Wsc1 distribution is localised in patches in the cell membrane of *S. cerevisiae*, and that the patches increase in size and density in response to heat shock or osmotic stress (Heinisch et al., 2010). Since *Sc*Wsc1 protein or transcript levels were not quantified before and after stress, it was not clear whether the proteins changed in their abundance as well as in their distribution. Furthermore, expression differences in Wsc transcripts in response to cell wall stress have not been reported in fungi to date. It is therefore possible that the putative *E. festucae* Wsc sensor proteins are constitutive in their expression as they act to monitor cell wall stress. However other explanations for this result include the possibility that they are not the true homologs of the functionally-characterised fungal Wsc proteins, or that mechano-sensing in *E. festucae* occurs through a different mechanism, such as the calcium channel regulator, MidA (see Chapter 3).

The amino acid sequence similarity of *E. festucae* Wsc proteins (EfM3.026360 and EfM3.072420) and their phylogenetic relationship to functional Wsc2 and Wsc3 proteins indicate that they have the potential to be either Wsc2 or Wsc3 homologs. However, their gene expression was unchanged in response to mechanical stretch compared to un-stretched controls. Lack of gene expression studies on Wsc proteins in the literature presents a problem for choosing a gene for functional analysis. Therefore, we searched for other potential cell

wall stress sensor proteins that changed in their gene expressions in my transcriptomics dataset.

5.3. Identification of a New Putative Cell Wall Stress Sensor Protein in *E. festucae*

To determine whether any *E. festucae wsc* gene homologues were differentially expressed in response to mechanical stretch, the transcriptomics dataset in this thesis (see Chapter 4) was searched for other potential DE stress sensor genes that were responsive to mechanical-stretch. DE genes of the early and late responses were aligned with the functional Wsc proteins in Table 5.1 using BLASTX. One protein (EfM3.023930) with limited amino acid similarity was found (Figure 5.5). The top hit was to *N. crassa* Wsc1, with 12% amino acid similarity (Figure 5.5). EfM3.023930 was differentially expressed in response to mechanical stretch, both the early (+1.65, $p \leq 0.05$) and late (+1.6, $p \leq 0.05$) treatments compared to the un-stretched control. To assess its potential to be a cell wall stress sensor, its protein structure and its sequence similarity to other Wsc proteins were analysed. EfM3.023930 possesses one SP domain in the N terminus, a THM domain and a CT in the C terminus (Figure 5.5).

Figure 5.5 Protein sequence alignment of *E. festucae* Wsc candidates *Ef*WscA, and EfM3.02930 (highlighted in red square) and other functionally characterized fungal Wsc proteins. Increase in similarity of amino acids is indicated by grey and black boxes, grey showing similar amino acids and black showing the same amino acids throughout the sequences along the sequences. Af: *A. fumigatus*, Ca: *C. albicans*, Cg: *C. glabrata*, Ef: *E. festucae*, Kl: *K. lactis*, Nc: *N. crassa*, Pp: *P. pastoris*, Sc: *S. cerevisiae.* The accession numbers for other proteins in the alignment can be found in Table 5.1. Protein domains are shown in black squares. SP: Signal peptide, WSC: Wsc domain, STR: Serine/threonine rich region, THM: Transmembrane domain, CT: Cytoplasmic tail.

	AfWsc1	AfWsc2	AfWsc3	CaWsc1	CgWsc1	EfM3.013010	EfM3.023930	EfM3.026360	EfM3.072420	KlWsc1	KlWsc2/3	NcWsc1	NcWsc2	PpWsc1	ScWsc1	ScWsc2	ScWsc3
AfWsc1		19.7%	20.8%	20.6%	14.1%	24.8%	8.7%	18.7%	16.1%	16.0%	18.1%	23.6%	15.8%	19.8%	17.4%	13.4%	14.2%
AfWsc2	19.7%		19.7%	20.3%	15.5%	16.6%	6.7%	17.3%	14.4%	16.1%	16.0%	14.9%	17.9%	20.6%	18.4%	15.4%	15.1%
AfWsc3	20.8%	19.7%		19.9%	15.0%	19.3%	11.0%	27.5%	24.5%	16.6%	17.2%	18.3%	29.2%	21.7%	14.9%	14.3%	13.5%
CaWsc1	20.6%	20.3%	19.9%		20.3%	21.4%	11.7%	22.1%	15.7%	24.8%	23.4%	17.9%	21.7%	28.5%	23.5%	19.0%	17.4%
CgWsc1	14.1%	15.5%	15.0%	20.3%		14.3%	9.3%	13.9%	12.0%	32.2%	20.6%	13.6%	15.7%	21.6%	45.6%	19.0%	18.5%
EfM3.013010 (EfWscA)	24.8%	16.6%	19.3%	21.4%	14.3%		8.6%	19.5%	15.9%	13.7%	15.6%	32.3%	15.9%	17.6%	15.5%	11.3%	10.2%
EfM3.023930	8.7%	6.7%	11.0%	11.7%	9.3%	8.6%		11.5%	9.6%	10.0%	9.6%	12.0%	11.5%	10.9%	9.6%	7.9%	7.9%
EfM3.026360	18.7%	17.3%	27.5%	22.1%	13.9%	19.5%	11.5%		26.9%	16.7%	18.6%	19.1%	34.7%	21.9%	18.1%	13.6%	14.1%
EfM3.072420	16.1%	14.4%	24.5%	15.7%	12.0%	15.9%	9.6%	26.9%		14.2%	15.8%	15.7%	24.1%	16.6%	15.4%	9.9%	11.8%
KlWsc1	16.0%	16.1%	16.6%	24.8%	32.2%	13.7%	10.0%	16.7%	14.2%		24.9%	14.7%	16.8%	24.3%	37.4%	19.9%	19.3%
KlWsc2/3	18.1%	16.0%	17.2%	23.4%	20.6%	15.6%	9.6%	18.6%	15.8%	24.9%		15.7%	15.5%	27.9%	25.7%	31.6%	30.5%
NcWsc1	23.6%	14.9%	18.3%	17.9%	13.6%	32.3%	12.0%	19.1%	15.7%	14.7%	15.7%		16.0%	17.2%	14.4%	12.4%	11.0%
NcWsc2	15.8%	17.9%	29.2%	21.7%	15.7%	15.9%	11.5%	34.7%	24.1%	16.8%	15.5%	16.0%		21.5%	17.7%	14.0%	13.3%
PpWsc1	19.8%	20.6%	21.7%	28.5%	21.6%	17.6%	10.9%	21.9%	16.6%	24.3%	27.9%	17.2%	21.5%		24.5%	19.3%	17.4%
ScWsc1	17.4%	18.4%	14.9%	23.5%	45.6%	15.5%	9.6%	18.1%	15.4%	37.4%	25.7%	14.4%	17.7%	24.5%		22.0%	21.8%
ScWsc2	13.4%	15.4%	14.3%	19.0%	19.0%	11.3%	7.9%	13.6%	9.9%	19.9%	31.6%	12.4%	14.0%	19.3%	22.0%		42.1%
ScWsc3	14.2%	15.1%	13.5%	17.4%	18.5%	10.2%	7.9%	14.1%	11.8%	19.3%	30.5%	11.0%	13.3%	17.4%	21.8%	42.1%	

Figure 5.6 Matrix of identity scores of *E. festucae* Wsc candidates, *Ef*WscA, EfM3.02930 (highlighted in red square) and other functionally characterized Wsc proteins in the alignment. The highest identity score between EfM3.02930 and other Wsc proteins is shown in the red square. Af: *A. fumigatus*, Ca: *C. albicans*, Cg: *C. glabrata*, Ef: *E. festucae*, Kl: *K. lactis*, Nc: *N. crassa*, Pp: *P. pastoris*, Sc: *S. cerevisiae*. The accession numbers for other proteins in the alignment can be found in Table 5.1.

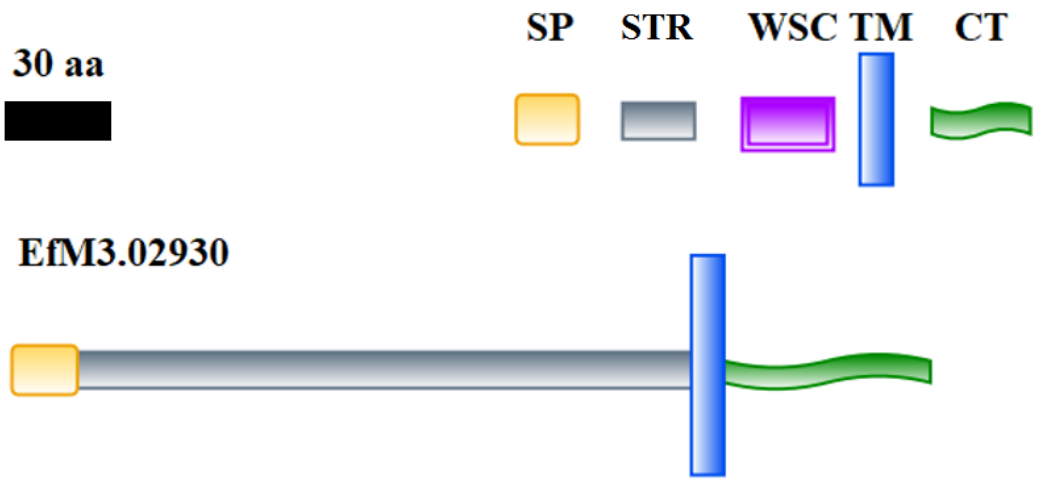

Figure 5.7 Predicted domain layout of *E. festucae* EfM3.023930 protein. SP: Signal peptide, WSC: Wsc domain, T: TM: Transmembrane domain, CT: Cytoplasmic tail. The diagram is drawn to scale. Sc: *S. cerevisiae*.

In order to assess the similarity between EfM3.023930 and known functional Wsc proteins, a protein alignment was made using MAFFT E-NS-i (Figure 5.9). The highest sequence identity observed between EfM3.023930 and other functional Wsc proteins was *Nc*Wsc1 with 12% (32.4% similarity) (Figure 5.9). The alignment revealed that the sequence similarity between EfM3.023930 and other Wsc proteins were in the SP, THM and where WSC domain is found in other proteins (Figure 5.5). Although a complete WSC could not be recognized by InterProScan, two conserved cysteine residues were found in EfM3.023930 in approximately 80 amino acid long sequence between SP and TM (Figure 5.8).

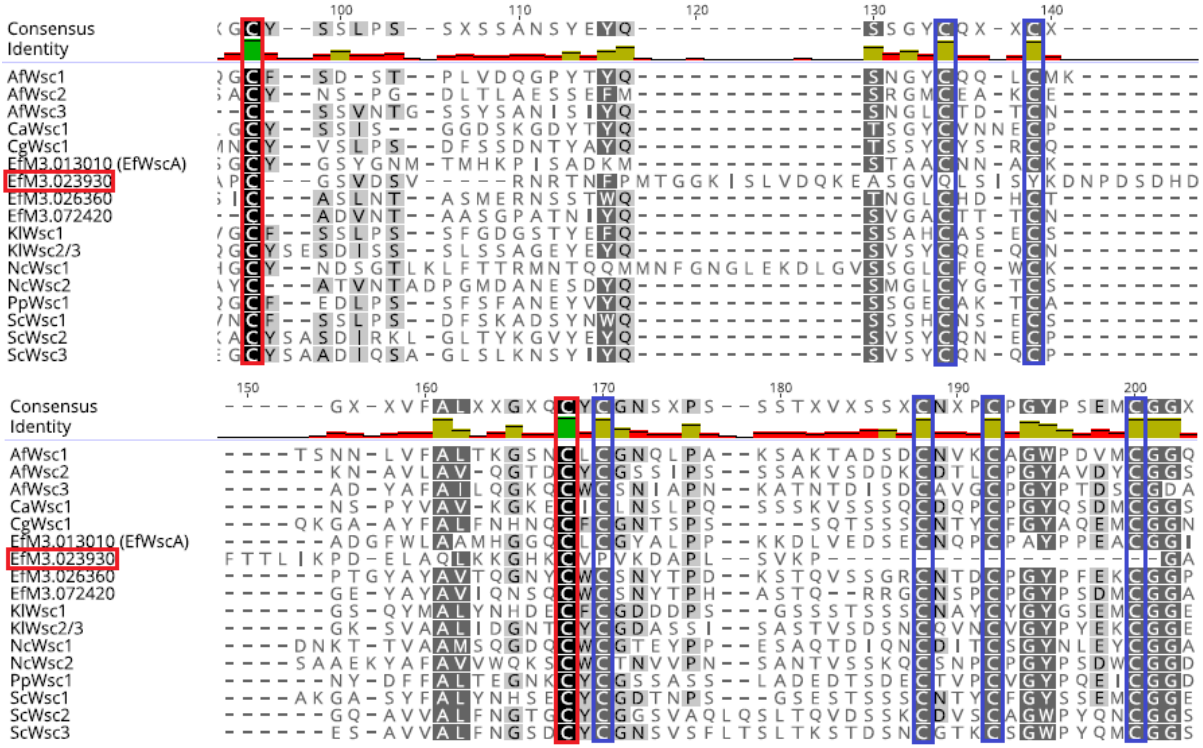

Figure 5.8 WSC domain alignment of two *E. festucae* Wsc candidates (EfM3.026360 and EfM3.072420), *Ef*WscA (EfM3.013010), EfM3.02930 (highlighted in red square) and other functionally characterized Wsc proteins. Two conserved cysteine residues in EfM3.023930 are marked with red squares, and other cysteine residues conserved throughout the domain of the other proteins, but not in EfM3.02930, are marked with blue squares.

In order to assess the evolutionary relationship between the Wsc proteins and EfM3.023930, a phylogenetic tree has been constructed using the protein alignment (Figure 5.5).

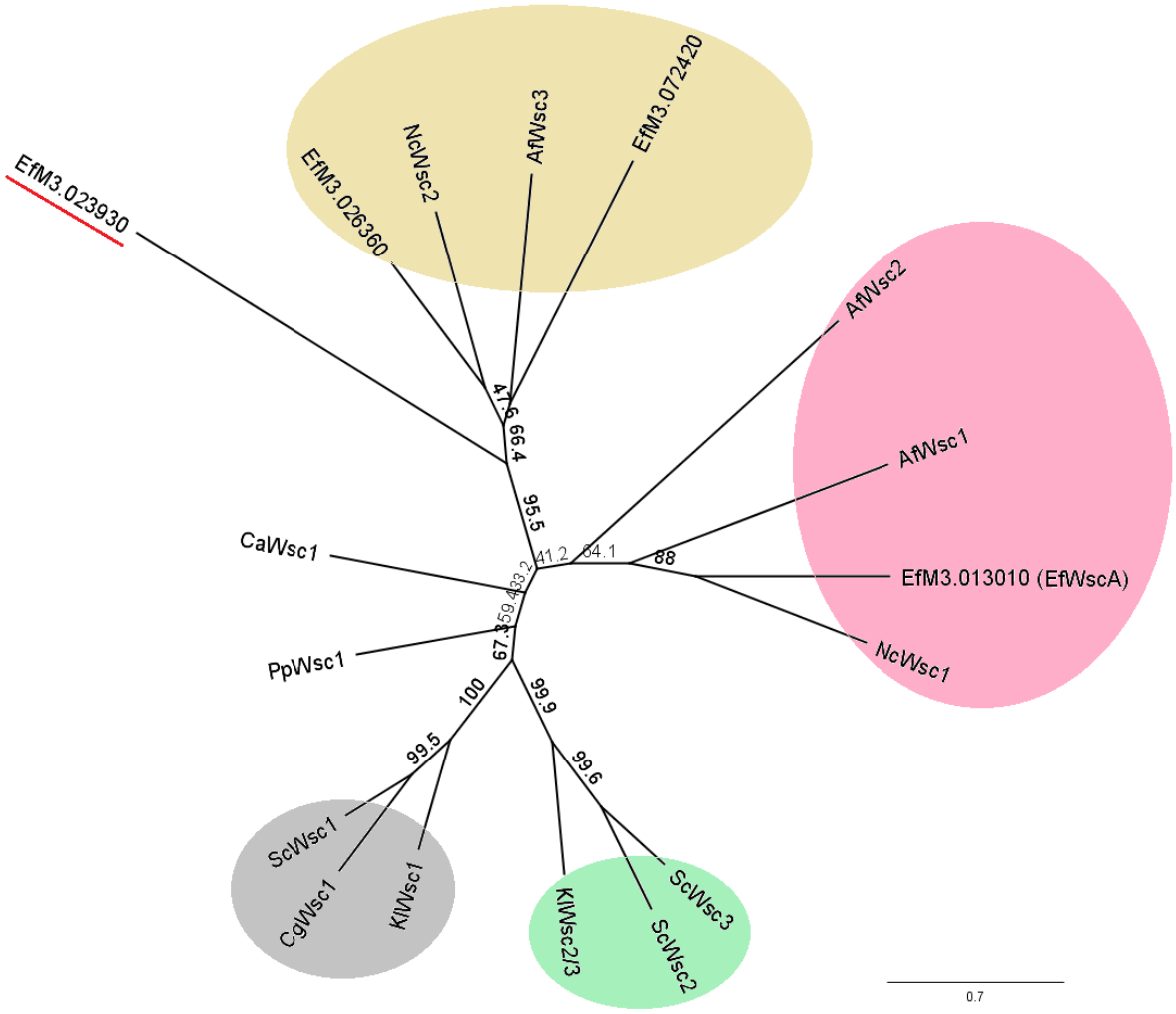

Figure 5.9 Phylogenetic relationship between two *E. festucae* Wsc candidates (EfM3.026360 and EfM3.072420), *Ef*WscA (EfM3.013010), EfM3.02930 (underlined in red) and other functionally characterized fungal Wsc proteins constructed using Maximum Likelihood from PhyML software with 1000 Bootstrap replicates. The organisms are labelled using their initials ● : Filamentous WscA group, ● : Filamentous WscB or WscC group, ● : Yeast Wsc1 group, ● : Yeast Wsc2 or Wsc3 group. Af: *A. fumigatus*, Ca: *C. albicans*, Cg: *C. glabrata*, Ef: *E. festucae*, Kl: *K. lactis*, Nc: *N. crassa*, Pp: *P. pastoris*, Sc: *S. cerevisiae*. The accession numbers for these proteins in the alignment can be found in Table 5.1.

EfM3.023930 was not closely related to any particular fungal Wsc protein but showed a slight agree of sequence similarity with *Af*Wsc3 and *Nc*Wsc2, as well as two other *Ef*Wsc candidates (EfM3.026360 and EfM3.072420) (Figure 5.5). Similar to other *E. festucae* proteins in the analysis, it did not show relatedness to any of the yeast species, *S. cerevisiae*, *K. lactis*, *C. glabrata* or *P. pastoris* Wsc proteins (Figure 5.9). The protein alignment of EfM3.023930 and other Wsc proteins show that this protein is not more similar to functional Wsc proteins than other *E. festucae* Wsc candidates (Figure 5.9). The highest identity

between EfM3.023930 and other Wsc proteins was 12% with *Nc*Wsc1, whereas the highest identity between *Ef*WscA (EfM3.013010) and other Wsc proteins was 30% with *Nc*Wsc1 (Figure 5.6). Although the presence of only two cysteine residues indicate that EfM3.023930 doesn't possess a complete WSC domain (Figure 5.8), slight sequence similarity of SP, WSC, TM and STR region between EfM3.023930 and other Wsc proteins suggests that EfM3.023930 shares some structural relatedness with fungal Wsc proteins (Figure 5.8).

To determine if the genomes of other *Epichloë* species have orthologous EfM3.023930 proteins, the genomes of 17*Epichloë* species on the *Epichloë* genome database of University of Kentucky, USA (http://www.endophyte.uky.edu) was searched using BLAST, with EfM3.023930 as the query. All 17 *Epichloë* species possessed one protein that was highly similar to EfM3.023930 (Appendix 5). The multiple alignment of these proteins to EfM3.023930 returned high similarity scores, the highest being 92.3% to *E. baconii* and lowest being 76.4% to *E. bromicola* 04262 (Appendix 4). The domain structure of the 17 proteins from *Epichloë* species were analysed using InterProScan and found that all of them carried a SP, TM and CT domains, plus an additional conserved region between the SP and TM domains. The protein alignment confirmed the two conserved cysteine residues in the region between SP and TM (Figure 5.8).

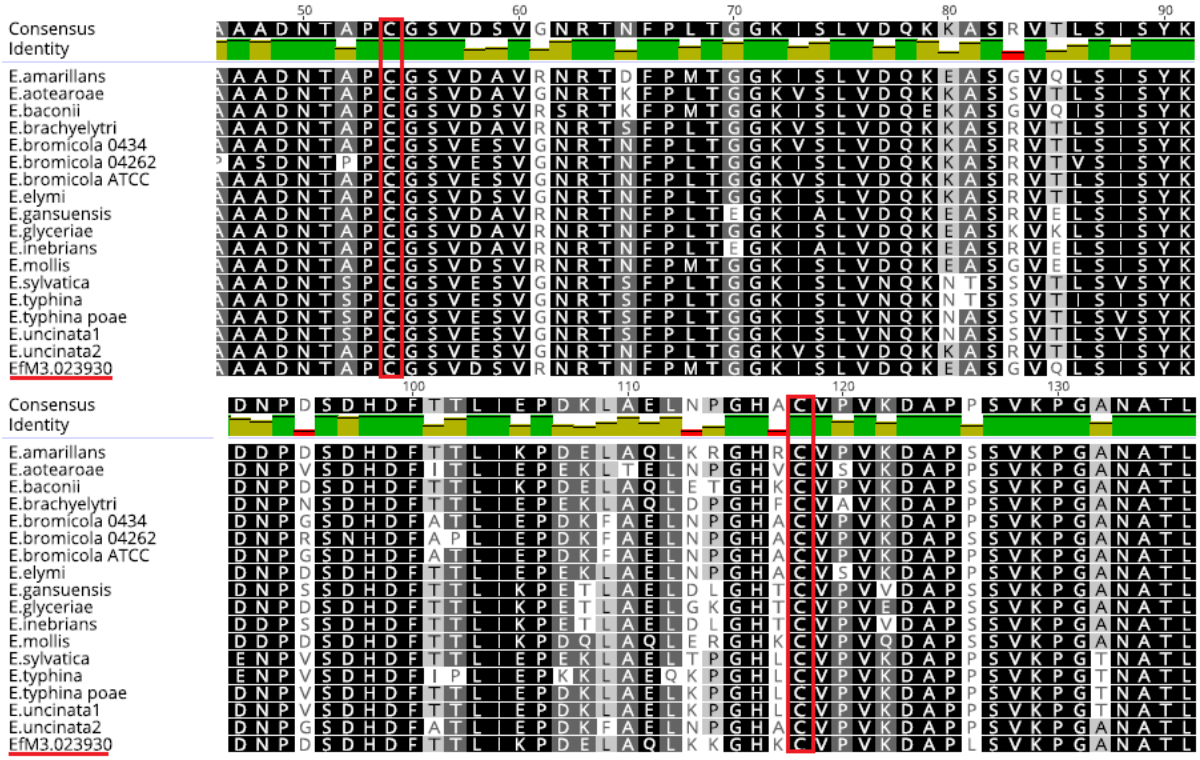

Figure 5.10 WSC domain alignment of Wsc protein sequences from 17 *Epichloë* species and EfM3.023930 in *E. festucae* (underlined in red). All the proteins share the two cysteine residues (are marked with red squares) conserved throughout WSC domains.

The presence of this highly conserved *Epichloë* protein raised the possibility that this protein may serve a specific function in this genus. Conserved cysteine residues are important for the structure and the function of proteins (Meitzler et al., 2013). During protein secretion or in proteins with extracellular parts, cysteine pairs form disulfide bonds to stabilize proteins and maintain the protein folding (Morand et al., 2004).

To determine the distribution of EfM3.023930 homologues in the genomes of other fungi, BLASTP analysis was used to retrieve similar proteins from Joint Genome Institute (JGI), (The Fungal Genomic Resource, http://genome.jgi.doe.gov/) (Nordberg et al., 2014) using EfM3.023930 as query. The result returned 100 hypothetical proteins from 28 different species. Among them, the second and the fifth most similar proteins were annotated as Wsc2 (the most similar protein was a hypothetical protein) in *Pochonia chlamydosporia* and *Metarhizium robertsii*, respectively (Appendix 1). The list included other proteins annotated as Wsc2, related to Wsc2 or Wsc2 glucoamylase III, GPI-anchored proteins, cell adhesion proteins and the rest were annotated as hypothetical proteins (Appendix 1). The e value 5e-72 was determined as cut off. The proteins computationally annotated as Wsc2, or related to Wsc2, were subjected to InterProScan analysis to determine the protein domain layout. All of them possessed a SP, TM, CT and an unidentifiable region between SP and TM. To

understand the similarity between EfM3.023930 and its closest homologues, plus the characterised Wsc proteins (Table 5.1), a protein alignment was made using MAFFT E-NS-i. EfM3.023930 and its homologues were more similar to each other than to the functionally characterized Wsc proteins as expected (Figure 5.11). The similarities between 48 proteins were observed mostly in the SP, TM, CT and the region where the WSC is located in the classical Wsc proteins (Figure 5.11).

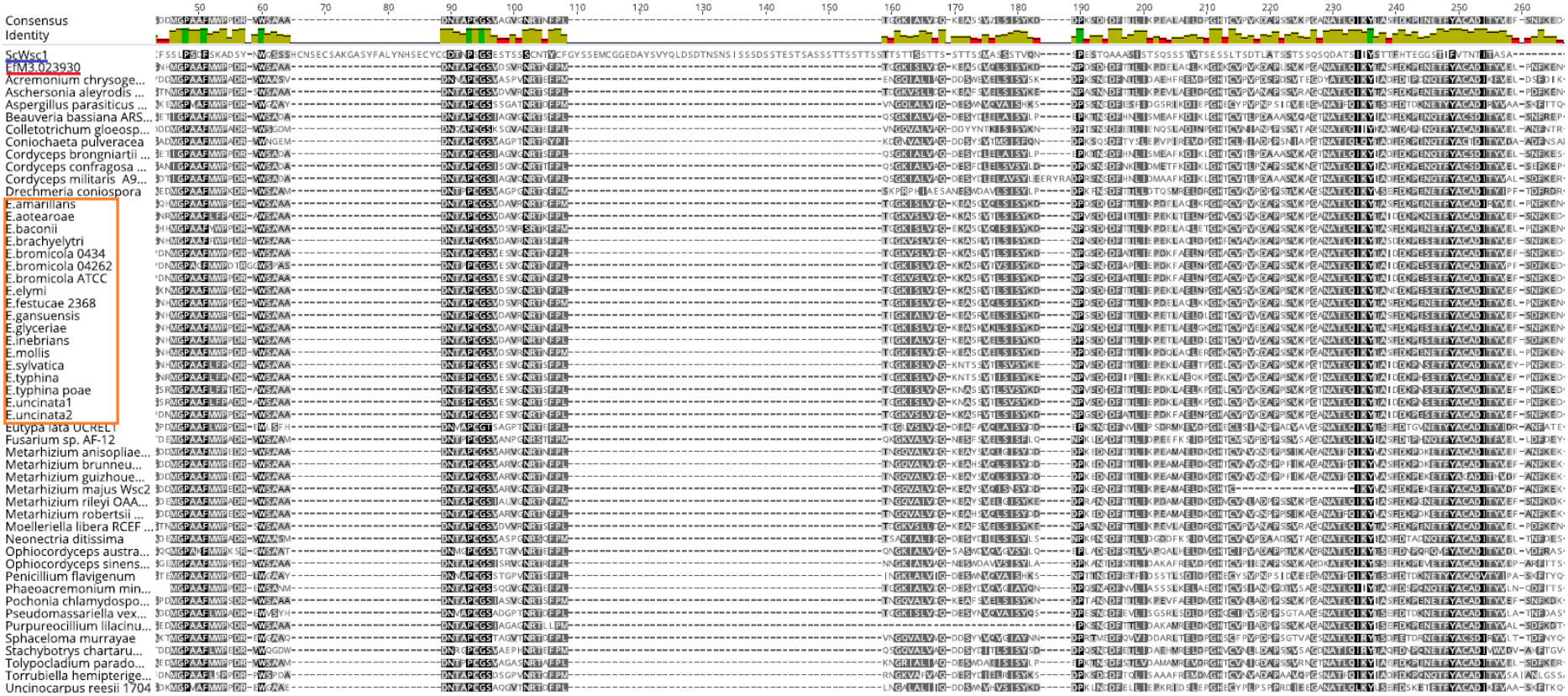

Figure 5.11 WSC domain alignment of hypothetical proteins annotated as Wsc similar from 28 species, *Sc*Wsc1 (underlined in blue), EfM3.023930 (underlined in red) and similar proteins from other *E. festucae* species (highlighted in orange square). *Sc*: *S. cerevisiae*, *Ef*: *E. festucae*.

To investigate the phylogenetic relationship of hypothetical Wsc similar proteins, EfM3.023930 and functionally characterized Wsc proteins, a phylogenetic tree was constructed using the protein alignment via Maximum Likelihood from PhyML software with 1000 Bootstrap replicates.

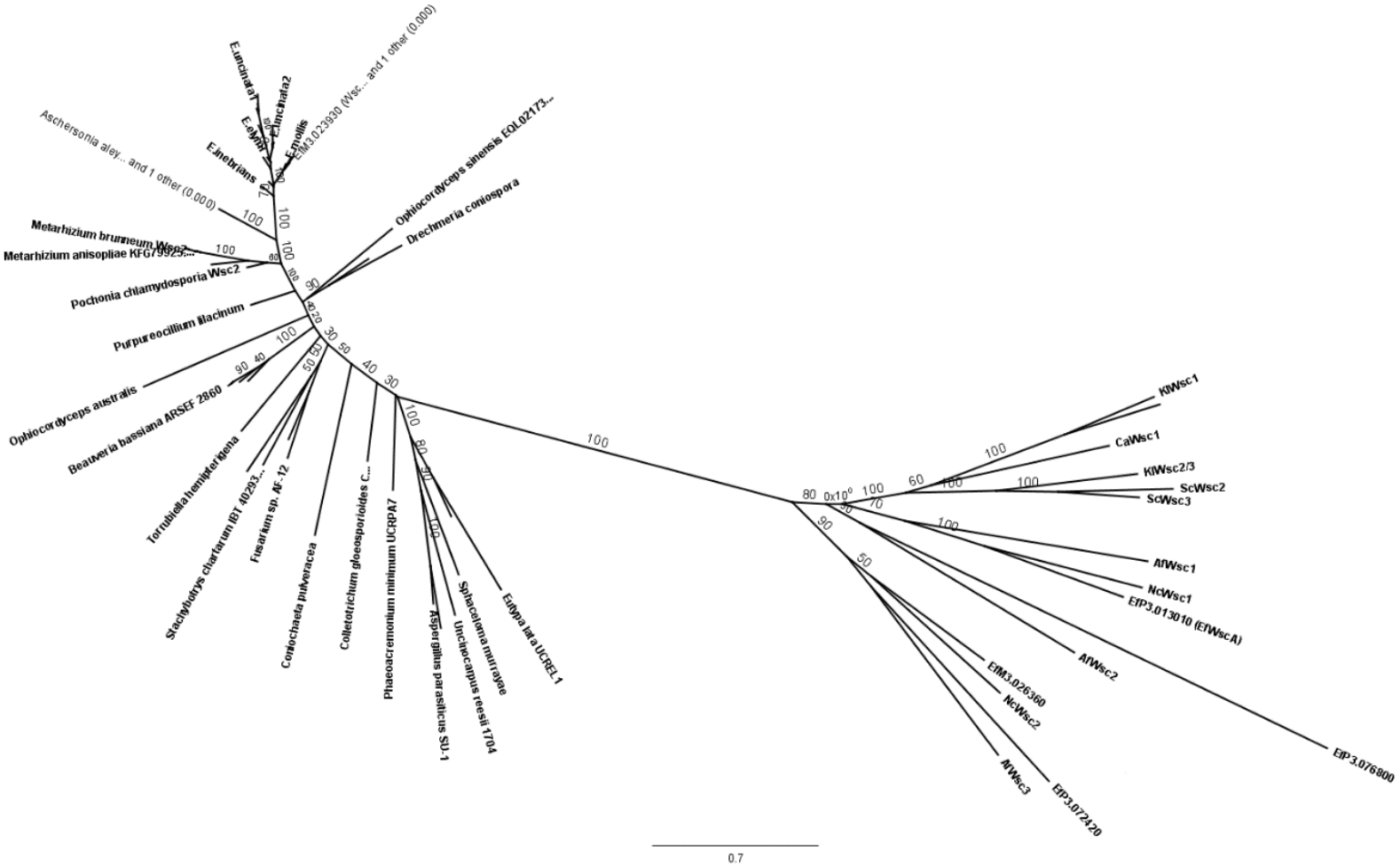

Figure 5.12 Phylogenetic tree of characterised Wsc proteins, EfM3.023930, and homologous proteins from other *Epichloë* species and fungal species. The alignment and phylogenetic tree was constructed using the MAFFT E-NS-i and Maximum Likelihood algorithms from PhyML software with 1000 Bootstrap replicates. The species, protein names and accession numbers of sequences used in this alignment is given in Appendix 1.

The phylogenetic tree showed that the hypothetical Wsc similar proteins from other fungi were not closely related to functionally characterized Wsc proteins (Figure 5.12). However, the protein domain layout of hypothetical Wsc similar proteins and the fact that they are present in all genome sequenced *Epichloë* species, and many other fungi, raised the possibility that these proteins could be another type of cell wall stress sensor. So far, none of the hypothetical Wsc2 proteins used in this study or other proteins with similar domain layout has been functionally characterized.

5.4. Development of Gene Replacement Constructs for Functional Analysis of EfM3.026360 and EfM3.023930

To understand the functions of EfM3.023930 and EfM3.026360 in *E. festucae*, the genes were selected for targeted gene replacement using the split marker method (Fairhead et al., 1996, Rahnama et al, 2017). EfM3.023930 was chosen as a novel putative stress sensor that may play a role in sensing mechanical stress since it was up-regulated in response to mechanical stretch, and similar to other hypothetical Wsc proteins from other fungi (Appendix 1). For functional characterization of these genes, 3' and 5' flank sequences of target gene were cloned into donor plasmids pDONR-SMR and pDONR-SML, which were then used as gene replacement vectors (Figure 5.13). The split marker system was chosen as the hygromycin selectable marker is split between the replacement vectors and only becomes functional after a three way homologous recombination between the two vectors and the gene of interest in the fungal chromosome. This results in fewer ectopic insertions of the deletion vectors. Replacement vectors were constructed (Figure 5.14), the inserts checked by sequencing and restriction digests and transformed into *E. festucae* Fl1 WT protoplasts with approximately 1.25 X 10^8 protoplasts/mL concentration as described previously (Ariyawansa, 2015). Initially, *E. festucae* Fl1 WT was chosen for transformation for both EfM3.023930 and EfM3.026360 deletion. *E. festucae* ΔwscA transformation for EfM3.026360 deletion was planned to observe the redundancy between Wsc proteins. Two transformation attempts were made until viable colonies could be obtained.

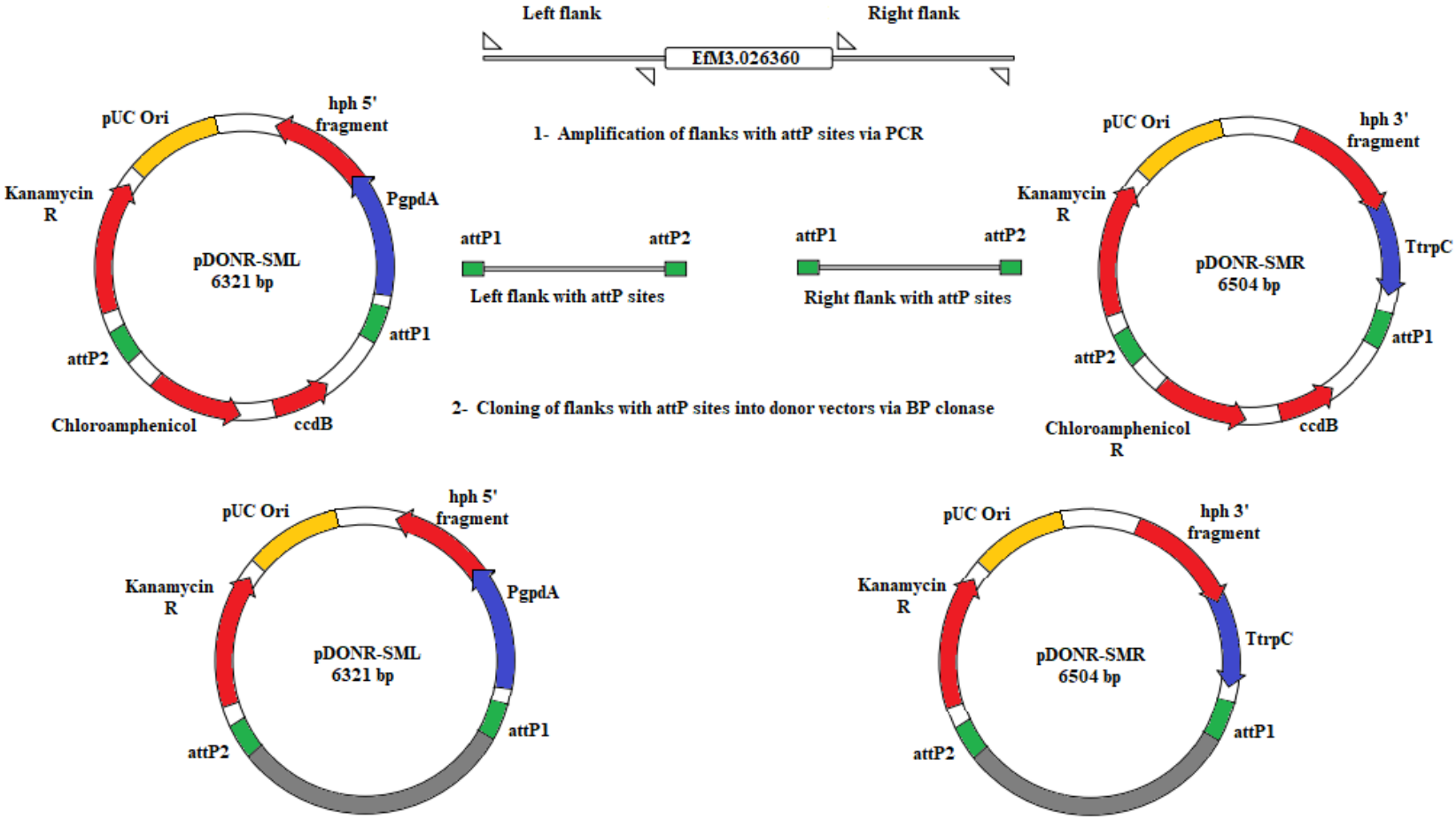

Figure 5.13 Schematic representation of the construction of split marker gene replacement vectors pDONR-SML and pDONR-SMR using MultiSite Gateway® Kit (Thermo Fisher, USA)

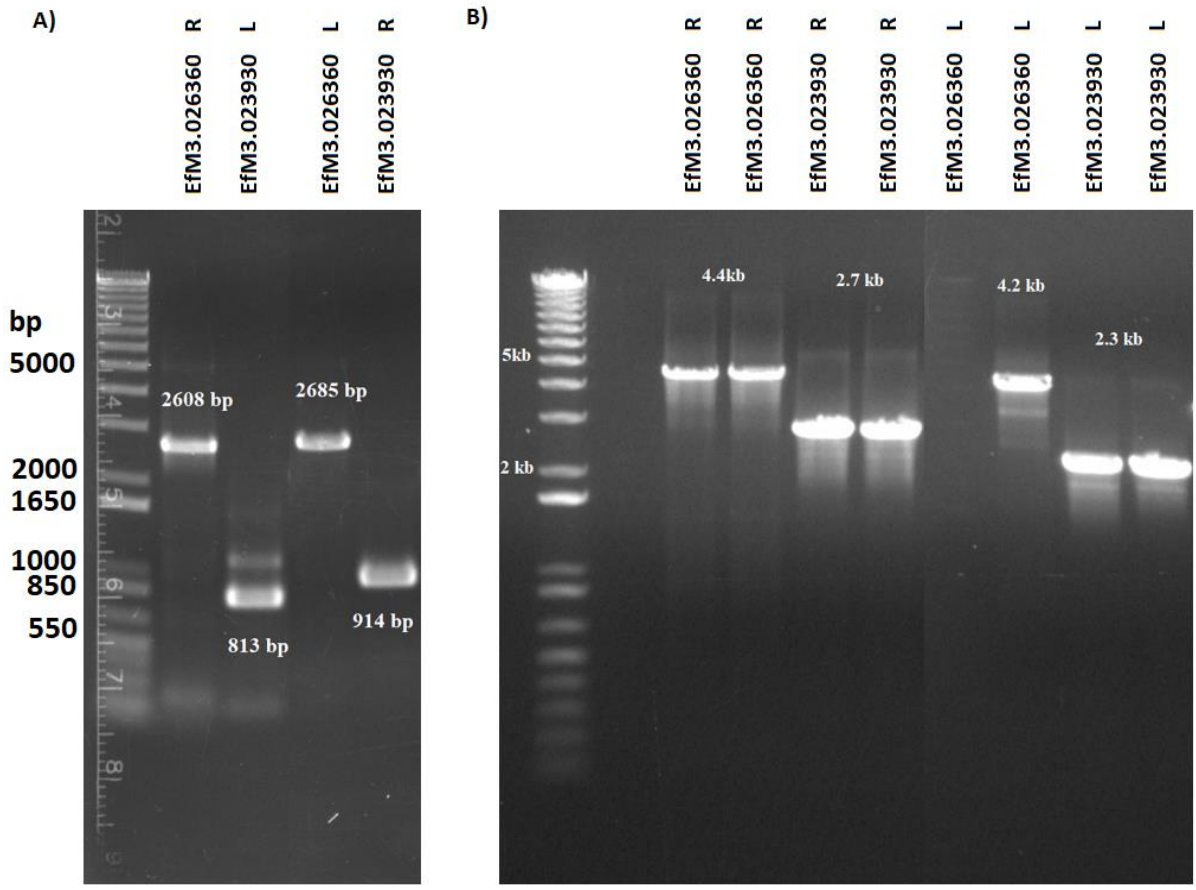

Figure 5.14 Vector construction for EfM3.023930 and EfM3.026360 deletions in *E. festucae* Fl1 WT. A) Right (R) and left (L) flank amplifications for targeted deletion of EfM3.023930 and EfM3.026360 via homologous recombination. The flanks were amplified using the primer pairs in the Appendix 3 and products were run on 0.8% agarose gel containing 25µg/ml Ethidium Bromide as described in Section 2.6. B) The confirmation PCR for EfM3.023930 and EfM3.026360 knock out constructs after cloning into donor vectors pDONR SMR or pDONR SML. The screening was carried out using the primer pairs in the Appendix V and products were run on 0.8% agarose gel containing 25µg/ml Ethidium Bromide as described in Section 2.6. For both agarose gels, 1kb Plus DNA Ladder (Thermo Fisher, USA) was used as marker. The visualization of gels was carried out using UV transilluminator gel documentation system (Gel Doc™, Bio-Rad, CA, USA).

Hygromycin-resistant colonies became visible within 7 d of growth in axenic culture at 24°C (Figure 5.15). Transformation yielded putative 96 EfM3.026360 mutant colonies that survived on hygromycin and except six of them, all displayed abnormal morphology and slow growth compared to WT protoplasts grown on PDA (Figure 5.15). Whereas for putative EfM3.023930 mutants, 62 colonies out of 78 transformants showed abnormal colony morphology and slow growth compared to WT (Figure 5.15). For screening of mutants, genomic DNA was extracted from hygromycin-resistant

E. festucae colonies. However, DNA extraction proved to be problematic for putative mutant colonies as sufficient DNA for PCR screening could not be yielded. The genomic DNA extraction from putative mutants were first carried out as described in Section 2.10 using Quick-DNA Fungal/Bacterial Miniprep Kit (Zymo Research, USA) by macerating the cultures in liquid N_2 in individual Eppendorf tubes and carrying out the extraction according to manufacturer's protocol. This methodology did not yield sufficient genomic DNA for PCR. Next, cultures were subjected to a crude DNA extraction protocol, which again resulted in insufficient genomic DNA quality and quantitiy for PCR screening. The slow growth and the unusual morphology of candidate cultures provided a challenge to proceed to PCR screening in the time context of this study. So far, these preliminary findings suggest that EfM3.026360 (putative *Ef*WscB) and EfM3.023930 might have a role in regulating vegetative growth of *E. festucae* in culture.

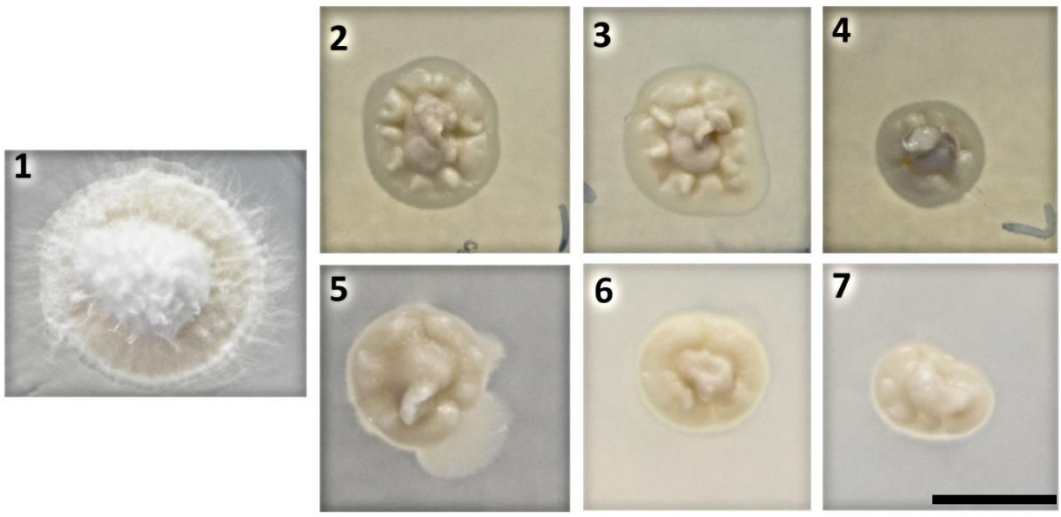

Figure 5.15 *E. festucae* WT (1) and putative EfM3.023930 (2, 3 and 4) and EfM3.026360 mutants (5, 6 and 7) at 1wk on PDA. WT cultures are grown on PDA without hygromycin supplement, whereas putative mutants were grown on 100 µg/ml hygromycin containing PDA plates. The scale bar shows 5 mm.

5.5. Discussion

In this chapter, identification and preliminary characterization of putative Wsc proteins in *E. festucae* has been carried out to pave the way for understanding their roles in sensing mechanical stretch and potentially regulating intercalary growth *in planta*. In *S. cerevisiae* and several other fungi, Wsc proteins have been characterized as a part of the Cell Wall Integrity (CWI) pathway that functions to sense external stress on the cell wall and transduce the signal to the cytoplasm and then the nucleus, to regulate vegetative growth in culture (Verna et al., 1999, Dichtl et al, 2012, Norice et al., 2007, Maddi et al., 2012, Heinisch et al., 2008, Rosenwald et al., 2016, Ohsawa et al., 2017). In *E. festucae*, WscA has been functionally analysed through gene deletion and similarly been found to be a regulator of vegetative growth in culture (Ariyawansa, 2015). Given the fact that the CWI pathway in fungi employs three Wsc proteins to sense external stress (Wsc1, Wsc2 and Wsc3), we hypothesized that *E. festucae* CWI pathway possessed Wsc2 and Wsc3 homologs (Jendretzki et al., 2011).

5.5.1. Identification of Putative Wsc Proteins In *E. festucae*

Studies to date on Wsc proteins in fungi show that these proteins have four domains in common (Ohsawa et al., 2017). A signal peptide (SP) at the N terminus, a wall stress sensor (WSC) domain that senses mechanical stretch and undergoes a conformational change, a transmembrane (TM) domain that anchors the protein to the cell membrane, and a cytoplasmic tail (CT) that relays the external stress signal downstream to the cytoplasmic signalling pathway (Verna et al., 1999). The only exception to this domain layout has been found in *A. fumigatus* Wsc2 that lacks a cytoplasmic tail but still functions as a regulator of growth in culture (Dichtl et al., 2012). In the *E. festucae* genome, aside from the previously studied WscA, two other candidate Wsc proteins (EfM3. 026360 and EfM3.072420) were found that translated into proteins with the classical fungal Wsc protein domain layout. The amino acid sequence similarity of these proteins to other functionally characterized Wsc proteins was concentrated in the protein domains (ST, WSC, TM), and the putative cytoplasmic tail (CT) of *E. festucae* proteins were more diverse (Figure 5.1).This is consistent with functionally characterized Wsc proteins from other filamentous fungi which also show low amino acid sequence similarity to *Sc*Wsc proteins. Currently the protein with the highest sequence similarity with *Sc*Wsc1 is from the yeast, *C. glabrata* (*Cg*Wsc1, 43.9%) (Ohsawa et al., 2017). The presence of conserved cysteine motifs in the WSC domain of

candidate *Ef*Wsc proteins suggested that they could be cell wall stress sensors, since this motif in WSC domain is thought to be important for redistribution and clustering of these proteins on cell wall in response to environmental stress and stress sensing in *S. cerevisiae* (Heinisch et al, 2010). When cysteine residues in WSC domain in *Sc*Wsc1 were substituted with other amino acids, the cells were more susceptible to heat stress, congo red and Calcofluor white compared to wild type (Heinisch et al, 2010). Also, atomic force microscopy of mutants with cysteine substitutions at the 4th and 5th, 6th and 7th, and 8th residues in the WSC domain revealed that these substitutions affected the ability of *Sc*Wsc1 to cluster in response to stress, pointing out to the role of WSC domain in regulating sensor clustering during sensing of external stress (Heinisch et al, 2010). Clustering of *Sc*Wsc1 is thought to be crucial for downstream signal amplification during prolonged exposure to external stress (Heinisch et al, 2010). Therefore, the presence of this cysteine motif in the candidate *Ef*Wsc proteins' WSC domain may be an indicator of their potential to be cell wall stress sensor proteins (Table 4.2).

The phylogenetic tree of characterized Wsc and candidate *E. festucae* proteins showed distinct grouping of yeast and filamentous fungi Wsc proteins, and that *N. crassa*, *A. fumigatus* and putative *E. festucae* Wsc proteins were closely related to each other compared to *S. cerevisiae*, *K. lactis* and *C. glabrata* (Figure 5.4). Moreover, EfM3.026360 was closely grouped with *Nc*Wsc2 and EfM3.072420 with *Af*Wsc3, suggesting that these could be putative *Ef*WscB and *Ef*WscC, respectively (Figure 5.12).

Most studies on the Wsc sensors to date have focussed on protein characterisation and localisation in filamentous fungi , and gene expression studies under cell wall stress have not yet been carried out. A transcriptomic study conducted on *S. cerevisiae* in no stress conditions showed that over-expression of mitogen activated protein kinase (MpkA) resulted in differential regulation of cell wall remodelling enzymes and cell wall proteins such as β-1,3-glucan synthase, chitin synthase, cell wall mannoproteins and cell surface glycoproteins (Jung et al., 2002). However, no expression changes in Wsc proteins were detected (Jung et al., 2002). The same study analysed the gene expression profiles of cell wall genes of *S. cerevisiae* WT, this time during heat shock and found that 25 cell wall remodelling and biogenesis genes that were differentially regulated in MpkA overexpression mutants were again differentially regulated in response to heat shock, however, since Wsc proteins were not differentially regulated in

the MpkA overexpression transcriptomics study, their expression profiles during heath shock were not studied (Jung et al., 2002). In the *E. festucae* transcriptomics data (Chapter 3.7), the *Ef*Wsc candidates EfM3.026360 and EfM3.072420 were not differentially regulated, also none of the other *E. festucae* protein candidates with WSC domains were differentially regulated ($p \leq 0.05$) in either the early or late responses to mechanical stretching compared to un-stretched controls (Table 5.3). This finding is in accordance with the findings from *S. cerevisiae* during MpkA overexpression, however more studies are needed to understand the expression profile of *wsc* genes during exposure to stress in fungi.

The overall low similarity of *Ef*Wsc candidates to other functionally characterized proteins raised the possibility that *E. festucae* might possess more diverse proteins that sense mechanical stretch. Therefore, the search for putative *E. festucae* sensor proteins (similar to Wsc proteins) that changed in gene expression in response to mechanical stretch, was widened. For this, the transcriptomics dataset in this thesis (see Chapter 4) was searched for other potential DE stress sensor genes that were responsive to mechanical-stretch by aligning the genes with the functional Wsc proteins in Table 3.14 using BLASTX. One such protein (EfM3.02930) with SP, STR, THM and CT domains was up-regulated slightly in early and late responses to mechanical stretch compared to the control ($p \leq 0.05$). The BLAST search showed that this protein was similar to other hypothetical Wsc similar proteins from other filamentous fungi (highest identity is between *P. chlamydosporia* Wsc2 with 63%), and the identity scores between proteins from different fungal genera and EfM3.02930 were much higher compared to the similarity between putative *Ef*Wsc and other characterized fungal Wsc proteins (Appendix 1). These hypothetical Wsc2 or Wsc2-like proteins from other filamentous fungi have not been characterized so far. The domain analysis of EfM3.02930 revealed a similar layout to characterized Wsc protein domain with SP, STR, THM and CT in the same order as Wsc proteins, except in the WSC domain, where only two of cysteine residues from the eight residues motif could be detected (Figure 5.5). The two-cysteines in the region where WSC domain sits in the conventional Wsc protein (between SP and STR) in EfM3.02930 and the other conserved serine, glycine and leucine residues in this region suggests that this sequence is not a completely different sequence as there are similarities between this region and other WSC domains (Figure 5.5). Moreover, the amino acid sequence alignment of WSC regions of EfM3.02930, EfM3.026360, EfM3.072420, *Ef*WscA functionally characterized Wsc proteins from other organisms

(Figure 5.6) showed that the region between SP and STR in EfM3.02930 shows identity to other functional WSC domains (highest amino acid identity is between *Nc*Wsc1 with 18.8%) however it was not recognized as a protein domain in InterProScan analysis, and there are no functional studies that shows its role in any organisms. Moreover, the finding that other known *Epichloë* species also possessed a very similar protein with the same characteristic region between SP and TM suggests that this protein might be a novel cell wall protein (Figure 5.8). The role of cysteine residues in WSC have been studied in *S. cerevisiae* Wsc1, where single substitutions of cysteine into other amino acids resulted in failure to grow and to form a sensosome under heat and osmotic stress compared to WT (Heinisch et al, 2010). However, the role of each cysteine in WSC domains of Wsc proteins during stress sensing has not been studied in filamentous fungi. Proteins homologous to EfM3.02930 in other fungi showed the same change in the region where WSC domain is located in functional Wsc proteins, and all of them possessed SP, STR, THM and CT domains, indicating a potential that this protein might be conserved and have an important function (Figure 5.15). A BLAST search of the JGI database revealed that the fungi that were found to have protein similar to EfM3.02930 only possessed one protein with the same domain layout and the same region between SP and STR resembling WSC domain, and when their genome was searched for other proteins similar to EfM3.02930 none could be found (data not shown). Among the 28 species of fungi that possessed this type of protein (Appendix 1), 19 of them were entomopathogenic fungal species, 4 of them were plant pathogens and 4 of them were pathogens of mammals and 1 of them is an endophytic fungus of willows (Appendix 5). The phylogenetic tree of these proteins with WSC resembling region and classical Wsc proteins indicate that these two types of proteins are largely diverse from each other, and EfM3.02930 is grouped with the proteins with WSC resembling region (Figure 5.12). Phylogenetic studies on associations between fungi of the Hypocreales and Clavicipitaceae and their hosts may offer a new perspective on this protein with a modified WSC domain. Ancestral character mappings of 69 fungal species, including *Epichloë typhina* were constructed using 6 gene sequences to build a phylogenetic tree, and hosts (insect, plant or other fungi) of each species were mapped onto the tree to reveal inter-kingdom host switches by the fungi (Spatafora et al., 2007). The result revealed that grass symbiont *E. typhina*, along with several other grass symbionts, switched plant to insect hosts, and then back to plants (Spatafora et al., 2007). This suggests that *Epichloë* species, plus other plant-associated fungi, might still possess

some genes that were necessary for the insect pathogenic lifestyle. Therefore, my finding of proteins with WSC resembling region possessing two cysteine residues is found in 27 known pathogenic fungal species raises the possibility that this putative cell wall sensor protein may have been retained from *E. festucae*'s ancestral life style as an insect pathogen. The fact that this unique protein remained in all genome sequenced *Epichloë* species and was up-regulated in early and late response to mechanical stretching in my transcriptomics data brings up the possibility that this protein might function during plant colonization. To understand the role of EfM3.02930 in intercalary growth, confirmation of the gene deletion needs to be completed, and observations on radial growth rate (in culture) and plant colonization made. Cell wall plasticity under mechanical stress should also be investigated.

5.5.2. Functional Characterization Attempts of Putative Wsc In *E. festucae*

In this study, an attempt was made to functionally characterize putative Wsc candidate EfM3.026360 and EfM3.02930 to understand their role in intercalary growth. Wsc proteins appear to exhibit functional redundancy in *S. cerevisiae,* where single or double mutation phenotypes manifests as heat sensitivity in either YPD or SC medium, whereas the phenotype is severely exacerbated (increased heat sensitivity and anti-fungal sensitivity) when three of them were deleted together, suggesting that stress sensing occurs through all three Wsc proteins, and that deletions in single genes do not markedly affect cell wall integrity signalling in S. *cerevisiae* (Verna et al.,1999).

The previous study in *E. festucae* demonstrated that Δ*wscA* mutants had reduced colony radial growth rates and abnormal hyphal morphology compared to WT, as well as increased sensitivity to Calcofluor white that could be rescued by osmotic stabilizer Sorbitol in the medium (Ariyawansa, 2015). However, the plant colonization pattern of the mutant did not differ significantly from WT (Ariyawansa, 2015). This finding lead to the hypothesis that *E. festucae* Wsc proteins were similarly redundant in function during plant colonization. One of the objectives of this PhD was to identify further Wsc proteins in *E. festucae* for deletion, both singly, and in combination with *wscA*. Unfortunately, it was not possible to confirm that the colonies obtained were truly *wscB* deletion mutants. Nevertheless, their morphology indicated they were not wild type as they presented smaller colonies and less mycelia compared to WT cultures on PDA similar to what has been observed in *E. festucae wscA* mutants (Figure 5.15)

(Ariyawansa, 2015). The genomic DNA extraction from these putative mutants proved to be more difficult than extraction from WT colonies, indicating that the cell wall of putative mutants was more difficult to break down. In the future, after successful Δ*wscB* confirmation, these mutants will be used to carry out radial colony growth assessment, cell wall morphology analysis using CR and CW and plant inoculation to assess colonization and plant morphology to understand the role of WscB in *E. festucae* intercalary growth. Moreover, a mechanical stretching experiment using *wscB* mutants could shed light on the role of WscB in sensing mechanical stress and regulating cell wall plasticity in *E. festucae* cultures.

5.5.3. Conclusion and Major Impact

In this chapter, an attempt was made to find other Wsc homologs in *E. festucae* and analyse the phylogenetic relationship between them and the functional Wsc proteins from yeast and filamentous fungi. Moreover, a potential stress sensing unique protein that resembles a Wsc protein and was differentially regulated in response to mechanical stretching was found and detected in known *Epichloë* species and 28 other pathogenic fungi. This study will provide basis for understanding mechanical stress sensing in *E. festucae* and the future characterization studies might shed light on the role of this unique Wsc resembling protein in not only in *Epichloë*, but also in other fungi.

6. Conclusions and Future Work

The aim of this PhD project was to expand on the understanding of the mechanisms used by *E. festucae* to perform intercalary growth through mechanical stretching experiments and transcriptomics analysis.

6.1. Understanding the Role of *E. festucae midA* in Plant Colonization and Intercalary Growth

One of the major objectives of this project was to widen the understanding of how *E. festucae* switches from tip growth in the host shoot apex to intercalary growth in developing leaves. Previous experiments have shown that mechanical stretching *in vitro* may be the stimulus required for hyphal extension and intercalary compartment division and that *E. festucae* MidA plays a role in polar growth in culture and intercalary growth in plants (Ariyawansa, 2015). To expand on these findings, host infection rates and the effects of *E. festucae* WT, Δ*midA* and complementation strains on the host plant were investigated. No differences between strains were found with respect to host infection rate indicating that MidA function is not essential for establishing an initial infection in the host shoot apex after artificial inoculation of seedlings. Phenotype assessments of plants infected with *E. festucae* WT, Δ*midA* or *mid1*-complemented strains also showed no effect of *midA* deletion on host phenotype. The only difference observed, but not quantified, was that the tillers of plants infected with *ΔmidA* strains were thinner and more fragile when they were pressed against the nitrocellulose membranes during the tissue print immunoassay. This was speculated to be due to altered cell wall content in these tillers, which warrants future study.

6.1.1. Loss of MidA Results in Reduced Hyphal Biomass in the SA Enriched Tissues

Previous confocal microscopy studies of *E. festucae* Δ*midA* expressing enhanced green fluorescent protein (EGFP) showed relatively numerous hyphae in the plant shoot apex but relatively sparse colonisation of the intercalary zone of leaves compared to wild type (Ariyawansa, 2015). To confirm these findings, a quantitative hyphal biomass analysis was conducted on SA-enriched and leaf-enriched samples of *L. perenne* infected with *E. festucae* WT, Δ*midA* and *mid1*-complemented strains but there were

inconsistencies in these results. One strain (Δ*midA*20) was not detectable in plant tissues, while for the other two strains, one infected the host at levels similar to wild type and the other had reduced hyphal biomass, making it difficult to draw a conclusion on the effect of MidA on hyphal density in SA-enriched tissues. The source of the variability was likely due to variable contamination of SA-enriched tissues with the surrounding leaf tissues, which were very low in hyphal biomass (see below). This question can only be resolved by refining the methods to isolate the SA from surrounding tissues, which is time consuming but achievable. The biomass of leaf enriched tissues gave a more conclusive result, which confirmed the previous visual observations that Δ*midA* hyphae only sparsely colonised the leaves of plants (Ariyawansa, 2015). These findings indicated that *midA* function is required for intercalary zone colonization and that calcium uptake is particularly important for intercalary hyphal growth in plants. However, the fact that hyphal biomass was still detectable with Δ*midA* strains suggests that *E. festucae* Δ*midA* is still able to undergo intercalary growth to a certain degree. This was speculated to be due to the presence of sugars, amino acids, K^+, $Fe^{2/3+}$ and Ca^{2+} ions that might function as osmotic stabilizers (O'Leary et al., 2014), or allow calcium uptake through alternative mechanisms, thus enabling *E. festucae* Δ*midA* strains to undergo intercalary growth. This hypothesis is supported by our findings in this study, where extracellular calcium supplementation was shown to restore reduced growth rates of *E. festucae* Δ*midA* to wild type levels, and in the previous study where the osmotic stabilizer sorbitol was found to rescue reduced growth rates of Δ*midA* strains (Ariyawansa, 2015). Given that calcium uptake through the Low Affinity Calcium Uptake System (LACS) calcium channel Fig1 may enable Δ*midA* strains to perform intercalary growth to a certain extent, further work to investigate the role of the LACS during intercalary growth should be conducted through deletion of the *E. festucae* homologue of *S. cerevisiae fig1*. Deletion of the *E. festucae cch1* calcium ion channel gene would also strengthen the findings of this study.

6.1.2. Calcium Increases the Elastomeric Potential of *E. festucae* WT

Similar to polar extension in fungi, the first step in intercalary growth in response to mechanical stretch is most likely to be stretching of the hyphal cell wall and plasma membrane. The elastomeric potential of *E. festucae* WT was investigated under mechanical stress using PDA with or without $CaCl_2$ supplementation, to understand the role of extracellular calcium on hyphal cell wall plasticity. Cultures grown on stretching

frames under PDA or PDA with 50 mM $CaCl_2$ were mechanically stretched in various amounts. *E. festucae* WT grown on PDA without supplemental calcium were able to undergo up to 2 mm of stretch (over 4.5 cm of membrane) without breaking, whereas the WT grown with 50 mM $CaCl_2$ were able to stretch for 12 mm without breaking. These findings pointed to the importance of extracellular calcium in the plasticity of the *E. festucae* cell wall under mechanical stress. Although calcium is an important signalling molecule for metabolism in eukaryotes, the mechanisms in which Ca^{2+} regulates cell wall remodelling enzymes in fungi are unknown. It is possible to speculate that calcium might be regulating the functions of cell wall remodelling enzymes such as β-glucan synthases and endo or exo-β glucanases. Examination of transcriptional responses to mechanical stress by the *E. festucae* WT showed that several cell wall degrading enzymes, putative endo-1,3-β-glucanase, exo-1,3-β-glucanase, glucan-1,3-β-glucosidase,glycosyl transferase and omega-6 fatty acid desaturase, were upregulated in response to stretch. Since there was 50 mM $CaCl_2$ in the growth medium, it is possible that calcium may elevate the enzymes involved in cell wall plasticity. This is consistent with observations on calcium influx in *E. festucae* hyphae undergoing polar growth, where there is a need for gradient of calcium from the apical compartment (Ariyawansa, 2015) with the highest concentrations in the tip where extension is taking place. Presumably, as the tip extends, and the calcium concentrations behind the tip diminish, these enzymes likely reduce in concentration and allows the wall to harden. This could be tested in a future transcriptomics analysis where *E. festucae* WT cultures are grown under PDA or PDA with 50 mM $CaCl_2$, and are mechanically stretched, and the expression of cell wall remodelling and biosynthesis genes and enzymes are investigated.

6.1.3. Calcium Increases the Elastomeric Potential of *E. festucae* Δ*midA*

The elastomeric potential of *E. festucae* Δ*midA* hyphae was investigated in a similar fashion to understand the role of MidA in regulating hyphal cell wall plasticity. *E. festucae* Δ*midA* cultures, grown under PDA or PDA with 50 mM $CaCl_2$ were mechanically stretched in incremental amounts. Cultures grown under PDA alone were not able to tolerate even 1 mm of mechanical stretch without hyphal breakage, whereas cultures grown on PDA with 50 mM $CaCl_2$ were able to tolerate a total of 3 mm of mechanical stretch, and showed consistent hyphal breakage at 4 mm stretching. These findings indicated that extracellular calcium (50 mM) was able to restore the cell wall

plasticity in Δ*midA* cultures to a certain extent. This finding supports the hypothesis that extracellular calcium may chemically complement the *midA* deletion, possibly by calcium uptake through another channel such as the Fig1 channel of the LACS, which imports calcium from a high to a low concentration gradient (Locke et al., 2001). This speculation is supported by previous findings, where calcium oscillations were investigated in *E. festucae* WT and Δ*midA* strains using GCaMP5, and it was shown that calcium oscillations in the wild type were rapid and observed in the hyphal tips, whereas in the Δ*midA* strain, calcium oscillations were still present, although markedly less frequent (Ariyawansa, 2015). It is unknown whether the calcium was entering the tip through the Fig1 channel or via a further calcium importer. In a future study, the calcium sensor GCaMP5 could be utilized in mechanical stretching to understand the calcium influx patterns under mechanical stress. For this, an automatic mechanical stretching frame could be devised to allow cultures to remain under the confocal microscope during stretching, and this would allow simultaneous visualization of calcium oscillations in hyphae at the time of mechanical stretching.

6.1.4. Calcium Increases the Intercalary Growth Capacity of *E. festucae*

The intercalary growth capacity of *E. festucae* was studied in the presence or absence of calcium to understand its effect on formation of new compartments in hyphae. *E. festucae* WT, Δ*midA* and *mid1*-complemented strains were grown under PDA or PDA with 50 mM $CaCl_2$, and subjected to mechanical stretch of various magnitudes. For all strains, supplementation with 50 mM $CaCl_2$ significantly increased the compartmentalization rates, in both the stretched and un-stretched treatments. The compartmentalization rates of *E. festucae* Δ*midA* could not be restored to WT levels, even in the presence of 50 mM $CaCl_2$, suggesting that *midA* function is crucial, not only for hyphal elasticity, but also for compartment division in *E. festucae*. The lower compartmentation rate in the presence of calcium may be due to slower calcium uptake (perhaps through the LACs system). Genetic complementation of mutant strains with *midA* restored compartmentalisation rates to WT levels confirming the role of MidA in calcium uptake and compartmentalisation.

6.2. Gene Responses of *Epichloë festucae* Hyphae to Mechanical Stretch in Culture

The current understanding of intercalary growth of *E. festucae* has been limited to microscopic observations of compartment extension and division in hyphae, therefore, an attempt to understand the molecular responses to mechanical stretching was made by conducting a transcriptomics experiment on hyphae immediately after (ER) and 3h after (LR) mechanical stretch.

6.2.1. Mechanical Stretching Induces Changes in Primary Metabolism in *E. festucae*

The early response to mechanical stretching resulted in 105 (63 up-regulated, 42 down-regulated) genes that were differentially regulated compared to control, and the late response showed a larger number of genes (403; 352 up regulated, 51 down regulated) that were differentially expressed compared to the control. Gene Ontology (GO) assessment of DEGs showed that early and late responses to mechanical stretching resulted in enrichment in nitrogen metabolism and changes in the extracellular layer of hyphae. These findings suggested that mechanical stretching increases the requirement for nitrogen metabolism in *E. festucae*.

6.2.2. Mechanical Stretching Induces Expressions of Genes Related to Cell Wall Remodelling, Symbiosis and Transcription

Transcriptomics analysis revealed unique DEG GO term enrichment in early and late responses of *E. festucae* to mechanical stretch. In the early response immediately after stretch, DEGs for GO terms for extracellular changes and urea catabolism were enriched, whereas the late response also showed DEG enrichment in carbohydrate, nitrogen and protein metabolism, plus hyphal growth and cell wall building, nucleic acid metabolism and oxidation/reduction. A greater number of genes were differentially regulated in the late response, and hyphal growth and cell wall related GO term enrichments in the late response indicated that mechanical stretching was likely being perceived as a stimulus for *E. festucae* growth.

Intercalary growth in response to mechanical stress is hypothesised to require a combination of cell wall plasticity and growth, all the while maintaining the integrity of the plasma membrane and cell wall. Evidence in support of this hypothesis included the discovery that 15 putative fungal growth and cell wall remodelling related genes were

found to be up-regulated response to mechanical stretching. These putative genes showed homology to endo-1, 43-β glucanase, exo-1, 3-β glucanase, glucan-1, 3 β glucosidase, glycosyl transferase which are known to function as cell wall loosening enzymes in fungi (Baladro´n et al., 2002, Adams et al., 2004). The rest of the up-regulated genes showed homology to membrane or cell wall structural proteins and cytoskeleton proteins, indicating a possible structural change in cell wall and rearrangement of cytoskeleton proteins in response to stretching. These findings suggest that mechanical stretching acted as a stimulus for cell wall remodelling, potentially to allow intercalary extension of *E. festucae* hyphae. Conversely, the hyphal wall remodelling enzyme, chitinase, was down-regulated by mechanical stretch. The reason for this is not clear but warrants further investigation. A further gene that was upregulated was a putative omega-6-fatty acid desaturase which introduces double bonds into membrane lipids and suggests a role for enhancing the fluidity of cellular membranes that may be subjected to strain when mechanical stretch is applied.

A further 13 genes previously shown to be important in symbiosis in fungi were upregulated by mechanical stretch. The functionally characterized *E. festucae* genes regulating synchronized growth between perennial ryegrass and *E. festucae*, *proA*, *soft*, *symC*, *noxD* and *acyA* were up-regulated in the late response compared to controls.

One of the key concepts of the intercalary growth hypothesis is that hyphae colonising growing host tissues are subjected to mechanical stretch due to their attachment to plant cells. In agreement with this hypothesis, a number of putative host attachment genes were upregulated in early and late transcriptional responses to mechanical stretch. These included the hydrophobic surface binding protein A (HsbA), a number of hydrophobins, plus a putative adhesin-like protein 1 homolog, and a CFEM domain-containing protein which has been associated with fungal pathogenesis in fungi (Kulkarni, 2003). The mechanism through which *E. festucae* may bind to host cell walls is not currently known, and these proteins are potential candidates that could be investigated in this regard. One hypothesis to explain their induction by mechanical stretch is that the proteins may become embedded in the nascent cell wall, thus strengthening the physical linkages between the host and the endophyte. One of the most highly upregulated gene in this mechanical stretch study was cutinase. Cutinase was differentially expressed in both responses implying an important role in response to mechanical stretch or intercalary growth. Cutinase degrades cutin, a lipid polymer embedded in a waxy layer which serves as a protective barrier around plant cells. Cutin degradation can be the first

step in invasion of plants by microbes, however, cutin can also serve as a carbohydrate source for fungi. Its role in symbiosis is currently unknown, and not all plant associated contain this enzyme. Its role in mechanical stretch or intercalary growth are currently unknown, but some hypotheses include surface recognition, cuticle degradation as a nutrient source or possibly for hyphal attachment to plant cells during intercalary growth. Functional characterization of cutinase in *E. festucae*, and investigation of plant colonization patterns of mutants during symbiosis might broaden our understanding of its role.

In this study, 13 putative transcription factors (TFs) were up-regulated in response to mechanical stretching. Putative homologs of *S. cerevisiae* Gal4 and Azf1 were among the up-regulated genes in the late response, which are known to regulate nitrogen metabolism and cell wall integrity, respectively (Burger 1991, Slattery et al., 2006). Future characterization of these TFs is required for better understanding of the pathways influenced by mechanical stretching in *E. festucae*.

6.2.3. Mechanical Stretching is a Stimulus Rather than Stress

Expression of stress-related genes in response to mechanical stretching was also investigated to understand the impact of mechanical stress on *E. festucae* hyphae. Among known HSPs in *E. festucae*, only two were found to be up-regulated in response to stretching. With the exception of *noxD* that interacts with NoxA and together regulate symbiotic interactions and cell to cell fusion (Green, 2016), no genes of the NADPH oxidase complex (involved in the production of super oxide) were up-regulated either. The lack of widespread stress responses to mechanical stretching in the transcriptomics data indicated that *E. festucae* hyphae that were stretched by 3 mm at one time appeared not to have been subjected to undue stress compared to un-stretched controls in our study, rather, biologically appropriate stretching appears to have been perceived as a stimulus for growth.

6.3. Identification of Putative Wsc Proteins in *Epichloë festucae* Through Bioinformatics

In this part of the project, identification and preliminary characterization of putative *E. festucae* Wsc proteins were carried out to shed light on their roles in sensing mechanical stretch. One Wsc protein in *E. festucae*, WscA has been functionally analysed through gene deletion previously, and found to be a regulator of vegetative

growth, hyphal morphology and cell wall integrity in the presence of cell wall perturbing agents in culture (Ariyawansa, 2015). However, the plant colonization pattern of mutants was found to be similar to WT, suggesting Wsc proteins in *E. festucae* could be redundant in function during host colonization (Ariyawansa, 2015). To test this hypothesis, putative *E. festucae* Wsc proteins were identified and analysed using a phylogenetics approach.

6.3.1. Identification of Putative *E. festucae* Wsc proteins and Phylogenetic Analysis

Putative *E. festucae* Wsc proteins were identified using the amino acid sequences of previously characterized Wsc proteins from yeast and filamentous fungi. The protein domain analysis resulted in two candidates (EfM3.026360 and EfM3.07240) with the same domain layout of a classical Wsc protein. The WSC domains in these two *E. festucae* proteins were found to possess the eight conserved cysteine residues that have been linked to functionality of Wsc proteins, previously. The phylogenetic analysis revealed that EfM3.026360 and EfM3.07240 were closely grouped with *A. fumigatus* and *N. crassa* Wsc proteins, while previously characterized *E. festucae* WscA was grouped with Wsc1 proteins of the same organisms. The phylogenetic tree resulted in distinct yeast and fungi clades, indicating that Wsc proteins of fungi were more closely related to each other than to yeast.

6.3.2. *E. festucae* WscA and Putative Wsc Proteins are Not Differentially Expressed under Mechanical Stretching

The expressions of CWI pathway related genes were investigated in the transcriptomics study to understand their responses to mechanical stretching. None of the characterized CWI pathway genes in *E. festucae* (MkkA, MpkA) were up-regulated in response to mechanical stretching, including the WscA and the putative Wsc proteins. It is possible that the signalling pathway proteins, including the Wsc sensor proteins, are constitutively expressed or not induced by mechanical stretch. Alternatively, gene responses may have occurred at a time point outside of the range of the study. So far, expression differences in Wsc transcripts in response to cell wall stress in fungi have not been reported in the literature. Given that mechanical stretching did not induce a stress response in the transcriptomics study in this project, a future study where *E. festucae* cultures are stretched repeatedly (as would occur in the plant), and then

subjected to gene expression analysis for WscA and putative Wsc proteins by techniques such as qPCR, might be a worthwhile experiment to conduct to better understand the expression patterns of mechanical stress sensors in *E. festucae*.

6.3.3. Identification of a New Putative Cell Wall Protein Responsive to Mechanical Stretching in *E. festucae*

A novel putative cell wall protein (EfM3.023930) that was responsive to mechanical stretching, and resembled a Wsc protein, was detected in the transcriptomics study. EfM3.023930 was found to be somewhat similar to *N. crassa* Wsc1 but with low (12%) amino acid similarity. This protein possessed SP, STR, THM and CP domains, along with an unidentifiable region between SP and STR that possessed two cysteine residues instead of the usual eight observed in the WSC domains of Wsc proteins. EfM3.023930 was differentially expressed in response to mechanical stretch, both during the early (+1.65, $p \leq 0.05$) and the late (+1.6, $p \leq 0.05$) responses compared to control. Construction of a phylogenetic tree to understand the relationship between characterized Wsc proteins, *E. festucae* WscA, previously identified putative *E. festucae* Wsc proteins (EfM3.026360 and EfM3.07240) and EfM3.023930 showed that this protein was somewhat similar to fungal Wsc proteins. However, given the very low amino acid conservation outside the functional domains, and the presence of only 2 of the 8 conserved cysteines, this protein has not been classified as a putative Wsc protein, and is referred to as "Wsc-like". Orthologs of EfM3.023930 were found in other known *Epichloë* species, and potential homologs were detected in 28 other pathogenic species of filamentous fungi. Phylogenetic tree analysis showed that these proteins grouped separately to functionally characterized Wsc proteins, *E. festucae* WscA and putative *E. festucae* Wsc proteins (EfM3.026360 and EfM3.07240), indicating a possibility that EfM3.023930 could be a new type of cell wall stress sensor, or alternatively linked with another process altogether.

6.3.4. Deletion of *E. festucae* EfM3.023930 and EfM3.026360 (Wsc2)

An initial attempt was made to functionally characterize EfM3.023930 and EfM3.026360 in *E. festucae* using targeted gene replacement (Fairhead et al., 1996, Rahnama et al, 2017). The resulting transformations yielded 96 putative EfM3.026360 mutant colonies that grew on hygromycin and except six of them, all displayed abnormal morphology and slow growth compared to WT protoplasts grown on PDA.

Whereas for putative EfM3.023930 mutants, 62 colonies out of 78 transformants displayed abnormal colony morphology and slow growth compared to WT. DNA extraction proved to be problematic for putative mutant colonies as sufficient DNA for PCR screening could not be produced using different methods, therefore successful mutants could not be confirmed for further experiments. In the future,confirmation of successful mutants will be required, followed by mechanical stretching of mutants to assess their role in sensing and responding to mechanical stress, Plant colonization studies will also be useful in understanding the role of these proteins in plant colonisation. Further, double deletions of *E. festucae* Δ*wscA* and these new candidate sensors may also give insights into redundancy of Wsc proteins in *E. festucae*.

6.4. General Conclusion

In conclusion, this study revealed the importance of MidA and extracellular calcium in regulating hyphal cell wall plasticity and intercalary growth in culture. Moreover, early and late gene responses to mechanical stretching in *E. festucae* were detected through transcriptomics and it was shown that mechanical stretching was a stimulus for expression of genes related to primary metabolism, growth, cell wall remodelling and plant fungal interactions in *E. festucae*. These findings can be used to further our understanding of intercalary growth in *E. festucae*, and hopefully the mechanical stretching devices can be utilized, not only for testing *E. festucae* mutants, but for other filamentous fungi, to discover their intercalary growth potential.

APPENDIX

Appendix 1 – BLASTp Result of EfM3.023930

Sequences producing significant alignments:

Select: All None Selected:0

Alignments Download GenPept Graphics Distance tree of results Multiple alignment

	Max score	Total score	Query cover	E value	Ident	Accession
hypothetical protein AAL_03377 [Moelleriella libera RCEF 2490]	337	337	97%	6e-114	64.93%	KZZ97413.1
WSC2 protein [Pochonia chlamydosporia 170]	293	293	97%	2e-96	63.30%	XP_018142334.1
hypothetical protein I1G_00008737 [Pochonia chlamydosporia 123]	292	292	95%	4e-96	63.60%	RZR58615.1
hypothetical protein NOR_05190 [Metarhizium rileyi RCEF 4871]	286	286	95%	7e-94	60.15%	OAA41682.1
hypothetical protein MANI_009204 [Metarhizium anisopliae]	274	274	88%	7e-89	59.43%	KFG79925.1
wsc2 [Metarhizium robertsii ARSEF 23]	271	271	88%	9e-88	57.85%	XP_007822388.1
hypothetical protein BBO_02779 [Beauveria brongniartii RCEF 3172]	270	270	91%	2e-87	57.09%	OAA47324.1
hypothetical protein CCM_07104 [Cordyceps militaris CM01]	268	268	90%	3e-86	55.91%	XP_006672305.1
Uncharacterized protein TPAR_06041 [Tolypocladium paradoxum]	267	267	97%	3e-86	56.88%	POR33767.1
hypothetical protein BB8028_0001g08470 [Beauveria bassiana]	264	264	99%	1e-84	54.77%	PQK08774.1
hypothetical protein A9K55_007805 [Cordyceps militaris]	264	264	90%	1e-84	55.21%	ATY63567.1
Carcinoembryonic antigen-related cell adhesion molecule 1 [Beauveria bassiana]	263	263	97%	3e-84	54.32%	PMB73111.1
GPI anchored protein, putative [Beauveria bassiana ARSEF 2860]	262	262	99%	5e-84	54.77%	XP_008595315.1
wsc2 [Metarhizium guizhouense ARSEF 977]	258	258	93%	8e-83	56.86%	KID91938.1
hypothetical protein LEL_00111 [Cordyceps confragosa RCEF 1005]	253	253	91%	1e-80	58.59%	OAA80566.1
hypothetical protein OCS_02117 [Ophiocordyceps sinensis CO18]	252	252	96%	4e-80	52.63%	EQL02173.1
wsc2 [Metarhizium brunneum ARSEF 3297]	248	248	92%	1e-78	57.71%	XP_014548516.1
hypothetical protein H634G_04823 [Metarhizium anisopliae BRIP 53293]	246	246	88%	8e-78	59.43%	KJK80584.1
wsc2 [Metarhizium majus ARSEF 297]	238	238	97%	3e-75	53.18%	KID94845.1
hypothetical protein ACRE_026430 [Acremonium chrysogenum ATCC 11550]	239	239	83%	9e-75	48.63%	KFH46563.1
hypothetical protein PENFLA_c028G08518 [Penicillium flavigenum]	238	238	91%	1e-74	47.24%	OQE16284.1
hypothetical protein S40293_04253 [Stachybotrys chartarum IBT 40293]	239	239	99%	2e-74	43.56%	KFA46487.1
hypothetical protein S7711_08684 [Stachybotrys chartarum IBT 7711]	238	238	99%	3e-74	43.56%	KEY63959.1
hypothetical protein CDD81_1921 [Ophiocordyceps australis]	234	234	85%	2e-73	50.64%	PHH60221.1
hypothetical protein S40288_00520 [Stachybotrys chartarum IBT 40288]	236	236	99%	2e-73	43.32%	KFA77730.1
hypothetical protein CDV36_000700 [Fusarium sp. AF-12]	234	234	91%	7e-73	47.48%	RMJ19606.1
hypothetical protein VHEMI05624 [Torrubiella hemipterigena]	233	233	94%	8e-73	50.94%	CEJ89800.1
Pc20g13980 [Penicillium rubens Wisconsin 54-1255]	231	231	91%	4e-72	45.70%	XP_002563876.1
hypothetical protein TOPH_01412 [Tolypocladium ophioglossoides CBS 100239]	231	231	97%	5e-72	52.99%	KND93682.1

Appendix 2 – Buffers and Solutions

All buffers and solutions were prepared in ddH_2O.

TAE buffer (50X) in 1000 mL

Tris base 242.0 g

Glacial acetic acid 57.1 mL

EDTA (pH 8.0) 100.0 mL from 0.5 M stock

For working solution, the stock was diluted 50:1

6x loading dye (6X) in 10 ml

Bromophenol blue 25 mg

Xylene cyanol FF 25 mg

Glycerol 3.3 mL

H2O 6.7 mL

Appendix 3 – List of PCR Primers Used in this Study

Primer name	Sequence	Study
NRPS-1F	gtccgatcattccaagctcgtt	Hyphal Biomass
NRPS-1R	tggtgggaagttccctgcac	Hyphal Biomass
Lp-EF1a-RT-F2/3	caccacgagtctatgct	Hyphal Biomass
Lp-EF1a-RT-R2	gacctgggcaacaaagc	Hyphal Biomass
Wsc2-FP-Right	gaggggaggtgagactagca	EfM3.026360 Right flank amplification
Wsc2-RP-Right	gctagcagcctcctcaaaca	EfM3.026360 Right flank amplification
Wsc2-FP-Left	cgacctacaatacccgtcgg	EfM3.026360 Left flank amplification
Wsc2-RP-Left	cacacttgctcgcgttttca	EfM3.026360 Left flank amplification
Wsc2like-FP-Right	ctactcttttgcgccagaagc	EfM3.023930 Right flank amplification
Wsc2like-RP-Right	cgcagcctccttgaaatgac	EfM3.023930 Right flank amplification
Wsc2like-FP-Left	ggattccggtgctacgagta	EfM3.023930 Left flank amplification
Wsc2like-RP-Left	cgcagcctccttgaaatgac	EfM3.023930 Left flank amplification
SML-Hyg-FP	gtccatcacagtttgccagt	pDONR-SMR/SML Hygromycin cassette screening
SMR-Hyg-RP	atccacgccctcctacatcg	pDONR-SMR/SML Hygromycin cassette screening
LJNTF002-077 LJNTF2-77	tgcctagtgaatgctccgta	pDONR-SMR Screening
M13-FP	gtaaaacgacggccag	pDONR-SMR/SML Screening
M13-RP	gtaaaacgacggccag	pDONR-SMR/SML Screening

Appendix 4- Amino acid identity scores of EfM3.023930 homologs of *Epichloë* species. The protein sequences were aligned using MAFFT E-NS-I in Geneious.

	E.amarillans	E.aotearoae	E.baconii	E.brachyelytri	E.bromicola ...	E.bromicola ...	E.bromicola ...	E.elymi	E.gansuensis	E.glyceriae	E.inebrians	E.mollis	E.sylvatica	E.typhina	E.typhina poae	E.uncinata1	E.uncinata2	EfM3.023930
E.amarillans		77.7%	90.5%	83.2%	80.3%	75.3%	79.6%	82.8%	82.5%	87.2%	82.5%	90.5%	75.9%	73.7%	77.4%	77.1%	79.9%	92.0%
E.aotearoae	77.7%		78.5%	83.2%	83.2%	77.4%	82.8%	85.7%	77.1%	81.4%	76.4%	77.7%	85.3%	83.8%	87.2%	87.2%	82.8%	78.5%
E.baconii	90.5%	78.5%		82.5%	80.7%	75.6%	80.3%	82.8%	82.1%	86.5%	81.4%	90.5%	76.3%	74.8%	77.1%	76.7%	80.3%	92.3%
E.brachyelytri	83.2%	83.2%	82.5%		88.3%	81.8%	87.5%	91.6%	84.0%	87.6%	83.3%	83.9%	79.2%	77.4%	79.2%	78.9%	87.9%	83.2%
E.bromicola 0434	80.3%	83.2%	80.7%	88.3%		90.9%	99.3%	92.3%	80.4%	84.3%	79.6%	81.8%	79.2%	78.5%	80.8%	80.4%	99.6%	81.4%
E.bromicola 04262	75.3%	77.4%	75.6%	81.8%	90.9%		90.9%	86.5%	76.1%	79.3%	75.4%	76.4%	74.1%	74.4%	75.9%	75.6%	90.5%	76.4%
E.bromicola ATCC	79.6%	82.8%	80.3%	87.5%	99.3%	90.9%		91.6%	80.0%	83.9%	79.3%	81.4%	78.9%	78.1%	80.4%	80.0%	98.9%	81.0%
E.elymi	82.8%	85.7%	82.8%	91.6%	92.3%	86.5%	91.6%		83.3%	87.2%	82.5%	83.6%	81.1%	80.0%	81.9%	81.5%	91.9%	83.6%
E.gansuensis	82.5%	77.1%	82.1%	84.0%	80.4%	76.1%	80.0%	83.3%		89.1%	99.3%	84.0%	75.3%	72.7%	74.9%	74.5%	80.0%	83.9%
E.glyceriae	87.2%	81.4%	86.5%	87.6%	84.3%	79.3%	83.9%	87.2%	89.1%		88.4%	89.4%	78.2%	76.3%	78.6%	78.2%	83.9%	88.7%
E.inebrians	82.5%	76.4%	81.4%	83.3%	79.6%	75.4%	79.3%	82.5%	99.3%	88.4%		84.0%	74.5%	71.9%	74.2%	73.8%	79.3%	83.2%
E.mollis	90.5%	77.7%	90.5%	83.9%	81.8%	76.4%	81.4%	83.6%	84.0%	89.4%	84.0%		76.7%	74.1%	77.4%	77.1%	81.4%	92.0%
E.sylvatica	75.9%	85.3%	76.3%	79.2%	79.2%	74.1%	78.9%	81.1%	75.3%	78.2%	74.5%	76.7%		92.4%	95.5%	95.1%	78.9%	77.4%
E.typhina	73.7%	83.8%	74.8%	77.4%	78.5%	74.4%	78.1%	80.0%	72.7%	76.3%	71.9%	74.1%	92.4%		92.4%	92.0%	78.1%	75.1%
E.typhina poae	77.4%	87.2%	77.1%	79.2%	80.8%	75.9%	80.4%	81.9%	74.9%	78.6%	74.2%	77.4%	95.5%	92.4%		99.2%	80.4%	78.5%
E.uncinata1	77.1%	87.2%	76.7%	78.9%	80.4%	75.6%	80.0%	81.5%	74.5%	78.2%	73.8%	77.1%	95.1%	92.0%	99.2%		80.0%	78.1%
E.uncinata2	79.9%	82.8%	80.3%	87.9%	99.6%	90.5%	98.9%	91.9%	80.0%	83.9%	79.3%	81.4%	78.9%	78.1%	80.4%	80.0%		81.0%
EfM3.023930	92.0%	78.5%	92.3%	83.2%	81.4%	76.4%	81.0%	83.6%	83.9%	88.7%	83.2%	92.0%	77.4%	75.1%	78.5%	78.1%	81.0%	

Appendix 5- Amino acid alignmnet of EfM3.023930 homologs of *Epichloë* species. The protein sequences were aligned using MAFFT E-NS-i in Geneious.

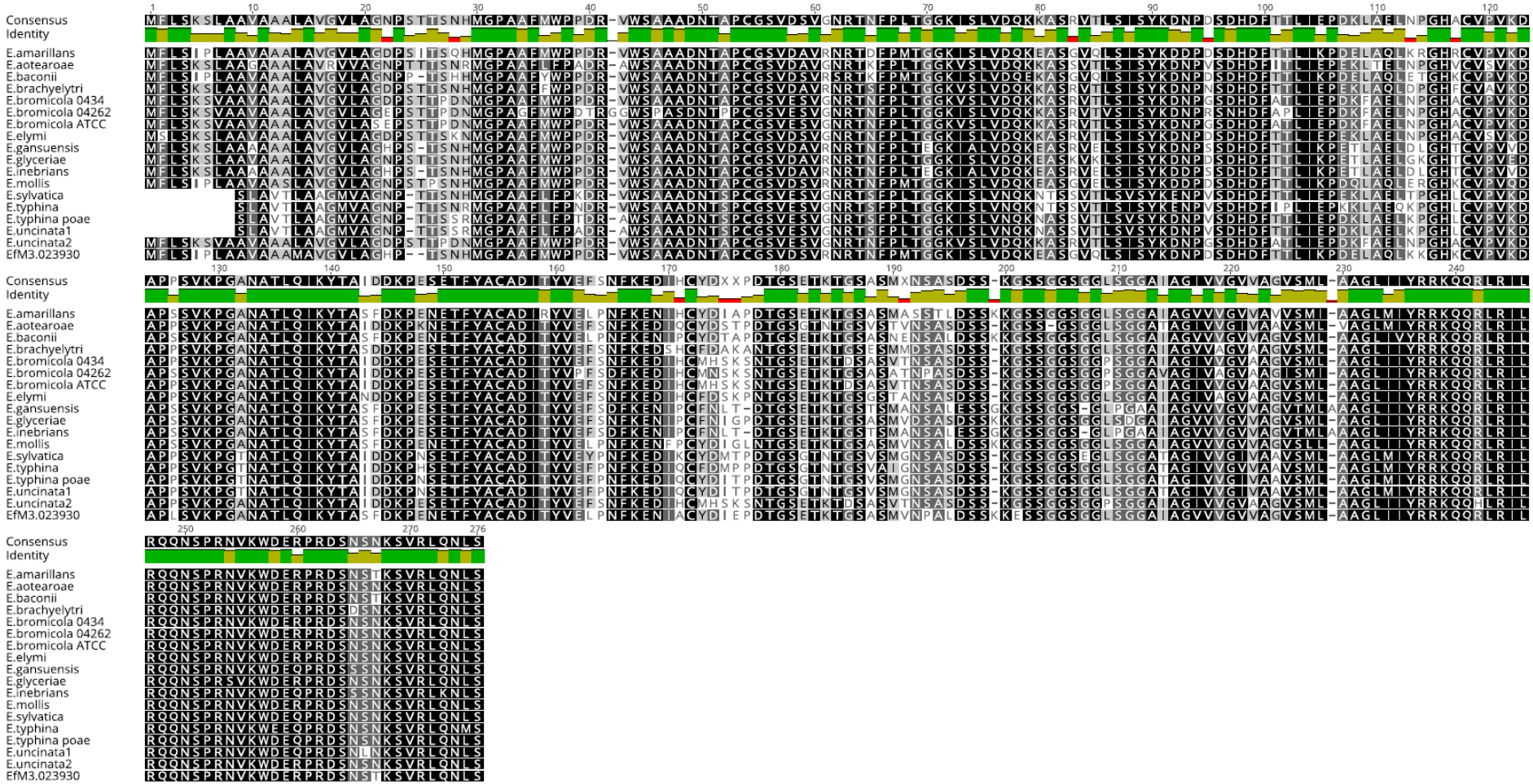

References

Adams, D. (2004). Fungal cell wall chitinases and glucanases. *Microbiology*, *150*(7), 2029-2035. http://doi.org/10.1099/mic.0.26980-0

Akerboom, J., Chen, T. W., Wardill, T. J., Tian, L., Marvin, J. S., Mutlu, S., Calderón,

Aguilar, P. S., Engel, A., & Walter, P. (2007). The plasma membrane proteins Prm1 and Fig1 ascertain fidelity of membrane fusion during yeast mating. *Molecular biology of the cell*, *18*(2), 547-56. http://doi.org/10.1091/mbc.E06-09-0776

Altschul, Stephen F., Gish, Warren., Miller, Webb., Myers, Eugene W., Lipman, David J. (1990). Basic local alignment search tool. *Journal of Molecular Biology*, *215*(3), 403-410. https://doi.org/10.1016/S0022-2836(05)80360-2

Ariyawansa, S. (2015). Sensing and Signalling Mechanical Stress During Intercalary Growth in *Epichloë* grass endophytes. (Doctoral Dissertation)

Bacon, C. W., & Hill, N. S. (2013). *Neotyphodium/Grass Interactions*. Springer Science & Business Media

Banuett, F. (1998) Signalling in the yeasts: an informationalcascade with links to the filamentous fungi. *Microbiol Mol Biol Rev*. *62*(2) 249–274. PMID: 9618441

Becker, Y., Eaton, C. J., Brasell, E., May, K. J., Becker, M., Hassing, B., … Scott, B. (2014). The Fungal Cell Wall Integrity MAPK Cascade is Crucial for Hyphal Network Formation and Maintenance of Restrictive Growth of *Epichloë festucae* in Symbiosis with *Lolium perenne*. *Molecular Plant-Microbe Interactions: MPMI*. http://doi.org/10.1094/MPMI-06-14-0183-R

Bormann, Jörg., Tudzynski, Paul. (2009). Deletion of Mid1, a putative stretch-activated calcium channel in *Claviceps purpurea*, affects vegetative growth, cell wall synthesis and virulence. *Microbiology*, *155*, 3922-3933. http://doi.org/10.1099/mic.0.030825-0

Brand, A., & Gow, N. A. (2009). Mechanisms of hypha orientation of fungi. *Current Opinion in Microbiology*, *12*(4), 350–357. http://doi.org/10.1016/j.mib.2009.05.007

Brand, A., Shanks, S., Duncan, V. M. S., Yang, M., Mackenzie, K., & Gow, N. A. R. (2007). Hyphal orientation of *Candida albicans* is regulated by a calcium-dependent mechanism. *Current Biology: CB*, *17*(4), 347–352. http://doi.org/10.1016/j.cub.2006.12.043

Cavinder, B., Hamam, A., Lew, R. R., & Trail, F. (2011). Mid1, a mechanosensitive calcium ion channel, affects growth, development, and ascospore discharge in the filamentous fungus *Gibberella zeae*. *Eukaryotic Cell*, *10*(6), 832–841. http://doi.org/10.1128/EC.00235-10

Cavinder, B., & Trail, F. (2012). Role of Fig1, a component of the low-affinity calcium uptake system, in growth and sexual development of filamentous fungi. *Eukaryotic Cell*, *11*(8), 978–988. http://doi.org/10.1128/EC.00007-12

Chardonnet, C.O., Sams, C.E., Conway, W.S. (1999). Calcium effect on the mycelial cell walls of *Botrytis cinerea*. *Phytochemistry*, *52*(6), 967-973. https://doi.org/10.1016/S0031-9422

Christensen, M. J., Bennett, R. J., Ansari, H. A., Koga, H., Johnson, R. D., Bryan, G. T., Voisey, C. R. (2008). *Epichloë endophytes* grow by intercalary hyphal extension in elongating grass leaves. *Fungal Genetics and Biology*, *45*(2), 84–93. http://doi.org/10.1016/j.fgb.2007.07.013

Christensen, M. J., Bennett, R. J., & Schmid, J. (2002). Growth of Epichloë / Neotyphodium and p-endophytes in leaves of Lolium and Festuca grasses. *Mycological Research*, *106*(1), 93–106. http://doi.org/10.1017/S095375620100510X

Christensen, M. J., Saulsbury, K., & Simpson, W. R. (2012). Conspicuous epiphytic growth of an interspecific hybrid *Neotyphodium sp*. endophyte on distorted host inflorescences. *Fungal Biology*, *116*(1), 42–48. http://doi.org/10.1016/j.funbio.2011.09.007

Chung, K., & Schardl, C. (1997). Sexual cycle and horizontal transmission of the grass symbiont, *Epichloë typhina*. *Mycological Research*, *101*(3), 295-301. https://doi.org/10.1017/S0953756296002602

Clay, K., & Schardl, C. (2002). Evolutionary origins and ecological consequences of endophyte symbiosis with grasses. *The American Naturalist*, *160 Suppl 4*, S99–S127. http://doi.org/10.1086/342161

Ronnie de Jonge, Melvin D Bolton, Bart PHJ Thomma. (2011). How filamentous pathogens co-opt plants: the ins and outs of fungal effectors. *Current Opinion in Plant Biology*, *14*(4), 400-406. https://doi.org/10.1016/j.pbi.2011.03.005

De rousset-hall, A., & Gooday, G. W. (1975). A Kinetic Study of a Solubilized Chitin Synthetase Preparation from *Coprinus cinereus*. *Microbiology*, *89*(1), 146–154. http://doi.org/10.1099/00221287-89-1-146

Dichtl, K., Helmschrott, C., Dirr, F. and Wagener, J. (2012). Deciphering cell wall integrity signalling in *Aspergillus fumigatus*: identification and functional characterization of cell wall stress sensors and relevant Rho GTPases. *Molecular Microbiology*, *83*(3), 506-519. doi:10.1111/j.1365-2958.2011.07946.x

Dichtl, K., Samantaray, S., and Wagener, J. (2016) Cell wall integrity signalling in human pathogenic fungi. Cellular Microbiology, *18*(9), 1228–1238. http://doi.org/doi: 10.1111/cmi.12612

Dickson, Robert C., Lester, Robert L. (2002). Sphingolipid functions in *Saccharomyces cerevisiae*. *Biochimica et Biophysica Acta (BBA) - Molecular and Cell Biology of Lipids, 1583*(1), 13-25. https://doi.org/10.1016/S1388-1981(02)00210-X

Dodds, Peter N., Rathjen, John. (2010). Plant immunity: towards an integrated view of plant–pathogen interactions. *Nature Reviews Genetics 11*(8), 539–548. http://doi.org/10.1038/nrg2812

Dupont, P., Eaton, C. J., Wargent, J. J., Fechtner, S. , Solomon, P. , Schmid, J. , Day, R. C., Scott, B. and Cox, M. P. (2015), Fungal endophyte infection of ryegrass reprograms host metabolism and alters development. *New Phytol*, *208*(4), 1227-1240. https://doi.org/10.1111/nph.13614

Eaton, C. J., Cox, M. P., Ambrose, B., Becker, M., Hesse, U., Schardl, C. L., & Scott, B. (2010). Disruption of signaling in a fungal-grass symbiosis leads to pathogenesis. *Plant physiology*, 153(4), 1780-94. http://doi.org/10.1104/pp.110.158451

Ene, I. V., Walker, L. A., Schiavone, M., Lee, K. K., Martin-Yken, H., Dague, E., Gow, N. A., Munro, C. A., … Brown, A. J. (2015). Cell Wall Remodeling Enzymes Modulate Fungal Cell Wall Elasticity and Osmotic Stress Resistance. *mBio*, *6*(4), e00986. http://doi.org/10.1128/mBio.00986-15

Fairhead, C., Llorente, B., Denis, F., Soler, M. and Dujon, B. (1996). New vectors for combinatorial deletions in yeast chromosomes and for gap-repair cloning using 'split-marker' recombination. *Yeast*, *12*(14), 1439-1457

Freeman, E. M. (1904). The Seed-Fungus of *Lolium temulentum*, L., the Darnel. *Philosophical Transactions of the Royal Society of London B: Biological Sciences*, *196*(214-224), 1–27. http://doi.org/10.1098/rstb.1904.0001

Gabriela Roca, M., Read, N. D., & Wheals, A. E. (2005). Conidial anastomosis tubes in filamentous fungi. *FEMS Microbiology Letters*, *249*(2), 191–198. http://doi.org/10.1016/j.femsle.2005.06.048

Garcia-Cantalejo JM, Boskovic J, Jimenez A. (1996). Sequence analysis of a 14.2 kb fragment of *Saccharomyces cerevisiae* chromosome XIV that includes the ypt53, tRNALeu and gsr m2 genes and four new open reading frames. *Yeast*, *12*(6), 599-608

Gonthier, D. J., Sullivan, T. J., Brown, K. L., Wurtzel, B., Lawal, R., VandenOever, K., Bultman, T. L. (2008). Stroma-forming endophyte *Epichloë glyceriae* provides wound-inducible herbivore resistance to its grass host. *Oikos*, *117*(4), 629–633. http://doi.org/10.1111/j.0030-1299.2008.16483.x

Green, K. (2016). A conserved Signalling Network Regulates *Epichloë festucae* Cell-Cell Fusion and the Mutualistic Symbiotic Interaction Between *E. festucae* and *Lolium perenne*. (Doctoral Dissertation)

Grigoriev, I. V., Nikitin, R., Haridas, S., Kuo, A., Ohm, R., Otillar, R., Riley, R., Salamov, A., Zhao, X., Korzeniewski, F., Smirnova, T., Nordberg, H., Dubchak, I., Shabalov, I. (2013). MycoCosm portal: gearing up for 1000 fungal genomes. *Nucleic acids research*, *42*(1), D699-704. https://doi.org/10.1093/nar/gkt1183

Goldman, Aaron., Roy, Jagoree., Bodenmiller, Bernd., Wanka, Stefanie., Landry, Christian R., Aebersold, Ruedi., Cyert, Martha S.(2004). The Calcineurin Signaling Network Evolves via Conserved Kinase-Phosphatase Modules that Transcend Substrate Identity. *Molecular Cell*, *55*(3), 422-435. https://doi.org/10.1016/j.molcel.2014.05.012

Guerre, P. (2015). Ergot alkaloids produced by endophytic fungi of the genus *Epichloë*. *Toxins*, *7*(3), 773–790. http://doi.org/10.3390/toxins7030773

Hahn, H., Huth, W., Schöberlein, W., Diepenbrock, W. and Weber, W. E. (2003). Detection of endophytic fungi in *Festuca* spp. by means of tissue print immunoassay. *Plant Breeding*, 122(3), 217-222. http://doi.org/10.1046/j.1439-0523.2003.00855.x

Hammad, F., Ji, J., Watling, R., & Moore, D. (1993). Cell population dynamics in *Coprinus cinereus*: co-ordination of cell inflation throughout the maturing basidiome. *Mycological Research*, *97*(3), 269–274. http://doi.org/10.1016/S0953-7562(09)81119-2

Harris, S. D. (2006). Cell polarity in filamentous fungi: shaping the mold. *International Review of Cytology*, *251*, 41–77. http://doi.org/10.1016/S0074-7696(06)51002-2

Heinisch, JJ., Dupres, V., Wilk, S., Jendretzki, A., Dufrene, YF. (2010). Single-molecule atomic force microscopy reveals clustering of the yeast plasma-membrane sensor Wsc1. *PLoS One, 5*(6), e11104. http://doi.org/f10.1371/journal.pone.0011104

Hohmann,Stefan., Mager, Willem H. (2003). Yeast Stress Responses. The Netherlands, Print: Springer Science & Business Media

Hickey, P. C., Jacobson, D., Read, N. D., & Glass, N. L. (2002). Live-cell imaging of vegetative hyphal fusion in *Neurospora crassa*. *Fungal Genetics and Biology: FG & B*, *37*(1), 109–119

Iida, H., Nakamura, H., Ono, T., Okumura, MS., Anraku, Y. (1994) MID1, a novel *Saccharomyces cerevisiae* gene encoding a plasma membrane protein, is required for Ca2+ influx and mating. *Mol Cell Biol*, *14*(12), 8259–8271. http://doi.org/10.1128/MCB.14.12.8259

Intercalary. (n.d.). Retrieved January 7, 2016, from http://www.merriam-webster.com/dictionary/intercalary

Jackson, S. L., & Heath, I. B. (1993). Roles of calcium ions in hyphal tip growth. *Microbiological Reviews*, *57*(2), 367–382

Jendretzki, Arne., Wittland, Janina., Wilk, Sabrina., Straede, Andrea., Heinisch, Jürgen J. (2011). How do I begin? Sensing extracellular stress to maintain yeast cell wall integrity. *European Journal of Cell Biology*, *90*(9), 740-744. https://doi.org/10.1016/j.ejcb.2011.04.006

Jung, U. S., Sobering, A. K., Romeo, M. J. and Levin, D. E. (2002), Regulation of the yeast Rlm1 transcription factor by the Mpk1 cell wall integrity MAP kinase. *Molecular Microbiology*, 46(3), 781-789. https://doi.org/doi:10.1046/j.1365-2958.2002.03198.x

Jewiss, O. R. (1972), TILLERING IN GRASSES—ITS SIGNIFICANCE AND CONTROL*. *Grass and Forage Science*, *27*(2), 65-82. https://doi.org/10.1111/j.1365-2494.1972.tb00689.x

Jin, C., Parshin, A. V., Daly, I., Strich, R., & Cooper, K. F. (2013). The Cell Wall Sensors Mtl1, Wsc1, and Mid2 Are Required for Stress-Induced Nuclear to Cytoplasmic Translocation of Cyclin C and Programmed Cell Death in Yeast. *Oxidative Medicine and Cellular Longevity*, *2013*. http://doi.org/10.1155/2013/320823

Ketela, T., Green, R., & Bussey, H. (1999). *Saccharomyces cerevisiae* mid2p is a potential cell wall stress sensor and upstream activator of the PKC1-MPK1 cell integrity pathway. *Journal of Bacteriology*, *181*(11), 3330–3340

Kües, U. (2000). Life History and Developmental Processes in the Basidiomycete *Coprinus cinereus*. *Microbiology and Molecular Biology Reviews*, *64*(2), 316–353. http://doi.org/10.1128/MMBR.64.2.316-353.2000

Kanzaki, M., Nagasawa, M., Kojima, I., Sato, C., Naruse, K., Sokabe, M., Ida, H. (1999). Molecular identification of a eukaryotic, stretch-activated nonselective cation channel. *Science*, *285*(5433), 882–886. https://doi.org/f10.1126/science.285.5429.882

Kocer, Armagan. (2015). Mechanisms of mechanosensing—mechanosensitive channels, function and re-engineering. *Current Opinion in Chemical Biology*, 29, 120-127. https://doi.org/10.1016/j.cbpa.2015.10.006

Kock, C., Dufrêne, Y. F., & Heinisch, J. J. (2015). Up against the wall: is yeast cell wall integrity ensured by mechanosensing in plasma membrane microdomains?. *Applied and environmental microbiology*, *81*(3), 806-11. http://doi.org/10.1128/AEM.03273-14

Kulkarni, Resham., D Kelkar, Hemant S., Dean, Ralph A. (2003). An eight-cysteine-containing CFEM domain unique to a group of fungal membrane proteins. *Trends in Biochemical Sciences*, *28*(3), 118-121. https://doi.org/10.1016/S0968-0004(03)00025-2.

Kumamoto, C. A. (2008). Molecular mechanisms of mechanosensing and their roles in fungal contact sensing. *Nature reviews*. Microbiology, *6*(9), 667-73. http://doi.org/10.1038/nrmicro1960

Langer, R. H. M. (1972). How Grasses Grow. London, Print: The Camelot Press Ltd.

Leuchtmann, A., Bacon, C. W., Schardl, C. L., White, J. F., & Tadych, M. (2014). Nomenclatural realignment of Neotyphodium species with genus Epicholë. *Mycologia*, *106*(2), 202–215. http://doi.org/10.3852/13-251

Lew, R. R., Abbas, Z., Anderca, M. I., & Free, S. J. (2008). Phenotype of a Mechanosensitive Channel Mutant, mid-1, in a Filamentous Fungus, *Neurospora crassa*. *Eukaryotic Cell*, *7*(4), 647–655. http://doi.org/10.1128/EC.00411-07

Lo Presti, Libera., Lanver, Daniel., Schweizer, Gabriel., Tanaka, Shigeyuki., Liang, Liang., Tollot, Marie., Zuccaro, Alga., Reissmann, Stefanie., Kahmann, Regine. (2015). Fungal Effectors and Plant Susceptibility. *Annual Review of Plant Biology*, *66*(1), 513-545. https://doi.org/10.1146/annurev-arplant-043014-114623

Locke, EG., Bonilla, M., Liang, L., Takita, Y., Cunningham, KW. (2000). A homolog of voltage-gated Ca ($^{2+}$) channels stimulated by depletion of secretory Ca ($^{2+}$) in yeast. *Mol Cell Biol*, *20*(18), 6686–6694. http://doi.org/10.1128/MCB.20.18.6686-6694.2000

Lichius, A., Yáñez-Gutiérrez, M. E., Read, N. D., & Castro-Longoria, E. (2012). Comparative live-cell imaging analyses of SPA-2, BUD-6 and BNI-1 in *Neurospora crassa* reveal novel features of the filamentous fungal polarisome. *PloS One*, *7*(1), e30372. http://doi.org/10.1371/journal.pone.0030372

Ligr, Martin., Madeo, Frank., Fröhlich, Eleonore., Hilt, Wolfgang., Fröhlich, Kai-Uwe., Wolf, Dieter H. (1998). Mammalian Bax triggers apoptotic changes in yeast. *FEBS Letters*, *438*(1-2), 61-65. https://doi.org/10.1016/S0014-5793(98)01227-7

Lim, L. L., Fineran, B. A., & Cole, A. L. J. (1983). Ultrastructure of Intrahyphal Hyphae of *Glomus Fascicula Tum* (thaxter) Gerdemann and Trappe in Roots of White Clover (trifolium Repens L.). *New Phytologist*, *95*(2), 231–239. http://doi.org/10.1111/j.1469-8137.1983.tb03489.x

Liu, F., Ng, S. K., Lu, Y., Low, W., Lai, J., & Jedd, G. (2008). Making two organelles from one: Woronin body biogenesis by peroxisomal protein sorting. *The Journal of Cell Biology*, *180*(2), 325–339. http://doi.org/10.1083/jcb.200705049

Li, X., Zhou, Y., Zhu, M., Qin, J., Ren, A., & Gao, Y. (2015). Stroma-bearing endophyte and its potential horizontal transmission ability in *Achnatherum sibiricum*. *Mycologia*, *107*(1), 21–31. http://doi.org/10.3852/13-355

Maddi, A., Dettman, A., Fu, C., Seiler, S., Free, SJ. (2012) WSC-1 and HAM-7 Are MAK-1 MAP Kinase Pathway Sensors Required for Cell Wall Integrity and Hyphal Fusion in *Neurospora crassa*. *Plos One*, *7*(8): e42374. https://doi.org/10.1371/journal.pone.0042374

Markham, P. (1994). Occlusions of septal pores in filamentous fungi. *Mycological Research*, *98*(10), 1089–1106. http://doi.org/10.1016/S0953-7562(09)80195-0

Markus, Albert. (2013). Peptides as triggers of plant defence. *Journal of Experimental Botany*, *64*(17), 5269–5279. https://doi.org/10.1093/jxb/ert275

Maruoka, Takashi., Nagasoe, Yurika., Inoue, Shinobu., Mori, Yasunori., Goto, June., Ikeda, Mitsunobu., Iida, Hidetoshi. (2002). Essential Hydrophilic Carboxyl-terminal Regions Including Cysteine Residues of the Yeast Stretch-activated Calcium-permeable Channel Mid1. *J. Biol. Chem*, *277*(14), 11645-11652. http://doi.org/doi:10.1074/jbc.M111603200

Maruyama, J.-I., & Kitamoto, K. (2013). Expanding functional repertoires of fungal peroxisomes: contribution to growth and survival processes. *Frontiers in Physiology*, *4*, 177. http://doi.org/10.3389/fphys.2013.00177

Mehlhorn H. (2015). Crystalloid Body. *Encyclopedia of Parasitology*. Springer, Berlin, Heidelberg.

Meitzler, J. L., Hinde, S., Bánfi, B., Nauseef, W. M., & Ortiz de Montellano, P. R. (2013). Conserved cysteine residues provide a protein-protein interaction surface in dual oxidase (DUOX) proteins. *The Journal of Biological Chemistry*, *288*(10), 7147-57. http://doi.org/10.1074/jbc.M112.414797

Moore, D. (1995). Tissue Formation. In N. A. R. Gow & G. M. Gadd (Eds.), The Growing Fungus (pp. 423–465). Springer Netherlands. Retrieved from http://link.springer.com/chapter/10.1007/978-0-585-27576-5_20

Morand, Philippe., Bille, Emmanuelle., Morelle, Sandrine., Eugene, Emmanuelle., Beretti, Jac-Luc., Wolfgang, Matthew., Meyer, F. Thomas., Koomey, Micheal., Nassif, Zavier. (2004). Type IV pilus retraction in pathogenic Neisseria is regulated by the PilC proteins. *The EMBO journal*, 23(9), 2009-17. http://doi.org/10.1038/sj.emboj.7600200

Moy, M., Li, H. M., Sullivan, R., White, J. F., & Belanger, F. C. (2002). Endophytic fungal beta-1,6-glucanase expression in the infected host grass. *Plant Physiology*, *130*(3), 1298–1308. http://doi.org/10.1104/pp.010108

Nagabhyru, Padmaja., Dinkins, Randy D. and Schardl, Christopher L. (2018). Transcriptomics of Epichloë-Grass Symbioses in Host Vegetative and Reproductive Stages. *Molecular Plant-Microbe Interactions*, *32*(2), 194-207. https://doi.org/10.1094/MPMI-10-17-0251-R

Norice, C. T., Smith, F. J., Solis, N., Filler, S. G., & Mitchell, A. P. (2007). Requirement for *Candida albicans* Sun41 in biofilm formation and virulence. *Eukaryotic cell*, 6(11), 2046-55. http://doi.org/10.1128/EC.00314-07

Nordberg, Henrik., Cantor, Michael., Dusheyko, Serge., Hua, Susan, Poliakov, Alexander, Shabalov, Igor., Smirnova, Tatyana., Grigoriev, Igor V., Dubchak, Inna. (2014) The genome portal of the Department of Energy Joint Genome Institute: 2014 updates. *Nucleic Acids Research*, 42(D1), D26–D31. https://doi.org/10.1093/nar/gkt1069

Ohsawa, S., Yurimoto, H. and Sakai, Y. (2017). Novel function of Wsc proteins as a methanol-sensing machinery in the yeast *Pichia pastoris*. *Molecular Microbiology*, *104*(2), 349-363. http://doi.org/doi:10.1111/mmi.13631

Owsianowski, E., Walter, D., Fahrenkrog, B. (2008). Negative regulation of apoptosis in yeast. *Biochim. Biophys. Acta*, 1783(7), 1303–1310. http://doi.org/10.1016/j.bbamcr.2008.03.006

Ozeki-Miyawaki, C., Moriya, Y., Tatsumi, H., Iida, H., and Sokabe, M. (2005). Identification of functional domains of Mid1, a stretch-activated channel component, necessary for localization to the plasma membrane and Ca2+ permeation. *Exp. Cell Res*, *311*(1), 84–95. http://doi.org/10.1016/j.yexcr.2005.08.014

O'Leary, B. M., Rico, A., McCraw, S., Fones, H. N., & Preston, G. M. (2014). The infiltration-centrifugation technique for extraction of apoplastic fluid from plant leaves using *Phaseolus vulgaris* as an example. *Journal of Visualized Experiments: JoVE*, (94), 52113. http://doi.org/10.3791/52113

O'Leary, B. M., Neale, H. C., Geilfus, C. M., Jackson, R. W., Arnold, D. L., & Preston, G. M. (2016). Early changes in apoplast composition associated with defence and

disease in interactions between *Phaseolus vulgaris* and the halo blight pathogen *Pseudomonas syringae* Pv. phaseolicola. *Plant, Cell & Environment*, *39*(10), 2172-84. http://doi.org/ 10.1111/pce.12770

Philip, B., & Levin, D. E. (2001). Wsc1 and Mid2 are cell surface sensors for cell wall integrity signaling that act through Rom2, a guanine nucleotide exchange factor for Rho1. *Molecular and Cellular Biology*, *21*(1), 271–280. http://doi.org/10.1128/MCB.21.1.271-280.2001

Philipson, M. N., & Christey, M. C. (1986). The relationship of host and endophyte during flowering, seed formation, and germination of *Lolium perenne*. *New Zealand Journal of Botany*, *24*(1), 125–134. http://doi.org/10.1080/0028825X.1986.10409724

R Core Team (2013). R: A language and environment for statistical computing. R Foundation for Statistical Computing, Vienna, Austria. ISBN 3-900051-07-0. http://www.R-project.org/

Rahnama, M., Forester, N., Ariyawansa, K. G. S. U., Voisey, C. R., Johnson, L. J. Johnson, R. D., Fleetwood, D. J. (2017). Efficient targeted mutagenesis in *Epichloë festucae* using a split marker system. *Journal of Microbiological Methods*, *134*(2017), 62-65. https://doi.org/10.1016/j.mimet.2016.12.017

R.C. Keogh, B.J. Deverall, Stella, McLeod. (1980). Comparison of histological and physiological responses to Phakopsora pachyrhizi in resistant and susceptible soybean. T*ransactions of the British Mycological Society*. *74*(2), 329-333. https://doi.org/10.1016/S0007-1536(80)80163-X

Rech, Christine., Engh, Ines., Kück, Ulrich. (2007). Detection of hyphal fusion in filamentous fungi using differently fluorescence-labeled histones. *Current Genetics*, *52*(259). https://doi.org/10.1007/s00294-007-0158-6

Regaladot, C. M. (1998). Roles of calcium gradients in hyphal tip growth: a mathematical model. *Microbiology*, *144*(10), 2771–2782. http://doi.org/10.1099/00221287-144-10-2771

Repussard, C., Zbib, N., Tardieu, D., & Guerre, P. (2014). Ergovaline and lolitrem B concentrations in perennial ryegrass in field culture in southern France: distribution in the plant and impact of climatic factors. *Journal of Agricultural and Food Chemistry*, *62*(52), 12707–12712. http://doi.org/10.1021/jf504581y

Riquelme, M. (2013). Tip growth in filamentous fungi: a road trip to the apex. *Annual Review of Microbiology*, *67*, 587–609. http://doi.org/10.1146/annurev-micro-092412-155652

Riquelme, M., & Sánchez-León, E. (2014). The Spitzenkörper: a choreographer of fungal growth and morphogenesis. *Current Opinion in Microbiology*, *20*, 27–33. http://doi.org/10.1016/j.mib.2014.04.003

Rodicio, Rosaura., Buchwald, Ulf., Schmitz, Hans-Peter., Heinisch, Jürgen J. (2008). Dissecting sensor functions in cell wall integrity signaling in *Kluyveromyces lactis*. *Fungal Genetics and Biology*, *45*(4), 422-435. https://doi.org/10.1016/j.fgb.2007.07.009

Rodicio, R., & Heinisch, J. J. (2010). Together we are strong—cell wall integrity sensors in yeasts. *Yeast*, *27*(8), 531–540. http://doi.org/10.1002/yea.1785

Rosenwald, A. G., Arora, G., Ferrandino, R., Gerace, E. L., Mohammednetej, M., Nosair, W., Rattila, S., Subic, A. Z., … Rolfes, R. (2016). Identification of Genes in *Candida glabrata* Conferring Altered Responses to Caspofungin, a Cell Wall Synthesis Inhibitor. *G3 (Bethesda, Md.)*, *6*(9), 2893-907. http://doi.org/doi:10.1534/g3.116.032490

Saikkonen, K., Young, C. A., Helander, M., & Schardl, C. L. (2015). Endophytic Epichloë species and their grass hosts: from evolution to applications. *Plant Molecular Biology*. http://doi.org/10.1007/s11103-015-0399-6

Schardl, C. L. (1996). EPICHLOE SPECIES: fungal symbionts of grasses. *Annual Review of Phytopathology*, *34*, 109–130. http://doi.org/10.1146/annurev.phyto.34.1.109

Schenk, Sebastian T., Schikora, Adam. (2015). Lignin Extraction and Quantification, a Tool to Monitor Defense Reaction at the Plant Cell Wall Level. *Bio-Protocol*, *5*(10), 1-6, http://doi.org/10.21769/BioProtoc.1430

Schardl, C. L. (2002). *Epichloë festucae* and related mutualistic symbionts of grasses. *Fungal Genetics and Biology: FG & B*, *33*(2), 69–82. http://doi.org/10.1006/fgbi.2001.1275

Scott, B. (2001). Epichloë endophytes: fungal symbionts of grasses. *Current Opinion in Microbiology*, *4*(4), 393–398. https://doi.org/10.1016/S1369-5274(00)00224-1

Sharman, B.C. (1945). Leaf and Bud Initiation in the Gramineae. *Botanical Gazette*, *106*(3), 269-289. https://doi.org/10.1086/335298

Shaw, B. D., Chung, D.-W., Wang, C.-L., Quintanilla, L. A., & Upadhyay, S. (2011). A role for endocytic recycling in hyphal growth. *Fungal Biology*, *115*(6), 541–546. http://doi.org/10.1016/j.funbio.2011.02.010

Slattery, M. G., Liko, D., & Heideman, W. (2006). The function and properties of the Azf1 transcriptional regulator change with growth conditions in *Saccharomyces cerevisiae*. *Eukaryotic cell*, *5*(2), 313-20

Spatafora, J. W., Sung, G., Sung, J., Hywel-Jones, N. L. and White, J. F. (2007). Phylogenetic evidence for an animal pathogen origin of ergot and the grass endophytes. *Molecular Ecology*, 16(8), 1701-1711. http://doi.org/doi:10.1111/j.1365-294X.2007.03225.x

Steinberg, G. (2007). Hyphal Growth: a Tale of Motors, Lipids, and the Spitzenkörper. *Eukaryotic Cell*, *6*(3), 351–360. http://doi.org/10.1128/EC.00381-06

Straede, A., & Heinisch, J. J. (2007). Functional analyses of the extra- and intracellular domains of the yeast cell wall integrity sensors Mid2 and Wsc1. *FEBS Letters*, *581*(23), 4495–4500. http://doi.org/10.1016/j.febslet.2007.08.027

Tadych, M., Bergen, M. S., & White, J. F. (2014). *Epichloë spp*. associated with grasses: new insights on life cycles, dissemination and evolution. *Mycologia*, *106*(2), 181–201

Takemoto, D., Tanaka, A., & Scott, B. (2006). A p67Phox-like regulator is recruited to control hyphal branching in a fungal-grass mutualistic symbiosis. *The Plant cell*, *18*(10), 2807-21. http://doi.org/10.1105/tpc.106.046169

Takeshita, N., Manck, R., Grün, N., de Vega, S. H., & Fischer, R. (2014). Interdependence of the actin and the microtubule cytoskeleton during fungal growth. *Current Opinion in Microbiology*, *20*, 34–41. http://doi.org/10.1016/j.mib.2014.04.005

Tanaka, A., Takemoto, D., Hyon, G., Park, P. and Scott, B. (2008). NoxA activation by the small GTPase RacA is required to maintain a mutualistic symbiotic association between *Epichloë festucae* and perennial ryegrass. *Molecular Microbiology*, *68*(5), 1165-1178. http://doi.org/doi:10.1111/j.1365-2958.2008.06217.x

Tanaka, A., Takemoto, D., Chujo, T., & Scott, B. (2012). Fungal endophytes of grasses. *Current Opinion in Plant Biology*, *15*(4), 462–468. http://doi.org/10.1016/j.pbi.2012.03.007

Tanaka, A., Cartwright, G. M., Saikia, S., Kayano, Y., Takemoto, D., Kato, M., Tsuge, T. and Scott, B. (2013). Symbiotic hyphal network regulation by ProA. *Molecular Microbiology*, *90*(3), 551-568. http://doi.org/10.1111/mmi.12385

Tan, Y. Y., Spiering, M. J., Scott, V., Lane, G. A., Christensen, M. J., & Schmid, J. (2001). In Planta Regulation of Extension of an Endophytic Fungus and Maintenance of High Metabolic Rates in Its Mycelium in the Absence of Apical Extension. *Applied and Environmental Microbiology*, *67*(12), 5377–5383. http://doi.org/10.1128/AEM.67.12.5377-5383.2001

Tenney, K., Hunt, I., Sweigard, J., Pounder, J. I., McClain, C., Bowman, E. J., & Bowman, B. J. (2000). Hex-1, a gene unique to filamentous fungi, encodes the major protein of the Woronin body and functions as a plug for septal pores. *Fungal Genetics and Biology: FG & B*, *31*(3), 205–217. http://doi.org/10.1006/fgbi.2000.1230

van den Burg, HA., Harrison, SJ., Joosten, MH., Vervoort, J., de Wit, PJ. (2006). Cladosporium fulvum Avr4 protects fungal cell walls against hydrolysis by plant chitinases accumulating during infection. *Mol Plant Microbe Interact*, *19*(12), 1420-30. http://doi.org/ 10.1094/MPMI-19-1420

Verghese, J., Abrams, J., Wang, Y., & Morano, K. A. (2012). Biology of the heat shock response and protein chaperones: budding yeast (*Saccharomyces cerevisiae*) as a model system. *Microbiology and molecular biology reviews: MMBR*, *76*(2), 115-58. http://doi.org/10.1128/MMBR.05018-11

Verna, J., Lodder, A., Lee, K., Vagts, A., & Ballester, R. (1997). A family of genes required for maintenance of cell wall integrity and for the stress response in *Saccharomyces cerevisiae*. *Proceedings of the National Academy of Sciences of the United States of America*, *94*(25), 13804–13809

Verna, J., Ballestar, R. (1999). A novel role for the mating type (MAT) locus in the maintenance of cell wall integrity in *Saccharomyces cerevisiae*. *Mol Gen Genet*. *261*(4), 681-689. PMID: 10394905

Voisey, C. R. (2010). Intercalary growth in hyphae of filamentous fungi. *Fungal Biology Reviews*, *24*(3–4), 123–131. http://doi.org/10.1016/j.fbr.2010.12.001

Wang Q. M., Liu W. Q., Liti G., Wang S. A., Bai F. Y. (2012). Surprisingly diverged populations of *Saccharomyces cerevisiae* in natural environments remote from human

activity. *Mol. Ecol, 21*(22), 5404–5417. http://doi.org/10.1111/j.1365-294X.2012.05732.x

Walter, David., Wissing, Silke., Madeo, Frank., Fahrenkrog, Birthe. (2006). The inhibitor-of-apoptosis protein Bir1p protects against apoptosis in *S. cerevisiae* and is a substrate for the yeast homologue of Omi/HtrA2. *Journal of Cell Science*, *119*(9), 1843-1851. https://doi.org/ 10.1242/jcs.02902

Wu, C., Yang, F., Smith, K. M., Peterson, M., Dekhang, R., Zhang, Y., Zucker, J., Bredeweg, E. L., Mallappa, C., Zhou, X., Lyubetskaya, A., Townsend, J. P., Galagan, J. E., Freitag, M., Dunlap, J. C., Bell-Pedersen, D., … Sachs, M. S. (2014). Genome-wide characterization of light-regulated genes in *Neurospora crassa*. *G3 (Bethesda, Md.)*, *4*(9), 1731-45. https://doi.org/ 10.1534/g3.114.012617

Yoshimura, Hitoshi., Tada, Tomoko., Iida, Hidetoshi. Subcellular localization and oligomeric structure of the yeast putative stretch-activated Ca2+ channel component Mid1. *Experimental Cell Research*, *293*(2), 185-195. https://doi.org/10.1016/j.yexcr.2003.09.020

Youatt, J., Gow, N. a. R., & Gooday, G. W. (1988). Bioelectric and biosynthetic aspects of cell polarity in *Allomyces macrogynus*. *Protoplasma*, *146*(2-3), 118–126. http://doi.org/10.1007/BF01405920

Zhang, S., Zheng, H., Long, N., Carbo, N., Chen, P., Aguilar, P. S., & Lu, L. (2014). FigA, a Putative Homolog of Low-Affinity Calcium System Member Fig1 in *Saccharomyces cerevisiae*, is Involved in Growth and Asexual and Sexual Development in *Aspergillus nidulans*. *Eukaryotic Cell, 13*(2), 295–303. http://doi.org/10.1128/EC.00257-13

Zdobnov, M. Evgeni., Apweiler, Rolf. (2001). InterProScan--an integration platform for the signature-recognition methods in InterPro. *Bioinformatics*, *17*(9), 847-848. PMID: 11590104